# ABSTRACT

**UYAR, TAMER.** NANOSTRUCTURING POLYMERS WITH CYCLODEXTRINS. (Under the direction of Prof. Alan E. Tonelli)

The formation of polymer-cyclodextrin inclusion compounds of polycarbonate (PC), poly(methylmethacrylate) (PMMA) and poly(vinylacetate) (PVAc) guests with host γ-cyclodextrin (γ-CD) have been successfully achieved. Coalesced bulk polymer samples were obtained by removal of γ-CD from their inclusion compounds (ICs). Spectroscopic findings indicated that the chain conformations of the bulk polymers were altered when they were included inside the CD channels and extended chain conformations were retained when coalesced from their ICs. Significant improvements were observed in the thermal transitions for the coalesced polymers, with glass transitions shifted to higher temperatures. Thermal studies reveal that the thermal stabilities of coalesced polymers increased slightly compared to the corresponding as-received polymers and degradation products of the polymers are affected once the polymers chains are included inside the γ-CD-IC cavities.

A procedure for the formation of intimate blends of binary and ternary polymer systems; PC/PMMA, PC/PVAc, PMMA/PVAc and PC/PMMA/PVAc was studied. PC/PMMA, PC/PVAc, PMMA/PVAc and PC/PMMA/PVAc were included in γ-CD channels and were then simultaneously coalesced from their common γ-CD-ICs to obtain intimately mixed blends. It was observed that the ratios of polymers in coalesced blends were significantly different than the starting ratios, and PC was found to be preferentially included in γ-CD channels when compared to PMMA or

PVAc. Physical mixtures of polymer blends were also prepared by co-precipitation and solution casting methods for comparison. The analysis indicates that the ternary and the binary blends of these polymers achieved by coalescence from their common γ-CD-IC results in a homogeneous polymer blends, possibly with improved properties, whereas co-precipitation and solution cast methods produced phase separated polymer blends. It was shown that coalescence of two or more normally immiscible polymers from their common CD-ICs appears to be an applicable method for obtaining well-mixed, intimate blends.

The solid complex of guest styrene included inside the channels of host γ-cyclodextrin (styrene/γ-$CD_{channel}$-IC) was formed in order to perform polymerization of styrene in a confined environment (γ-CD channels). Modeling of polystyrenes (PS) with various stereosequences in the narrow cylindrical channels corresponding to those found in γ-CD ICs has been conducted. It was calculated that only isotactic PS stereoisomers can fit into the γ-CD cavity. Thus, based on the modeling of stereoisomeric PSs in narrow γ-CD channels, it was suggested that polystyrene with unusual microstructures might be produced *via* constrained polymerization of styrene monomer in its γ-CD-IC crystals. The *in situ* polymerization of styrene inside the narrow channels of its γ-CD-IC crystals was performed in aqueous media. Alternatively, the solid-state polymerization of styrene/γ-CD IC has also been carried out by radiation polymerization. It was found that most styrene monomer migrates from the γ-CD channels and polymerizes outside of the channels. Yet, a rotaxaned structure has been obtained where some CD molecules entrapped along the PS chains after the polymerization.

# NANOSTRUCTURING POLYMERS WITH CYCLODEXTRINS

By

**TAMER UYAR**

A dissertation submitted to the
Graduate Faculty of North Carolina State University
in partial fulfillment of the requirements for the
Degree of Doctor of Philosophy

## FIBER & POLYMER SCIENCE

**Raleigh, NC**

**September 2005**

**APPROVED BY**

Dr. Maurice Balik

Dr. Richard Kotek

Dr. Juan P. Hinestroza

Dr. Alan E. Tonelli
*Chair of Advisory Committee*

# TO MY FAMILY

# BIOGRAPHY

Tamer Uyar was born in Mersin, Turkey and attended Middle East Technical University (METU) in Ankara, Turkey from 1994 to 1998. He graduated with a B. S. in Chemistry Education double major with Chemistry both with honors. In 1998, Tamer began the master's program also at METU in Chemistry and conducted research on the structural and thermal characterization of conducting polymers. He graduated with a M. Sc. in Chemistry with a minor in Polymer Sci & Tech in 2000.

In August 2000, Tamer came to the United States to study at the Materials Science & Engineering Department of the University of Cincinnati. There, he studied multi-functional polymeric composite coatings and then obtained a M. S. degree. In 2002, Tamer began studying for a Ph. D. in Fiber & Polymer Science at North Carolina State University with Professor Alan E. Tonelli. He studied polymer-cyclodextrin inclusion compounds. In the summers of 2002, 2003 and 2004, he interned in R & D at Procter & Gamble in Cincinnati, OH where he gained industrial experience and practice on various subjects.

He is an author/co-author of more than 20 scientific papers and he presented his studies in more than 15 international conferences. He was awarded at "Excellence in Graduate Polymer Research Symposium", American Chemical Society 228$^{th}$ National Meeting (Philadelphia, PA, August 2004). He was a Student Presentations Award Winner at National Textile Center Forum 2004 (Hilton Head, SC, February 2004). He was also First Place Award Winner in Graduate Students Presentations, Richard Gilbert Award Symposium 2004 organized by North Carolina Polymer Section-American Chemical Society (Feb 12$^{th}$ 2004)

# ACKNOWLEDGEMENTS

I would like to express my sincere thanks and gratitude to my adviser, my mentor, my chair of my advisory committee Prof. Alan E. Tonelli for his guidance, support, encouragement and patience during my graduate studies.

I also thank the other members of the advisory committee: Dr. Maurice Balik, Dr. Richard Kotek, Dr. Juan P. Hinestroza, Dr. Bruce M. Novak and Dr. Samuel Hudson for their discussions and directions.

I would like to express my special thanks to Dr. Cristian C. Rusa and Dr. Mariana Rusa for their guidance, help and discussions. They have been an invaluable asset for my studies.

I would like to thank Marcus A. Hunt for his useful discussions and for his assistance in some of the characterization techniques.

I would like to thank our collaborators: Dr. Jale Hacaloglu, Dr. Hanna S. Gracz and Dr. Ahmed El-Shafei for carrying out Pyrolysis Mass Spectroscopy, Nuclear Magnetic Resonance Spectroscopy and Molecular Modeling studies, respectively.

Many thanks Dr. Hanna S. Gracz, Dr. Xingwu Wang and Dr. Daniel Shin for performing NMR experiments and their discussions. They spent many hours including night and weekend hours to get the data and I really appreciated their efforts.

I would like to thank Birgit Anderson (Analytical Lab Manager) for giving me the analytical instrumentation trainings and Carolyn Krystoff (Academic Programs Coordinator) for her assistance and directions with the paperwork during my graduate studies.

I acknowledge Dr. Stephen J. Bilyj and Gerald D. Wicks for their assistance in using gamma radiation source in Nuclear Engineering department.

National Textile Center and NC State University, College of Textile are acknowledged for funding and support.

Finally, I would like to express my very deep gratitude to my family and to my fiancée, Basak Bengu, for their support and love.

# TABLE OF CONTENTS


List of Tables..... viii
List of Figures..... x
1. **Introduction**..... 1
1.1 General Properties of Cyclodextrins..... 1
1.1.1 Solubility of Cyclodextrins..... 4
1.1.2 Structural Characteristics of Cyclodextrins..... 5
1.2 Cyclodextrin Inclusion Complexes..... 6
1.2.1 Preparation of Cyclodextrin Inclusion Complexes..... 7
1.2.2 Industrial Applications of Cyclodextrin Complexes..... 9
1.2.3 Inclusion Complexes of Small Molecules with Cyclodextrins..... 16
1.2.4 Inclusion Complexes of Polymers with Cyclodextrins..... 17
1.2.5 Structural Characteristics of Cyclodextrin Inclusion Complexes..... 21
1.2.6 Characterization of Cyclodextrin Inclusion Complexes..... 24
1.2.7 Thermodynamics of Cyclodextrins Complexation..... 29
1.2.8 Proposed Models for Polymer-Cyclodextrin Inclusion Phenomena..... 35
1.2.9 Parameters Affecting the Formation of Polymer-Cyclodextrin Inclusion Complexes..... 38
1.2.10 Characteristics of Polymers Included In the Channels of Their CD-ICs..... 44
1.3 Coalescence of Polymers from Their Cyclodextrin Inclusion Compounds..... 50
1.3.1 Concept of Coalescence..... 50
1.3.2 Characteristics of Polymers Coalesced from Their CD ICs..... 50
1.3.3 Polymer Blends Coalesced From Their Common CD-ICs..... 55
1.3.4 Polymerization in the Presence of Cyclodextrins..... 60
1.4 Modeling of Polystyrenes in Channels..... 66
1.5 Motivation..... 68
1.5.1 Reorganization and Improvement of Bulk Polymers by Processing with Their Cyclodextrin Inclusion Compounds..... 68
1.5.2 Intimate Blending of Polymer Systems from Their Common Cyclodextrin Inclusion Compounds..... 69
1.5.3 Inclusion of Monomers in the CD Channels and Their Polymerization..... 70
1.6 References..... 71
2 **Reorganization and Improvement of Bulk Polymers by Processing with Their Cyclodextrin Inclusion Compounds**..... 83
2.1 Summary..... 83
2.2 Introduction..... 84
2.3 Experimental..... 85
2.3.1 Materials..... 85
2.3.2 Formation of Polymer- $\gamma$-CD Inclusion Compounds..... 86

2.3.3 Coalescence of PC, PMMA and PVAc from Their CD-ICs ..... 88
2.4 Characterization ..... 89
2.4.1 Wide-Angle X-ray Diffraction (WAXD) ..... 89
2.4.2 Fourier Transform Infrared Spectroscopy (FT-IR) ..... 89
2.4.3 Modulated Differential Scanning Calorimetry (M-DSC) ..... 89
2.4.4 Thermogravimetric Analysis (TGA) ..... 90
2.4.5 Direct Insertion Probe Pyrolysis Mass Spectrometry (DIP-MS): ..... 90
2.5 Results and Discussion ..... 90
2.5.1 Wide-Angle X-ray Diffraction (WAXD) ..... 90
2.5.2 Fourier Transform Infrared Spectroscopy (FT-IR) ..... 93
2.5.3 Differential Scanning Calorimetry (DSC) ..... 99
2.5.4 Thermogravimetric Analysis (TGA) ..... 103
2.5.5 Direct Insertion Probe Pyrolysis Mass Spectrometry (DIP-MS) ..... 106
2.6 Conclusions ..... 117
2.7 References: ..... 118
3 **Intimate Blending of Polymer Systems from Their Common Cyclodextrin Inclusion Compounds** ..... 121
3.1 Binary Polymer Systems: Polycarbonate/Poly(methyl methacrylate), Polycarbonate/Poly(vinyl acetate) and Poly(methyl methacrylate)/ Poly(vinyl acetate) ..... 121
3.1.1 Summary ..... 121
3.1.2 Introduction ..... 122
3.1.3 Experimental ..... 129
3.1.4 Characterization ..... 132
3.1.5 Result and Discussion ..... 133
3.1.6 Conclusions ..... 162
3.2 An Intimate Polycarbonate/Poly(methyl methacrylate)/Poly(vinyl acetate) Ternary Blend *via* Coalescence from Their Common γ-Cyclodextrin Inclusion Compound ..... 163
3.2.1 Summary ..... 163
3.2.2 Experimental ..... 164
3.2.3 Results and Discussion ..... 167
3.2.4 Conclusion ..... 181
3.2.5 References ..... 182
4 **Crystalline Cyclodextrin Inclusion Complexes with Aromatic Molecules** ..... 186
4.1 The Solid Channel Structure Inclusion Complex Formed Between Guest Styrene and Host γ-Cyclodextrin ..... 186
4.1.1 Summary ..... 186
4.1.2 Introduction ..... 187
4.1.3 Experimental Section ..... 189
4.1.4 Results and Discussion ..... 193
4.1.5 Conclusions ..... 212
4.2 Crystalline Cyclodextrin Inclusion Compounds Formed with Aromatic Guests: Guest-Dependent Stoichiometries and Hydration-Sensitive Crystal Structures ..... 213

4.2.1 Summary ..... 213
4.2.2 Introduction ..... 214
4.2.3 Experimental ..... 214
4.2.4 Characterization ..... 217
4.2.5 Results and Discussion ..... 219
4.2.6 Conclusions ..... 238
5 **Polymerization of Styrene in Cyclodextrin Channels: Can Confined Free Radical Polymerization Yield Stereoregular Polystyrene?** ..... 243
5.1 Summary ..... 243
5.2 Molecular Modeling of γ-CD/PS Complexation ..... 244
5.3 Experimental ..... 245
5.3.1 Formation of Styrene/Cyclodextrin Inclusion Compounds ..... 245
5.3.2 Stability of Styrene/γ-$CD_{channel}$ IC in Aqueous Medium ..... 249
5.3.3 Polymerization of Styrene/γ-$CD_{channel}$ IC ..... 250
5.3.4 Characterization of Polystyrene Obtained from Polymerization of Styrene-γ-Cyclodextrin Inclusion Compound ..... 252
5.4 References ..... 257
6. **Conclusions and Future Directions of the Research** ..... 258
7. **Appendix** ..... 260
7.1 List of Publications ..... 260

# LIST OF TABLES

## CHAPTER 1


**Table 1.** General properties of cyclodextrins 4

**Table 2.** Selected market products containing Cyclodextrins 10

**Table 3.** US companies with issued US Patents on cyclodextrin based inventions & applications by October 2004. 11

**Table 4.** Inclusion complex formation between CD and PEG terminated with various small end groups. 19

**Table 5.** List of monomers polymerized in the presence of methylated β-CD in water. 62

**Table 6.** Overview of the Reaction Parameters and Results of the Polymerization of Styrene under Semicontinuous Conditions in the Presence of Different Amounts of Randomly Methylated *β*-Cyclodextrin (RAMEB) (2 h at 80 °C, Then 1 h at 85 °C) 63

**Table 7.** Overview of the Reaction Parameters and Results of the Polymerization of MMA (1a) and Styrene (2a) in the Presence of Different Amounts of Randomly Methylated *β*-Cyclodextrin (RAMEB). 64

**Table 8.** Polystyrene Stereoisomer Channel Conformations 67


## CHAPTER 2


**Table 1.** The relative intensities and the assignments of characteristic and intense peaks in the pyrolysis mass spectra of as-received, and coalesced PVAc and the physical mixture of PVAc and γ-CD at temperatures corresponding to maxima in the TIC curves. 109

**Table 2.** The relative intensities and assignments of characteristic and intense peaks in the pyrolysis mass spectra of as-received and coalesced PMMA at temperatures corresponding to maxima in the TIC curves. 113

## CHAPTER 3


**Table 1.** $T_{1\rho}(^1H)$ of binary (PC/PMMA) blend (ms) 146

**Table 2.** $T_{1\rho}(^1H)$ of binary (PMMA/PVAc) blend (ms) 146

**Table 3.** The relative intensities and assignments of characteristic and intense peaks in the pyrolysis mass spectra of physical and coalesced PMMA/PVAc blends at temperatures corresponding to maxima in the TIC curves. 157

**Table 4.** The relative intensity ratios of some selected peaks in the pyrolysis mass spectra of PVAc, c-PVAc, PMMA, c-PMMA, and their coalesced and physical blends, which correspond to maxima in their TIC curves. 161

**Table 5.** $T_{1\rho}(^1H)$ of Ternary PC/PMMA/PVAc Blends (ms) 177


## CHAPTER 4


**Table 1.** Energy of host, guest and complex, and energy of stabilization upon complexation, computed using PM3 parameters. 206

**Table 2.** Stabilization energies of ICs formed from γ-CD channel structure and different number of styrene molecules in different orientation. 210

**Table 3.** Crystallographic characteristics of $\gamma$-$CD_{channel}$ and styrene/$\gamma$-$CD_{channel}$ IC. 228

**Table 4.** Crystallographic characteristics of hexagonal styrene/$\gamma$-$CD_{channel}$ IC crystal structure. 230


## CHAPTER 5


**Table 1.** An overview of PS polymerization parameters and results 251

# LIST OF FIGURES

## CHAPTER 1


**Figure 1**. The chemical structure of γ-cyclodextrin. 2

**Figure 2**. The truncated cone structure of cyclodextrin. 2

**Figure 3.** Approximate dimensions of α-CD, β-CD and γ-CD. 3

**Figure 4.** A 3-D view of the "collapsed cylinder" structure of δ-CD. 3

**Figure 5.** Molecular lipophilicity patterns (MLP's) projected onto the solid state structure derived contact surfaces of the non-complexed forms of α- (upper left) , β- (upper right) , γ- (lower left) , and δ-CD (lower right, respectively) . Blue colors indicate the most hydrophilic surface regions, while oily yellow-brown colors designate the most hydrophobic surface areas in all cases. 6

**Figure 6**. α-Cyclodextrin-Nitromethane Inclusion Complex. 7

**Figure 7.** Schematic representation of the production of a CD-drug complex. 13

**Figure 8.** The solubility of nimesulide and nimesulide/β-cyclodextrin complex. 13

**Figure 9.** Illustration of an inclusion compound formed on the fabric's surface. 15

**Figure 10.** Guest exchange, for example, perfume release and sweat component entrapment. a) Loading the fixed cyclodextrin with perfume molecule. b) During wearing,sweat humidity excrets short chain fatty acids which displace and release the perfume molecules and in turn become entrapped. 15

**Figure 11**. Chemical structures of dye molecule (left) and it's Inclusion Compound with γ-Cyclodextrin (right) Two of the dye molecules fit into the γ-CD cavity and three γ-CD units are required to fully encapsulate the dye molecule. 16

**Figure 12**. Number of publications related to cyclodextrins between 1980 and 2004 (data of 2004 is incomplete). 17

**Figure 13**. 3-D representation of γ-Cyclodextrin-PDMS Inclusion Complex. 18

**Figure 14.** a.) Time course for the turbidity development after mixing the α-CD solution and the PEG solution, b.) Yields of the complexes of a-CD with PEG as a function of the molecular weight of PEG. 20

**Figure 15**. Crystalline structure of CDs a.) cage, b.) layer and c.) channel. 22

**Figure 16.** Schematic representation of the packing of CD molecules within their crystal lattices: (a) head-to-head:tail-to-tail and (b) head-to-head:tail-to-head:tail-to-tail channel structures. 23

**Figure 17.** WAXD pattern of as-received γ-CD and PMMA-γ-CD IC. 25

**Figure 18.** 1H-NMR spectrum of styrene/methylated-β-CD complex in $D_2O$ (green spectrum) in comparison to uncomplexed m-β-CD (blue spectrum). 26

**Figure 19.** $^{13}$C-CP/MAS NMR spectra of (a) DM-β-CD and (b) polythiophene polymerized with $FeCl_3$ initiator in water from DM-*β*-CD-2T inclusion complex. 28

**Figure 20.** The inclusion complexation of β-CD with poly(thiophene-2,5-diyl). 29

**Figure 21.** Changes of UV-vis absorption of the supernatant obtained from the reaction of PTh and β-CD. 29

**Figure 22.** Schematic representation of CD inclusion complex formation: Salicylic acid is the guest molecule; the small circles represent the water molecules. 30

**Figure 23.** The definition of the equilibrium constant for 1:1 complexation. 32

**Figure 24.** Thermodynamic quantities ($\Delta G°$, $\Delta H°$, and $T\Delta S°$ at 298 K) for the complexation of various classes of guests with α-cyclodextrin as a function of the number of methylenes ($N_C$) in the guest molecules: (a) 1-alkanols (O), (b) *sec*-alkanols (▲), (c) 1,2-alkanediols (⊡), (d) α,*ω*-alkanediols (■), (e) alkylammoniums (×), (f) alkylamines (△), (g) alkanoates (●), (h) alkanoic acids (□), (i) alkanedioates (+), (j) alkanedioic acids (◆), (k) alkylureas (♢). Insets are partial enlargements. 34

**Figure 25.** Turbidity plot at λ=400 nm during the formation and precipitation of a PEG-α-CD complex. 36

**Figure 26.** Schematic representation of the threading of α-CDs on a PEG chain. 37

**Figure 27.** Turbidities of PEG-α-CD complexation as a function of temperature. 39

**Figure 28.** Effects of temperature and solvent on the threading of PEG by α-CD. 40

**Figure 29.** Variation of polymer and $H_2O$ $^1$H-NMR peak intensities relative to the intensity of solvent (acetone) peak, as PNAI chains in solution are included by γ-CD. 41

**Figure 30.** Decrease of polymer $^1$H-NMR peak intensity with time as a result of inclusion from polymer solution into channels of suspended γ-$CD_{channel}$ crystals. 42

**Figure 31.** Water release from γ-$CD_{cage}$ crystals and γ-$CD_{channel}$ crystals suspended in acetone and γ-$CD_{cage}$ crystals suspended in $CDCl_3$. 42

**Figure 32.** Decrease of polymer peak intensities with time as a result of inclusion in γ-$CD_{cage}$ or γ-$CD_{channel}$ crystals suspended in PNAI/acetone solutions. PNAI2 (MW= 9,000 g/mol) has a higher molecular weight than PNAI1 (MW= 3,200 g/mol). 43

**Figure 33.** Illustration of extended polymer chains inside the channels of their CD-ICs. 44

**Figure 34.** STM images of the inclusion complex between β-CD and PANi where fields of view are (a) 1200 nm x1200 nm and (b) 350 nm x 350 nm. (c) The height profile of the cross section. 45

**Figure 35**. The STM image of the polymer cyclodextrin inclusion complex (PEG-α-CD) (a) and its schematic representation (b). 46

**Figure 36.** (a) Structure of the "molecular necklace", and three modes (b, c, and d) of the shuttle manipulation by STM. 47

**Figure 37.** STM images of the simple-shuttling of α-CDs along the PEG chain. 47

**Figure 38.** Proposed structures of the PCL-α- and γ-CD-ICs. 49

**Figure 39.** All trans crystalline (Top) and γ-CD-IC included and coalesced kink, $g^{\pm}$ $tg^{\mp}$ (Bottom) PET conformers. 49

**Figure 40.** Schematic representation of polymer-CD IC formation and the coalescence process. 51

**Figure 41.** X-ray diffraction patterns of (a) as-received and (b)coalesced PC, and (c) as-received and (d) coalesced PET. 52

**Figure 42.** X-ray diffraction patterns of (a)coalesced nylon-6 (b) as-received nylon-6. 53

**Figure 43.** Expanded FTIR spectra of (a) as-received and (b) IC coalesced nylon-6. 54

**Figure 44.** The DSC cooling curves of coalesced and as-received isotactic-PP. 55

**Figure 45.** Formation of intimate polymer blends by coalescence of common polymer-CD Inclusion compounds. 56

**Figure 46.** The second heating DSC scans of (a) coalesced PC, (b) coalesced PC/PMMA blend (PC:PMMA = 4:1 molar ratio), (c) coalesced PC/PMMA blend (PC:PMMA = 1:1 molar ratio), (d) coalesced PC/PMMA blend ( PC:PMMA = 1:4 molar ratio), and (e) coalesced PMMA. 57

**Figure 47.** Polarized photomicrographs of (a) PLLA, (b) PCL, (c) solution-cast, and (d) coalesced PLLA/PCL blends. 58

**Figure 48.** $^{1}$H-NMR spectra of (a) precipitated PET/PEN and (b) coalesced PET/PEN blend. 59

**Figure 49.** Schematic presentation of complexation and polymerization of cyclodextrin complexed monomers. 61

**Figure 50.** SEM image of PS particles: (a) 0 wt % cyclodextrin, broad PSD; (b) 5.6 wt % cyclodextrin, narrow PSD; (c) 11.1 wt % cyclodextrin, narrow PSD. 63

**Figure 51.** Crystal structure of $\beta$-CD-bithiophene inclusion complex. Carbon and oxygen of $\beta$-CD are shown in gray and red, respectively. Carbon and sulfur of bithiophene are shown in blue and yellow, respectively. 65

**Figure 52.** Polythiophene prepared from the DM-$\beta$-CD-2T inclusion complex polymerized with $FeCl_3$ initiator in water. 65

**Figure 53.** PS tetrad fragment (mmm = dddd) used in the search for channel conformers. 67

## CHAPTER 2


**Figure 1.** (a) γ-CD chemical structure; (b) approximate dimensions of α-CD, β-CD and γ-CD; schematic representation of packing structures of (c) cage-type and (d) head-to-tail channel-type CD crystals; (f) cyclodextrin-inclusion compound (CD-IC) channels with included polymer guests. 84

**Figure 2.** Schematic representation of polymer-CD IC formation, the coalescing process and the coalesced polymer. 87

**Figure 3.** X-ray diffraction patterns of (a) as-received γ-CD, (b) γ-CD channel structure, (c) vacuum-dried γ-CD channel structure, and (d) vacuum-dried PMMA-γ-CD IC. 91

**Figure 4.** X-ray diffraction patterns of (a) PC-γ-CD IC, (b) PMMA-γ-CD-IC and (c) PVAc-γ-CD-IC. 93

**Figure 5.** FT-IR spectra of (a) as received γ-CD, (b) PMMA-, (c) PC-, and (d) PVAc-γ-CD-ICs. 94

**Figure 6.** FT-IR spectra of as-received (a) PMMA, (b) PVAc, and (c) PC. 95

**Figure 7.** FT-IR spectra of coalesced (a) PMMA, (b) PVAc, and (c) PC. 95

**Figure 8.** FT-IR spectra of (a) as-received PMMA and (b) coalesced PMMA. 97

**Figure 9.** FT-IR spectra of (a) as-received PC and (b) coalesced PC. 99

**Figure 10.** Modulated DSC thermograms of (a) first heating scan of coalesced PC (b) second heating scan of coalesced PC, (c) first heating scan of precipitated PC (d) second heating scan of precipitated PC, (e) first heating scan of as-received PC (f) second heating scan of as-received PC. 100

**Figure 11.** X-ray diffraction patterns of (a) coalesced PC, (b) precipitated PC and (c) as-received PC. 101

**Figure 12.** Modulated DSC thermograms of (a) second heating scan of coalesced PMMA (b) second heating scan of as-received PMMA. 102

**Figure 13.** DSC thermograms of (a) second heating scan of coalesced PVAc (b) second heating scan of as-received PVAc. 103

**Figure 14.** TGA thermograms of as-received γ-cyclodextrin. 104

**Figure 15.** TGA thermograms of (a) coalesced PMMA, (b) as-received PMMA, (c) coalesced PVAc (d), as-received PVAc (e), coalesced PC (f), and as-received PC. 105

**Figure 16.** TIC curves and pyrolysis mass spectra recorded at the maximum of the peaks and shoulders in the TIC curves of a.) as-received γ-CD, b.) i. as-received PVAc, ii. coalesced PVAc, c.) i. as-received PMMA, ii. coalesced PMMA, d.) i. as-received PC ii. coalesced PC. 107

**Figure 17.** Evolution profiles of some characteristic products recorded during the pyrolysis of γ-CD. 108

**Figure 18.** Evolution profiles of some characteristic products recorded during the pyrolysis of a) as-received PVAc, b) coalesced PVAc, and c) γ-CD/PVAc physical mixture. 111

**Figure 19.** Evolution profiles of some characteristic products recorded during the pyrolysis of a) as-received PMMA, and b) coalesced PMMA. 114

**Figure 20.** Evolution profiles of $CO_2$ (m/z= 44 Da) , $C_3H_5O_2$ (m/z=73 Da), $C_6H_5$-O-COO-$C_6H_4$ (m/z=213 Da) and $C_6H_5$-$C(CH_3)_2$-$C_6H_4$-O-$C_6H_4$-$C(CH_3)_2$-$C_6H_4$ (m/z=405 Da) recorded during pyrolysis of a.) as-received PC, b.) Coalesced PC, c.) PC-γ-CD-IC and d.) as-received γ-CD. 116

## CHAPTER 3

**Figure 1.** Schematic representation of polymer-CD IC formation, the coalescence process and the coalesced polymer. 130

**Figure 2.** X-ray diffraction patterns of vacuum-dried crystals (a) γ-CD channel, (b) PC/PMMA-γ-CD-IC, (c) PC/PVAc-γ-CD-IC, and (d) PMMA/PVAc-γ-CD-IC. 134

**Figure 3.** $^1$H-NMR spectra of coalesced (a) PC/PMMA, (b) PC/PVAc and (c) PMMA/PVAc binary blends. 136

**Figure 4.** FT-IR spectra of (a) as received γ-CD, (b) PC/PMMA-γ-CD-IC, (c) PC/PVAc γ-CD-IC, and (d) PMMA/PVAc-γ-CD-IC. 137

**Figure 5.** FT-IR spectra of co-precipitated polymer blends (a) PC/PMMA, (b) PC/PVAc and (c) PMMA/PVAc. 139

**Figure 6.** FT-IR spectra of coalesced polymer blends: (a) PC/PMMA, (b) PC/PVAc, and (c) PMMA/PVAc. 139

**Figure 7.** DSC thermograms of (a) first heating scan and (b) second heating scan of coalesced PC/PMMA blend and (c) first heating scan of co-precipitated PC/PMMA blend. 141

**Figure 8.** DSC thermograms of (a) first heating scan and (b) second heating scan of coalesced PC/PVAc blend and (c) first heating scan of co-precipitated PC/PVAc blend. 143

**Figure 9.** DSC thermograms of (a) first heating scan (b) and second heating scan of co-precipitated PMMA/PVAc blend and (c) second heating scan of coalesced PMMA/PVAc blend. 144

**Figure 10.** TGA thermograms of (a) coalesced and (b) co-precipitated PC/PMMA blends; (c) coalesced and (d) co-precipitated PC/PVAc blends; and (e) coalesced and (f) co-precipitated PMMA/PVAc blends. 147

**Figure 11.** TIC curves (left) and pyrolysis mass spectra (right) recorded at the maximum of the peaks and shoulders in the TIC curves of a) PC/PMMA physical mixture, b) coalesced PC/PMMA, c) PC/PVAc physical mixture d) coalesced PC/PVAc, e) PMMA/PVAc physical mixture, and f) coalesced PMMA/ PVAc blends. 150

**Figure 12.** Evolution profiles of $C_6H_5$-$C(CH_3)_2$-$C_6H_4$-O-$C_6H_4$-$C(CH_3)_2$-$C_6H_4$ (m/z=405Da), $C_6H_5$-O-COO-$C_6H_4$ (m/z=213 Da), MMA (m/z=100Da), $CH_2C(CH_3)CO$ (m/z=69Da), $CH_2CCH_3$ (m/z= 41Da) , and $C_2H_4O_2$ (m/z=60Da), recorded during the pyrolysis of a) physical b) coalseced PC/PMMA blends. 152

**Figure 13.** Evolution profiles of $C_6H_5$-$C(CH_3)_2$-$C_6H_4$-O-$C_6H_4$-$C(CH_3)_2$-$C_6H_4$ (m/z=405Da), $C_6H_5$-O-COO-$C_6H_4$ (m/z=213 Da), $C_2H_4O_2$ (m/z=60Da), $C_2H_3O$ (m/z=43 Da), and $C_7H_7$ (m/z= 91Da) recorded during the pyrolysis of a) physical and b)coalseced PC/PVAc blends. 155

**Figure 14.** TIC curves (left) and pyrolysis mass spectra (right) recorded at the maximum of the peaks and shoulders in the TIC curves of a) $\gamma$-CD, b)as-received PVAc, c) coalesced PVAc, d)as-received-PMMA, e) coalesced PMMA, f) PMMA/PVAc physical mixture, and g) coalesced PMMA/ PVAc blend. 156

**Figure 15.** Evolution profiles of some characteristic products recorded during the pyrolysis of a) PMMA/PVAc physical mixture and b) coalesced PMMA/ PVAc blend. 158

**Figure 16.** $^{1}$H-NMR spectra of coalesced PC/PMMA/PVAc-1 ternary blend. 168

**Figure 17.** FT-IR spectra of a.) as-received γ-CD b.) PC/PMMA/PVAc-γ-CD IC. 170

**Figure 18.** FT-IR spectra of coalesced-1 (a), -2 (b), and co-precipitated PC/PMMA/PVAc ternary blends (c). 172

**Figure 19.** DSC thermograms of the coalesced PC/PMMA/PVAc-1 blend, first heating scan (a) and second heating scan (b); co-precipitated PC/PMMA/PVAc blend, first heating scan (c). Annealing time between first and second heating scans of the coalesced blend is 1 min. 173

**Figure 20.** MDSC scans of the first (a), and second (b) heating runs recorded for the PC/PMMA/PVAc-2 blend. The sample was held 3 min at 170° C after the first heating. 175

**Figure 21.** TGA thermograms of (a) coalesced (-1), (b) precipitated, and (c) coalesced (-2) PC/PMMA/PVAc blends. 180

## CHAPTER 4

**Figure 1.** (a) γ-CD chemical structure; (b) approximate dimensions of α-, β- and γ-CDs; schematic representation of packing structures of (c) cage-type and (d) head-to-head:tail-to-head:tail-to-tail channel-type γ-CD crystals. 188

**Figure 2.** DSC scans of a.) styrene/γ-CD-IC b.) physical mixture of styrene and γ-CD. 194

**Figure 3.** CP/MAS $^{13}$C-NMR of a.) physical mixture of styrene and γ-CD and b.) styrene/γ-$CD_{channel}$-IC, and c.) single pulse $^{13}$C-NMR of styrene/γ-$CD_{channel}$-IC. 196

**Figure 4.** **(i)** TGA thermograms of a.) as-received γ-CD, b.), styrene/γ-CD-IC, and c.) physical mixture of styrene and γ-CD. **(ii)** Isothermal TGA thermograms of styrene/γ-CD-IC, a.) 180, b.) 200, c.) 220, and d.) $265^{0}$ C. All samples were rapidly heated ($200^{0}$ C/min.) to reach these constant target temperatures. 198

**Figure 5.** Total ion current (TIC) curves and pyrolysis mass spectra recorded at the maximum of the peaks and shoulders in the TIC curves of a.) styrene/γ-CD-IC and b.) the physical mixture of styrene and γ-CD. 201

**Figure 6.** Evolution profiles of $C_2H_4O_2$ (m/z= 60 Da), $C_3H_5O_2$ (m/z=73Da), $C_6H_6$ (m/z=78 Da), $C_8H_8$ (m/z=104 Da), and $H_2O$ (m/z= 18 Da) in a.) styrene/γ-CD-IC and b.) the physical mixture of styrene and γ-CD. 202

**Figure 7.** **(i)** Predicted absorption spectrum ($\lambda_{max}$= 353.9 nm) of two parallel and overlapping styrene molecules at an intermolecular distance (2.55 Å). **(ii)** Two views of the MO orbitals responsible for the electronic transition at 353.9nm, superimposed on two locked styrene molecules: a) two overlapped styrene molecules parallel to the plane of the paper, b) two styrene molecules perpendicular to the plane of the paper. 204

**Figure 8.** **(i)** UV-Vis absorbance spectrum of styrene in methanol. **(ii)** Solid-state UV-Vis spectrum of styrene/γ-CD-IC. 205

**Figure 9.** (i) Optimized geometry of host (a), guest (b), and IC (c) containing one styrene molecule using semi-empirical PM3 parameters and the MOZYME algorithm. (ii) Optimized geometry of two styrene molecules initially set at a.) 2.55 and b.) 3.3 Å. (iii) Starting a.) and optimized geometry b.) of γ-CD-IC containing two overlapped, parallel styrene molecules. (iv) Starting (a) and optimized geometry (b) of IC containing two styrene molecules. (v) Optimized geometry of non-overlapped styrenes (a) and two views (b and c) of the optimized IC containing two styrene molecules with no overlap and no π-π interactions. 208

**Figure 10.** (a)Equilibrium molecular geometry of γ-CD channel structure. (b) Equilibrium molecular geometry of the IC of γ-CD channel structure and 6-styrene molecules inside. The starting intermolecular distance was 3.3 A. Following geometry optimization, it was 4.3 Å. (c) Equilibrium molecular geometry of the IC of γ-CD channel structure and 6-styrene molecules. The starting intermolecular distance was 2.55 Å. Following geometry optimization, it was 4.0 Å. (d) Equilibrium molecular geometry of the IC of γ-CD channel structure and 4-styrene molecules next to each other in a chain-like structure. 211

**Figure 11.** FT-IR spectra of a.) as received γ-CD and b.) aniline/γ-CD IC. The insert window shows the overlay of the expanded region (1800 - 1300 $cm^{-1}$) for i.) aniline/, ii.) styrene/, iii.) ethylbenzene/, iv.) benzene/, v.) toluene/, vi.) p-xylene/, and vii.) phenol/γ-CD ICs. 222

**Figure 12.** TGA thermograms of a.) as-received γ-CD and b.) toluene/, c.) benzene/, d.) styrene/, e.) aniline/, f.) phenol/, g.) ethylbenzene/, and h.) *p*-xylene/γ-CD ICs. 224

**Figure 13.** X-ray diffraction patterns of a.) γ-$CD_{cage}$, b.) γ-$CD_{channel}$, and c.) γ-$CD_{channel}$ vacuum dried for 24 hrs at $40^0$ C. 226

**Figure 14.** X-ray diffraction patterns of a.) α-$CD_{cage}$, b.) styrene/α-$CD_{channel}$ IC. 227

**Figure 15.** X-ray diffraction patterns of a.) styrene/γ-CD IC, b.) styrene/γ-CD IC vacuum dried for 24 hrs at 40 $^0$C and c.) vacuum dried styrene/γ-CD IC stored at 100% humidity for 51 hours. 231

**Figure 16.** Time-dependent X-ray diffraction patterns of vacuum dried styrene/γ-CD IC subsequently stored at 100% humidity. 232

**Figure 17.** Time-dependent x-ray peak area changes for 1,2, and 3 dehydration- hydration cycles of styrene/γ-CD IC: (i) variation of the 2θ = 6.0º (hexagonal) and (ii) 7.5º peak (tetragonal) areas. 233

**Figure 18.** Equilibrium anhydrous weight after vacuum-drying at 40° C (●)and hydrated weight after sorption at 25° C and a = 1.0 (■) of styrene/γ-CD IC as a function of hydration cycle. The difference in anhydrous and dehydrate weights is also plotted(▲). 235

**Figure 19.** Interval sorption and desorption of styrene/γ-CD IC at 40° C. 236

**Figure 20.** X-ray diffraction patterns of a.) aniline/γ-CD IC, b.) aniline/γ-CD IC vacuum dried for 24 hrs at $40^0$ C. and c.) vacuum dried aniline/γ-CD IC stored at 100% humidity for 24 hours. 237

## CHAPTER 5


**Figure 1.** (a) Molecular geometry of a tetrade isotactic PS. (b) isotactic-PS-γ-CD inclusion compound. (c) Molecular geometry of syndiotactic PS. (d) Representation of the collision between the hydrogen atoms of syndiotactic and γ-CD. 245

**Figure 2.** The variation of $^{1}$H-NMR peak intensity of styrene relative to the solvent peak in the suspensions of α-$CD_{cage}$, β-$CD_{cage}$, γ-$CD_{cage,}$ and γ-$CD_{channel.}$ 247

**Figure 3.** Overlay of $^{1}$H-NMR spectra of (a) γ-CD solution in $D_2O$. The addition of styrene in γ-CD aqueous solution after (b) 5 min, (c) 25 min and (d) 60 min. 248

**Figure 4.** FT-IR overlay of (a) □-CD, (b) poystyrene, (c) PS-γ-CD IC obtained by solution polymerization and (d) PS-γ-CD IC obtained by solid-state polymerization. 253

**Figure 5.** TGA overlay of (a) PS-γ-CD IC obtained by solid-state polymerization, (b) γ-CD, (c) poystyrene and (d) derivative weight % loss of PS-γ-CD IC. 253

**Figure 6.** DSC scan of PS-γ-CD IC obtained by solid-state polymerization. 254

**Figure 7.** $^{13}$C-NMR of aromatic C-1 regions of PSs at 120$^{o}$ C. d-dichlorobenzene and mixture of d-dichlorobenzene/d-DMSO were used as solvent for polystyrene and PS-γ-CD IC, respectively: (a) PS synthesized in toluene, AIBN, 24hr, 60$^{o}$ C (b) PS-γ-CD IC obtained by solution polymerization and (c) PS-γ-CD IC obtained by solid-state polymerization. 256

# CHAPTER 1

## LITERATURE REVIEW

### 1. Introduction

### 1.1 General Properties of Cyclodextrins

Cyclodextrins (CDs), small cyclic oligosaccharides are produced from starch by the action of cyclodextrin glycosyltransferase (CGTase), an enzyme produced by several organisms.[1] These cyclic oligosaccharides consist of (α-1,4)-linked α-D-glucopyranose units (Figure 1). Due to the chair conformation of the glucopyranose units, the CDs are shaped like a truncated cone rather than perfect cylinders. The hydroxyl functions are orientated to the cone exterior, with the primary hydroxyl groups of the sugar residues at the narrow edge of the cone and the secondary hydroxyl groups at the wider edge (Figure 2). CDs possess the unique characteristic of having a hydrophobic central cavity and a hydrophilic outer surface. The central cavity is lined by the skeletal carbons and ether oxygens of the glucose residues, which gives it a hydrophobic character.

Cyclodextrins consist of a family of three major, well-known industrially produced, and several rare, minor cyclic oligosaccharides. The three major cyclodextrins are crystalline, homogeneous substances, which are named α-, β- and γ-cyclodextrin and consist of six, seven and eight glucopyranose units, respectively. Although the depth of the cavities for the three CDs is the same (~7.9 Å), their cavity diameters are ~ 5, 7, and 9 Å, respectively, for α-, β- and γ-CD (Figure 3). [2]

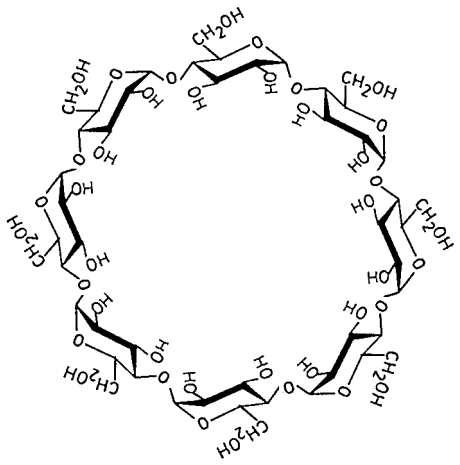

**Figure 1**. The chemical structure of γ-cyclodextrin.

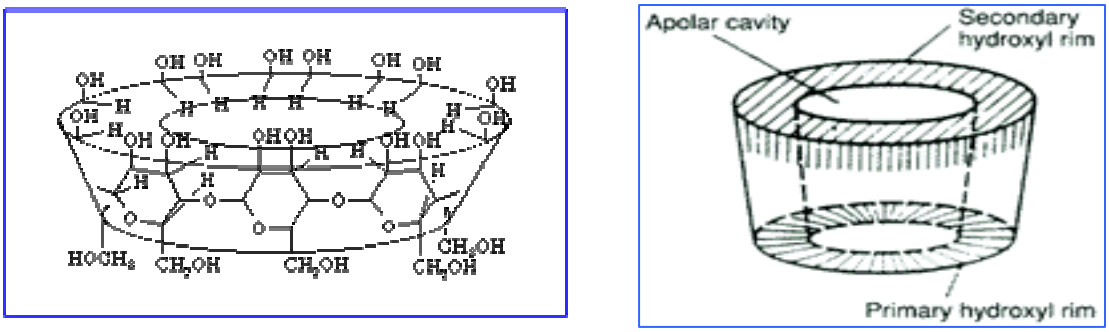


**Figure 2**. The truncated cone structure of cyclodextrin.

In the past decade, a series of larger CDs have also been isolated and studied.[3-6] For example, the nine-membered $\delta$-CD was isolated from the commercially available CD conversion mixture by chromatography. The larger CDs are not regular truncated cone shaped structures. They are collapsed, and their cavity cross sections are even smaller than in $\gamma$-CD (Figure 4). $\delta$-CD is less stable than the three common CDs ; their hydrolysis rates increases in the order α-CD < β-CD < γ-CD < δ-CD.

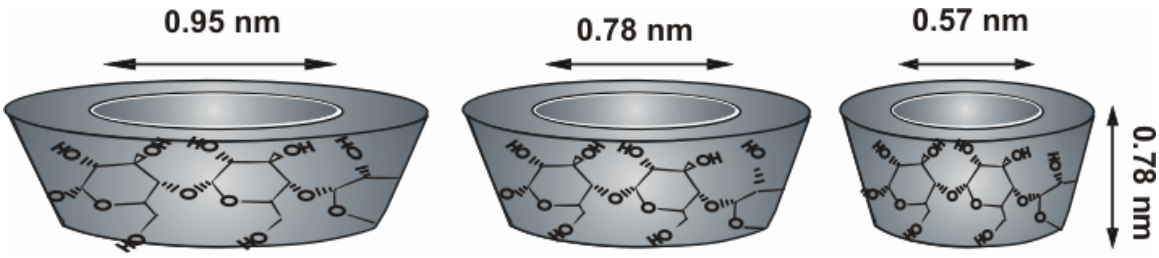


**Figure 3.** Approximate dimensions of α-CD, β-CD and γ-CD.

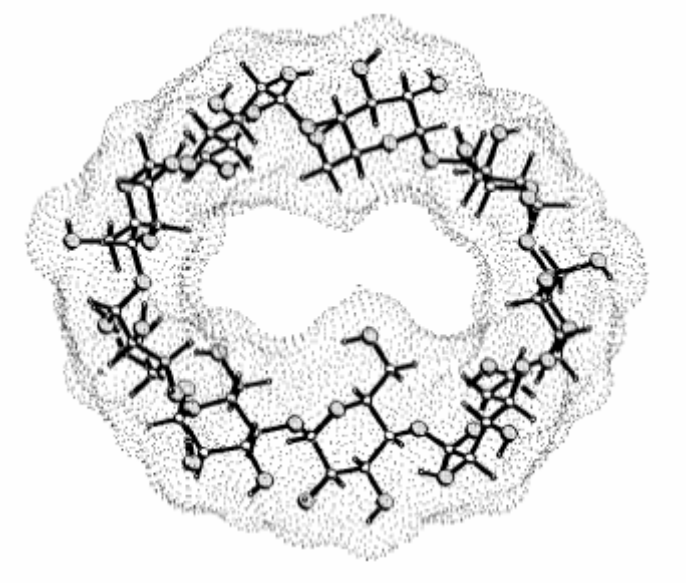

**Figure 4.** A 3-D view of the "collapsed cylinder" structure of δ-CD.[7]

Cyclodextrins (CDs) have some distinctive physical and chemical properties which are listed in Table 1.[8] CDs are stable in alkaline solutions, but they are susceptible to acid hydrolysis. Partial acid hydrolysis of CDs produces glucose and a series of acylic maltosaccharides. The stability of CDs toward acid hydrolysis depends on the temperature and acidity. Under normal experimental conditions (pH higher than 3.5 and temperature below 60 °C), CDs are fairly

stable. They are also resistant to light within the ultraviolet-visible (UV-Vis) and infrared (IR) ranges, and CDs are non-reducing, with glucose the only product of their acid hydrolysis.

**Table 1.** General properties of cyclodextrins.[8]

| Cyclodextrin | α | β | γ |
|---|---|---|---|
| Number of Glucose Unites | 6 | 7 | 8 |
| Molecular Weight (g/mol) | 972 | 1135 | 1297 |
| Inner Diameter (Å) | 4.5-5.7 | 6.2-7.8 | 7.9-9.5 |
| Outer Diameter (Å) | 13.7 | 15.3 | 16.9 |
| Height (Å) | 7.9 | 7.9 | 7.9 |
| Approximate volume cavity ($Å^3$) | 174 | 262 | 427 |
| Solubility in $H_2O$ (g/ml) | 14.5 | 1.85 | 23.2 |
| p*K* (by potentiometry) at 25 °C | 12.33 | 12.2 | 12.08 |
| Crystal water content, wt % | 10.2 | 13.2-14.5 | 8.13-17.7 |
| Hydrolysis by *A. oryzae* α-amylase | negligible | Slow | rapid |

### 1.1.1 Solubility of Cyclodextrins

The aqueous solubility of the CDs is much lower than that of comparable acyclic saccharides which is due to relatively strong intermolecular hydrogen bonding in the crystal state. Substitution of any of the hydrogen bond forming hydroxyl groups results in dramatic improvement in their aqueous solubility.[9] The C-2-OH group of one glucopyranoside unit can form a hydrogen bond with the C-3-OH group of the adjacent glucopyranose unit. In CDs, a complete secondary belt is formed by these hydrogen bonds, therefore β-CD is a rather rigid

structure. β-CD has the lowest water solubility of all CDs and the intramolecular hydrogen bond formation in β-CD is possibly the explanation of its low solubility. The hydrogen-bond belt is incomplete in the α-CD molecule, since one glucopyranose unit is in a distorted position. As a result, instead of the six possible H-bonds, only four can be fully established. γ-CD is a non-coplanar, more flexible structure; therefore, it is the most soluble of the three common CDs. δ-CD has a greater aqueous solubility than β-CD, but less than that of α- or γ-CD.

### 1.1.2 Structural Characteristics of Cyclodextrins

Cyclodextrins are shaped like truncated cones with primary and secondary hydroxyl groups crowning the narrower and wider rims, respectively. They have a distinctive hydrophobic central cavity and a hydrophilic outer surface. Due to the hydrophobic internal cavity, various organic and inorganic molecules of appropriate dimension can be bound inside the cavity to form inclusion complexes.[1] Hydrophobic effects are found to be the major driving force directing the formation of inclusion complexes by cyclodextrins.[10] Immel studied the calculation of molecular lipophilicity patterns (MLP's) of CDs on molecular surfaces and visualized them in color-coded form on solid contact surface models by using the MOLCAD-molecular modeling program.[7] The relative MLP's for the four different non-complexed cyclodextrins are shown in Figure 5, with blue colors as a reminder of water corresponding to hydrophilic surface regions, while oily yellow-brown colors designate the most hydrophobic areas. Due to the accumulation of twice as many secondary hydroxyl groups, the wider rim openings of the cyclodextrins are significantly more hydrophilic. Because of

considerable puckering of the macrocycle and the irregular tilting of the glucose moieties, the separation of hydrophilic and hydrophobic surface areas on the front- and back-side becomes less pronounced for the largest ring homolog, δ-CD.

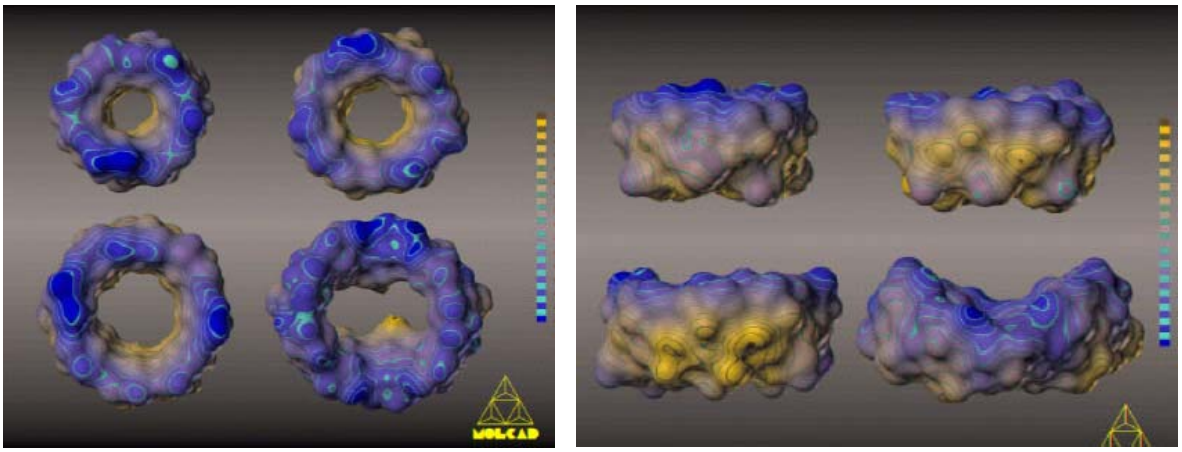

**Figure 5.** Molecular lipophilicity patterns (MLP's) projected onto the solid state structure derived contact surfaces of the non-complexed forms of α- (upper left) , β- (upper right) , γ- (lower left) , and δ-CD (lower right, respectively) . Blue colors indicate the most hydrophilic surface regions, while oily yellow-brown colors designate the most hydrophobic surface areas in all cases.[7]

## 1.2 Cyclodextrin Inclusion Complexes

Due to the chemical structure and doughnut-like molecular shape of α-, β-, γ-CDs, one of their most significant characteristics is the formation of inclusion compounds (ICs) with a variety of guests, where the guest molecules are included in the cavities of the host cyclodextrins molecules.[1] Figure 6 illustrates a cyclodextrin inclusion complex formed with host α-CD and guest nitromethane.[11] Guest molecules can be acids[12], ionic compounds[13], halogen compounds,[14] aliphatic alcohols,[15] aromatic compounds,[16] monomers,[17] dyes,[18] and drug molecules[19] etc., Besides small molecules, polymers[20], including

proeins and polypeptides[21] have also been found to be included as guests in CD cavities.

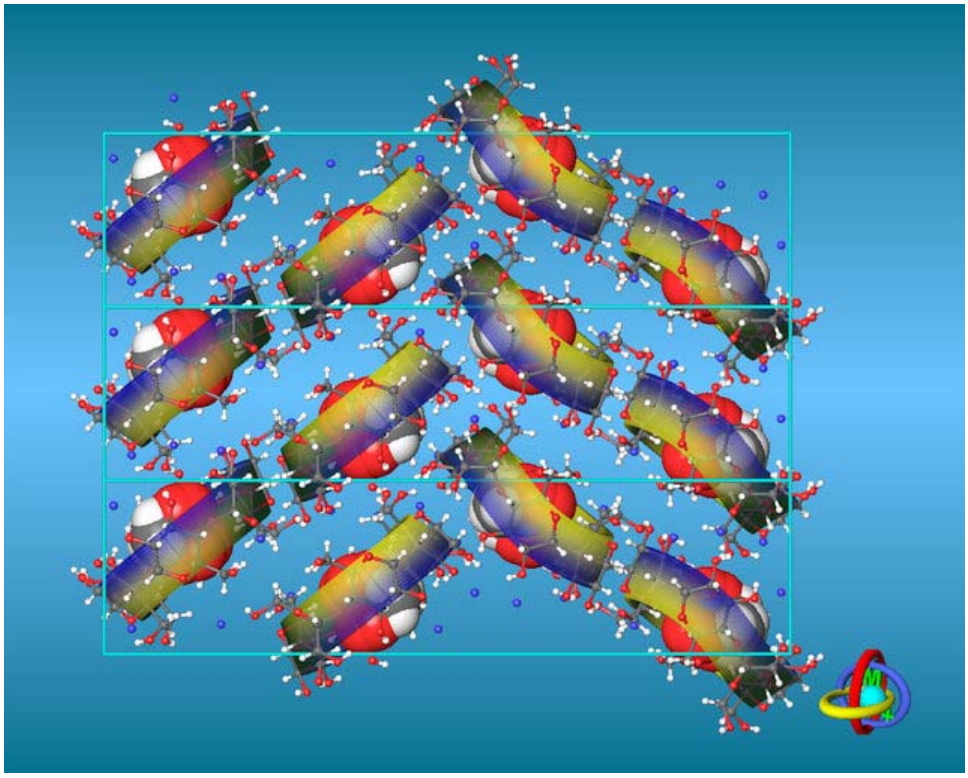

**Figure 6**. α-Cyclodextrin-Nitromethane Inclusion Complex.[11]

### 1.2.1 Preparation of Cyclodextrin Inclusion Complexes

Cyclodextrin inclusion complexation is a molecular phenomenon, where the guest and host cyclodextrin molecules come into contact with each other to associate and form a complex. Cyclodextrin inclusion complexes (CD-ICs) can be easily formed under ambient conditions. The presence of water is very important and plays a key factor in the formation of CD-ICs, because water is usually the medium for dissolution of both the host cyclodextrin and the guest molecules. Moreover, water is a driving force for the hydrophobic interaction of

the guest with the cavity of the cyclodextrin. In some cases, water is required to stabilize the CD-ICs, since water molecules can form a bridge between the hydroxyl groups of adjacent molecules of cyclodextrin to form a cage structure. The most commonly used methods are the co-precipitation, slurry, paste, and dry mixing methods.[22] These methods are very similar to each other except for the quantities of water employed.

#### 1.2.1.1 Co-precipitation Method

In this method, the guest compound is added to an aqueous solution of cyclodextrin, while the solution is being stirring. Conditions are optimized so that the solubility of the complex is exceeded and the complex can then be collected as a precipitate by filtration or centrifugation. This method is widely used in the laboratory, since it demonstrates feasibility of complexation of a particular guest. Small quantities of complex can be obtained for testing the functioning of the complex in applications, and for characterizing the complex to determine the properties of the complex. However, this method is not frequently used for large-scale formation of complexes, because of the large amount of water used, the size of tanks required, and wastewater disposal considerations.

#### 1.2.1.2 Slurry Method

In the slurry method, cyclodextrin is suspended in water up to 50% w/w concentration, because CDs do not have to be completely dissolved to form complexes. As the dissolved portion of the cyclodextrin forms a complex and the complex precipitates, more of the cyclodextrin dissolves and forms additional complex. Heating can be used if desired and is compatible with the physical

requirements of the guest. The complex is generally collected by filtration and dried.

#### 1.2.1.3 Paste Method

A minimum amount of water (20-30% w/w) is used in the paste method. The cyclodextrin, water, and guest are added to a mixing device and mixed. Various mixers, such as an extruder, blade mixer, or other kneading type of mixer, can be used and the mixing time varies with the guest to be complexed, amount of water, and mixing device used. A mixing device providing high shear generally completes the complexation in a shorter amount of time than a low shear mixer. Because of the high viscosity, this method is usually not performed in the laboratory.

#### 1.2.1.4 Dry Mixing Method

In the dry mixing method, the cyclodextrin is mixed with the guest with no added water. This is generally not an efficient method of making complexes since mixing times can range from hours to days. In some cases, the guest might also be serving as a solvent for the cyclodextrin, which accelerate the time for complexation.

### 1.2.2 Industrial Applications of Cyclodextrin Complexes

Cyclodextrins have unique characteristic molecular structures and they are capable of forming inclusion complexes with various organic and inorganic compounds by incorporating them as guests into their cavities. Since the physical and chemical properties of incorporated guest compounds can be tailored by

complexation with CDs, inclusion compounds of CDs are used in many applications, such as foods,[23] textiles,[24] cosmetics and home/personal care,[25] chemical, agricultural,[26] but mostly in pharmaceuticals.[27] Some of the selected applications[22] of CDs are given in Table 2. There are also a large number of patents[28] on cyclodextrin based inventions and applications, and some of them are summarized in Table 3, along with the number of patents held as of 2004.

**Table 2.** Selected market products containing Cyclodextrins. [22]

| Drug | Administration route | Trade name | Market |
|---|---|---|---|
| **α-Cyclodextrin** | | | |
| Alprostadil ($PGE_1$) | IV | Prostavastin | Europe, Japan, USA |
| Cefotiam hexetil HCl | Oral | Pansporin T | Japan |
| **β-Cyclodextrin** | | | |
| Benexate HCl | Oral | Ulgut, Lonmiel | Japan |
| Dexamethasone | Dermal | Glymesason | Japan |
| Iodine | Topical | Mena-Gargle | Japan |
| Nicotine | Sublingual | Nicorette | Europe |
| Nimesulide | Oral | Nimedex, Mesulid | Europe |
| Nitroglycerin | Sublingual | Nitropen | Japan |
| Omeprazol | Oral | Omebeta | Europe |
| $PGE_2$ | Sublingual | Prostarmon E | Japan |
| Piroxicam | Oral | Brexin | Europe |
| Tiaprofenic acid | Oral | Surgamyl | Europe |
| **2-Hydroxypropyl-β-cyclodextrin** | | | |
| Cisapride | Rectal | Propulsid | Europe |
| Hydrocortisone | Buccal | Dexocort | Europe |
| Indomethacin | Eye drops | Indocid | Europe |
| Itraconazole | Oral, IV | Sporanox | Europe, USA |
| Mitomycin | IV | Mitozytrex | USA |
| **Randomly methylated β-cyclodextrin** | | | |
| 17β-Estradiol | Nasal spray | Aerodiol | Europe |
| Chloramphenicol | Eye drops | Clorocil | Europe |
| **Sulfobutylether β-cyclodextrin** | | | |
| Voriconazole | IV | Vfend | Europe, USA |
| Ziprasidone maleate | IM | Geodon, Zeldox | Europe, USA |
| **2-Hydroxypropyl-γ-cyclodextrin** | | | |
| Diclofenac sodium | Eye drops | Voltaren | Europe |

**Table 3.** US companies with issued US Patents on cyclodextrin based inventions & applications by October 2004.[28]

| Name of Company | # of Issued US Patents |
|---|---|
| **PHARMACEUTICAL COMPANIES** | |
| Abbott Laboratories | 6 |
| Alcon Laboratories | 7 |
| Alza Corporation | 2 |
| Bausch & Lomb, Inc. | 1 |
| Bristol Myers Squibb | 2 |
| Ciba Geigy Corporation | 6 |
| Ciba Vision | 3 |
| Glaxo Corporation | 4 |
| Hoffmann La Roche | 2 |
| Merck & Co. Inc. | 4 |
| Pfizer Inc. | 6 |
| Sandoz | 2 |
| Smith-Kline Beacham | 2 |
| Sterling Winthrop Inc. | 5 |
| **INDUSTRIAL COMPANIES** | |
| Chevron Research & Technology Co. | 1 |
| Exxon Research & Engineering Co. | 2 |
| General Electric Co. | 9 |
| Hewlett Packard Co. | 1 |
| Rohm & Haas Co. | 7 |
| Sony Corp. | 2 |
| Xerox Corp. | 6 |

| Name of Company | # of Issued US Patents |
|---|---|
| **CONSUMER PRODUCTS COMPANIES** | |
| 3M Co. | 3 |
| Campbell Soup Co. | 1 |
| General Foods Corp. | 1 |
| Gillette Co. | 2 |
| Kimberly-Clark Worldwide Corp. | 38 |
| Lever Brothers Co. | 2 |
| Nabisco Brands, Inc. | 1 |
| Phillip Morris Products, Inc. | 2 |
| Procter & Gamble Co. | 84 |
| **CHEMICAL COMPANIES** | |
| American Cyanimid | 5 |
| Calgon Corp. | 2 |
| Dow Chemical | 3 |
| Eastman Kodak | 3 |
| E.I. DuPont | 5 |
| Monsanto | 2 |
| **COSMETIC COMPANIES** | |
| Andrew Jergens & Co. | 6 |
| Chesebrough Ponds USA Co. | 7 |
| Estee Lauder, Inc. | 1 |
| Helene Curtis, Inc. | 2 |
| L'Oreal | 1 |
| Revlon Consumer Products Corp. | 2 |

#### 1.2.2.1 Food Applications

The application of cyclodextrin inclusion compounds (CD-ICs) formed with food ingredients offers many advantages.[23] Some of them can be summarized as: a.) Protection of active ingredients against oxidation, heat-promoted decomposition, light-induced reactions, loss by volatility, etc. b.) Elimination (or reduction) of undesired tastes/odors, microbiological contamination, fibers/other undesired components, hygroscopicity, etc. c.) Technological advantages typically include stabilization of flavors and spices, standardizable compositions, simple dosing and handling of dry powders, and reduced packing and storage costs.

#### 1.2.2.2 Pharmaceutical Applications

Cyclodextrins increase the water solubility of poorly soluble drugs to improve their bioavailability.[27] The bioavailability of a poorly soluble drug will be improved by CD complexation, because; it will be dissolved faster, it will attain a higher solubility , it will be absorbed faster and the time between administration and onset of biological effect (e.g. pain-reduction) will be shorter. Figures 7 and 8 show the schematic preparation of CD-drug complexes and the solubility enhancement of nimesulide with β-cyclodextrin complexation, respectively. Additionally, light, thermal and oxidative stability of drug molecules can be improved through the formation of cyclodextrin complexes.

Cyclodextrins have also been used to reduce dermal, gastrointestinal or ocular irritation, mask unpleasant tastes or odors, prevent adverse drug-ingredient interactions and convert oils/liquids into powders to improve handling.

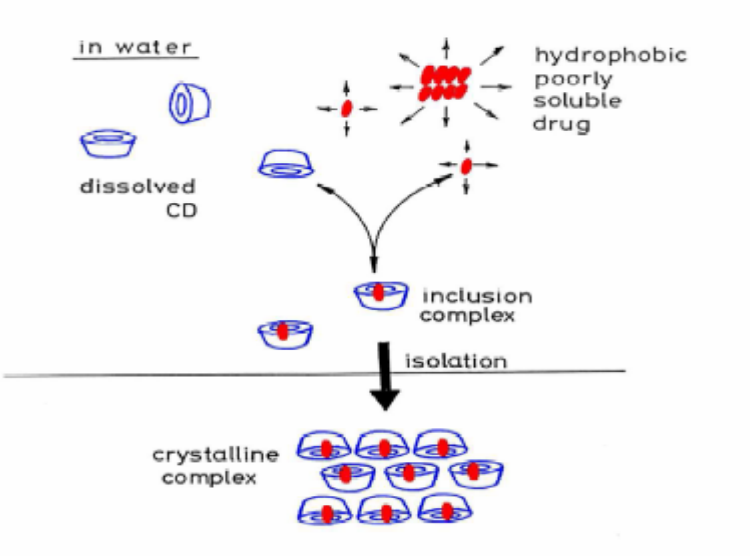


**Figure 7.** Schematic representation of the production of a CD-drug complex.[27a]

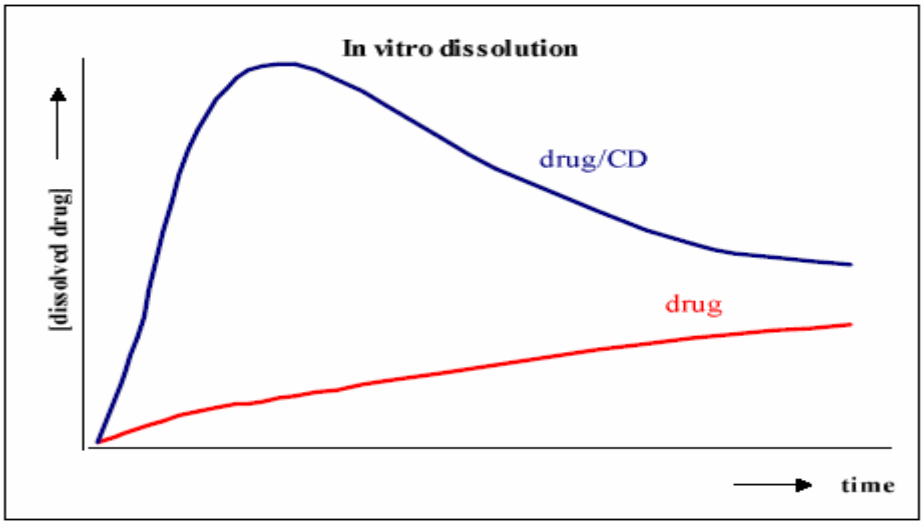


**Figure 8.** The solubility of nimesulide and nimesulide/β-cyclodextrin complex

#### 1.2.2.3 Textile Applications

Cyclodextrins plays a significant role in the textile industry[24] and are being used for: (1) to remove surfactants from washed textiles; (2) to substitute surfactants in textiles finishing; (3) to improve dyeability of fabrics when bound chemically to fibers. They provide enhanced hydrophilicity and they immobilize perfumes, insect repellents, antimicrobial agents, etc.. Figures 9 and 10 schematically illustrate CD covalently attached on the fabric surface[29] and it's function as a perfume releaser and sweat component trapper, respectively.[24a] Cyclodextrins are also very effective in stabilizing dye molecules[30] and enhancing the dyeability of fabrics. Figure 11 shows a CD-Dye inclusion compound.

#### 1.2.2.4 Personal Care, Cosmetics and Toiletries Applications

The main advantages of cyclodextrins in this area are odor control, stabilization, and process improvement upon conversion of a liquid ingredient to a solid form. Applications include sprays, toothpaste, skin creams, liquid and solid fabric softeners, paper towels, tissues and underarm shields.[25]

#### 1.2.2.5 Chemical and Agricultural Applications

In the chemical industry, cyclodextrins are widely used to separate enantiomers[31a] and isomers[31b]. Additionally, CDs are used to catalyse reactions[32] and to remove or detoxify waste materials.[33] Cyclodextrins form complexes and stabilize/increase the solubility of various agricultural chemicals including herbicides, insecticides, fungicides, repellents, pheromones, and growth regulators.[26]

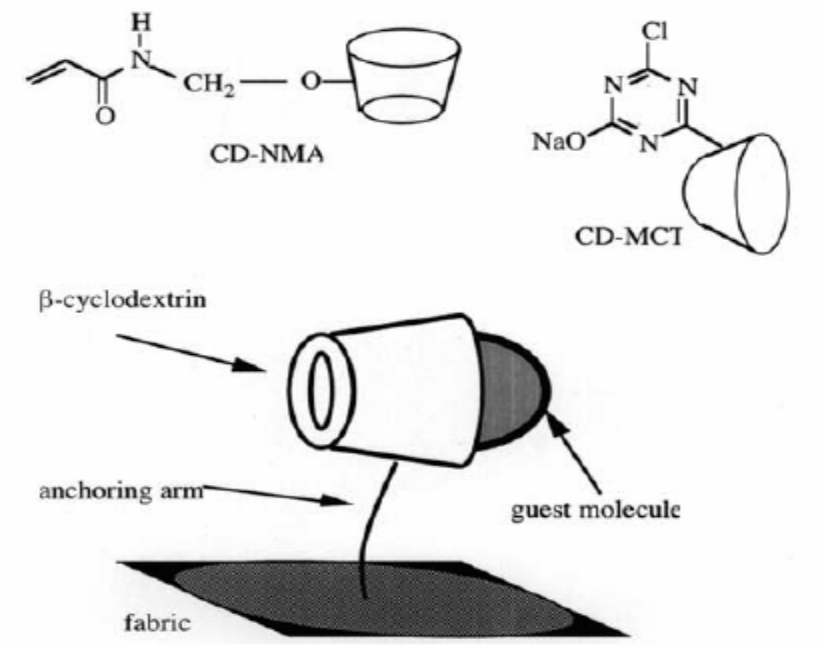


**Figure 9.** Illustration of an inclusion compound formed on the fabric's surface.[29]

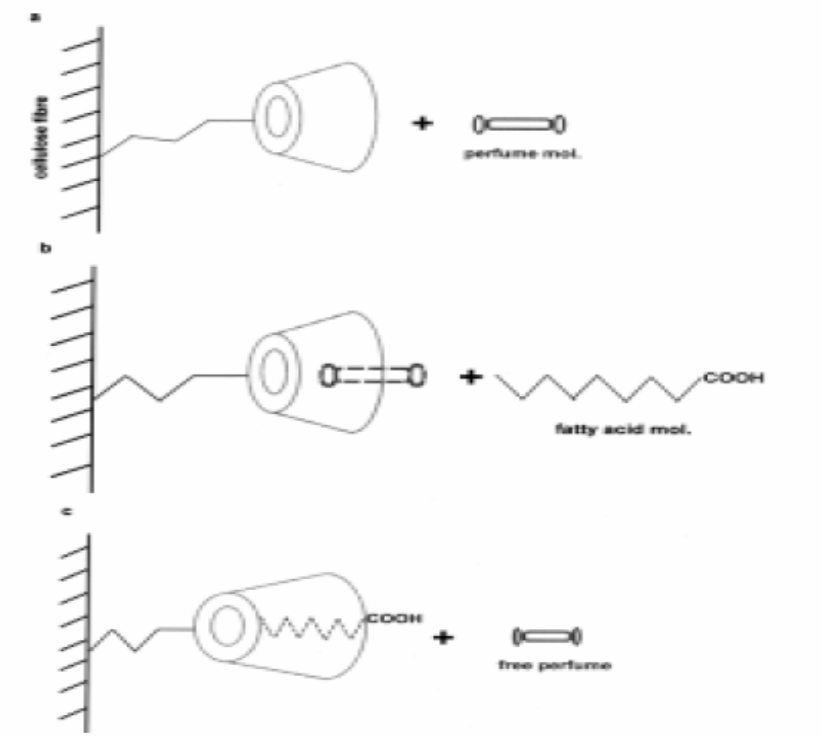


**Figure 10.** Guest exchange, for example, perfume release and sweat component entrapment. a) Loading the fixed cyclodextrin with perfume molecule. b) During wearing,sweat humidity excrets short chain fatty acids which displace and release the perfume molecules and in turn become entrapped.[24a]

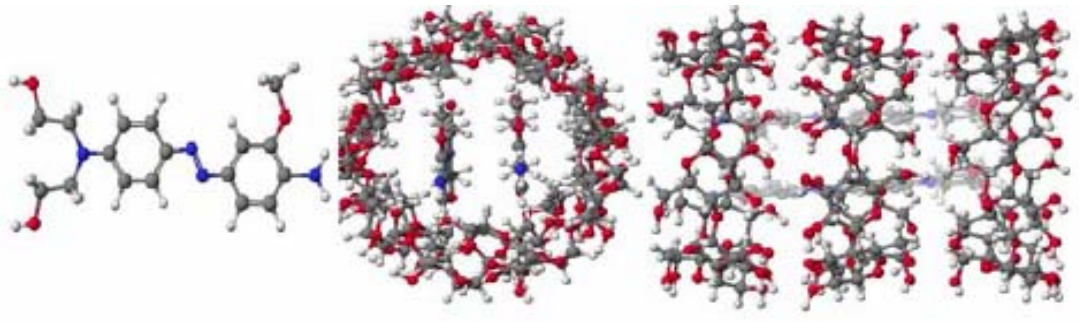

**Figure 11**. Chemical structures of dye molecule (left) and it's Inclusion Compound with γ-Cyclodextrin (right) Two of the dye molecules fit into the γ-CD cavity and three γ-CD units are required to fully encapsulate the dye molecule.[30]

### 1.2.3 Inclusion Complexes of Small Molecules with Cyclodextrins

A massive number of studies related to cyclodextrins and their inclusion compounds have been published in the last two decades (Figure 12). A variety of cyclodextrin inclusion compounds (CD ICs) with small molecules have been formed and characterized. The common parameters found for the inclusion of small molecules are: (a) Stoichoimetry (guest : CD): 1:1, 1:2, 2:1, 2:3, 3:2, (b) Formation rate $T_{1/2}$ ~ 0.001 - 1 ms, (c) Complex stability constants, (d) Size of the molecules suitable for complexation (diameter less than 1 nm) and (e) Solubility in water <10 mg/mL .

Because CD complex are held together purely by noncovalent interactions, they function as excellent models for the study of chiral and molecular recognition mechanisms. Moreover, naturally occurring CDs and their chemically modified derivatives have been widely applied for improving the oral delivery of drugs, in particular for increasing the rate of absorption through an increase in the rate of dissolution. The size of the guest and host molecules also

plays an important role for inclusion complexation and its stability. For instance, the study of the inclusion of naproxen by CDs showed that α-CD forms a 1:2 complex, β-CD and derivatives form 1:1 complexes, and γ-CD forms both 1:1 and 1:2 complexes. The higher stability of the complex with γ-CD was explained in terms of a better inclusion of the naproxen naphthalene ring.[35]

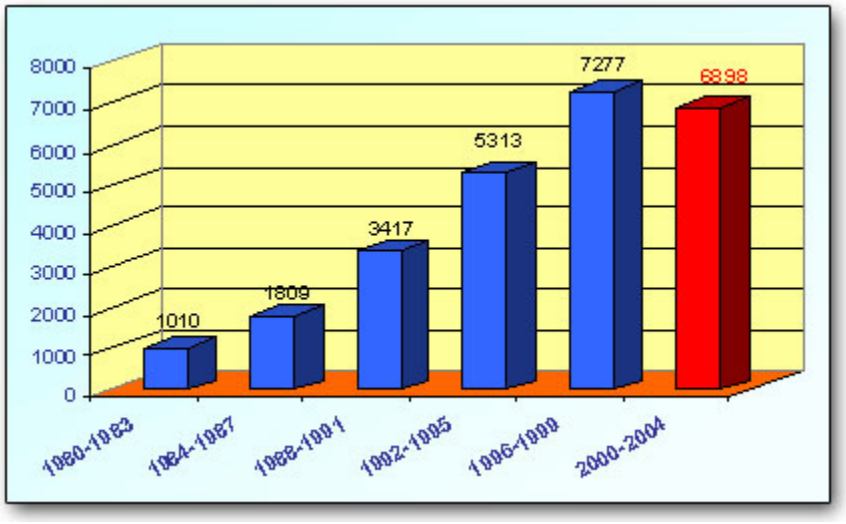


**Figure 12**. Number of publications related to cyclodextrins between 1980 and 2004 (data of 2004 is incomplete).[34]

### 1.2.4 Inclusion Complexes of Polymers with Cyclodextrins

Studies related to polymer-cyclodextrin inclusion compounds (polymer-CD-ICs) (Figure 13) have increased dramatically in the last decade. Harada and Kamachi were the first researchers to report the formation of polymer-CD-ICs in 1990.[36] They found that α-cyclodextrin forms complexes with polyethylene glycol (PEG) of various molecular weights to give stoichiometric complexes in high yields when aqueous solutions of PEG were added to a saturated aqueous

solution of α-CD at room temperature. Prior to their work, there were only a few reports related to the *in situ* polymerization of monomers within a cyclodextrin complex. For instance, Ogata et al.[37], prepared hexamethylenediamene complexed with β-CD and polymerized it to obtain polyamide-CD-ICs. Additionally, Maciejewski reported the polymerization and copolymerization of vinylidene chloride as adducts of β-CD.[38]

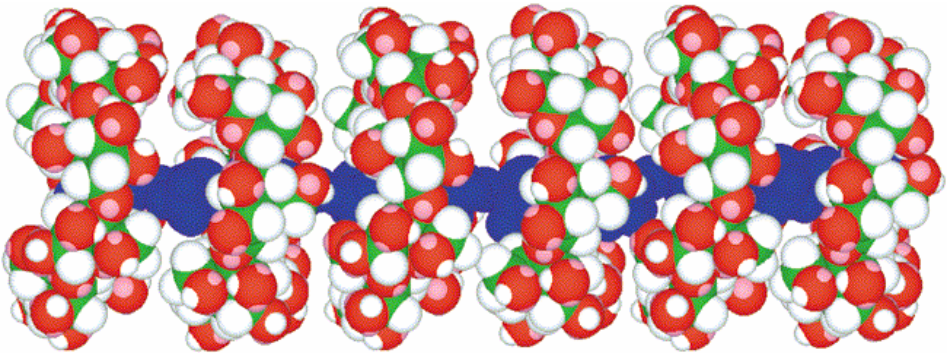

**Figure 13**. 3-D representation of γ-Cyclodextrin-PDMS Inclusion Complex.[39]

The research groups of Harada[40] and Tonelli[41] have carried out extensive investigations on polymer-CD ICs to get a better understanding of the inclusion and confinement of polymer chains in host CD cavities. They prepared inclusion compounds of cyclodextrins with various polymers. These polymers differ in nature: hydrophobic[40-41a] or hydrophilic[40-41b], low molecular weight[40c] or high molecular weight[41a], amorphous[40d,41c] or semi-crystalline[41d], aliphatic[40-41e] or aromatic[41f], biodegradable[40f, 41g], and inorganic polymers[40g, 41h].

Harada and co-workers reported noteworthy findings on PEG-CD ICs.[42] They observed that α-CD forms ICs with PEG in a ratio of 2:1 (monomer unit: CD=2:1) with various molecular weights to give stiochometric complexes in a crystalline state. They reported the complexes between α-CD and PEG with molecular weight in the range of 200-10,000, however, they were not able to obtain ICs with α-CD and the lower molecular weight analogs of PEG like ethylene glycol, diethylene glycol and triethylene glycol.[36,43] They also studied the effect of end groups on the PEG backbone. Table 4 lists the results of complex formation between α-CD and PEG with different end groups. PEG's with small end groups, such as methyl, dimethyl, and amino groups, formed complexes and their yields were found to be higher than for unmodified guest PEGs.

**Table 4.** Inclusion complexes formation between CD and PEG terminated with various small end groups.[42]

| $R(CH_2CH_2O)_nCH_2CH_2R^*$ | | | Yields (%) | |
|---|---|---|---|---|
| R | **R*** | **$M_n$** | **α-CD** | **β-CD** |
| **-OH** | *-OH* | 1000 | 90 | 0 |
| **$-NH_2$** | *$-NH_2$* | 1450 | 94 | 0 |
| | | 2000 | 96 | 0 |
| **$-OCH_3$** | *$-OCH_3$* | 500 | 88 | 0 |
| | | 1000 | 93 | 0 |
| | | 2000 | 98 | 0 |
| **$-OCH_3$** | *-OH* | 750 | 89 | 0 |

These results indicate that interactions (hydrogen bonds) between the -OH groups of PEG and -OH groups of α-CD may not be the key driving force for

complex formation. PEG having bulky substituents, such as a 3,5-dinitrobenzol group and a 2,4-dinitophenyl group at the chain ends, do not fit or pass through the $\alpha$-CD cavity, and did not form any complex with $\alpha$-CD. It was also observed that polypropylene glycol (PPG) did not form a complex with $\alpha$-CD, since it is bulkier than PEG. However, PPG formed complexes with $\beta$-CD and $\gamma$-CD, since they have wider cavities. It was also found that the rate of complex formation and the yield of complex depend on the molecular weight of PEG, where PEG of 1000 g/mol forms complexes most rapidly and the yield increases as the molecular weight increases. Figure 14 shows the rates of complex formation and the yields of the PEG-$\alpha$-CD complex as a function of different PEG molecular weights.

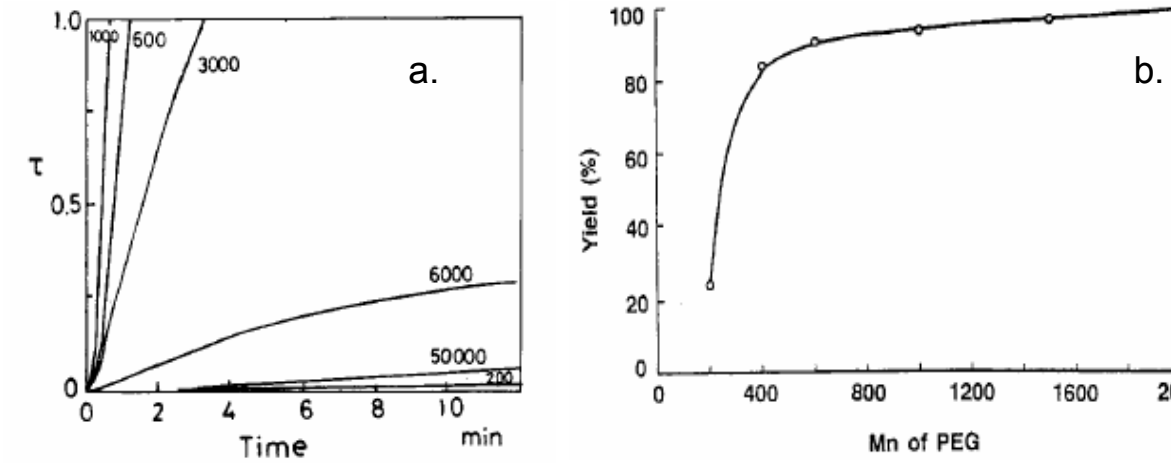


**Figure 14.** a.) Time course for the turbidity development after mixing the $\alpha$-CD solution and the PEG solution, b.) Yields of the complexes of a-CD with PEG as a function of the molecular weight of PEG.[42]

### 1.2.5 Structural Characteristics of Cyclodextrin Inclusion Complexes

Generally speaking, two types of crystal structures[44] have been observed for solid CD IC's; cage and channel structures (Figure 15). In cage type crystal structures, the cavity of each CD molecule is blocked off on both sides by adjacent CD's, thereby leading to isolated cavities. Depending on the packing of the CD molecules, two classes of cage complexes are observed. In the first, CDs are packed crosswise in a "herringbone" arrangement which is most common in pure $\alpha$-, $\beta$-, and $\gamma$-CDs. In the other, thus far observed only for $\alpha$-CD and $\beta$-CD complexes, a motif suggestive of bricks in a wall is found and called a "layer" type. There, the CDs are arranged in sheets with all $O_2H/O_3H$ hydroxyls on one side and all $O_6H$'s on the other side. Adjacent sheets face each other with lateral displacements, so the CDs cavities are closed on both sides by adjacent molecules. In the channel type structure, CD molecules are stacked on top of each other constructing linearly aligned, "endless" channels in which guest molecules are included. The stacks of CDs are stabilized by hydrogen bonds producing a head-to-tail pattern or a head-to-head/tail-to-tail arrangement.

As-received (pure) $\alpha$-, $\beta$-, and $\gamma$-CDs have cage structures with just water molecules residing in the CD cavities. CDs adopt cage or channel type crystal structure in their inclusion compounds depending on the characteristics of the guest molecules. Crystalline $\alpha$-CD inclusion complexes form cages with small molecular guests, whereas long molecular and ionic guests prefer channels. For instance, $\alpha$-CD complexes with acetic, propionic, and butyric acids crystallize in

cages, whereas valeric acid and higher analogues form channels; a clear and well-defined size selectivity for guests.[45]

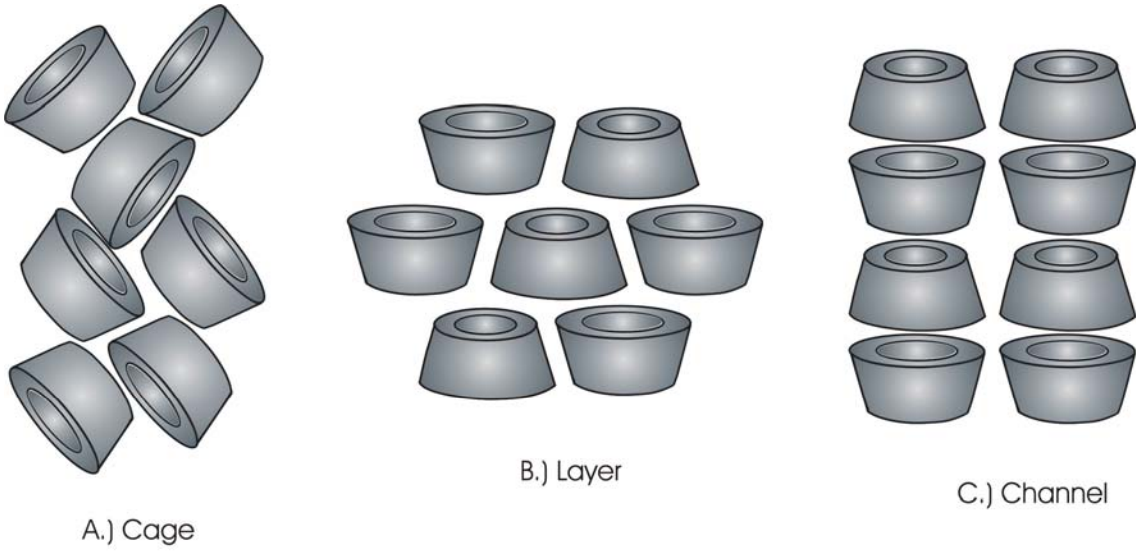


**Figure 15**. Crystalline structure of CDs a.) cage, b.) layer and c.) channel.

The situation for β-CD appears to be different, and prediction of channel or cage forming guests is not possible so far. In any case, the dodecahydrate as well as methanol, ethanol, and hydroiodide complexes of β-CD crystallize as cage-type complexes. However, 1-propanol, which easily fits into the cavity, induces a change to the channel type structure for β-CD, in contrast to α-CD which crystallizes in the cage type with this guest molecule.[45]

For γ-CD, a herringbone cage-type complex has only been obtained with water as the guest, ie., pure γ–CD, whereas for other guest molecules, even small methanol or styrene guests, induced the channel form.[46] It appears,

therefore, that generalizations can be made only for γ-CD, and extrapolations to α-CD and β-CD are not possible.

The channels formed by α-CD are mostly of the head-to-head:tail-to-tail form (Figure 16). By contrast, in most β-CD channel structures, the β-CD molecules are arranged head-to-head. The orientation of γ-CD in the columns, however, is neither exclusively head-to-head nor head-to-tail; it is instead head-to-head:tail-to-head:tail-to-tail, resulting in a 3-molecule repeating unit.[45]

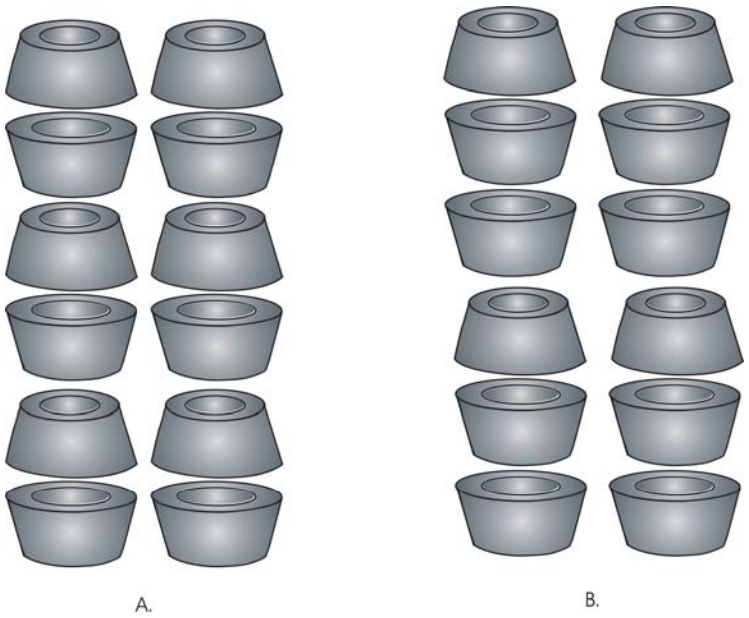


**Figure 16.** Schematic representation of the packing of CD molecules within their crystal lattices: (a) head-to-head:tail-to-tail and (b) head-to-head:tail-to-head:tail-to-tail channel structures.

Recent studies have also shown the possibility of preparing empty CD channels without any guest molecules. For instance, Topchieva *et al.*[47] initially prepared α-CD in the channel structure by first preparing a polymer-CD IC, then

removing the guest polymer chains. On the other hand, Rusa *et al.*[48] directly prepared α-CD in the channel structure by rapid precipitation of α-CD from its aqueous solution using chloroform. Rusa *et al.* have also prepared channel γ-CD with this method using acetone instead of chloroform. The preparation of empty CD channels makes it possible to put small molecules inside these channels. For instance, styrene is included inside the preformed γ-CD channels and polymerized in this confined environment to control the stereoregularity of the resulting polystyrene.[46]

### 1.2.6 Characterization of Cyclodextrin Inclusion Complexes

Cyclodextrin inclusion complexes that are formed either in a solution or in the crystalline state can be characterized by a variety of techniques. Once the complex is formed, there are characteristic changes, like a decrease in solubility, changes in chemical reactivity and stability, UV/Vis and fluorescence absorbance shifts, NMR chemical shifts, changes in crystalline structure, changes in pKa values etc., Furthermore, since complexation will influence the physicochemical properties of the aqueous complexation media, methods that monitor these media changes can be applied to study the complexation. For example, measurements of conductivity changes, determinations of freezing point depression, viscosity measurements and calorimetric titrations may be used.

Once the guest molecules are included within the cavities of cyclodextrins, the crystalline phase transition from cage to channel likely occurs if the guest is a long chain molecule, such as a polymer. Wide angle X-ray diffractometry

(WAXD) is a useful characterization technique for investigating the formation of CD-guest complexation by studying the crystalline phase transition between the cage structure of pure CD and the channel structure of polymer-CD ICs (Figure 17). Once the host CD molecules are threaded onto the polymer chains, it is expected that the final IC crystals adopt a channel-type structure. The WAXD pattern for cage γ-CD has characteristic reflections at 2θ = 12.4, 16.5, and 18.8, and 23.4°, and polymer-γ-CD IC crystals have one major reflection occurring at 2θ = 7.5°, which is characteristic of γ-CD in the channel structure and has been assigned to the 200 plane of a tetragonal lattice.[49]

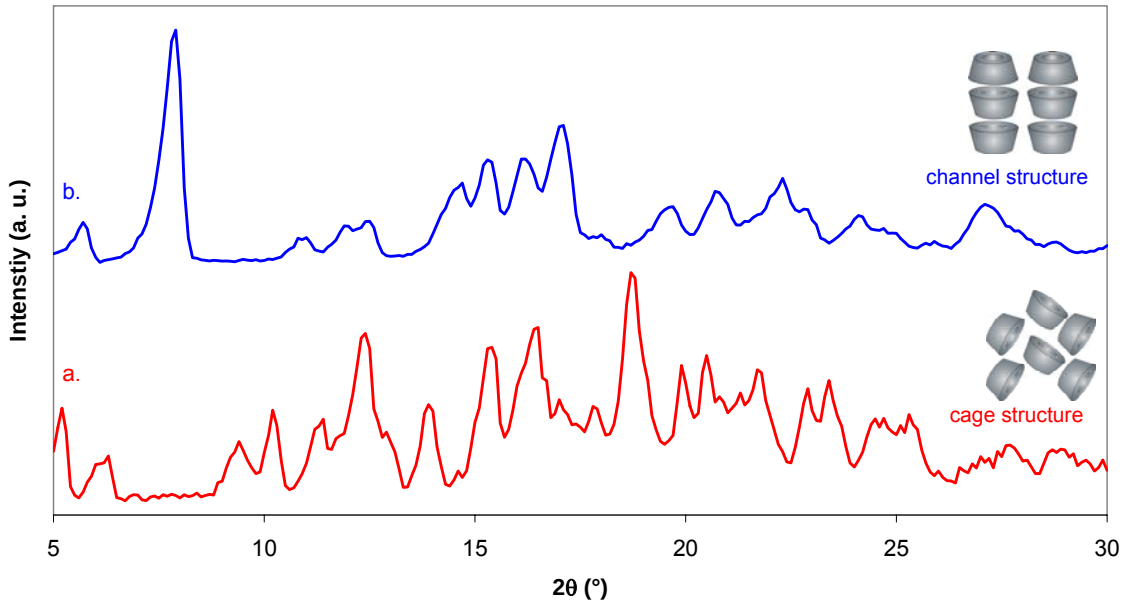


**Figure 17.** WAXD pattern of as-received γ-CD and PMMA-γ-CD IC.[50]

Nuclear Magnetic Resonance (NMR) spectroscopy is also a very useful tool for the investigation of CD complexes. As the environments around the hydrogen and carbon atoms in the cavity changes during association with the guest, shifts in the resonance peaks for the cyclodextrin can be observed, as well as for the peaks corresponding to the atoms of the guests which penetrate into the cavities of the cyclodextrins. For example, Figure 18 shows the characteristic $^{1}$H-NMR-shifts of styrene-CD-IC.[51] Typical shifts of CD protons induced by the included guest styrene molecules are observed compared to uncomplexed CD. The inner CD protons 3 and 5 are shifted towards higher field indicating that the styrene molecule is positioned within the cavity of the CD.

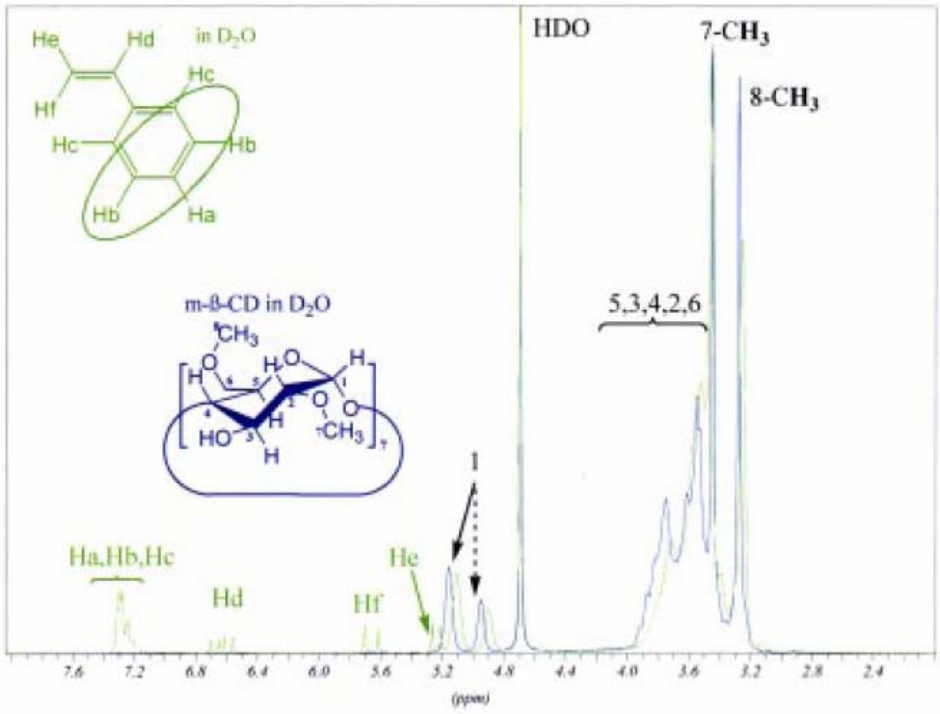


**Figure 18.** 1H-NMR spectrum of styrene/methylated-β-CD complex in $D_2O$ (green spectrum) in comparison to uncomplexed m-β-CD (blue spectrum).[51]

Additionally, solid-state $^{13}$Carbon NMR has also been used as a powerful technique to identify crystalline CD complexes. CD molecules assume a less symmetrical conformation in the crystal when they do not include guests in their cavities.[52-53] In this case, the spectrum shows resolved C-1 and C-4 resonances from each of the 1,4-linked glucose residues. However, in the spectrum of the CD complex each carbon of glucose can be observed as a single broader peak. The observation of single carbon peaks indicates that CD adopts a symmetrical conformation and each glucose unit of CD is in a similar environment. X-ray studies of pure CD single crystals also show that CDs assume a less symmetrical conformation when they do not include guests in their cavities and CDs adopt a more symmetrical conformation when they include guests in their cavities. Figure 19 shows the $^{13}$C-CP/MAS NMR spectra of dimethyl (DM)-β-CD and the pseudorotaxane (DM-β-CD-poly(2T)) prepared from the *in situ* polymerization of bithiophene (2T) in its DM-β-CD-bithiophene inclusion complex.[53] DM- β-CD-poly(2T) has a symmetrical cyclic conformation in the complex, although DM-β-CD assumes a less symmetrical conformation in the crystal when not including a guest into the cavity. Polythiophene chains are included into the cavities of DM-β-CDs following polymerization.

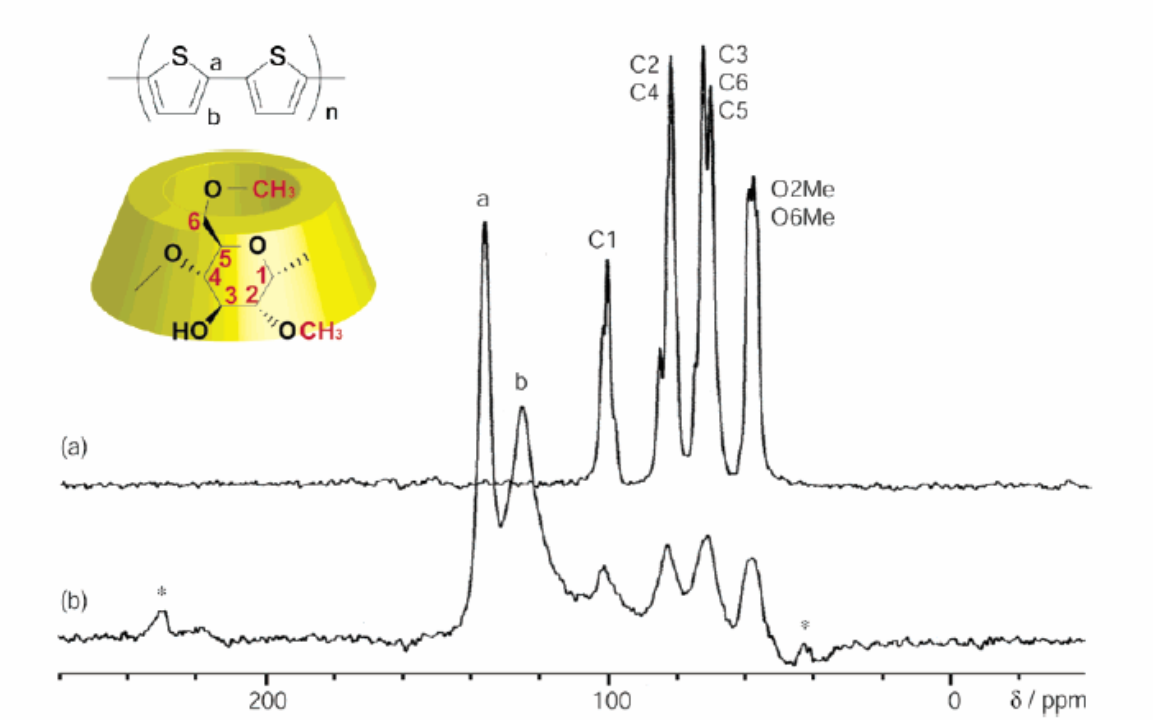


**Figure 19.** $^{13}$C-CP/MAS NMR spectra of (a) DM-β-CD and (b) polythiophene polymerized with $FeCl_3$ initiator in water from DM-*β*-CD-2T inclusion complex.[53]

The inclusion of guest molecules in CD cavities can also be followed by UV-vis spectroscopy. For instance, the inclusion into β-CD of poly(thiophene-2,5-diyl)( PTh) in water (Figure 20) was studied by UV/Vis spectroscopy.[54] Figure 21 shows the changes in the UV-vis spectra of the aqueous solution containing the water-soluble pseudopolyrotaxane and β-CD. The UV-vis spectrum shows no obvious change in the range of 200–700 nm after 9 days. The threading of β-CD on PTh seemed to be very slow, but, after 15 days, the absorption peak at about 445 nm, which agrees with the peak position of the π–π* transition of PTh appeared and its intensity gradually increased until 22 days. After 23 days, the absorbance observed to decrease gradually due to the formation of water-

insoluble pseudopolyrotaxane by further threading of β-CD onto the water-soluble pseudopolyrotaxane.

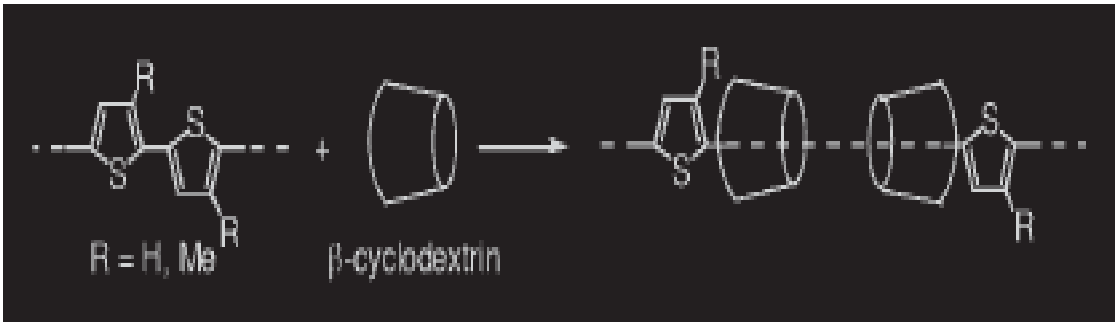


**Figure 20.** The inclusion complexation of β-CD with poly(thiophene-2,5-diyl)[54]

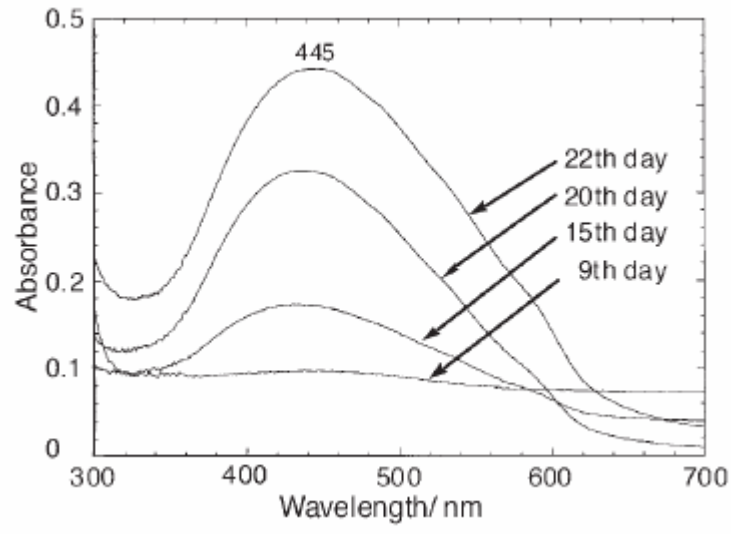


**Figure 21.** Changes of UV-vis absorption of the supernatant obtained from the reaction of PTh and β-CD.[54]

### 1.2.7 Thermodynamics of Cyclodextrins Complexation

In an aqueous solution, the apolar cyclodextrin cavity is occupied by water molecules which are unfavored energetically (polar-apolar interaction), and

therefore can be readily replaced by “proper“ guest molecules which are less polar than water (Figure 22). The dissolved cyclodextrin is the “host” molecule, and the “driving force” for complex formation is the substitution of the high enthalpy water molecules by an “appropriate“ guest molecule. One, two, or three cyclodextrin molecules can contain one or more entrapped “guest” molecules. Most frequently the host:guest ratio is 1:1. This is the essence of “molecular encapsulation”. However, 2:1, 1:2, or even more complicated associations and higher order equilibria also exist.

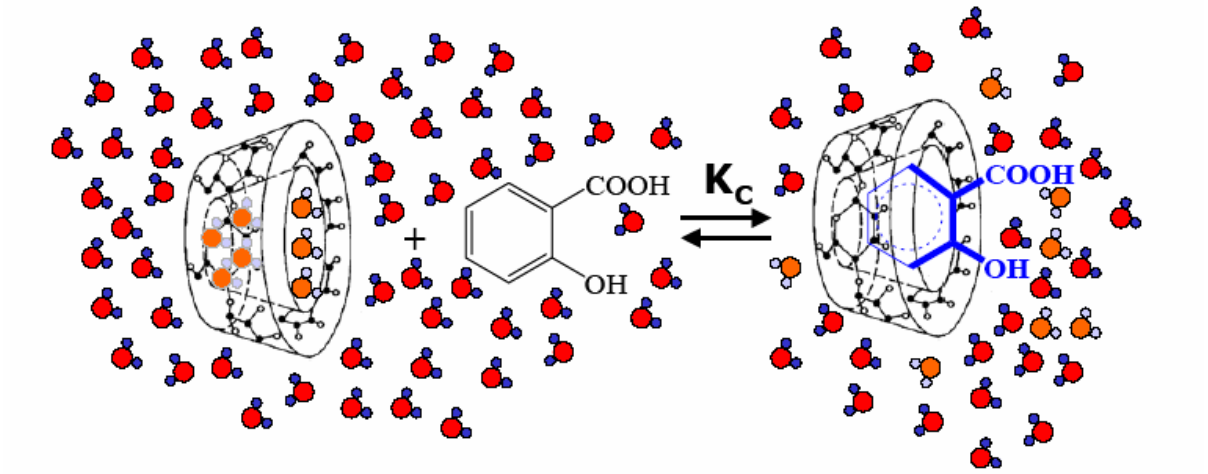


**Figure 22.** Schematic representation of CD inclusion complex formation: Salicylic acid is the guest molecule; the small circles represent the water molecules.[55]

The complexation thermodynamics of cyclodextrins have been studied extensively and various reports have been published.[10,56-58] The primary factors involved in complexation of guest-host molecules are believed to be mainly van der Waals and hydrophobic interactions,[10] although hydrogen bonding and steric effects also have certain functions[10] In summary, the thermodynamic quantities

obtained for the inclusion complexation by cyclodextrins are a consequence of the weighted contributions of these interactions.

A wide variety of experimental methods have been employed in the determination of thermodynamic quantities for the complexation reactions of cyclodextrins. These include calorimetry[59], titration[60], UV-vis absorption spectroscopy[61], circular dichroism (CD)[62], fluorescence[63], nuclear magnetic resonance (NMR)[64], electron spin resonance (ESR) spectroscopy[65], gas and liquid-phase chromatography[66-67] and pH potentiometry[68]. Additionally, kinetic experiments[69], solubility determinations[70] and vapor pressure[71] and conductivity[72] measurements were also employed in the thermodynamic investigation of cyclodextrin complexation.

The most significant contributions to the complexation thermodynamics of cyclodextrins are assumed to originate from (1) penetration of the hydrophobic part of the guest molecule into the cyclodextrin cavity and (2) dehydration of the organic guest. Since the cyclodextrin cavity is highly hydrophobic, the transfer of the hydrophobic part of the guest molecule from water into the cyclodextrin cavity occurs; a process which accomodates the combined effects of both contributions mentioned above.

However, charged groups, such as ammonium and carboxylate or hydrophilic groups, such as hydroxyl, amino, and carboxyl remain exposed to the bulk solvent even after the inclusion of the hydrophobic moiety. An exception to this general observation is the aromatic hydroxyl group, which can penetrate deeply into the cyclodextrin cavity where it hydrogen-bonds to one of

cyclodextrin's peripheral hydroxyl groups. Therefore, hydrogen bonding interactions may function as a third factor (3) contributing to the stabilization of cyclodextrin complexes with such guest molecules. There are two additional factors that can contribute to the complexation thermodynamics of cyclodextrins, which differ from the classical hydrophobic effect. These are (4) the release of the water molecules originally included in the cyclodextrin cavity to bulk water and (5) the conformational changes or strain release of the cyclodextrin molecule upon complexation. It should be noted that the nature and driving forces of cyclodextrin complexation in pure organic solvents may differ significantly from those in water.

The equilibrium constants for 1:1 complexation reactions can be defined as indicated in Figure 23. The general trends of the thermodynamic quantities ($\Delta G°$, $\Delta H°$ and $\Delta S°$) for the complexation reactions can be calculated from the equilibrium constant ($K$) in the standard state, and the standard Gibbs free energy change ($\Delta G°$) can also be determined from the experimental observation of enthalpy ($\Delta H°$) and entropy ($\Delta S°$) changes.

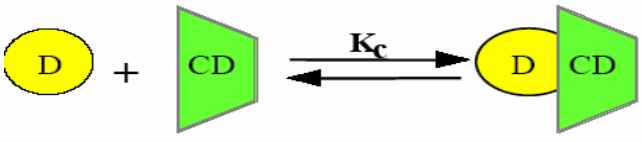


$$K_c = \frac{[D\text{-}CD]}{[D]\,[CD]}$$

**Figure 23.** The definition of the equilibrium constant for 1:1 complexation.

The equilibrium constant ($K$) depends on the hydrophobic nature of the host-guest interactions. Apparently, much higher affinities: as defined by $-\Delta G°$, are obtained for neutral compounds compared to those of the corresponding charged species derived from the same original guest molecules. Thus, neutral phenols, acids, and amines give larger $K$ values than the corresponding ionized or protonated species. Shape-matching and steric effects upon host-guest interaction, the hydrogen-bonding ability of functional groups on the guests, the position of substituents on aromatic or aliphatic guests, and the flexibilities of the guest molecules are also found to be important and affect the $K$ value.

Rekharsky and Inoue studied the effect of hydrophobic units on guest molecules.[10] They determined the $\Delta G°$, $\Delta H°$ and $\Delta S°$ values for the complexation reactions of $\alpha$-cyclodextrin observed with 1-alkanols, *sec*-alkanols, 1,2-alkanediols, $\alpha,\omega$-alkanediols, neutral alkylamines, alkylammonium ions, neutral alkanoic acids, alkanoate ions, neutral alkanedioic acids, alkanedioate ions, and monoalkylureas. The values were plotted as a function of the number of aliphatic carbon atoms ($N_C$) present in the guest molecules (Figure 24). They observed that the $\Delta G°$ and $\Delta H°$ values become more negative with increasing $N_C$, suggesting that the complexation itself is evidently driven by enthalpy, but that the entropic term controls the complex's ultimate stability. Similar findings have been found when the host was changed to $\beta$-CD.

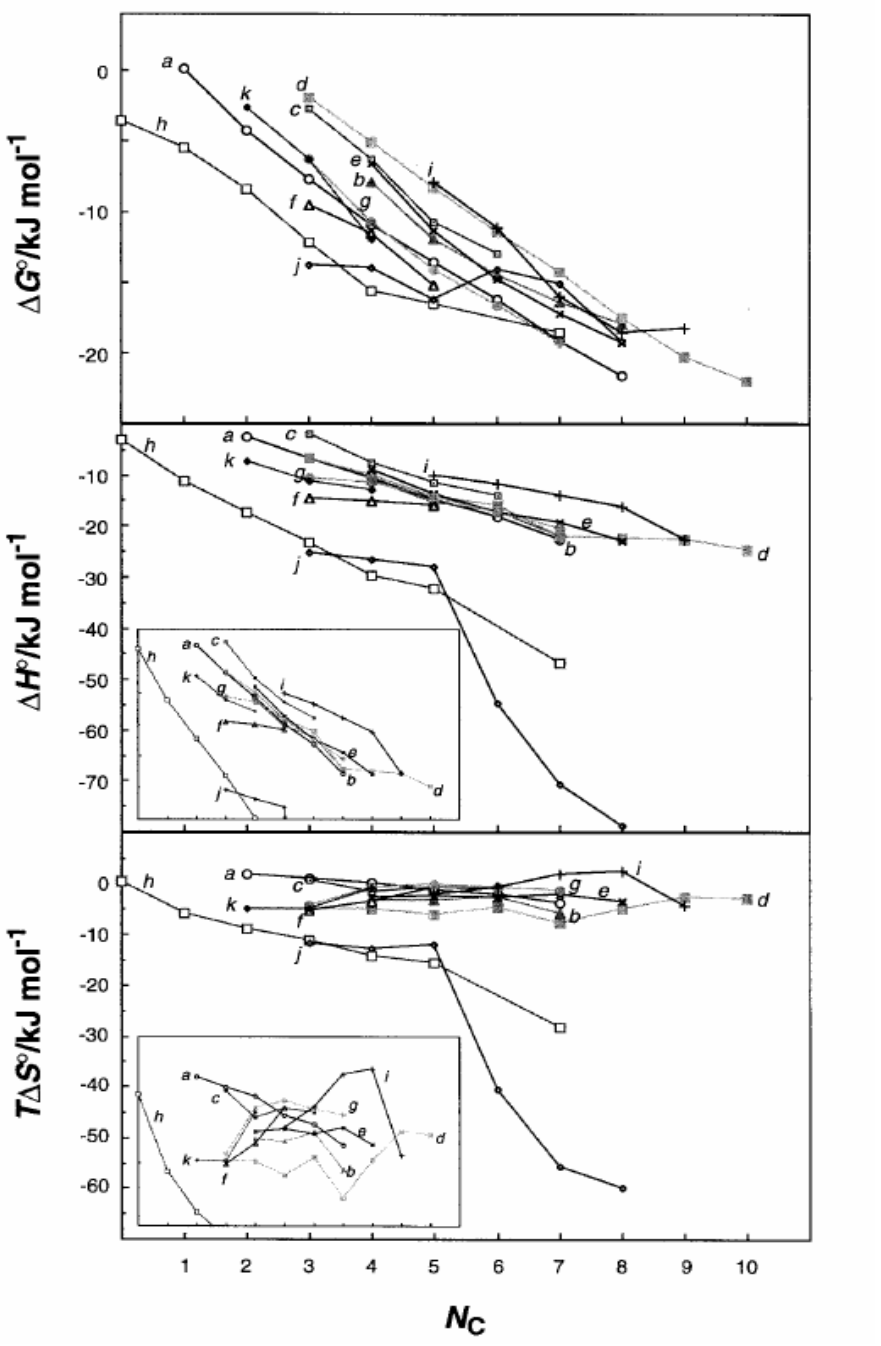


**Figure 24.** Thermodynamic quantities ($\Delta G°$, $\Delta H°$, and $T\Delta S°$ at 298 K) for the complexation of various classes of guests with $\alpha$-cyclodextrin as a function of the number of methylenes ($N_C$) in the guest molecules: (a) 1-alkanols (O), (b) *sec*-alkanols (▲), (c) 1,2-alkanediols (⊡), (d) $\alpha,\omega$-alkanediols (■), (e) alkylammoniums (×), (f) alkylamines (△), (g) alkanoates (●), (h) alkanoic acids (□), (i) alkanedioates (+), (j) alkanedioic acids (◆), (k) alkylureas (◊). Insets are partial enlargements.[10]

### 1.2.8 Proposed Models for Polymer-Cyclodextrin Inclusion Phenomena

Inclusion of polymers is a very fascinating phenomenon, in which one or more cyclic molecules (cyclodextrins) are threaded around a linear chain that penetrates their empty cavities. In the literature, there have been noteworthy studies to get an in-depth understanding of the inclusion process of guest polymer chains inside the host CD cavities.[73]

Baglioni and co-workers reported the study of the threading process of several $\alpha$-cyclodextrin molecules on PEG at different temperatures and in different solvents, and they proposed a model for the interpretation of the threading mechanism.[73a] The threading process was followed by UV-Vis absorbance measurements of the solution at $\lambda$ = 400 nm. Figure 25 shows absorbance versus *time* (s). The whole curve was divided into three parts, depending on the variation of absorbance with time. In the first part, between $t$ = 0 and the arrow, absorbance remains constant suggesting that $\alpha$-CD molecules are penetrated by PEG chains during this time. Then the absorbance increases steeply, because PEG-CD complexes aggregate and then precipitate, and finally absorbance reaches an asymptotic value. *Threading time* ($T_{th}$) was defined as the time required to record a detectable increment in absorbance during the formation of the PEG-CD complex.

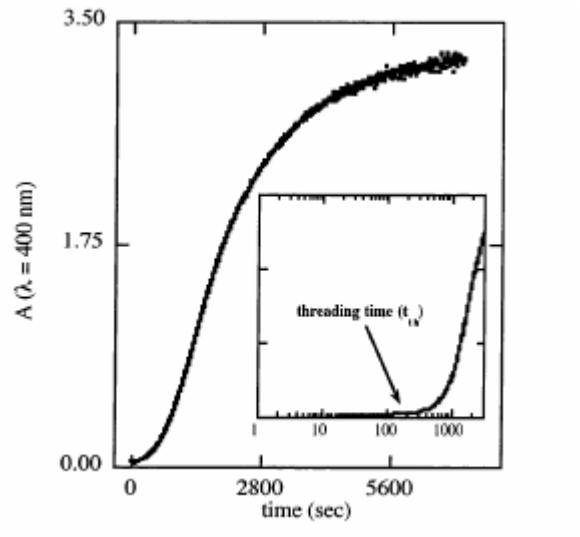


**Figure 25.** Turbidity plot at λ=400 nm during the formation and precipitation of a PEG-α-CD complex.[73a]

Additionally, they calculated the Gibbs free energy of activation and the number of α-CD molecules that take part in the threading process.

$$\text{PEG} + m(\alpha\text{-CD}) \rightleftharpoons \sigma^* \rightarrow \text{Polyrotaxane}$$

$\sigma^*$ represents the activated complex in the formation of the polyrotaxane (PEG-CD Complex), where the rate limiting step is the formation of $\sigma^*$ and is written as

$$\frac{\mathrm{d}[\sigma^*]}{\mathrm{d}t} = k^*[\sigma^*] = k^* K^{\ddagger}[\text{PEG}][\alpha\text{-CD}]^m$$

where $k^*$ is the rate constant, $K^{\ddagger}$ is the equilibrium constant, and $m$ is the number of α-CD molecules that participate in the formation of the activated complex $\sigma^*$.

The model they proposed for the inclusion phenomenon takes into account five distinct steps:

(1) diffusion of the polymer chains and cyclodextrin molecules in the solvent;

(2) initial threading of polymer chain ends into CD cavities;

(3) sliding of CD molecules over the polymer chains;

(4) dethreading of CD molecules from the polymer chain;

(5) precipitation of the final large aggregate.

(1) It was suggested that, when a-CD and PEG are dissolved in the solvent, they will randomly move by diffusion and some of the $\alpha$-CD molecules will be located in the proper position for the entrance of the PEG end into the CD cavity. Schematic representation of the threading process of CD on PEG chain is shown in Figure 26.

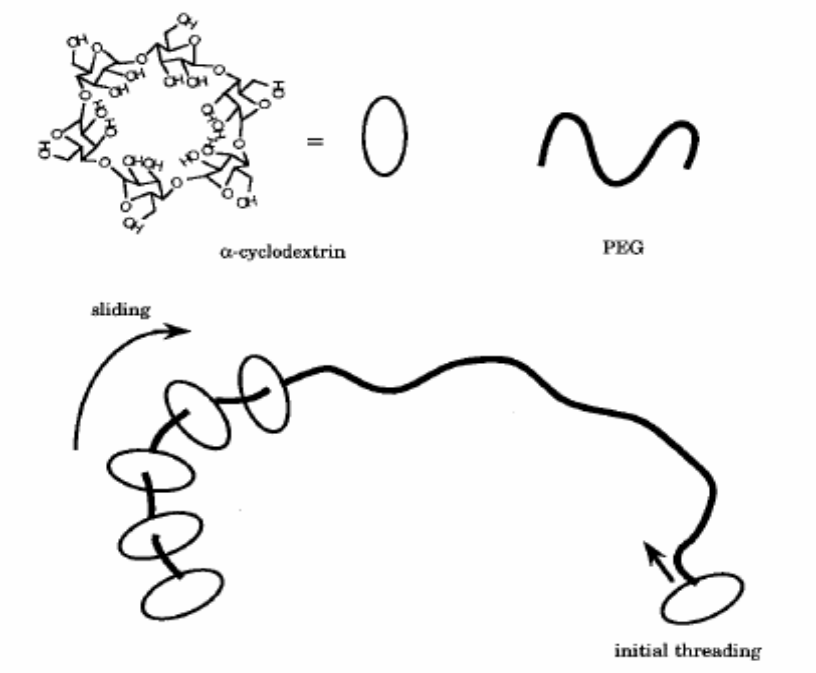


**Figure 26.** Schematic representation of the threading of α-CDs on a PEG chain.[73a]

(2) Once the α-CD cavity faces the PEG chain end, the initial threading occurs. The initial threading is favored by the attractive interactions that are established between the a-CD hydrophobic internal cavity and the -O-CH2-CH2- units of the linear PEG chain. It was observed that this second step is favored by low temperatures and highly structured solvents, where the random thermal motion of the two reactants is reduced.

(3) When additional α-CD molecules approach the PEG chain ends, the cyclodextrin molecules already threaded must slide along the PEG chain, moving toward the center of the long linear polymer. This process requires the unfolding and stretching out of the coiled PEG chains, and therefore will be favored by low temperatures and strong hydrogen bonding in the solvent.

(4) When the PEG chain is almost fully covered with a-CD, a dethreading of cyclodextrins from the chain ends is possible, in particular when the PEG has a high mobility due to an increase in temperature or to a lower hydrogen bonding strength of the solvent.

(5) When the PEG-CD complex is finally obtained, attractive interactions are established between different particles and produce large aggregates that easily precipitate and form a white thick gel that entraps a significant amount of solvent.

### 1.2.9 Parameters Affecting the Formation of Polymer-Cyclodextrin Inclusion Complexes

The diffusion process is expected to be dependent upon temperature and the nature of the solvent. Shorter threading times ($t_{th}$) (faster process) are expected when the temperature increases and when the solvent possesses weaker hydrogen

bonds. However, Baglioni *et al*., observed that $t_{th}$ increases as temperature increases.[73b] Figure 27 demonstrates the turbidity plots as a function of temperature where the $t_{th}$ is longer for higher temperatures.

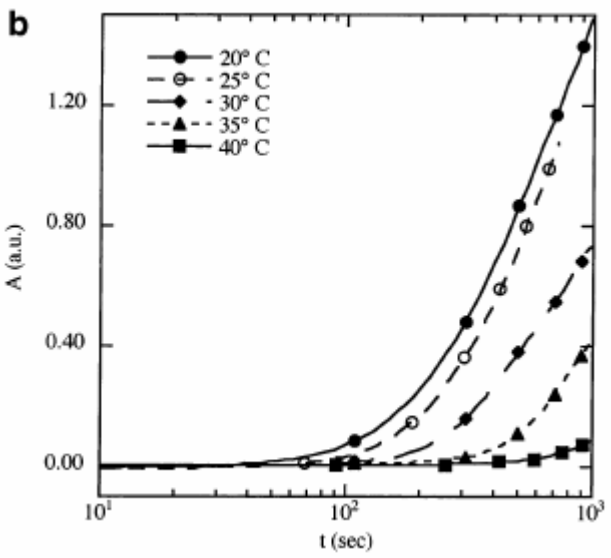


**Figure 27.** Turbidities of PEG-α-CD complexation as a function of temperature. [73b]

Additionally, the effect of solvent was also tested. Four different solvent systems were used: water ($H_2O$), heavy water ($D_2O$), mixture of $H_2O/D_2O$(1:1) and urea (0.1 M in water). The choice of these solvents was made on the basis of the different hydrogen bonding networks that they possess, where the strength of hydrogen bonds is as follows: $D_2O$ > $H_2O$ > urea. Figure 28 displays $t_{th}$ versus temperature (T, K) in the range between 283 and 313 K for four different solvent systems. The plot indicates that the threading process also depends on the solvent composition with a significant increase of $t_{th}$ in going from $D_2O$ to $H_2O/D_2O$ (1:1), to $H_2O$, and to urea for each temperature. The increase in $t_{th}$ with the weakening of the

solvent structure indicates that the diffusion is not the critical step in the overall threading process.

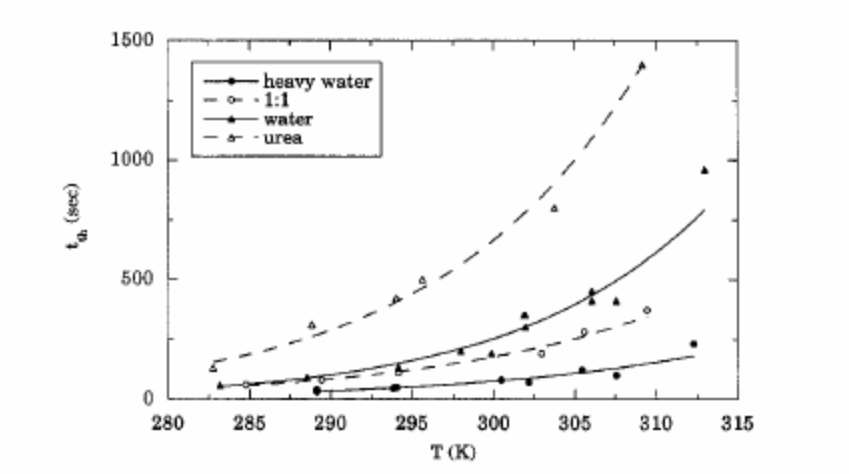


**Figure 28.** Effect of temperature and solvent on the threading of PEG by α-CD.[73b]

Rusa *et al.* have also reported that the solvent system plays an important role in the kinetics of the inclusion polymers in CDs.[41b] They studied the kinetics of formation of poly(*N*-acylethylenimine)- γ-CDs (PNAI-γ-CD-ICs) by a $^1$H-NMR technique. The PNAI-*g*-CD-ICs were obtained by suspension of as-received cage structure γ-Cyclodextrin (γ-$CD_{cage}$) or preformed channel structure γ-Cyclodextrin (γ-$CD_{channel}$) into polymer solutions. The decrease in polymer proton peak intensities was observed as a result of inclusion of polymer chains once the γ-$CD_{cage}$ crystals were suspended in acetone-PNAI solutions. An increase of the water peak intensity was reported as a result of its release from the γ-CD cavities as the polymer chains were included (Figure 29).

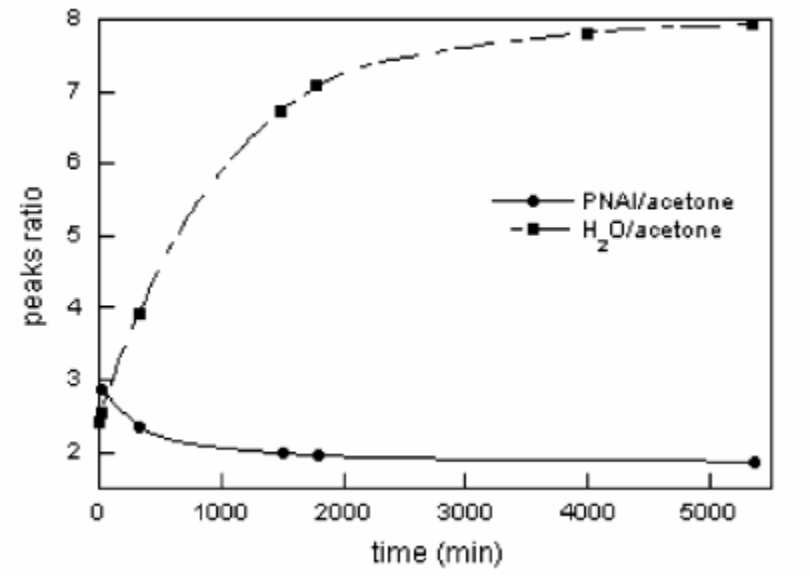


**Figure 29.** Variation of polymer and $H_2O$ $^1$H-NMR peak intensities relative to the intensity of solvent (acetone) peak, as PNAI chains in solution is included by CD. [41b]

They studied two PNAI solvent systems; acetone (water miscible) and chloroform (water immiscible), and observed that PNAI chains were included when acetone was used as a solvent, but the inclusion of PNAI did not occur when chloroform was used. Figure 30 shows the trend of polymer $^1$H-NMR peak intensity with time in two different solvent systems, where no decrease of the polymer peaks was observed when chloroform was used as solvent. This behavior was explained by the release of water, a hypothesis accepted as a driving force for polymer inclusion and which was supported by the trend of water release from γ-CD cavities when suspended in different systems. Rusa et al. found that the rate released and quantity of water was greater for γ-$CD_{channel}$ crystals compared to γ-$CD_{cage}$ crystals when suspended in acetone, and there was almost no water release from γ-$CD_{cage}$ in the case of chloroform as a PNAI solvent (Figure 31). This finding explains why

there is a faster and more pronounced decrease of PNAI peaks when included in γ-$CD_{channel}$ compared with γ-$CD_{cage}$.

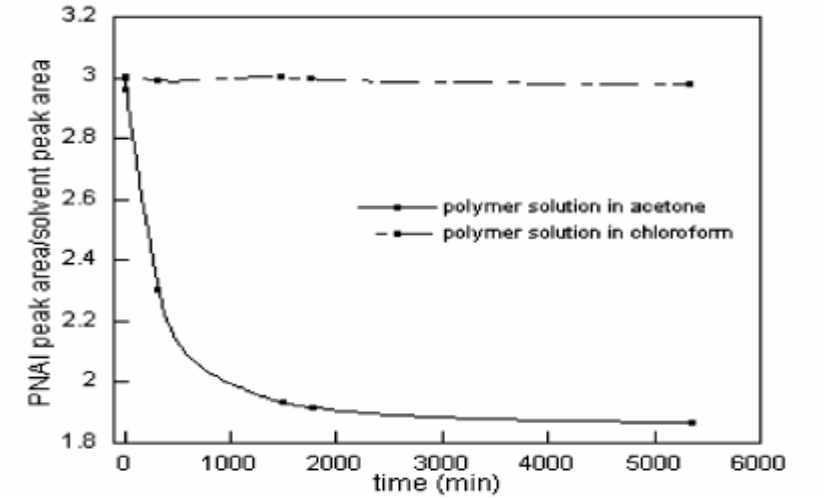


**Figure 30.** Decrease of polymer $^1$H-NMR peak intensity with time as a result of inclusion from polymer solutions into channels of suspended γ-$CD_{channel}$ crystals.[41b]

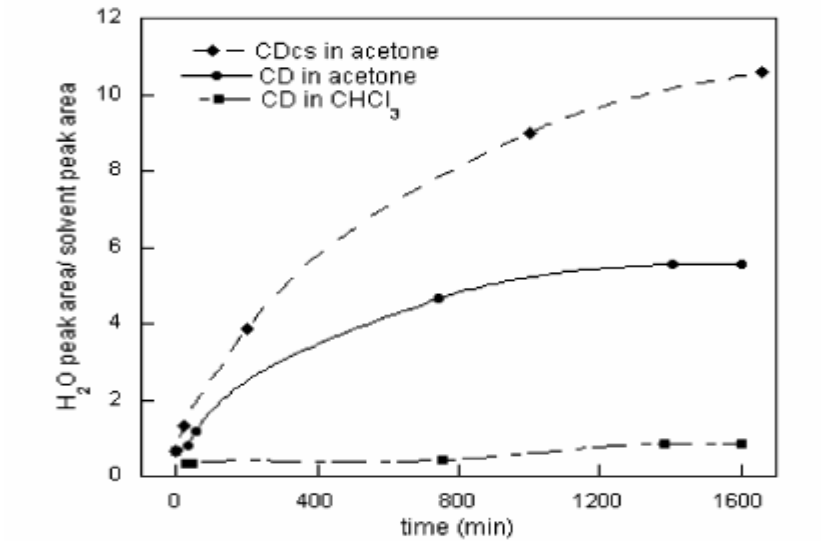


**Figure 31.** Water release from γ-$CD_{cage}$ crystals and γ-$CD_{channel}$ crystals suspended in acetone and γ-$CD_{cage}$ crystals suspended in $CDCl_3$.[41b]

The inclusion of PNAIs with different molecular weights was also studied by suspending γ-$CD_{channel}$ and γ-$CD_{cage}$ crystals into their acetone solutions. The rate

and amount of PNAI included by suspended $\gamma$-$CD_{channel}$ were found to be higher than that of suspended $\gamma$-$CD_{cage}$. The slow inclusion kinetics of PNAI chains by suspended $\gamma$-$CD_{cage}$ was explained by the necessary and concomitant solid-solid, crystal-crystal transition from $\gamma$-$CD_{cage}$ to $\gamma$-$CD_{channel}$ that must occur with the inclusion of PNAI chains. They also observed a greater ability to form a $\gamma$-CD complex for PNAI having a higher molecular weight (MW=9,000 g/mol) compared to a lower molecular weight PNAI1 (MW = 3,200 g/mol) (Figure 32).

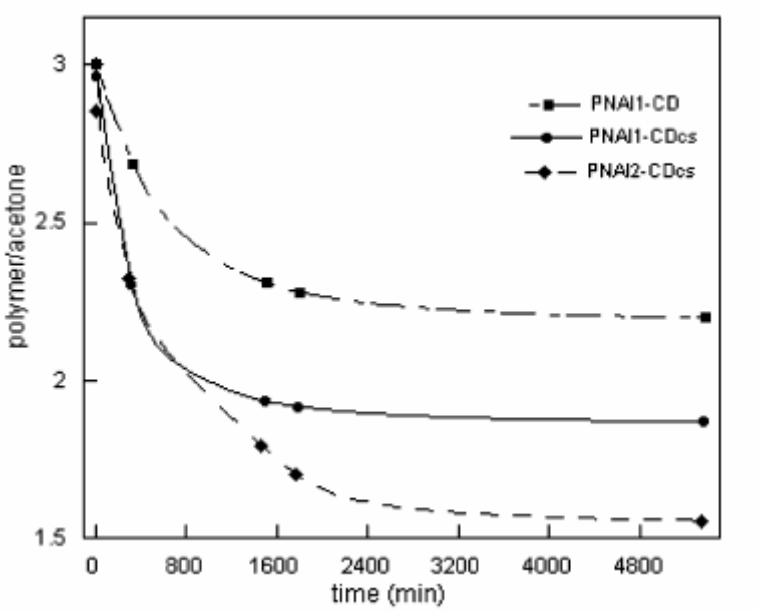


**Figure 32.** Decrease of polymer peak intensities with time as a result of inclusion in $\gamma$-$CD_{cage}$ or $\gamma$-$CD_{channel}$ crystals suspended in PNAI/acetone solutions. PNAI2 (MW= 9,000 g/mol) has a higher molecular weight than PNAI1 (MW= 3,200 g/mol).[41b]

Rusa *et al*.[74] used $\alpha$-CD in order to separate a mixture of PEGs with two different molecular weights, PEG600 (MWt=600 g/mol) and PEG20000 (MW=20,000 g/mol) by forming PEG-α-CD-ICs. It was found that α-CD strongly prefers the inclusion of PEG20000 over PEG600, which suggested that $\alpha$-CD included high

molecular weight PEG chains rather than the low molecular weight PEG. Similar results have also been observed by us in the formation of ICs between γ-CD and poly(vinylacetate) (PVAc).[50] We found that low molecular weight PVAc ($M_w$ = 12,800 g/mol) does not form an IC with γ-CD, whereas high molecular weight PVAc ($M_w$ = 167,000 g/mol). This result is particularily surprising, since low molecular weight PVAc ($M_w$ = 12,800 g/mol) forms common ICs in binary polycarbonate (PC)/PVAc and poly(methyl methacrylate) (PMMA)/PVAc pairs[75] and in ternary PC/PMMA/PVAc systems.[76]

### 1.2.10 Characteristics of Polymers Included In the Channels of Their CD-ICs

In order to form an inclusion complex with CD, the polymer chains must adopt an extended conformation which can fit into the CD cavity (Figure 33). Studies reporting the observation of extended chain conformations for polymers in their CD-ICs are available in the literature.[77-83]

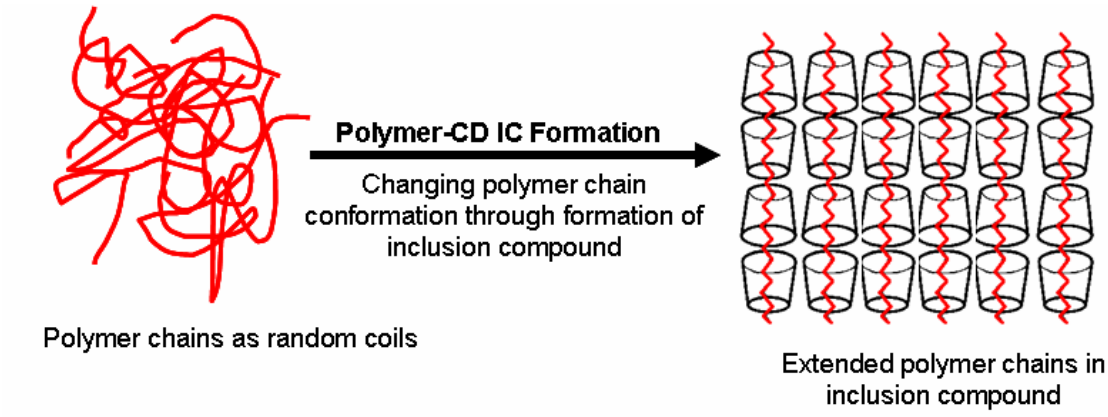


**Figure 33.** Illustration of extended polymer chains in the channels of their CD-ICs.

For example, the complex formation of emeraldine-base polyaniline (PANi) with β-cyclodextrin has been studied by scanning tunneling microscopy (STM).[77] It

was observed that PANi in the solution complexed with CD changed its conformation from coil to rod at low temperature below 275 K and the rod-like structure was imaged by STM (Figure 34). This finding suggested that β-CD molecules were threaded onto PANi and the polymer chains adopted an extended conformation in this confined environment and formed a rod-like structure. Moreover, it was found that the threaded β-CDs prevented the doping of PANi with iodine. The aurthors characterized this finding as the formation of an "insulated molecular wire", since a conjugated conducting polymer (PANi) was covered by insulating cyclic CD molecules.

Harada et al.[78] have studied the (PEG)-α-CD polyrotaxane with the scanning tunneling microscope (STM) in order to visualize the alignment of polymer chains inside the α-CD cavities (Figure 35). Regularly aligned PEG was clearly imaged by STM where the main chain of PEG runs along the surface of the substrate, and the α-CDs lie with their longitudinal axis parallel to the surface.

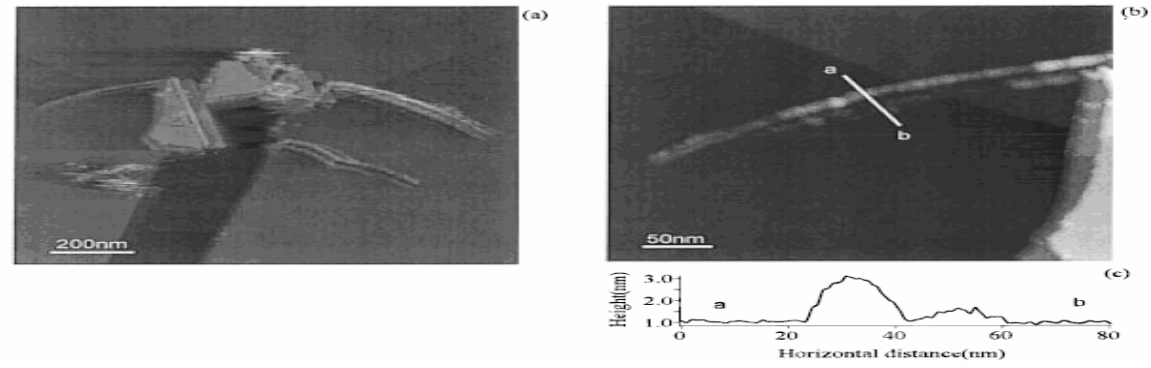


**Figure 34.** STM images of the inclusion complex between β-CD and PANi where fields of view are (a) 1200 nm x1200 nm and (b) 350 nm x 350 nm. (c) The height profile of the cross section.[77]

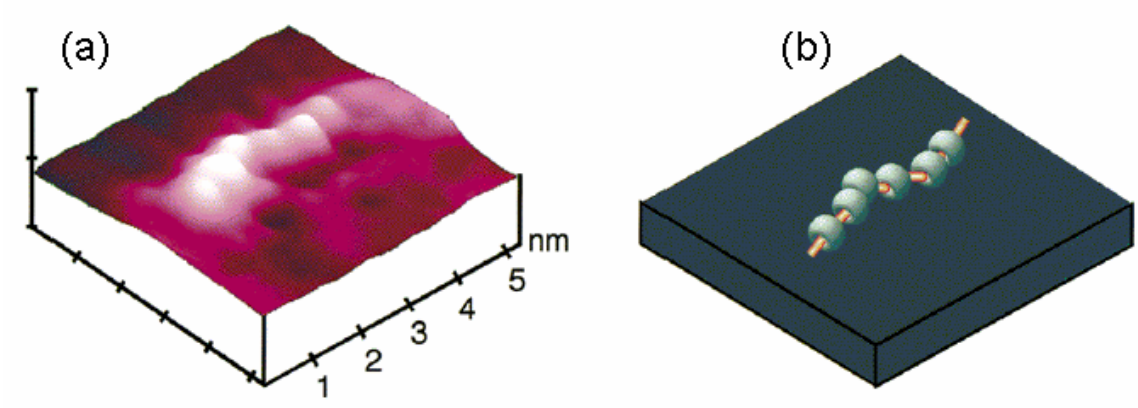


**Figure 35**. The STM image of the polymer cyclodextrin inclusion complex (PEG-α-CD) (a) and its schematic representation (b).[78]

They also demonstrated that the selected α-CD molecule(s) in a PEG/α-CD polyrotaxane could be reversibly shuttled using a STM since the α-CD molecules are noncovalently bound to PEG chains. One of the α-CDs in the molecular necklace was mechanically pushed by the STM tip along the main chain of PEG. The modes of shuttling and the shuttling of CD along the PEG chain are shown in Figures 36 and 37, respectively. The STM images were obtained before and after each manipulation. As designed, the target α-CD moved by sweeping the tip from right to left and the rest of the α-CDs retained their initial positions. Upon moving the tip in the reverse direction, the α-CD retraced its path and returned to its original position. Thus, the shuttling of one α-CD could be stably repeated.

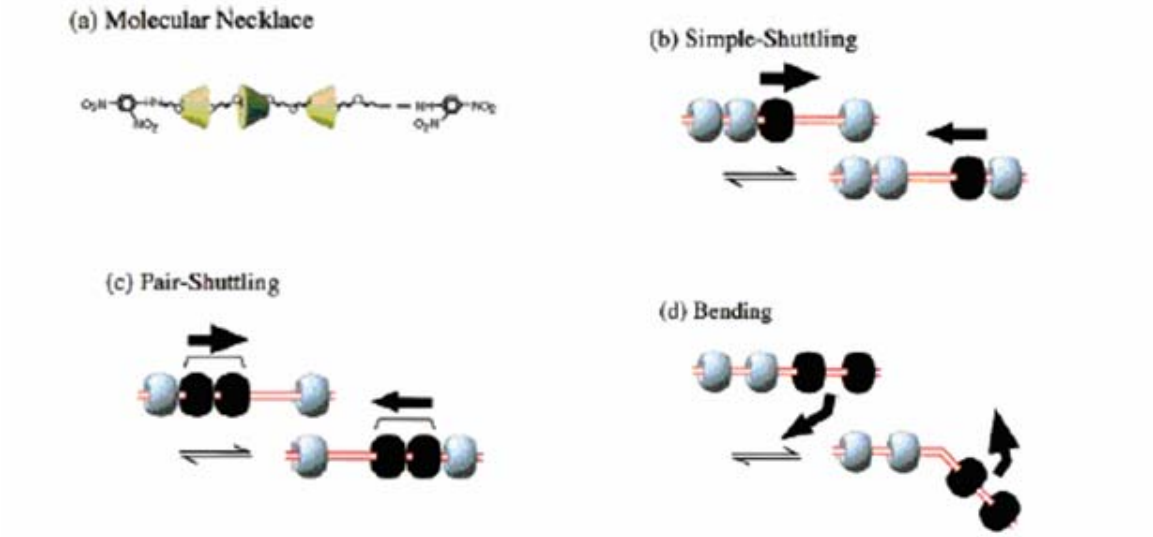


**Figure 36.** (a) Structure of the "molecular necklace", and three modes (b, c, and d) of the shuttle manipulation by STM.[78]

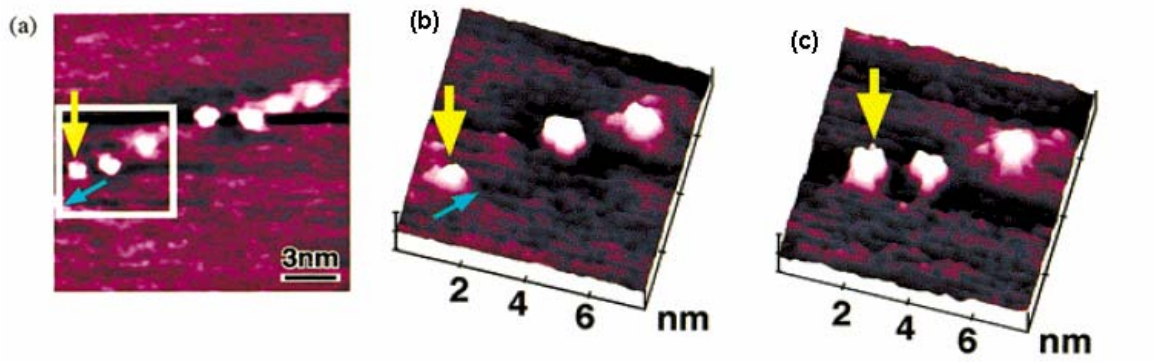


**Figure 37.** STM images of the simple-shuttling of $\alpha$-CDs along the PEG chain.[78]

Manipulation of polymers by including them in a confined environment, such as cyclodextrin channels, and subsequently removing the host CDs and coalescing them into bulk samples, can result in dramatic changes in crystalline structure, morphology, chain conformation, and chain dynamics. Polymer-CD-ICs have attracted the attention of Tonelli's research group, because the guest polymer chains

residing in and confined to the narrow CD channels provide a unique environment for the polymers. Through the formation of polymer-CD-ICs, it is possible to create an environment in which the behavior and dynamics of individual polymer chains can be studied, since, unlike their bulk samples, they are isolated and separated from neighboring polymer chains.

They have carried out extensive studies of polymer-CD-ICs and reported findings on the conformations and dynamics of the isolated polymer chains in this confined environment.[79-83] Solid-state carbon NMR with magic-angle spinning ($^{13}$C-NMR/MAS) has been used to study the structure and dynamics of various polymer-CD-ICs, with guest polymers, such as nylon-6, polycaprolactone (PCL) and the latter's copolymers. In nylon6-CD-ICs, a nearly fully extended, all trans conformation is adopted by nylon-6 chains included inside the CD channels.[80] It was found that in PCL-ICs formed with $\alpha$-CD and $\gamma$-CD the CD channels are occupied by single and two parallel, side-by-side PCL chains, respectively (Figure38).[81] It was reported that the intermolecular interactions in the $\alpha$-CD-PCL-IC channels restrict the dynamics of some PCL carbons more than $\gamma$-CD, but that the PCL chains in both CD complexes were found to be more mobile than in semicrystalline bulk PCL samples. In the case of PCL copolymers; PCL-polystyrene (PCL-PS) and PCL-poly(ethylene oxide)-PCL (PCL-PEO-PCL) di- and triblock copolymer-CD-ICs, only the PCL blocks were included in the CD channels.[82]

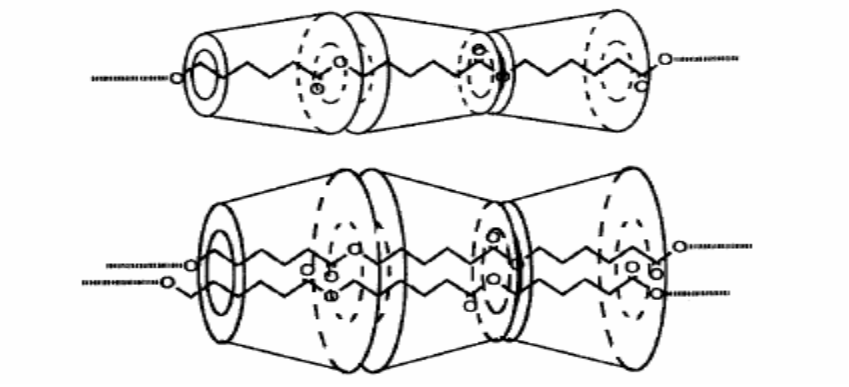

**Figure 38.** Proposed structures of the PCL-α- and γ-CD-ICs.[81]

It was also reported that poly(ethylene terephthalate) (PET) chains were isolated from neighboring PET chains when included in the narrow channels of its γ-CD-IC crystals and the ethylene glycol (EG) units adopted the highly extended g± t g∓ kink conformations (Figure 39). When coalesced from its PET-γ-CD-IC, they found i.) high levels of crystalinity (~ 50%), and ii.) in the non-crystalline regions of the sample the PET chains are retaining the kink conformations required for inclusion.[41f,83]

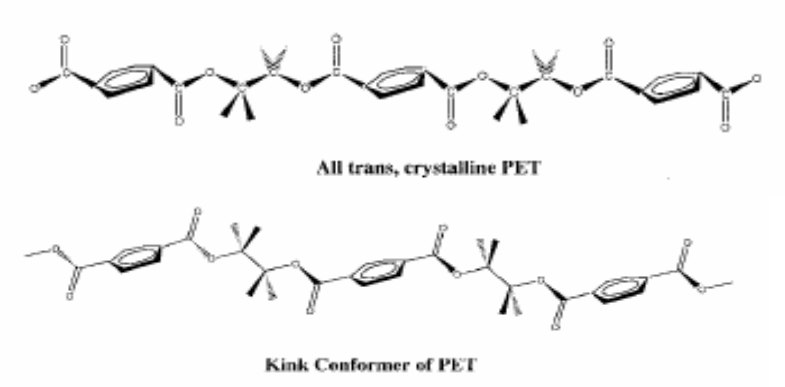


**Figure 39.** All trans crystalline (Top) and γ-CD-IC included and coalesced kink, $g^{\pm}\,tg^{\mp}$ (Bottom) PET conformers.[83]

## 1.3 Coalescence of Polymers from Their Cyclodextrin Inclusion Compounds

### 1.3.1 Concept of Coalescence

Polymer-CD ICs are crystalline compounds obtained by threading of the doughnut shaped CD molecules onto the guest polymer chains. Once guest polymer chains are included inside the CD cavities, they are segregated from neighboring polymers chains by the walls of the CD crystalline lattice and are forced to adopt highly extended conformations by the narrow host CD channels. When CD molecules are removed from polymer-CD IC crystals by dissolving the CD molecules (washing with water or dimethylsulfoxide) or breaking the CD molecules (enzymatic degradation of CD with an α-amylase enzyme) by means which does not have any influence on the polymer, the guest polymer chains are forced to collapse into reorganized bulk solids. This process is called “coalescence” of polymers from their inclusion complexes. Figure 40 illustrates the formation and coalescence of polymer-CD ICs. It has been shown that coalescence of polymers from their CD ICs can result in a significant improvement of their physical properties caused by modification of the structures, morphologies, and even conformations observed for their coalesced samples.

### 1.3.2 Characteristics of Polymers Coalesced from Their CD ICs

The polymer chains in CD channels must adopt highly extended conformations, as confirmed by theoretical calculations and experimental results.[83-86] It is expected that homopolymer chains coalesced from their ICs will retain more extended stretched conformations than samples formed from solutions or melts, where they randomly-coil and entangle. Certain instrumental techniques such as;

wide-angle x-ray diffraction (WAXD),[83] fourier transform infrared spectroscopy (FT-IR)[83], differential scanning calorimetry (DSC)[80] and solid state carbon nuclear magnetic resonance ($^{13}$C-NMR)[80] verify the presence of extended-chain conformations for the coalesced polymers. Some of the findings regarding the characteristics of coalesced polymers are summarized below.

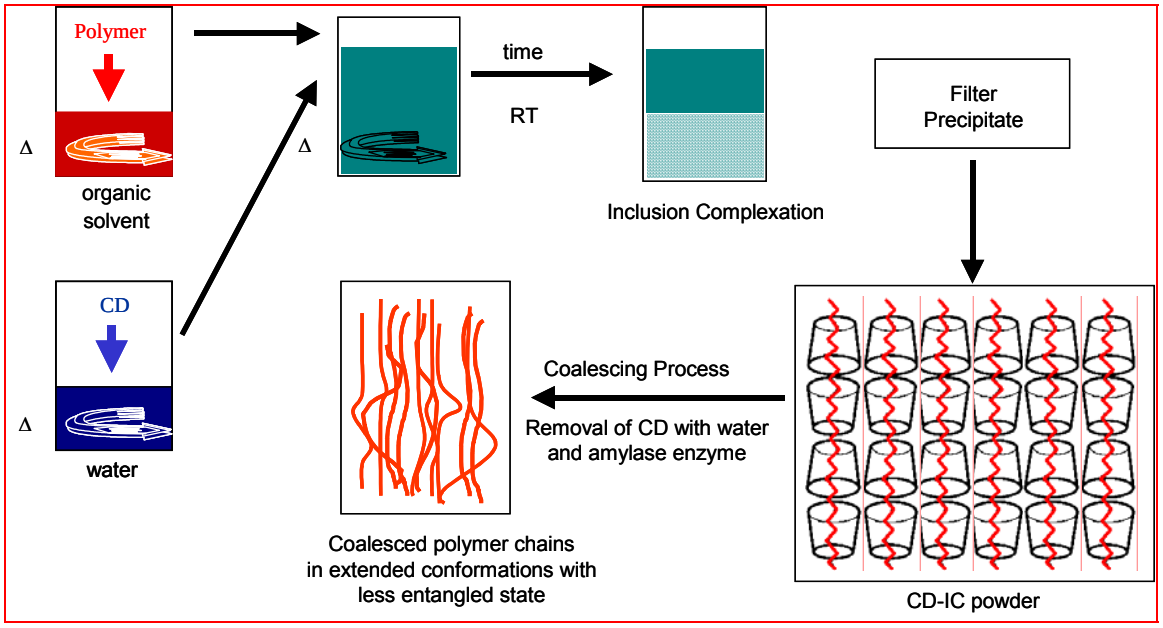


**Figure 40.** Schematic representation of polymer-CD IC formation and the coalescence process.

Bulk poly(ethylene terephthalate) (PET) and bisphenol-A polycarbonate (PC) samples have been formed by the coalescence of their segregated, extended chains from ICs formed between γ-CD host and PET and PC guests.[41f] DSC, FTIR, and WAXD results revealed that coalesced PET and PC samples have different crystalline structures, morphologies and conformations than that of polymer samples obtained by ordinary solution and melt processing techniques. It was demonstrated that PET and PC crystals formed upon coalescence of the highly extended and

segregated polymer chains from the narrow channels of the γ-CD host lattice. Figure 41 show the X-ray diffraction patterns of coalesced PET and PC compared to as-received samples.

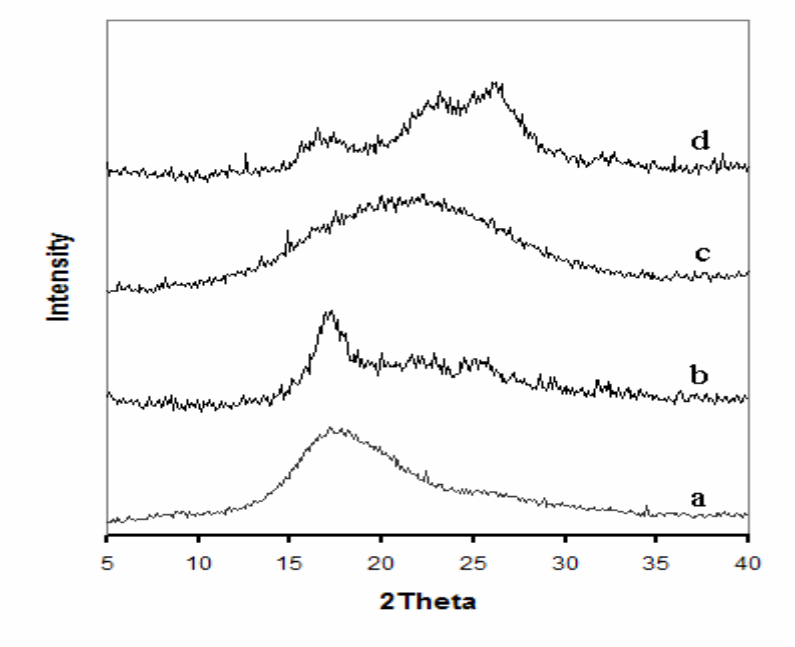


**Figure 41.** X-ray diffraction patterns of (a) as-received and (b)coalesced PC, and (c) as-received and (d) coalesced PET[41f]

As-received PC and PET appear to be amorphous, while the coalesced PC and PET samples are noticeably crystalline as seen in the diffractograms. A weak peak at 2θ ~ 25º is observed in the diffractogram of coalesced PC, and was attributed to an increase in the ordering along the PC chain axis as retained from its highly extended conformation in the PC-γ-CD IC. Diffraction peaks at 2θ = 16.5, 23.2, and 26.0º, which have been assigned[87] to the (010), (110), and (100) lattice planes, are evident in the diffractograms of coalesced PET. The (100) peak, which is

commonly enhanced in oriented samples, such as uniaxially drawn PET fibers and films[88], is clearly more pronounced in the coalesced sample.

Nylon-6 exhibits polymorphism with two types of stable crystal forms: monoclinic α-form and monoclinic γ-form. The γ-form crystal of nylon-6 can be transformed into the α-form crystal by annealing or by drawing of nylon-6. The principal structural difference between α and γ forms is that α is nearly all trans, having a more extended conformation compared to the γ form, and with axial tension, the γ form can usually be converted to the α form[89]. In order to fit in the channel of CD, nylon-6 has to maintain an extended conformation; therefore, the α crystalline conformation would be more favorable than that of the γ form. Wei et al. showed that the γ to α crystal transformation could be induced by coalescence from nylon6-CD-IC.[80] Figure 42 shows the X-ray diffraction patterns of as-received nylon-6 and coalesced nylon-6, where the large increase in the two crystalline peaks intensities confirms the crystal transformation.

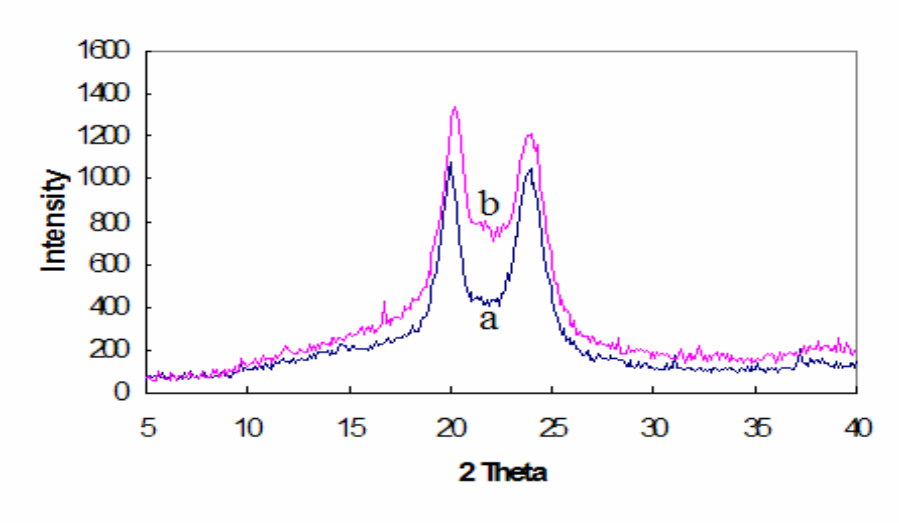


**Figure 42.** XRD patterns of (a) coalesced nylon-6 (b) as-received nylon-6.[80]

The structural manipulation of nylon-6 was also confirmed by FT-IR study. Figure 43 shows the FT-IR spectra of as-received and coalesced nylon-6 samples. The bands at 928, 959 and 1200 $cm^{-1}$ were attributed to the $\alpha$-crystalline phase, whereas the band at 973 $cm^{-1}$ was attributed to the $\gamma$-crystalline phase. For the as-received nylon-6 sample, there is a strong band at 973 $cm^{-1}$, showing that this sample contains a considerable amount of the $\gamma$-crystal form, with a small amount of the $\alpha$-crystal form indicated by the weak bands at 928, 959, and 1200 $cm^{-1}$. In contrast, the FTIR spectrum of coalesced nylon-6 sample does not show the band at 973 $cm^{-1}$, but strong bands at 930, 959 and 1200 $cm^{-1}$, indicating a much higher fraction of $\alpha$-crystal form. According to FTIR studies of nylon-6 yarns, the intensity of the absorption peak at 1030 $cm^{-1}$ increases with increasing draw ratio.[90] In the FTIR spectrum of the coalesced nylon-6, there is a very strong 1030 $cm^{-1}$ peak compared to as-received nylon-6. This may demonstrate that the extended, planar conformation adopted by nylon-6 in the cyclodextrin inclusion complex is substantially retained after coalescence.

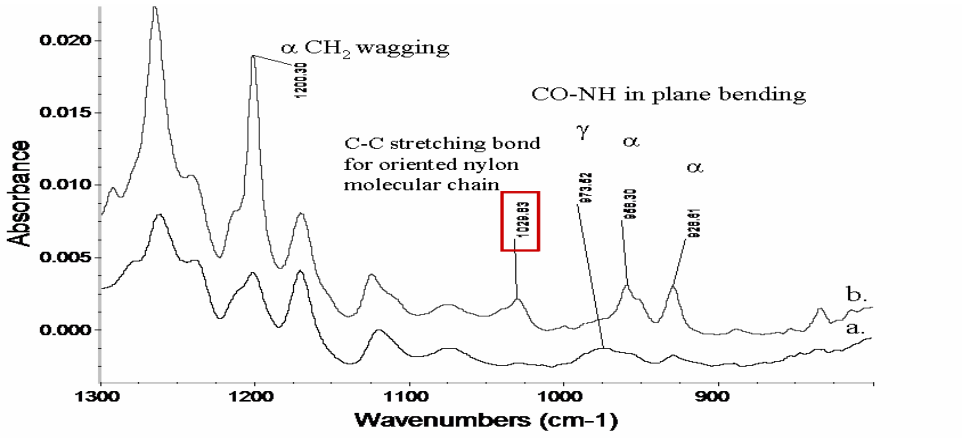


**Figure 43.** FT-IR spectra of (a) as-received and (b) IC coalesced nylon-6.[80]

The crystallization behavior of isotactic polypropylene (i-PP) coalesced from its γ-CD-IC was observed to be different from as-received and precipitated i-PPs.[41a] The crystallization temperature from the melt is found to be higher for the coalesced sample (Figure 44).

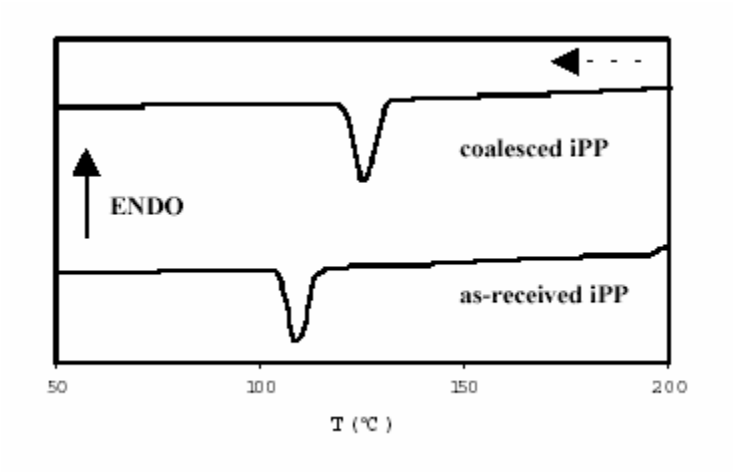


**Figure 44.** The DSC cooling curves of coalesced and as-received isotactic-PP.[41a]

### 1.3.3 Polymer Blends Coalesced From Their Common CD-ICs

The blending of two or more polymer components is a very common commercial approach to obtain new polymeric materials with improved characteristics. The conventional methods for producing polymer blends are melt blending, co-precipitation and solvent casting.[91] When two or more polymer components are blended together, it is likely to obtain phase-separated materials due to the small entropy of mixing and the generally unfavorable enthalpy of mixing when there is no specific interaction (hydrogen bonds, van der Waals and/or polar interactions, etc.) between the polymer side groups. In the case of poor mixing, polymer blends exhibit reduced/inferior properties due to the poor degree of

interfacial adhesion between the components, which creates a multiplicity of defects in the system.[92]

Recently, we have developed a novel approach for mixing of polymer pairs and triplets that are normally incompatible to form blends that possess molecular-level homogeneity (Figure 45).[93] This is achieved by the simultaneous formation of crystalline inclusion compounds (ICs) between host cyclodextrins (CDs) and two or more guest polymers, followed by coalescing the included guest polymers from their common CD–ICs to form intimate blends. This method has successfully produced intimate blends of PCL/poly(L-lactic acid) (PLLA),[94] PC/PMMA,[95] PET/poly(ethylene 2,6-naphthalate) (PEN)[96] and the ternary blend of PC/PMMA/PVAc.[97] Some of these findings are summarized below.

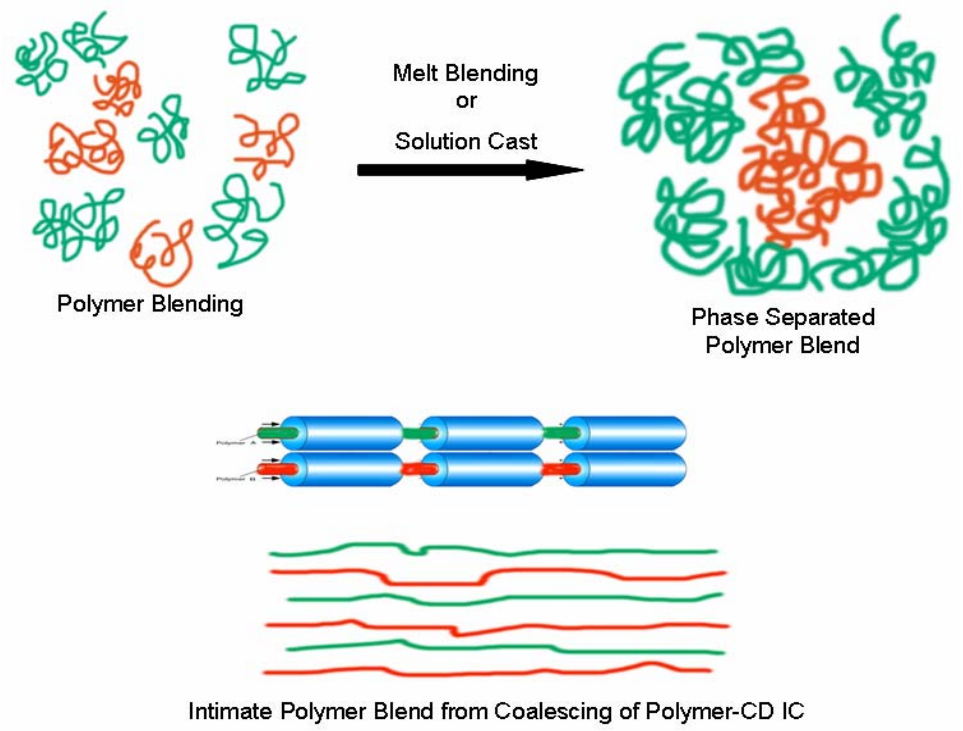


**Figure 45.** Formation of intimate polymer blends by coalescence of common polymer-CD Inclusion compounds.

Intimate blends of PC/PMMA have been prepared by coalescing of the PC/PMMA-γ-CD ICs.[95] Figure 46 presents the second DSC scans of the coalesced PC/PMMA blends with different weight ratios of the individual polymers. DSC thermograms show that only single glass transition temperatures ($T_g$) are observed for each coalesced blend sample, indicating initimate belnding of this polymer pair over the complete composition range. It was also observed, as expected, that the single $T_g$'s decrease with an increase of PMMA content in the coalesced CD-IC blend samples (pure PC and PMMA have $T_g$ at 145 and 118$^o$ C, respectively). The thermal stability of the coalesced blends has also been examined by repeated heating scans after annealing for 2 hours at 200$^o$ C. The continual observation of a single $T_g$ for PC/PMMA blends revealed that there is no phase separation taking place after repeatedly heating to 200$^o$ C or annealing at 200$^o$ C for 2 hours.

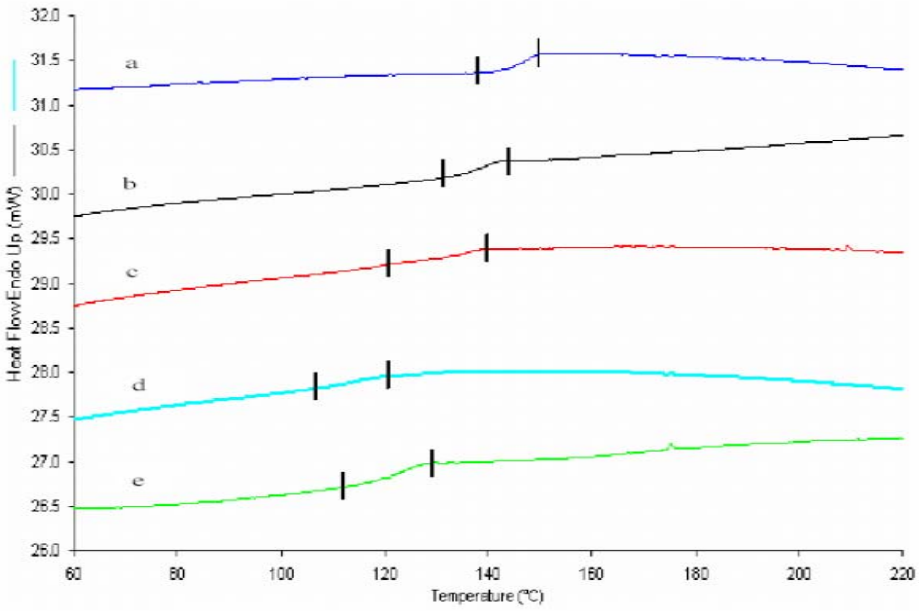


**Figure 46.** The second heating DSC scans of (a) coalesced PC, (b) coalesced PC/PMMA blend (PC:PMMA = 4:1 molar ratio), (c) coalesced PC/PMMA blend (PC:PMMA = 1:1 molar ratio), (d) coalesced PC/PMMA blend ( PC:PMMA = 1:4 molar ratio), and (e) coalesced PMMA.[95]

The ability of α-CD to form ICs with both PLLA and PCL has lead us to prepare an intimately compatible blend by coalescence of PLLA/PCL-α-CD-IC. The miscibility of the PLLA/PCL blend extracted from the α-CD IC channels has been investigated and compared to those of a PLLA/PCL blend cast from their common solution in dioxane. Figure 47 shows the polarized optical photomicrographs of PLLA, PCL and their blends cast from dioxane and coalesced from their common α-CD-IC. It is apparent in the solution-cast blend that a phase-separated morphology was formed, indicating that PLLA and PCL were not fully miscible. The spherulites with a maximum radius of 100 μm are attributed to PCL, whereas the smaller spherulites with a radius of about 20 μm are attributed to PLLA. On the contrary, the homogeneous morphology observed for the coalesced PLLA/PCL blend strongly suggests the intimate blending of these polymer pairs.

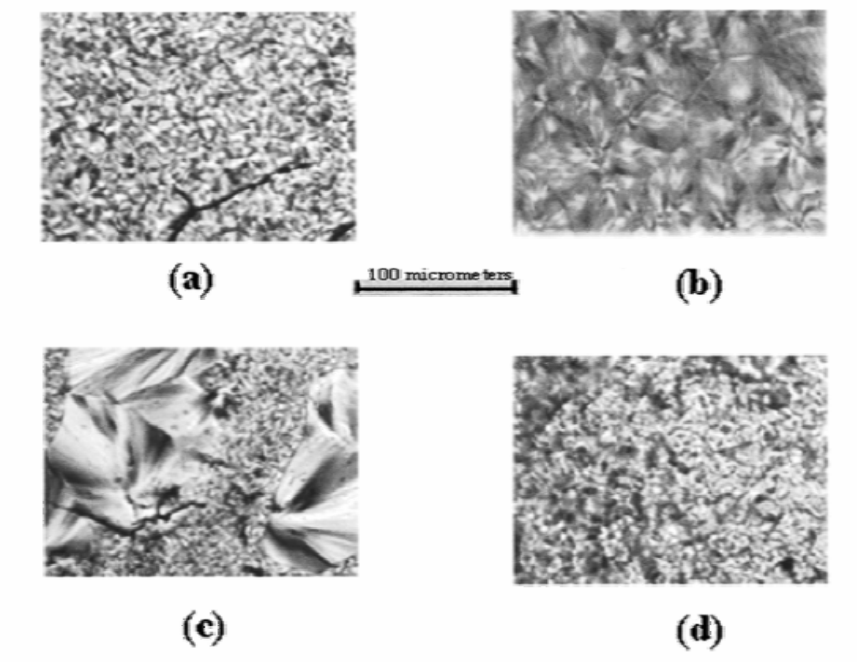


**Figure 47.** Polarized photomicrographs of (a) PLLA, (b) PCL, (c) solution-cast, and (d) coalesced PLLA/PCL blends.[94]

The simultaneous complexation of the aromatic polyesters PET and PEN with γ-CD was also studied[96]. Coalescence of these simultaneously complexed molecules generates an intimate blend of the two polymers. Thermal analysis, *via* differential scanning calorimetry, reveals thermal behavior indicative of an intimate blend of PET and PEN. Proton nuclear magnetic resonance spectroscopy ($^1$H-NMR) confirms that the homogeneous blending is not due to trans-esterification during thermal analysis (Figure 48). The detailed findings regarding intimate blending of the binary pairs of PMMA/PVAc, PC/PVAc, PC/PMMA and the ternary PC/PMMA/PVAc blend will be presented subsequently in the Results and Discussion section.

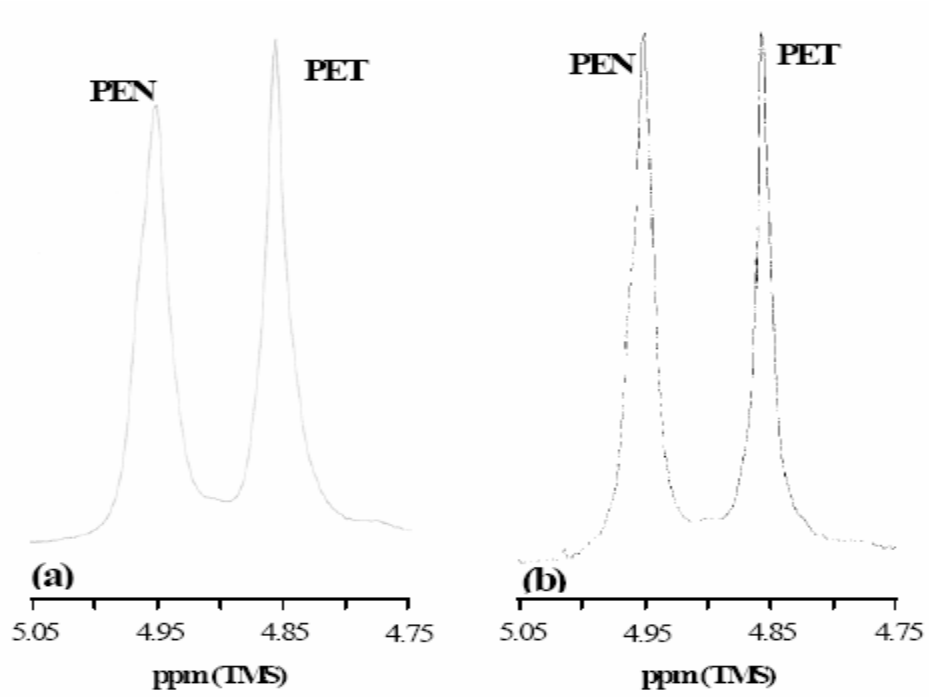


**Figure 48.** $^1$H-NMR spectra of (a) precipitated PET/PEN and (b) coalesced PET/PEN blend.[96]

### 1.3.4 Polymerization in the Presence of Cyclodextrins

The polymerization of various monomers in the presence of CD has been studied extensively in the last decade. Prior to that, there were only a few studies reported in the late 1970s related to the *in situ* polymerization of monomers within soluble cyclodextrin complexes. For instance, hexamethylenediamene complexed with β-CD was prepared and polymerized to obtain polyamide-CD-ICs.[37] The polymerization and copolymerization of vinylidene chloride as adducts of β-CD was also reported.[38]

Cyclodextrins are able to enclose hydrophobic molecules to form host-guest compounds. The hydrophobic guest monomers are encapsulated by the cyclodextrin cavities which results in significant changes of solution properties and reactivity of the guest molecule. Water-insoluble molecules (hydrophobic monomers) become water-soluble on treatment with aqueous solutions of cyclodextrins without any chemical modification of the guest molecule. This is because there are no covalent bonds formed in the host-guest interaction of cyclodextrin and the water-insoluble monomers. Therefore, CDs are being used to obtain complexes with various monomers in aqueous environments and those complexed monomers are being successfully polymerized *via* free radical initiation in water. The resulting polymer precipitates rapidly in high yields and the cyclodextrin slips off step by step from the growing chain and thus remains nearly quantitatively in the water phase.[98] The unthreaded cyclodextrin is soluble in water and thus can be reused to entrap new monomer (Figure 49).

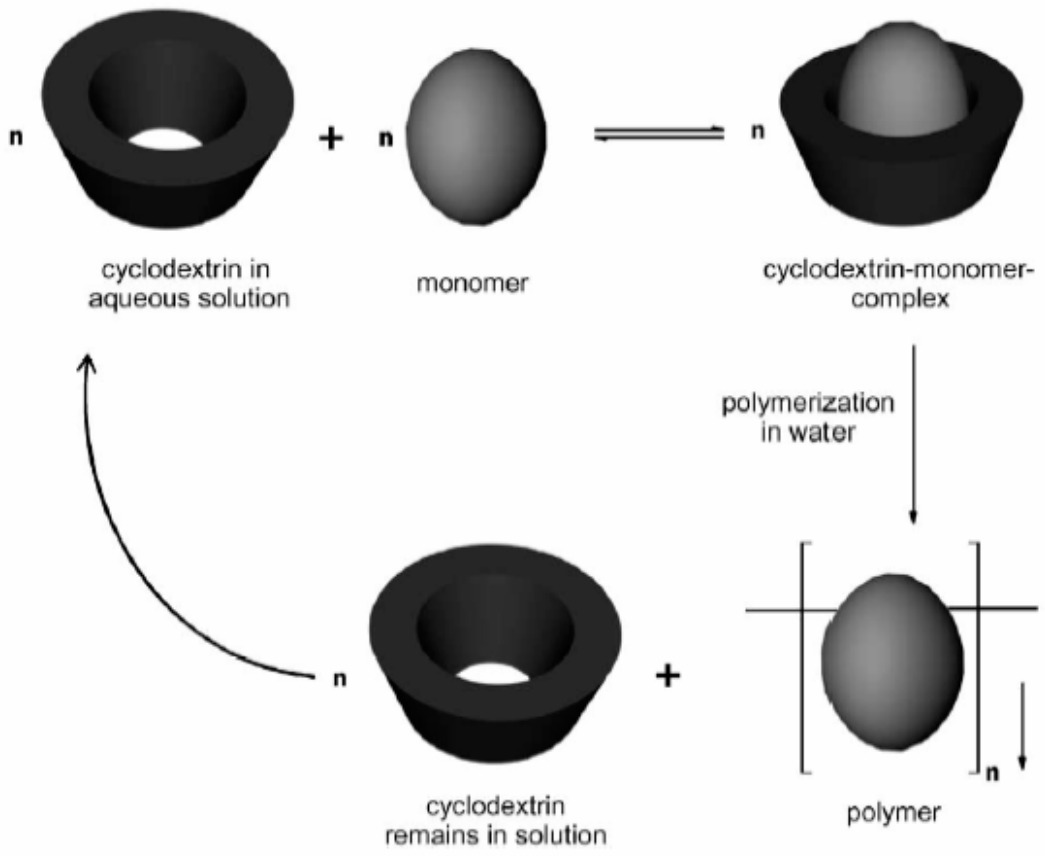


**Figure 49.** Schematic presentation of complexation and polymerization of cyclodextrin complexed monomers.[98]

Replacing organic solvents with an aqueous medium makes the polymerization environmentally friendly. This "green route" for polymerization has been extensively studied by Ritter and his research group[98-113]. They used various monomers to obtain homopolymers and copolymers by using CDs in polymer synthesis. The monomers used for polymerization by free radicals in aqueous medium are summarized in Table 5.

**Table 5.** List of monomers polymerized in the presence of methylated β-CD in water.

| *Monomers* | *Reference* |
|---|---|
| diethyl fumarate | *100* |
| fluorinated 2-vinylcyclopropane | *101* |
| tert-butyl methacrylate | *102* |
| N-methacryloyl phenylalanine methyl ester | *103* |
| N-alkyl methacrylamides | *104* |
| styrene | *105,106,112* |
| methyl methacrylate | *105,106,112* |
| N-methacryloyl-L-tyrosine methyl ester and ethyl ester | *107* |
| 4-vinylbenzaldehyde | *108* |
| fluorinated methacrylates | *109* |
| N-isopropylacrylamide | *110* |
| pyrrole and 3,4-Ethylenedioxythiophene | *111* |

In addition to environmental advantageous, utilization of CDs in polymer synthesis can also provide polymers with narrower particle size distributions and narrower molecular weight polydispersities.[99] For instance, Table 6 and Figure 50 show the results of the polymerization of styrene in the presence of randomly methylated β-cyclodextrin (RAMEB) and the particle size distribution of the resulting polystyrene, respectively.

**Table 6.** Overview of the Reaction Parameters and Results of the Polymerization of Styrene under Semicontinuous Conditions in the Presence of Different Amounts of Randomly Methylated $\beta$-Cyclodextrin (RAMEB) (2 h at 80 °C, Then 1 h at 85 °C)[99]

| polymer 3 | RAMEB (g) | water (g) | $K_2S_2O_8$ (g) | styrene (g) | PD | APS (nm) | PSD |
|---|---|---|---|---|---|---|---|
| a | 0 | 50 | 0.05 | 4.5 | 6.46 | 403 ± 16 | broad |
| b | 0.25 | 50 | 0.05 | 4.5 | 4.02 | 358 ± 2 | narrow |
| c | 0.5 | 50 | 0.05 | 4.5 | 3.07 | 267 ± 3 | narrow |
| d | 1.0 | 50 | 0.05 | 4.5 | 2.77 | 318 ± 2 | narrow |

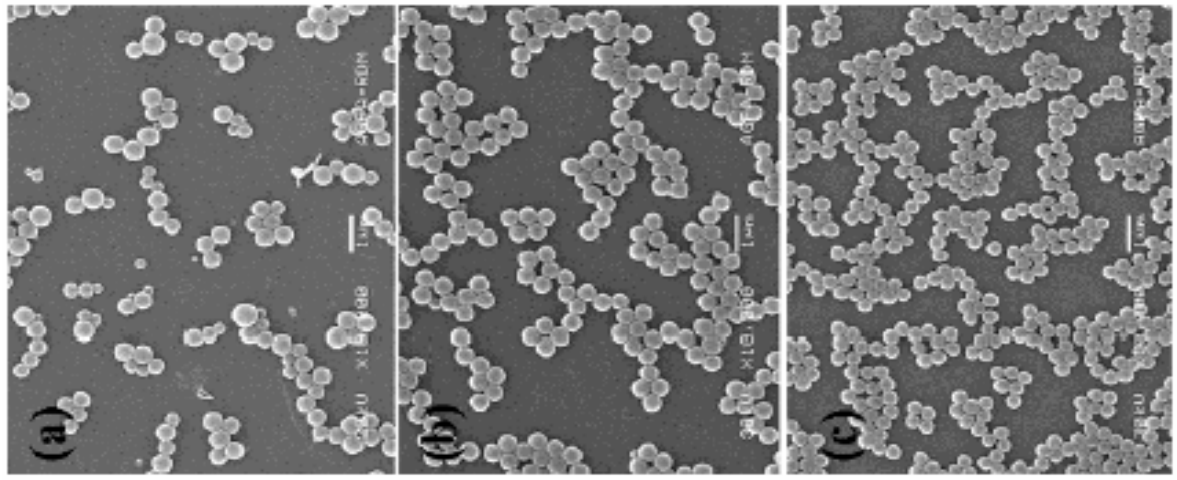


**Figure 50.** SEM image of PS particles: (a) 0 wt % cyclodextrin, broad PSD; (b) 5.6 wt % cyclodextrin, narrow PSD; (c) 11.1 wt % cyclodextrin, narrow PSD.[99]

It was also shown that yields and molecular weights of polymers obtained by polymerization of MMA or styrene from homogenous aqueous m-β-CD solution were significantly higher than those obtained from organic solvents.[106] Thus, this method may provide a means for rapid polymerization to high conversion using water as solvent (Table 7). It was also shown that the degree of polymerization can be controlled effectively by the use of chain-transfer agents. [112]

**Table 7**. Overview of the Reaction Parameters and Results of the Polymerization of MMA (1a) and Styrene (2a) in the Presence of Different Amounts of Randomly Methylated $\beta$-Cyclodextrin (RAMEB).[106]

| Monomer | Solvent | [Monomer] / mol × l$^{-1}$ | [m-$\beta$-CD] / mol × l$^{-1}$ | Total volume / ml | Initiator | $T$ / °C | $t$ / h | $x_p$ | $\overline{M}_n$ / g × mol$^{-1}$ |
|---|---|---|---|---|---|---|---|---|---|
| **2** | EtOH | 0.2 | – | 50 | AIBN 2.5 mol-% | 60 | 24 | 0.25 | 4800 |
| **2a** | water | 0.2 | 0.2 | 50 | $K_2S_2O_8$/$NaHSO_3$ 5 mol-% | 60 | 24 | 0.84 | 10000 |
| **1** | EtOH | 0.2 | – | 50 | AIBN 2.5 mol-% | 60 | 24 | 0.33 | 13000 |
| **1a** | water | 0.2 | 0.2 | 50 | $K_2S_2O_8$/$NaHSO_3$ 5 mol-% | 60 | 24 | 0.88 | 25000 |
| **1** | MeOH | 0.375 | – | 20 | VA O44 5 mol-% | 40 | 6 | 0.05 | 11000 |
| **1a** | water | 0.375 | 0.375 | 20 | VA O44 5 mol-% | 40 | 6 | 0.95 | 33000 |

Using CDs can also lead to surfactant-free polymerization. The polymer particles, with narrow PSD, prepared with CDs, but without using surfactants and solvent mixtures, can be used directly as taken from the reaction vessel without further purification steps. This could find use in the direct production of solid acrylic resins for powder clear coats by avoiding the processes of distillation and grinding.[113]

A series of $\beta$-CD or 2,6-dimethyl-$\beta$-CD (DM-$\beta$-CD) inclusion complexes with bithiophene (2T) were prepared by Harada et al. (Figure 51)[53]. These inclusion complexes were polymerized by $FeCl_3$, an oxidative initiator, in water to obtain pseudo-rotaxane with high molecular weight of poly(ethylenedioxythiophene) (poly(2T)) (Figure 52). The number-average molecular weight of poly(2T) was found to be up to 5,000 by the MALDI-TOF mass spectroscopy technique. It was observed that the resulting poly(2T) did contain cyclodextrins, suggesting that the poly(ethylenedioxythiophene) has a rotaxane structure where CD molecules located along the polymer chains after the polymerization. This observation is not consistent

with Ritter et al.,[106-107], where the CD molecules dethread from the resulting polymer chains and dissolve in the aqueous medium.

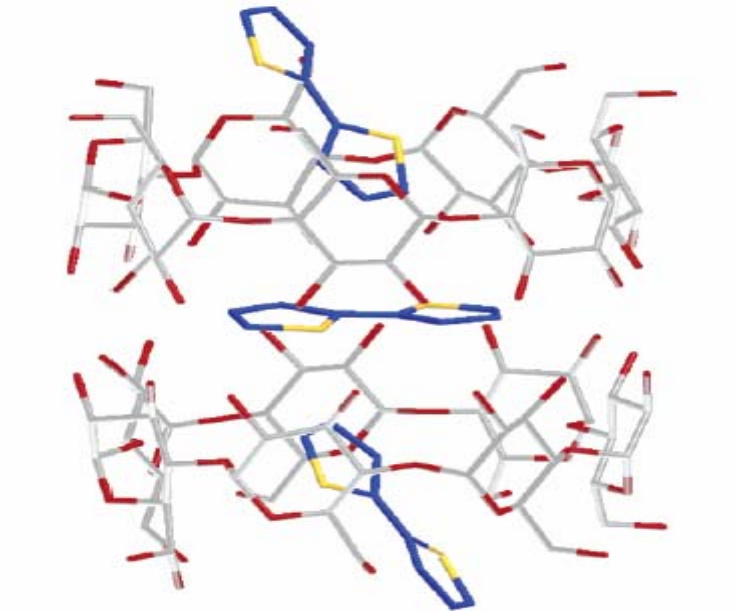

**Figure 51.** Crystal structure of $\beta$-CD-bithiophene inclusion complex. Carbon and oxygen of $\beta$-CD are shown in gray and red, respectively. Carbon and sulfur of bithiophene are shown in blue and yellow, respectively.[53]

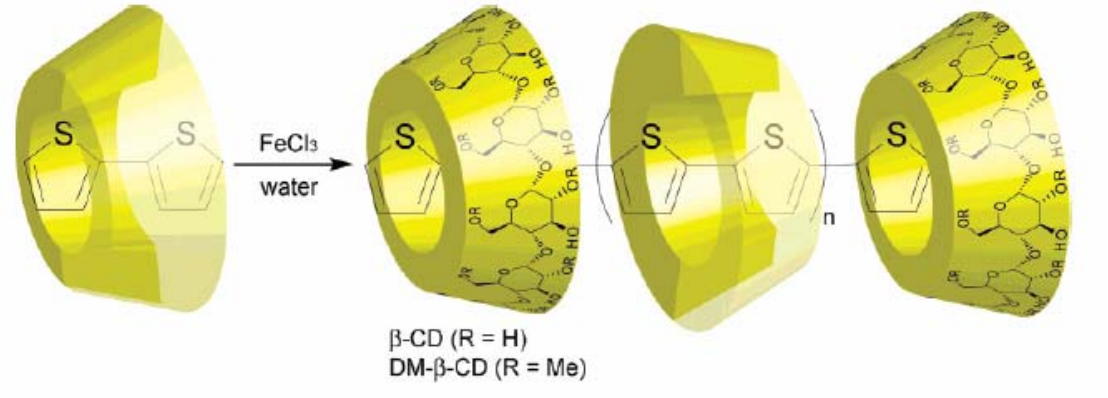


**Figure 52.** Polythiophene prepared from the DM-$\beta$-CD-2T inclusion complex polymerized with $FeCl_3$ initiator in water.[53]

## 1.4 Modeling of Polystyrenes in Channels

Polystyrenes (PS) with various stereosequences have been modeled in narrow cylindrical channels corresponding to those found in polymer-CD-ICs, where the polymers reside as guests inside the CD channels (Figure 53). Isotactic (i) PS is found to fit in channels with narrower diameters (D) than syndiotactic (s) PS, when both adopt conformations permitted by the Yoon, Sundararajan, Flory RIS conformational model[114] of PSs, while atactic (a) PS can be included in channels with D intermediate to those for i- and s-PS. In ICs formed with host $\gamma$-CD and guest a-PS homopolymer and guest PCL-b-a-PS diblock copolymer, it was observed that the a-PS homopolymer and the a-PS copolymer blocks were and were not included, respectively.[115] Thus, it appears that a-PS is barely able to be threaded by $\gamma$-CD, whose internal diameter is ~9 Å. Because the channel conformers found for i- and s-PS have smaller and larger diameters, respectively, than those found for a-PS, we would expect i-PS to be complexed by $\gamma$-CD, while s-PS might not.

In Table 8, we present a summary of our search for potential channel conformers for the tetrad stereoisomers of PS.[116] The most striking observation to be made is the disparity in the channel sizes (D) required to accommodate the different PS stereoisomers. While the i-PS stereoisomer (mmm) requires an 8.5 Å channel, the s-PS stereoisomer (rrr) cannot be accommodated in a cylindrical channel with a D , 10:5 Å , or an ~25% greater cross-section than that of the narrowest channel conformer found for the i-PS stereoisomer. The details of modeling and the calculation for the PS conformers can be found in the referenced article.[116] Also note that with the exception of the mrm and rmr PS tetrads, the probabilities of other

channel conformers found for the PS stereoisomers are very small. In contrast, the probability for the mrm and rmr PS stereoisomer channel conformers are much higher.

**Table 8.** Polystyrene Stereoisomer Channel Conformations.[116]

| Stereoisomer | Channel Diameter, Å | Conformer | Probability* |
|---|---|---|---|
| ***mmm*** | 8.5 | tttttgg and gttttgg | 0.0000003 |
| ***mrm*** | 9.0 | ttgttgt | 0.0012 |
| ***rrm*** | 9.2 | tgttgtt | 0.0000002 |
| ***mmr*** | 9.3 | tttttgg | 0.000007 |
| ***rmr*** | 10.4 | tttggtt | 0.00005 |
| ***rrr*** | 10.5 | tgttttg and tgttgtt | 0.000005 |

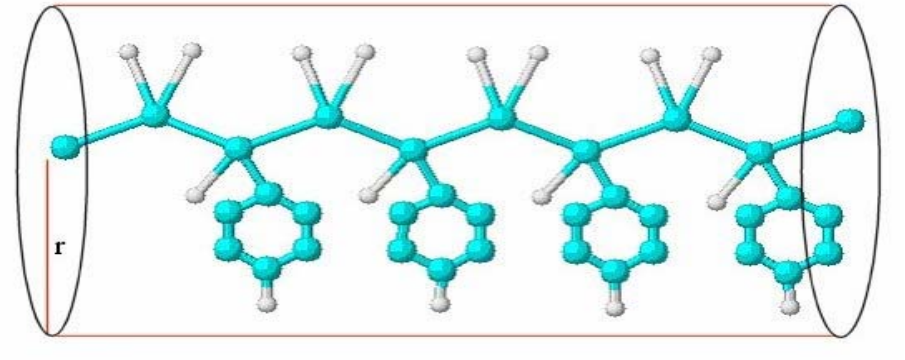


**Figure 53.** PS tetrad fragment (mmm = dddd) used in the search for channel conformers.

This would imply that the free-radical polymerization of styrene in the narrow channels of its IC formed with γ-CD, for example, might produce a PS with alternating m and r diads or i-PS rather than a- or s-PSs. This suggestion is made by analogy to our previous modeling[117] of polypropylene (PP) stereoisomers in channels with diameters (D, 5:5 Å) appropriate to ICs formed with PHTP and urea hosts. There it was observed that all PP tetrad stereoisomers could be included in a

5.5 Å channel, but the probability of the channel conformers for the rrr isomer, or s-PP, were again at least two orders of magnitude greater than those of the other stereoisomeric channel conformers. When propylene monomer was formed into an IC with PHTP and then free-radically polymerized in situ, the resulting PP was found[118] to be predominantly syndiotactic, as suggested by our modeling of PP stereoisomers in channels appropriate to PHTP-ICs.

## 1.5 Motivation

### 1.5.1 Reorganization and Improvement of Bulk Polymers by Processing with Their Cyclodextrin Inclusion Compounds

The properties of polymers, such as glass transition temperature ($T_g$), melting point ($T_m$), crystallinity and thermal degradation ($T_d$) etc., are significantly affected by their chain conformations, entanglements between the chains and by the intra and intermolecular attractions between the individual polymer chains. It is very essential to understand the nature of the isolated individual polymer chains in order to modify and enhance the properties of bulk polymers. The motivation for studying polymer-CD-ICs is due to the unique environment provided for the included polymer chains by the narrow channels of CD molecules.

Through the formation of polymer-CD-ICs, it is possible to create an environment for individual polymer chains which are extended and segregated in the narrow channels of their ICs. The guest polymer chains are confined to narrow, cylindrical channels created by the CD host, where the polymer chains are highly extended and are isolated from neighboring polymer chains by the IC channel walls. When polymers are coalesced from their ICs, the resulting consolidated bulk phase

may have a structure, morphology, and even constituent chain conformations different from those found in bulk polymer samples formed from their disordered, randomly coiling, and possibly entangled melts and solutions. Our aim is to obtain bulk polymers having extended, ordered, and unentangled chains. Polymer chains in such an alternatively organized state should produce polymers with enhanced physical properties and this can be achieved by coalescing polymer-CD-ICs.

In this work, we aim to improve the characteristics of commercial polymers namely; polycarbonate (PC), poly(methylmethacrylate) (PMMA) and poly(vinylacetate) (PVAc), through the formation of and coalescence from their inclusion compounds formed with cyclodextrins. It is expected chains will have extended conformations and less entangled chains for PC, PMMA and PVAc once they are coalesced form their CD-ICs. Therefore, the reorganization of polymer chains in the bulk would improve the physical properties of PC, PMMA and PVAc, such as glass transition temperature, crystallinity, thermal stability etc.

### 1.5.2 Intimate Blending of Polymer Systems from Their Common Cyclodextrin Inclusion Compounds

When two or more chemically distinct polymers are included in a common IC and then are subsequently coalesced, the consolidated polymer blend that is produced may be intimate and well-mixed, unlike similar blends formed by casting from their common solutions or obtained by melt blending. Here, we seek to develop an approach for mixing of polymer pairs and triplets that are normally incompatible to form blends that possess molecular-level homogeneity. In this study, our objective is to obtain intimately mixed binary blends of PC/PMMA, PC/PVAc, PMMA/PVAc and

their ternary blend PC/PMMA/PVAc by formation of and coalescence from their common inclusion compounds with γ–CD.

### 1.5.3 Inclusion of Monomers in the CD Channels and Their Polymerization

Polystyrenes (PS) with various stereosequences have been modeled in narrow cylindrical channels corresponding to those found in polymer-inclusion compounds (ICs), such as those formed with host cyclodextrins (CDs), where the polymers reside as guests. Isotactic (i) PS is found to fit in channels with narrower diameters (D) than syndiotactic (s) PS, while atactic (a) PS can be included in channels with D intermediate to those for i- and s-PS. Additionally, molecular modeling studies showed that only isotactic PS stereoisomers can fit into the γ-CD cavity. As a consequence of our molecular modeling findings, we can make the following suggestions:

(1) The free-radical initiated polymerization of styrene monomer in the narrow channels of the styrene-γ-CD-IC, if it is possible, is likely to produce a PS with isotactic stereosequences and atactic/syndiotactic stereosequences would be eliminated.

(2) While the formation of a γ-CD-IC with i-PS should be possible, it appears that a-PS or s-PS may not be included in the channels of the γ-CD-IC crystalline lattice, and so the process of IC formation with γ-CD may be used to separate stereoregular i-PS from a-PS or s-PS. Our aim is to achieve separation of i-PS from a-PS or s-PS from their common solution by using γ-CD. If this can be achieved, we would demonstrate that CD molecule functions as a “nano-filter” which can be used for separation of stereoregular PSs as well as other stereoregular polymers.

## 1.6 References


1. Szejtli, J., Osa, T., *Eds. Comprehensive Supramolecular Chemistry;* Pergamon: Oxford; Vol. 3 (Cyclodextrins), 1996.
2. Harada, A.; Li, J.; Kamachi, M. *Nature*, *370*, 126, 1994.
3. T. Fujiwara, N. Tanaka, and S. Kobayashi: *Chem. Lett.* 739, 1990.
4. T. Endo, H. Nagase, H. Ueda, A. Shigihara, S. Kobayashi and T. Nagai: *Chem. Pharm. Bull.* 45, 1856,1997.
5. K. Koizumi, H. Sanbe, Y. Kubota, Y. Terada, and T. Takaha: *J. Chromatogr. A.* 852, 407,1999.
6. K. L. Larsen, *Journal of Inclusion Phenomena and Macrocyclic Chemistry* 43: 1–13, 2002.
7. S. Immel, *Ph.D. Thesis*, Darmstadt University of Technology, 1995.
8. Szejtli, J., *Chem. Rev.*, 98:1743-1753, 1998.
9. Szejtli, J., *Journal of Inclusion Phenomena and Molecular Recognition in Chemistry*, 14 (1): 25-36, 1992
10. M. V. Rekharsky and Y. Inoue, *Chem. Rev.*, 98:1875-1917, 1998.
11. T. Nakagawa, S. Immel, F. W. Lichtenthaler, and H. J. Lindner, *Carbohydr. Res.*, 324:141-146, 2000.
12. Makedonopoulou S, Tulinsky A, Mavridis IM., *Supramolecular Chemistry,* 11 (1): 73-81 1999
13. (a) Ohtsuki H, Kamei K, Nagata T, Yamamoto T, Matsui Y., *Journal of Inclusion Phenomena and Macrocyclic Chemistry*, 50: 25–30, 2004.

(b) Fu Y, Liu L, Guo QX., *Journal of Inclusion Phenomena and Macrocyclic Chemistry*, 43 (3-4): 223-229, 2002.

14. Fei X, Hui YZ, Rudiger V, Schneider HJ., *Journal of Physical Organic Chemistry*, 10 (5): 305-310,1997.
15. Bojinova T, Coppel Y, Lauth-de Viguerie N, Milius A, Rico-Lattes I, Lattes A., *Langmuir* 19 (13): 5233-5239, 2003.
16. Setnicka V, Urbanova M, Kral V, Volka K., *Spectrochimica Acta Part A-Molecular and Biomolecular Spectroscopy,* 58 (13): 2983-2989, 2002.
17. Rimmer S., *Macromolecular Symposia*, 150: 149-154, 2000.
18. Wu M, Yuguchi Y, Kumagai T, Endo T, Hirotsu T., *Chemical Communications* (11): 1288-1289, 2004.
19. (a) Nasongkla N, Wiedmann AF, Bruening A, Beman M, Ray D, Bornmann WG, Boothman DA, Gao JM., *Pharmaceutical Research*, 20(10):1626, 2003.

    (b) Wen XH, Liu ZY, Zhu TQ, Zhu MQ, Jiang KZ, Huang QQ., *Bioorganic Chemistry*, 32 (4): 223-233, 2004
20. (a) Harada, A., Li, Kamachi, J. *Carbohydrate Res.,305*, 127, 1998.

    (b) Bullions TA, Wei M, Porbeni FE, Gerber MJ, Peet J, Balik M, White JL, Tonelli AE., *J Polymer Sci. Part B-Polymer Physics*, 40 (10): 992-1012, 2002.
21. (a) Aachmann FL, Otzen DE, Larsen KL, Wimmer R., *Protein Engineering*, 16 (12): 905-912, 2003.

    (b) Rusa CC, Bridges C, Ha, S-W, Tonelli AE. *Macromolecules*, 38:5640-5646, 2005
22. (a) Hedges, A. R., *Chem. Rev.*, *98,* 2035-2044, 1998.

(b) E.M. M. Del Valle, *Process Biochemistry,* 39, 1033-1046, 2004.

(c) Szejtli, J., *J. Mater. Chem.,* 7(4):575-587, 1997.

23. (a) Lajos Szente and Jozsef Szejtli, *Trends in Food Science & Technology,* 15:137–142, 2004.

(b) Reineccius TA, Reineccius GA, Peppard TL, *Journal of Food Science*, 68 (4): 1234-1239, 2003.

(c) Hedges A, McBride C, *Cereal Foods World*, 44 (10): 1999.

(d) Bhesh R. Bhandari, Bruce R. D'Arcy, and Indra Padukka *J. Agric. Food Chem.*, *47,* 5194-5197, 1999.

(e) Avinash Kant, Robert S. T. Linforth, Joanne Hort, Aandrew J. Taylor, *J. Agric. Food Chem.*, *52,* 2028-2035, 2004.

(f) Sri Yuliani, Bhesh Bhandari, Rulande Rutgers, and Bruce D'Arcy, *Food Reviews International*, 20(2):163-185, 2004.

24. (a) J. Szejtli , *Starch/Stärke*, 55, 191-196, 2003.

(b) Lo Nostro P, Fratoni L, Baglioni P., *Journal of Inclusion Phenomena and Macrocyclic Chemistry*, 44 (1-4): 423-427, 2002.

(c) Buschmann HJ, Knittel D, Schollmeyer E., *Journal of Inclusion Phenomena and Macrocyclic Chemistry*, 40 (3): 169-172, 2001.

25. (a) Prasad; Nikhil, Straus; David, Reichart; Glen, *United States Patent:* 6,287,603, 1999.

(b) Moldenhauer; Jens-Peter, Regiert; Marlies, Wimmer; Thomas, *United States Patent*: 5,985,296, 1998.

(c) Borgher, Sr.; Thomas A., Palmer; Clyde D., Trinh; Toan, Wendland; Paul A., *United States Patent:* 5,139,687, 1990.

(d) Chapman; B. Edgar, Trinh; Toan, *United States Patent*: 5,990,070, 1998.

(e) Turner; John Christopher, Demeyere; Hugo Jean Marie, Wendt; Hans, et al. *United States Patent*: 6,794,356, 2002.

26. Pitha; Josef , *United States Patent*: 6,001,821, 1998.

(b) Loftsson; Thorsteinn, *United States Patent*: 5,472,954, 1995.

27. (a) Szejtli, J. *Medicinal Research Reviews,* 14(3): 353-386, 1994.

(b) Thorsteinn Loftsson, Marcus E. Brewster, *Journal of Pharmaceutical Sciences,* 85(10): 1017-1025.

(c) Enrico Redenti, Lajos Szente, József Szejtli, *Journal of Pharmaceutical Sciences,* 89(1): 1-8.

(d) Oda M, Saitoh H, Kobayashi M, Aungst BJ, *International Journal of Pharmaceutics,* 280 (1-2): 95-102, 2004.

(e) Daniel-Mwambete K, Torrado S, Cuesta-Bandera C, Ponce-Gordo F, Torrado JJ, *International Journal of Pharmaceutics,* 272 (1-2): 29-36, 2004.

(f) Norased Nasongkla, Andy F. Wiedmann, Andrew Bruening, Meghan Beman, Dale Ray, William G. Bornmann, David A. Boothman, and Jinming Gao , *Pharmaceutical Research*, Vol. 20, No. 10.

28. http://www.cyclodex.com/

29. Pierandrea Lo Nostros, Laura Fratoni, Piero Baglioni, *Journal of Inclusion Phenomena and Macrocyclic Chemistry* 44: 423–427, 2002.

30. Brian George, Muthu Govindaraj, Hitoshi Ujiie); Harold Freeman, Sam Hudson, *NTC Project: C02-PH03*

31. (a) Foulon C, Danel C, Vaccher MP, Bonte JP, Vaccher C, Jean-Francois J, *Electrophoresis,* 25 (16): 2735-2744, 2004.

    (b) Singh M, Sharma R, Banerjee UC, *Biotechnology Advances*, 20 (5-6): 341-359, 2002.

32. Inokuma S, Kimura K, Funaki T, Nishimura J, *Journal of Inclusion Phenomena and Macrocyclic Chemistry,* 39 (1-2): 35-40, 2001.

33. Hilmi A, Luong JHT, Nguyen AL, *Chemosphere,* 36 (15): 3137-3147, 1998.

34. http://www.cyclolab.hu

35. Bettinetti, G., Melani, F., Mura, P., Monnanni, R., Giordano, F. *J Pharm Sci.,* 1991, *80*,1162.

36. Akira Harada and Mikiharu Kamachi, *Macromolecules* 1990,23, 2823-2824.

37. Ogata, N., Sanui, K., Wada, *J. J Polym Chem.,* 1976, *14*, 459.

38. Maciejewski, M. *J Macromol. Sci. Chem.,* 1976, *14*, 459.

39. Hiromichi Okumura, Miyuko Okada, Yoshinori Kawaguchi, and Akira Harada, *Macromolecules* 2000, *33,* 4297-4298.

40. (a) Takeshi Michishita, Yoshinori Takashima, Akira Harada, *Macromol. Rapid Commun.* 2004, 25, 1159–1162.

    (b)Miyuko Okada, Mikiharu Kamachi, and Akira Harada, *Macromolecules* 1999, *32,* 7202-7207

    (c) Harada A, Okada M, *Polymer Journal*, 31 (11): 1095-1098 Part 2, 1999,

(d) Michishita T, Okada M, Harada A, *Macromol. Rapid Commun.* 22 (10): 764-767, 2001.

(e) Okada M, Kawaguchi Y, Okumura H, Kamachi M, Harada A, *Journal of Polymer Science: Part A-Polymer Chemistry* 38: 4839-4849 Suppl. S, 2000.

(f) Kawaguchi Y, Nishiyama T, Okada M, Kamachi M, Harada A, *Macromolecules* 33 (12): 4472-4477, 2000.

(g) Okumura H, Kawaguchi Y, Harada A, *Macromolecules* 36 (17): 6422, 2003.

41. Rusa CC, Rusa M, Gomez M, Shin ID, Fox JD, Tonelli AE, *Macromolecules* 37 (21): 7992-7999, 2004.

(b) Rusa M, Wang XW, Tonelli AE, *Macromolecules,* 37(18): 6898-6903, 2004.

(c) Huang L, Tonelli AE, *J Macromolecular Sci. Reviews in Macromolecular Chem. and Phys.* C38 (4): 781-837 1998.

(d) Huang L, Allen E, Tonelli AE, *Polymer*, 40 (11): 3211-3221 MAY 1999.

(e) Shin ID, Huang L, Tonelli AE , *Macromolecular Symposia*, 138:21-40, 1999.

(f) Bullions TA, Wei M, Porbeni FE, Gerber MJ, Peet J, Balik M, White JL, Tonelli AE, *J Polymer Sci: Part B-Polymer Physics* 40 (10): 992-1012, 2002.

(g) Shuai XT, Porbeni FE, Wei M, Bullions T, Tonelli AE, *Macromolecules,* 35 (8): 3126-3132, 2002.

(h) Porbeni FE, Edeki EM, Shin ID, Tonelli AE *Polymer*, 42 (16): 6907, 2001.

42. A. Harada, J. Li, and M. Kamachi, *Macromolecules* 1993,26, 5698-5703.

43. (a) Harada, A. Li, J.; Kamachi, M. *Nature* 1992, *356*, 325.

(b) Harada A., Li J., Nakamitsu T., et al., *J. Org. Chem*. 1993,*58*, 7524.

44. Saenger, W. in *Inclusion Compounds*, Vol. 2 (Atwood J., Davies J., MacNiclol D.Eds) Academic, London, 1984 chap 8.

45. W. Saenger, J. Jacob, K. Gessler, T Steiner, D Hoffmann, H Sanbe, K Koizumi, S. M. Smith, T Takaha, *Chem. Rev.* 1998, *98,* 178Ỹ1802.

46. Uyar T, Rusa M, Tonelli AE, *Macromol. Rapid Commun.* 25(15):1382, 2004.

47. Topchieva, I.; Panova, I.; Popova, E.; Matukhina, E.; Grokhovskaya, T.; Spiridonov, V.; Gerasimov, V. *J. Polym. Sci., Part A* 2002, *44*, 352-358.

48. Rusa, C.; Bullions, T.; Fox J.; Porbeni, F.; Wang, X.; Tonelli, A. *Langmuir* 2002, *18*, 10016-10023.

49. Lind TK, Kuge T. *Agr Biol Chem* 1970; 34(4): 568-574.

50. T. Uyar, C. C. Rusa, M. A. Hunt, E. Aslan, J. Hacaloglu, A. E. Tonelli. *Polymer* (46) 4762, 2005.

51. J. Storsberg, H. Ritter, *Macromol. Rapid Commun*. 21, 236–241, 2000.

52. Lu J, Mirau PA, Shin ID, Nojima S, Tonelli AE, *Macromolecular Chem. and Phys.* 203 (1): 71-79, 2002.

53. Y.Takashima, Y. Oizumi, K. Sakamoto, M. Miyauchi, S. Kamitori, A.Harada, *Macromolecules* 2004, *37,* 3962-3964.

54. I. Yamaguchi, K. Kashiwagi, T. Yamamoto, *Macromol. Rapid Commun.* 2004, 25, 1163–1166.

55. A. Magnúsdóttir, M. Másson and T. Loftsson, *J. Incl. Phenom. Macroc. Chem.* 44,213-218, 2002.

56. C. DE Brauer, P. Germain and M. P. Merlin, *Journal of Inclusion Phenomena and Macrocyclic Chemistry* 44: 197–201, 2002.

57. Frieder W. Lichtenthaler, Stefan Immel, *Starch/Stärke* 1996, *48*, 145-154.

58. J. Pozuelo, F. Mendicuti, W.L. Mattice, *Macromolecules* 1997,*30,*3685-3690

59. Andini S.; Castronuovo G.; Elia V.; Gallotta, E. *Carbohydr. Res.* 1991,*217*,87.

60. Rekharsky, M. V.; Mayhew, M. P.; Goldberg, R. N.; Ross, P. D.;Yamashoji, Y.; Inoue, Y.; A *J. Phys. Chem*. 1997, *101*, 87-100.

61. Kitamura, K.; Imayoshi, N. *Anal. Sci*. 1992, *8*, 497-501.

62. Ueno, A.; Chen, Q.; Suzuki, I.; Osa, T. *Anal. Chem*. 1992, *64*, 1650-1655.

63. Hamasaki, K.; Ikeda, H.; Nakamura, A.; Ueno, A.; Toda, F.; Suzuki, I.; Osa, T. *J. Am. Chem. Soc.* 1993, *115*, 5035-5040.

64. Suzuki, M.; Sasaki, Y. *Chem. Pharm. Bull*. 1984, *32*, 832-838.

65. Eastman, M. P.; Freiha, C. C.; Hsu, C. C.; Lum, K. C.; Chang, C. A. *J. Phys. Chem.* 1987, *91*, 1953-1956.

66. Ito K.; Kikuchi K.; Okazaki N.; Kobayashi S., *Agric. Biol. Chem*. 1988,*52*,2763.

67. Vazquez, M. L.; Franco, C. M.; Cepeda, A.; Prognon, P.; Mahuzier, G*. Anal. Chim. Acta* 1992, *269*, 239-247.

68. Aversa, A.; Etter, W.; Gelb, R. I.; Schwartz, L. M. *J. Inclusion Phenom. Mol. Recognit. Chem*. 1990, *9*, 277-285.

69. Cohen, J.; Lach, J. L. *J. Pharm. Sci*. 1963, *52*, 132-136.

70. Lach, J. L.; Pauli, W. A. *J. Pharm. Sci.* 1966, *55*, 32-38.

71. Tucker, E. E.; Christian, S. D. *J. Am. Chem. Soc*. 1984, *106*, 1942-1945.

72. Gelb, R. I.; Schwartz, L. M.; Laufer, D. A. *Bioorg. Chem*. 1980,*9*, 450-461.

73. (a) M. Ceccato, P. Lo Nostro, P. Baglioni, *Langmuir* 1997, *13,* 2436-2439.

    (b) A. Becheri, P. Lo Nostro, B. W. Ninham, P. Baglioni, *J. Phys. Chem. B* 2003, *107,* 3979-3987.

74. Rusa, C. C.; Tonelli, A. E. *Macromolecules* 2000, *33*, 1813.

75. Uyar T., Rusa C. C., Rusa M., Wang X., J. Hacaloglu, Tonelli A. E., *Journal of Polymer Science: Part B-Polymer Physics,* (42) 2005.

76. Rusa CC, Uyar T, Rusa M, Wang X, Hunt MA, Tonelli AE. *Journal of Polymer Science: Part B-Polymer Physics* 2004; 42 (22): 4182-4194.

77. Yoshida, K., Shimomura, T., Ito, K., Hayakawa, R. *Langmuir*, 1999,*15*, 910.

78. Shigekawa, H., Miyake, K., Sumaoka, J., Harada, A., Komiyama, M. *J. Am. Chem. Soc.*, 2000, *122*, 5411.

79. Tonelli AE, *Macromolecular Symposia* 203: 71-87, 2003.

80. Wei M, Davis W, Urban B, Song YQ, Porbeni FE, Wang XW, White JL, Balik CM, Rusa CC, Fox J, Tonelli AE, *Macromolecules* 35 (21): 8039-8044, 2002.

81. Jin Lu, Peter A. Mirau, and Alan E. Tonelli, *Macromolecules* 2001, *34,* 3276.

82. Lu J, Mirau PA, Shin ID, Nojima S, Tonelli AE, *Macromolecular Chem. and Phys.* 203 (1): 71-79, 2002.

83. Wei M, Bullions TA, Rusa CC, Wang XW, Tonelli AE, *Journal of Polymer Science: Part B-Polymer Physics* 42 (3): 386-394, 2004.

84. Tonelli AE, *J Polymer Sci: Part B-Polymer Physics* 40 (12): 1254-1260, 2002.

85. Tonelli AE, *Polymer* 43 (2): 637-642, 2002.

86. Tonelli AE, *Polymer* 43 (22): 6069-6072, 2002.

87. Lindner, W. L. *Polymer*, 1973, *14*, 9.

88. Goschel, U. *Polymer*, 1996, *37*, 4049.

89. Dasgupta, S., Hammond, W. B., Goddard, W. A. *J. Am. Chem. Soc.* 1996, *118,* 12291.

90. Vashanthan, N., Salem D. R., *J. Polym. Sci. Polym.: Part B: Phys. Ed.* 2001, *39*, 536

91. Utracki L. A., '*Polymer Alloys and Blends-Thermodynamics and Rheology*', Oxford University Press, New York, 1990.

92. D. R. Paul, S. Newman, '*Polymer Blends*', Academic Press, New York, Volume 1-2, 1978.

93. Rusa C. C., Wei M., Shuai X., Bullions T. A., Wang X., Rusa M., Uyar T., Tonelli A. E., *J Polymer Sci: Part B-Polymer Physics*, 42(23):4207-4224, 2004.

94. Rusa C. C., Tonelli A. E., *Macromolecules,* 33 (15): 5321-5324, 2000.

95. Wei, M. Tonelli, A. E. *Macromolecules, 34,* 4061, 2001.

96. Bullions T. A., Edeki E. M., Porbeni F. E., Wei M., Shuai X., Rusa C. C., Tonelli A. E., *J Polymer Science: Part B-Polymer Physics*, 41 (2): 139-148, 2003.

97. Rusa C. C., Uyar T., Rusa M., Hunt M. A., Wang X., Tonelli A. E., *Journal of Polymer Science: Part B-Polymer Physics*, 42 (22): 4182-4194, 2004.

98. Helmut Ritter, Monir Tabatabai, *Prog. Polym. Sci.* 27 (2002) 1713–1720.

99. J. Storsberg, H. V. Aert, C. V. Roost, H. Ritter, *Macromolecules* 2003,*36,*50.

100. Choi SW, Ritter H *Macromol. Rapid Commun.* 25 (6): 716-719, 2004.

101. Choi SW, Kretschmann O, Ritter H, Ragnoli M, Galli G, *Macromolecular Physics and Chemistry*, (12): 1475-1479, 2003.

102. Schwarz-Barac S, Ritter H, *Journal of Macromolecular Science: Pure and Applied Chemistry,* A40 (5): 437-448 2003.

103. Schwarz-Barac S, Ritter H, Schollmeyer D, *Macromol. Rapid Commun,* 24 (4): 325-330, 2003.

104. Ritter H, Schwarz-Barac S, Stein P, *Macromolecules* 36 (2): 318-322, 2003.

105. Storsberg J, V Aert H, V Roost C, Ritter H, *Macromolecules* 36 (1):50, 2003.

106. Storsberg J, Ritter H, *Macromol. Rapid Commun* 21 (5): 236-241, 2000.

107. Tabatabai M, Ritter H, Schmelzer M, *E-Polymers* Art. No. 039, 2002.

108. Heinenberg M, Ritter H, *Macromol. Phys. & Chem.*, 203 (12): 1804, 2002.

109. Storsberg J, Ritter H, *Macromol. Phys. & Chem.*, 203 (5-6): 812-818, 2002.

110. Alupei IC, Alupei V, Ritter H, *Macromol. Rapid Commun* 23 (1): 55-58, 2002.

111. Storsberg J, Ritter H, Pielartzik H, Groenendaal L, *Advances Materials*, 12 (8): 567-569, 2000.

112. Glockner P, Metz N, Ritter H, *Macromolecules* 33 (11): 4288-4290, 2000.

113. Flosbach C, Herm M, Ritter H, Glockner P, *Progress in Organic Coatings*, 48 (2-4): 177-182, 2003.

114. Yoon DY, Sundararajan PR, Flory PJ. *Macromolecules* 1975;8:776.

115. Lu J, Mirau PA, Nojima S, Tonelli AE. In: Cheng HN, English AD, editors. *NMR spectroscopy of polymers in solution and in the solid state. ACS Symposium Series* # 834, Washington, DC: 2002. Chapter 4.

116. M.A. Hunt, D.-W. Jung, M. Shamsheer, T. Uyar, A.E. Tonelli, *Polymer* 45 (2004) 1345–1347

117. Tonelli AE. *Macromolecules* 1991;24:3069.

118. DiSilvestro G, Sozzani P, Farina M. *Polym Prepr (Am Chem Soc, Div Polym Chem* 1986;27(1):92.

# CHAPTER 2

## 2 Reorganization and Improvement of Bulk Polymers by Processing with Their Cyclodextrin Inclusion Compounds

### 2.1 Summary

The formation of polymer-cyclodextrin inclusion compounds of polycarbonate (PC), poly(methylmethacrylate) (PMMA) and poly(vinylacetate) (PVAc) guests with host γ-cyclodextrin (γ-CD) have been successfully achieved. Coalesced bulk polymer samples were obtained by removal of γ-CD from their inclusion compounds (ICs). The chemical and crystalline structures of ICs and coalesced PC, PMMA and PVAc were studied by fourier transform infrared spectroscopy (FT-IR) and wide-angle x-ray diffraction (WAXD). The thermal transitions, thermal stability, and degradation mechanisms of the samples were investigated by differential scanning calorimetry (DSC), thermogravimetric analysis (TGA), and direct insertion probe pyrolysis mass spectrometry (DIP-MS). FT-IR findings suggested that the chain conformations of the bulk polymers were altered when they were included inside the CD channels and these extended chain conformations may have been retained when coalesced from their ICs. Significant improvements were observed in the thermal transitions observed for the coalesced polymers, with glass transitions shifted to higher temperatures. The TGA results reveal that the thermal stabilities of coalesced polymers increased slightly compared to the corresponding as-received polymers. The DIP-MS observations indicated that the thermal stability and degradation products of the polymers are affected once the polymers chains are included inside the γ-CD-IC cavities.

## 2.2 Introduction

Cyclodextrins (CDs), cyclic starch oligomers, may be represented as shallow truncated cones consisting of 6, 7, or 8 glucose units, and are named alpha (α-), beta (β-), or gamma (γ-) cyclodextrins (CDs), respectively (see Figure 1a-b). Although the depth of the cavities for the three CDs is the same (~7.9 Å), their cavity diameters are ~ 4.5, 7, and 8.5-9 Å for α-, β- and γ-CD, respectively.[1] CD molecules can complex and host both polar and nonpolar molecules, as well as polymers (see Figure 1f), as guests inside their cavities due to their unique structure.[2-7]

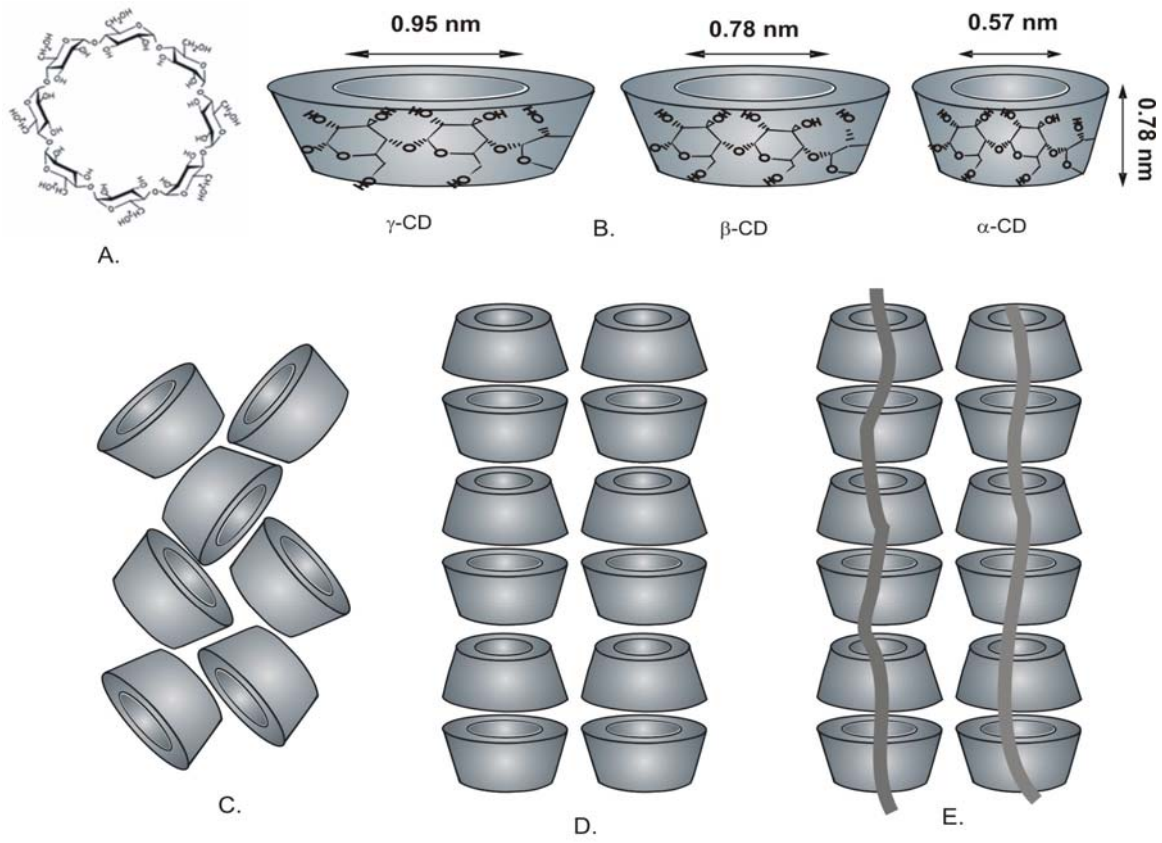


**Figure 1**. (a) γ-CD chemical structure; (b) approximate dimensions of α-CD, β-CD and γ-CD; schematic representation of packing structures of (c) cage-type and (d) head-to-tail channel-type CD crystals; (f) cyclodextrin-inclusion compound (CD-IC) channels with included polymer guests.

Our research group has recently reported that cyclodextrins (CDs) may act as hosts in the formation of inclusion compounds (ICs) with various high molecular weight polymers. Polymer-CD ICs are crystalline compounds obtained by threading of the doughnut shaped CD molecules onto the guest polymer chains. Once guest polymer chains are included inside the CD cavities, they are segregated from neighboring polymers chains by the walls of the CD crystalline lattice and are forced to adopt highly extended conformations by the narrow host CD channels. We have shown that coalescence (removal of CD) of guest polymers from their CD IC crystals can result in a significant improvement of their physical properties caused by modification of the structures, morphologies, and even conformations that are observed for their coalesced bulk samples.[8-9] Recently, we have also developed a novel approach for forming intimately mixed polymer blends by coalescing (removal of CD) bulk polymer pairs from their common CD ICs.[10-14]

Here, we describe the formation of ICs formed between γ-CD and polycarbonate (PC), poly(methylmethacrylate) (PMMA) and poly(vinylacetate) (PVAc) homopolymers. The coalesced bulk polymers were obtained by removal of γ-CD and it was observed that the physical properties of the coalesced polymers were improved when compare to as-received polymers.

## 2.3 Experimental

### 2.3.1 Materials

Polycarbonate (PC) ($M_w$ = 28,800 g/mol, $M_n$ = 17,300 g/mol), atactic-poly(methyl methacrylate) (PMMA) ($M_w$ = 15,000 g/mol), and atactic-

poly(vinylacetate) (PVAc), with $M_w$ = 12,800 and 167,000 g/mol, were purchased from Aldrich Co., and used as received. Tetrahydrofuran (THF) (Aldrich, 99+ %), dioxane (Aldrich, 99+ %), methyl ethyl ketone (MEK) (Fluka, 99+ %) were used without any purification. γ-cyclodextrin (γ-CD), β-cyclodextrin (β-CD) and α-cyclodextrin (α-CD) were obtained from Cerestar (Hammond, IN). The water used in this study was deionized (DI-$H_2O$).

### 2.3.2 Formation of Polymer- γ-CD Inclusion Compounds

The formation of inclusion compounds of γ-cyclodextrin with PC, PMMA and PVAc were carried our separately. According to the literature, we assumed that one γ-CD molecule may host three repeat units of PMMA or PVAc and 0.66 repeat units of PC.[1] For the formation of inclusion compounds, a quantity of 0.480 g (1.88 mmol, repeating unit) of PC or 0.858 g (8.58 mmol, repeating unit) of PMMA or 0.7376 g (8.58 mmol, repeating unit) of PVAc was dissolved in 100 mL of dioxane at 50° C. The γ-CD (3.712 g, 2.86 mmol) was dissolved in 10 mL of DI-$H_2O$ at 50° C and then added drop-wise to the polymer solution, while the stirring rate was kept at maximum and the temperature at 50° C. As the γ-CD solution was added, a white, turbid solution was formed (Figure 2). After stirring for three hours at 50° C, the white suspension was allowed to cool down to room temperature, while the stirring rate was kept low for another three days, because, after many attempts, the time required for obtaining these polymer inclusion compounds with γ-CD in high yield was found to be three days. Yet, the yield of polymer-CD IC was around or less than 30% depending on the guest polymer and more studies needs to be conducted to

optimize the inclusion parameters to increase the yield. The resulting white suspension was then vacuum filtered and the collected precipitate vacuum dried at 60° C for 24 h. The abbreviation for these polymer inclusion compounds are PC-, PMMA- and PVAc-γ-CD IC. It was found that low molecular weight PVAc ($M_w$ = 12,800 g/mol) does not form an inclusion compound with γ-CD. Different solvent systems like THF and MEK other than dioxane, were attempted for the formation of the the PVAc-γ-CD inclusion compound, but these failed. The host (γ-CD) was also changed to α-CD and β-CD, but neither formed an IC with the low molecular weight PVAc sample. The reason could be the branched structure of the PVAc since the CD molecules would exclude the branched chains due to their bulky size (the supplier (Aldrich) reported a branched structure for this polymer by GPC). However, we were able to obtain PVAc-γ-CD IC by using the high molecular weight linear PVAc sample ($M_w$ = 167,000 g/mol).

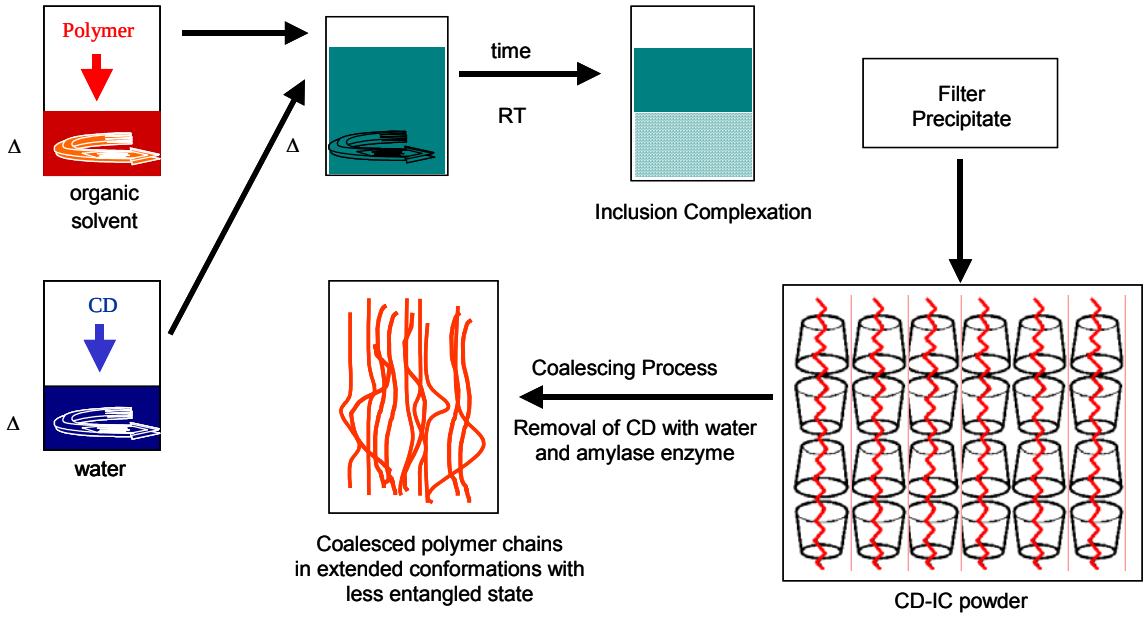


**Figure 2.** Schematic representation of polymer-CD IC formation, the coalescing process and the coalesced polymer.

### 2.3.3 Coalescence of PC, PMMA and PVAc from Their CD-ICs

Host γ-CD was removed from the ICs by washing the white crystals with deionized water overnight at 50° C and the α-amylase enzyme (Clarase L-4000) was used when necessary. The coalesced polymers were then vacuum filtered and rinsed several times with water, and finally vacuum dried at 30-40° C for 2 days.

The inclusion formation of PC with γ-CD was previously reported by our research group.[8] In the present study, a "greener" approach has been applied in the formation of polymer-CD inclusion compounds, in which the organic solvent (dimethyl sulfoxide) used previously for the γ-CD solution is replaced by water. However, the use of organic solvents for dissolution of polymer in the formation of polymer-CD-ICs still remains, and more work needs to be done in order to achieve totally environmentally "friendly" methods for their production. On the other hand, we observed that the coalesced polymers have the same characteristic properties independent of the IC preparation method.

We observed that the process of coalescing PC from its cyclodextrin inclusion compound resulted in a crystalline morphology, whereas the starting material (as-received PC) is completely amorphous. This observation can be explained by self-aggregation of extended and unentangled PC chains into a tighter and more ordered structure, which results in a crystalline phase. Solvent-induced crystallization was ruled out for the coalesced PC sample, because PC chains are segregated from neighboring polymer chains by the walls of the CD in ICs and the host γ-CD was washed out with water, which is a non-solvent for PC.

The control PC sample was prepared by applying the same procedure as the formation of the PC-γ-CD inclusion compound. The same amount of PC was dissolved in dioxane and water added dropwise, instead of CD aqueous solution, into the polymer solution. The precipitation of PC was observed overnight and the powder was collected by filtration after three days of stirring the solution. It was observed that precipitated PC also contains a crystalline phase.

## 2.4 Characterization

### 2.4.1 Wide-Angle X-ray Diffraction (WAXD)

Wide-angle X-ray diffraction (WAXD) measurements were performed with a Siemens type-F X-ray diffractometer using a Ni-filtered $CuK_\alpha$ radiation source ($\lambda$ = 1.54 Å). The diffraction intensities were measured every 0.1° from $2\theta$ = 5 to 30° at a rate of $2\theta$ = 3°/minute. The supplied voltage and current were 30 kV and 20 mA, respectively.

### 2.4.2 Fourier Transform Infrared Spectroscopy (FT-IR)

A Nicolet 510P FT IR spectrometer was utilized to obtain the infrared spectra of samples mixed with potassium bromide (KBr) and pressed into pellets. The spectra were taken over a range of 4000 to 400 $cm^{-1}$, with a resolution of 2 $cm^{-1}$ obtained after 64 scans.

### 2.4.3 Modulated Differential Scanning Calorimetry (M-DSC)

The M-DSC experiments were performed with a Thermal Analysis (TA) DSC Q1000 in modulated mode. Nitrogen was used as purge gas. All samples studied in this work were subjected to heating and cooling cycles consisting of: 1.0 minute

hold at 0° C, ramping to target temperature at 5° C/min, hold there for 1 minute, and samples were then quenched by ramping to 0° C at 200° C/min. Samples were subjected to a second cycle to investigate the change in thermal behavior following the first heat.

### 2.4.4 Thermogravimetric Analysis (TGA)

Thermogravimetric analyses of the PC, PMMA, and PVAC samples were performed with a Perkin-Elmer Pyris 1 thermogravimetric analyzer (TGA). Thermal decompositions were recorded between 25 and 650° C. The heating rate was 20° C/min, and nitrogen was used as a purge gas.

### 2.4.5 Direct Insertion Probe Pyrolysis Mass Spectrometry (DIP-MS):

The direct insertion probe pyrolysis mass spectrometry (DIP-MS) system consists of a 5973 HP quadruple mass spectrometer coupled to a JHP SIS direct insertion probe pyrolysis system. 0.01 mg samples were pyrolyzed in flared glass sample vials. The temperature was increased at a rate of $10^{o}$ C/min and the scan rate was 2 scans/s.

## 2.5 Results and Discussion

### 2.5.1 Wide-Angle X-ray Diffraction (WAXD)

WAXD is a useful characterization technique for investigating the crystalline phase transition between the cage structure of as-received γ-CD·$7H_2O$ (Figure 3a) and the channel structure of polymer-γ-CD ICs (Figure 4). Once the host γ-CD molecules are threaded onto the polymer chains, it is expected that the final IC crystals adopt a channel-type structure. Complicating polymer-CD IC formation is

the ability of dioxane, the polymer solvent used in this work, to precipitate γ-CD in the channel structure from its aqueous solution (Figure 3b). Rusa *et al.* previously observed this behavior by precipitating γ-CD in the channel structure, γ-$CD_{cs}$, using acetone.[15] There, γ-$CD_{cs}$ was reported to only contain water, suggesting that γ-CD channel structure can be preformed in solution. Subsequent vacuum drying destabilizes the channel structure, resulting in an amorphous diffraction pattern (Figure 3c).

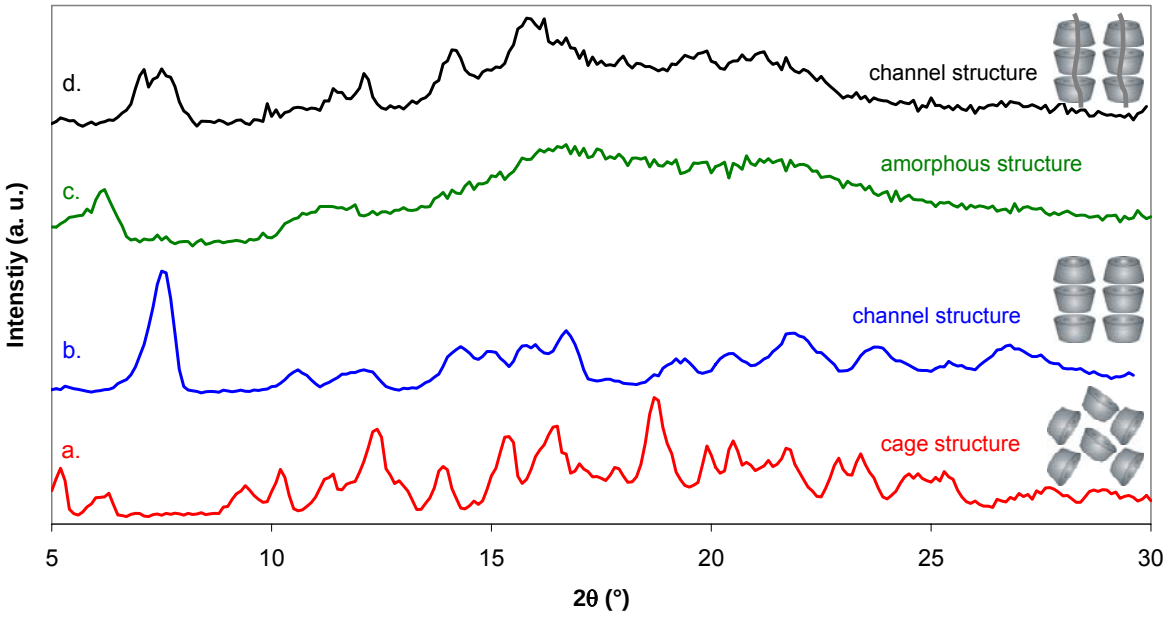


**Figure 3.** X-ray diffraction patterns of (a) as-received γ-CD, (b) γ-CD channel structure, (c) vacuum-dried γ-CD channel structure, and (d) vacuum-dried PMMA-γ-CD IC.

Figure 4 shows WAXD patterns for the three polymer-γ-CD ICs. Each exhibit a pattern consistent with those presented in the literature.[8,12] To confirm the formation of polymer-γ-CD IC crystals, the precipitates resulting from the addition of the cyclodextrin solution to the polymer solutions were vacuum-dried after filtration.

This destroys any γ-CD channel structure with only water included, since γ-$CD_{cs}$ collapses into an amorphous structure upon dehydration of the crystals.[15] However, in case of the polymer-CD ICs, the included polymer chains in the γ-CD channels would preserve the channel structure. The X-ray diffraction pattern of vacuum-dried PMMA-γ-CD-IC crystals is given in Figure 3d. It was observed that the reflections consistent with γ-CD in the channel structure persisted after vacuum drying of PMMA-γ-CD IC. One reflection in particular occurring at 2θ = 7.5° for polymer-γ-CD IC crystals is indicative of γ-CD in the channel structure and has been assigned to the 200 plane of a tetragonal lattice by Takeo and Kuge.[16] Yet, the diffraction pattern of PMMA-γ-CD-IC also indicated the existence of some amorphous structure, which is due to the presence of some γ-$CD_{cs}$, with only water included, that then collapsed into an amorphous structure upon vacuum drying. Diffraction patterns similar to that of PMMA-γ-CD IC were also observed for vacuum dried PC- and PVAc-γ-CD IC samples (not shown).

The presence of a peak at 2θ = 7.5° represents the first evidence that γ-CD molecules formed a channel structure IC with the possible inclusion of polymer guests residing in the γ-CD cavities. FT-IR (next section) and DSC studies were carried out to confirm that the polymers are included in the IC channels. DSC is a useful tool to determine whether or not the polymer chains are included inside the CD cavities: thermal transitions for polymers are observed if there is any uncomplexed polymer present in the CD ICs. None of the DSC scans of PC-, PMMA- or PVAc-γ-CD ICs (data not shown) exhibited glass transitions for any of the

potentially uncomplexed polymers. This result reveals that polymer chains are threaded and covered by γ-CD molecules in the ICs.

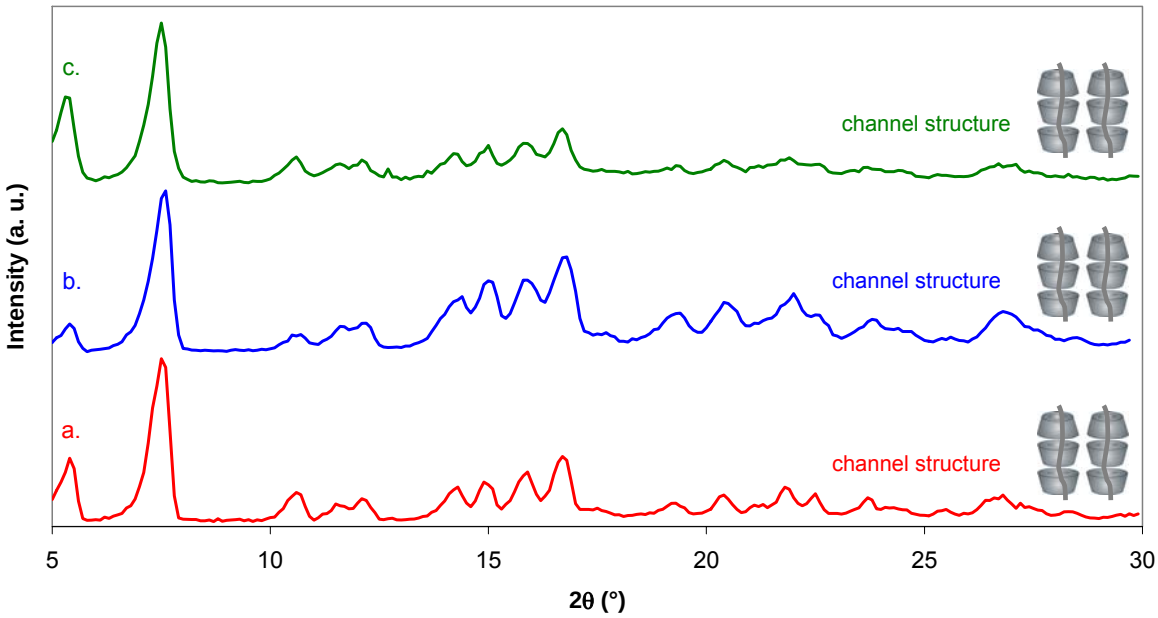


**Figure 4.** X-ray diffraction patterns of (a) PC-γ-CD IC, (b) PMMA-γ-CD-IC and (c) PVAc-γ-CD-IC.

### 2.5.2 Fourier Transform Infrared Spectroscopy (FT-IR)

The FTIR spectra of each polymer-γ-CD IC showed evidence of the presence of each polymer by virtue of C=O absorptions observed at 1730, 1739, and 1775 $cm^{-1}$ for PMMA, PVAc, and PC, respectively (figure 5). The overlayed FT-IR spectra of the as-received PMMA, PVAc and PC and coalesced samples are given in Figures 6 and 7, respectively. No heat treatment has been applied to any of the samples prior to the FT-IR scans. PMMA has an absorption band (C=O stretch) at 1730 $cm^{-1}$ (Figure 6a.), whereas the C=O stretch of PVAc absorbs at 1736 $cm^{-1}$ (Figure 6b.). The absorption peaks observed at 1148 and 1243 $cm^{-1}$ (C-O-C stretching) are from PMMA and the peaks observed at 1376 and 1242 $cm^{-1}$ are from PVAc.[17]

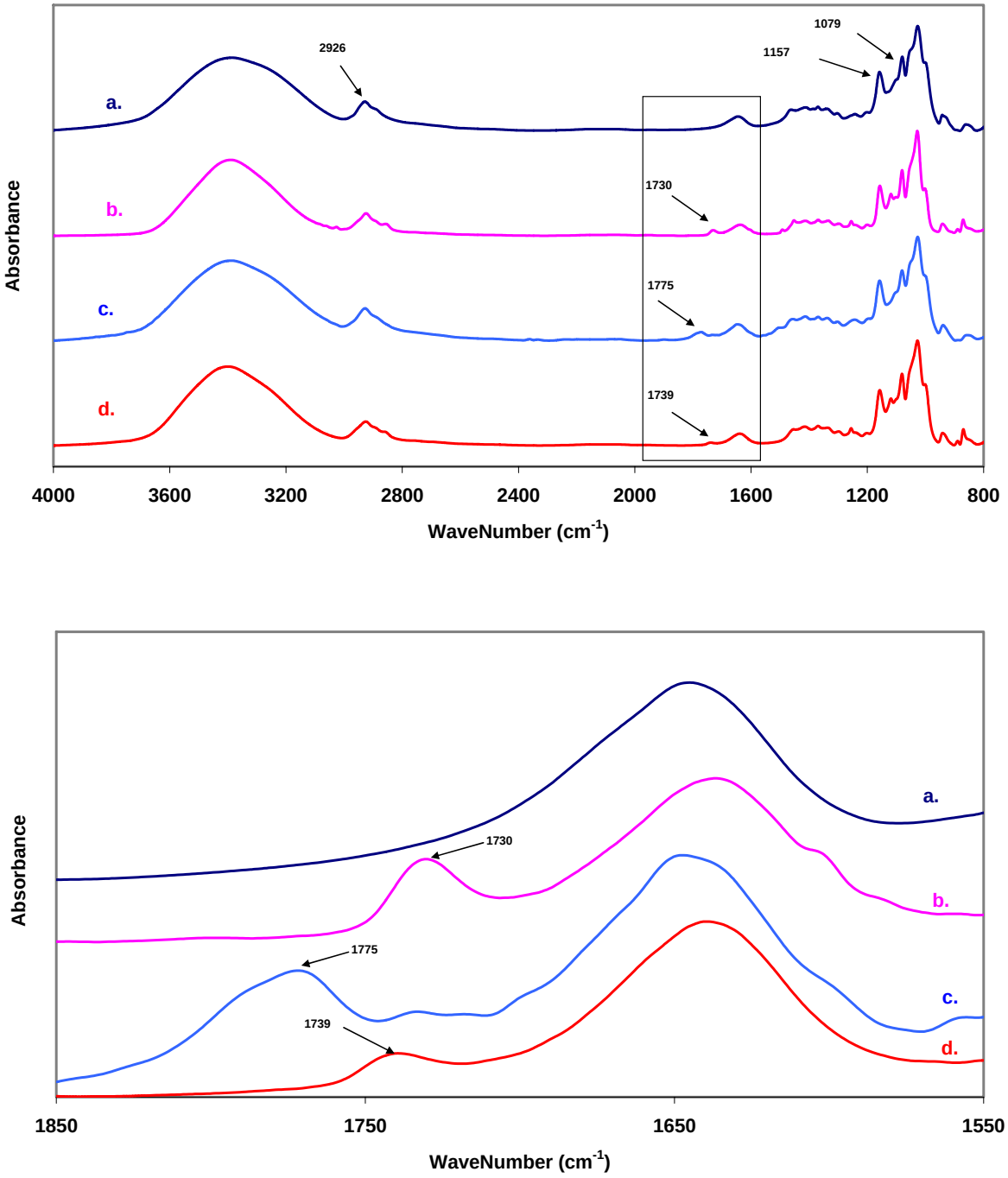


**Figure 5.** FT-IR spectra of (a) as received γ-CD, (b) PMMA-, (c) PC-, and (d) PVAc-γ-CD-ICs.

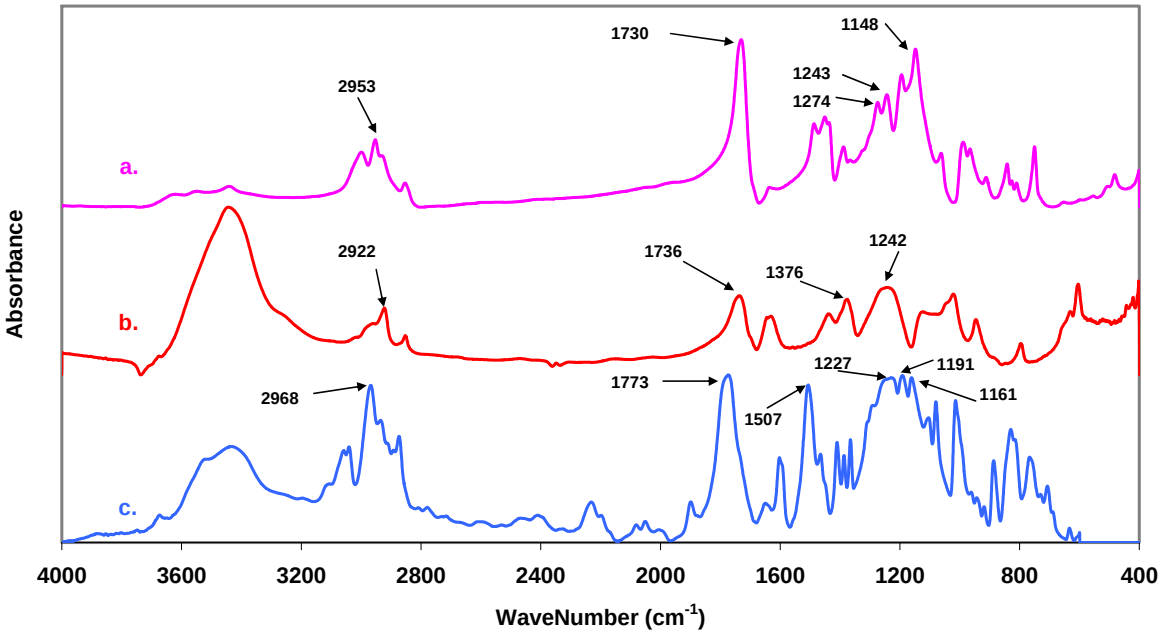


**Figure 6.** FT-IR spectra of as-received (a) PMMA, (b) PVAc, and (c) PC.

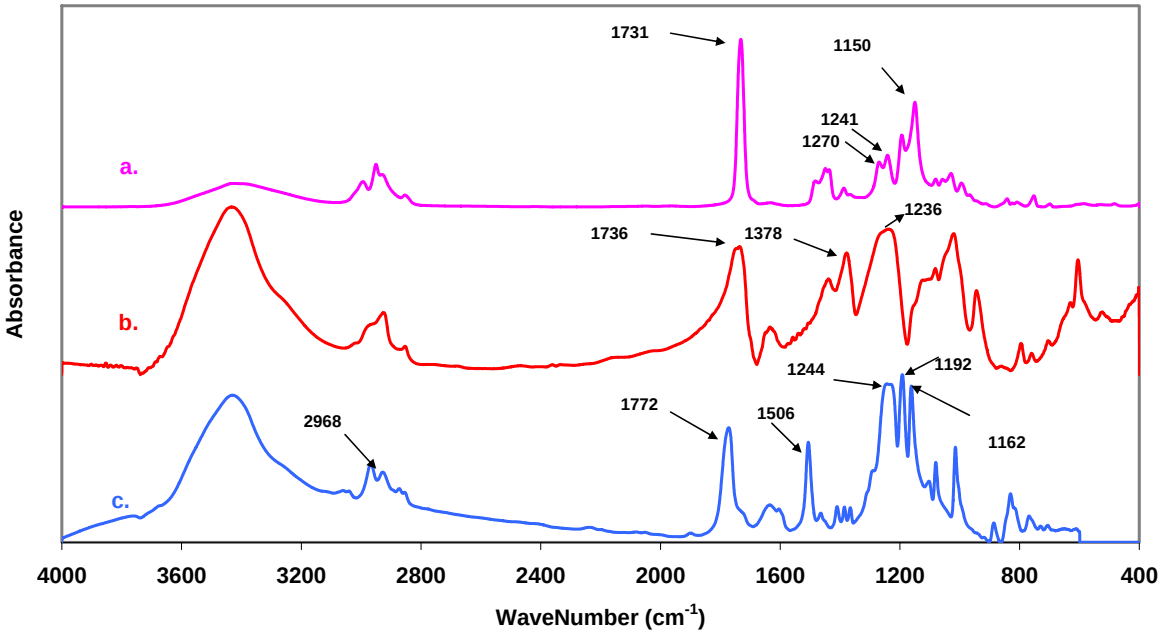


**Figure 7.** FT-IR spectra of coalesced (a) PMMA, (b) PVAc, and (c) PC.

It is usual to observe vibrational absorbance shifts when the interactions between or the local environments around polymer chains are different. Additionally, conformational changes can also be followed by infrared spectroscopy, since some absorption bands are conformationally sensitive. It is likely that when polymer chains are coalesced from their inclusion compounds they solidify in extended conformations that are less entangled. . The infrared spectra of as-received (Figure 6) and coalesced polymers (Figure 7) were examined in order to identify any possible conformational differences between their constituent polymer chains.

In the PMMA polymer backbone, the absorption band at 840 $cm^{-1}$ sensitive to the trans,gauche± conformations is characteristic of random coil chains, , while the absorption band at 860 $cm^{-1}$ is characteristic for the all trans or close to the all trans conformation.[18-21] In Figure 8a, the as-received PMMA has an absorption band at 842 $cm^{-1}$, which is characteristic of random coil chains. In coalesced PMMA (figure 8b), the absorption band due to trans, gauche± conformations is observed at 841 $cm^{-1}$, with a shoulder at 860 $cm^{-1}$, which indicates the presence of the all trans conformation as well, and confirms the existence of some extended chains in coalesced PMMA.

Furthermore, in the coalesced PMMA sample, some small shifts were also observed in other conformationally sensitive absorption bands (1150, 1190, 1240 and 1275 $cm^{-1}$, which are assigned to the C-C-O vibration coupled to the C-O vibration). For instance, the peaks observed at 1148, 1244, and 1274 $cm^{-1}$ in the as-received sample were shifted to 1150, 1241, and 1270 $cm^{-1}$ in the coalesced

sample, respectively. Similarly, in the coalesced PVAc sample, peaks at 1242 and 1376 $cm^{-1}$ shifted to 1236 and 1378 $cm^{-1}$, respectively.

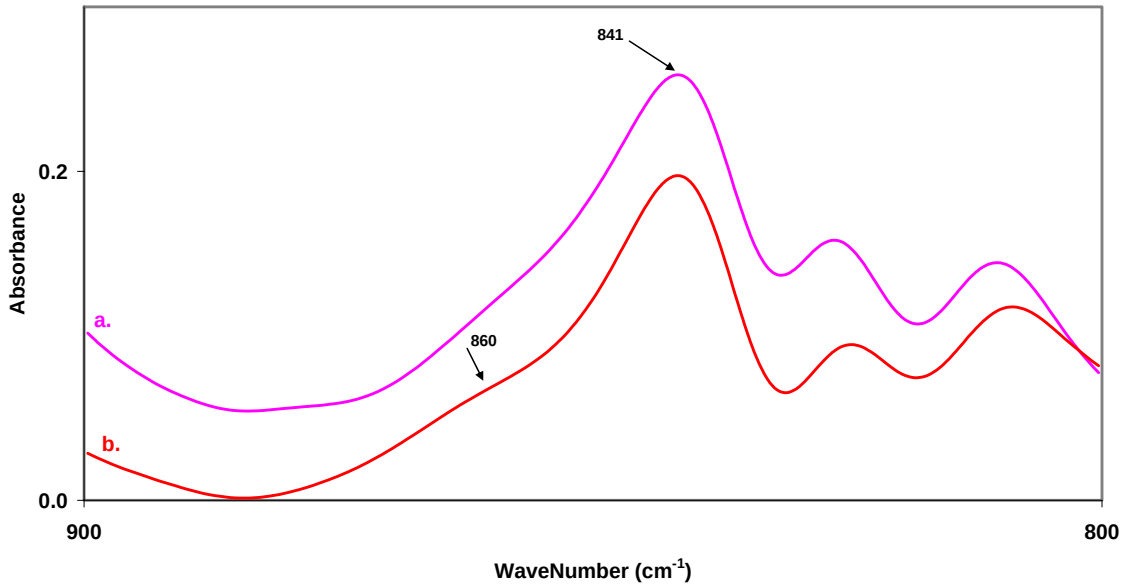


**Figure 8.** FT-IR spectra of (a) as-received PMMA and (b) coalesced PMMA.

Additionally, the most significant difference is the much improved resolution observed in the FTIR spectra of the coalesced samples when compared to the as-received sample spectra. This improved resolution may due to the presence of less entangled and more extended chains, which is anticipated for the coalesced polymers. Generally, broad infrared bands observed in polymer samples are due to the large variety of polymer conformations and various chain-packing environments surrounding each vibrating bond or group. In coalesced polymers, vibrating bonds or groups are subjected to smaller conformational and chain-packing variations due to their more ordered structures.

The infrared spectrum of as-received PC is given in figure 6c. The absorption bands at 1161 and 1191 $cm^{-1}$ due to carbonate C-O stretch, carbonate aryl-O-aryl C-

O stretching at 1227 $cm^{-1}$, para-aromatic ring stretching at 1507 and 1602 $cm^{-1}$, carbonate C=O stretching at 1773 $cm^{-1}$ and $CH_3$ asymmetric stretching at 2968 $cm^{-1}$ are characteristic of PC.[17] Conformationally sensitive infrared bands were reported in the literature for polycarbonate.[22-24] The broad carbonyl C=O band has its maximum around 1775 $cm^{-1}$ and is subdivided into contributions from the *trans-trans* (*t-t*) conformer at 1767 $cm^{-1}$ and the *trans-cis* (*t-c*) conformer of the carbonate groups at 1785 $cm^{-1}$. The C-C aromatic in-plane stretching exhibits a doublet at 1600 $cm^{-1}$, which is divided into *t-t* and *t-c* conformational contributions at 1594 and 1604 $cm^{-1}$, respectively. The C-O-C antisymmetric vibration at 1235 $cm^{-1}$ consists of *t-t* and *t-c* conformational contributions at 1252 and 1223 $cm^{-1}$, respectively.

The conformationally sensitive regions of the IR spectra for PC, 1200-1800 $cm^{-1}$ are examined in detail in Figure 9. For as-received PC, the carbonyl band was observed at 1773 $cm^{-1}$ along with a shoulder at 1785 $cm^{-1}$, which is a contribution of the *t-c* conformation. For the coalesced PC, a narrower absorption band with maximum at 1772 $cm^{-1}$ was observed and the shoulder at 1785 $cm^{-1}$ was absent. The C-C aromatic in-plane stretching was similar for both as-received and coalesced PC and the absorption bands were observed at around 1604 $cm^{-1}$, with a shoulder at 1594 $cm^{-1}$. The most noticeable difference observed between the two samples was for the C-O-C antisymmetric vibration. For as-received PC, the peak contributed by the *t-t* conformation at 1252 $cm^{-1}$ has a lower intensity than the peak at 1227 $cm^{-1}$, which is a contribution from the *t-c* conformation. In the case of coalesced PC, these absorption bands were shifted to 1244 $cm^{-1}$ and 1230 $cm^{-1}$. Moreover, the intensity

of the 1244 $cm^{-1}$ peak is higher than that of the 1230 $cm^{-1}$ band, which indicates the presence of a higher content of *t-t* conformation when compared to as-received PC.

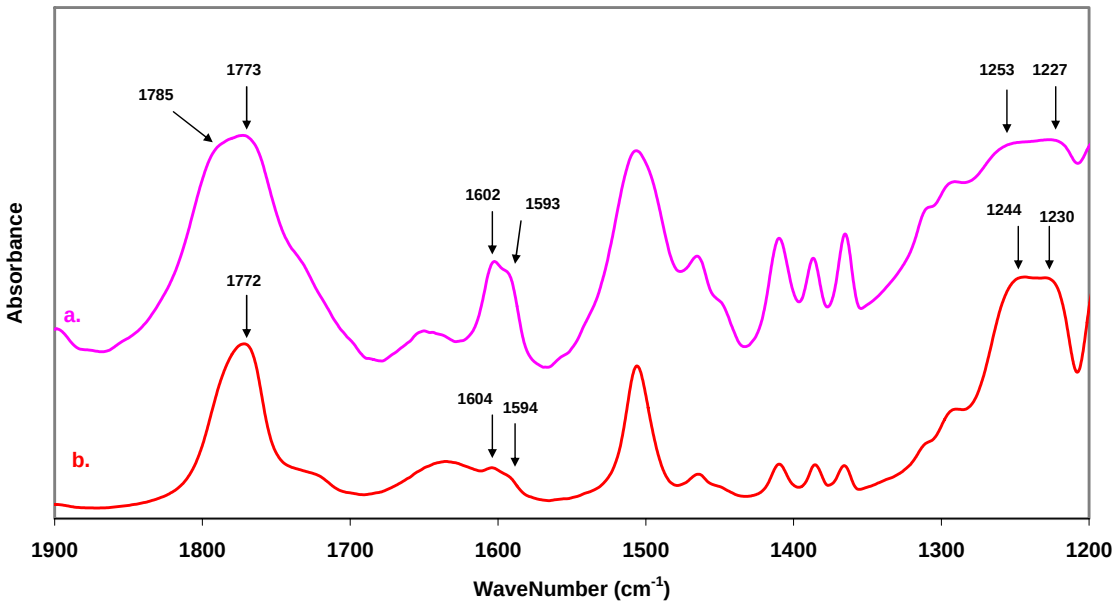


**Figure 9**. FT-IR spectra of (a) as-received PC and (b) coalesced PC.

To sum up, the observation of some differences in the infrared spectra of as-received and coalesced polymers indicates that the conformations and packing of polymer chains, when they are coalesced from their inclusion compounds, is different from those in the as-received bulk polymers.

### 2.5.3 Differential Scanning Calorimetry (DSC)

Figure 10 displays the modulated differential scanning calorimetry (MDSC) scans recorded for as-received, precipitated and coalesced PC. The absence of a melting point ($T_m$) in its DSC scans indicates that as-received PC does not contain a crystalline phase, and is completely amorphous. The glass transition temperature

($T_g$) for this sample is observed at 145° C. The first scan of precipitated PC shows two melting points: the main melting at $T_m$=239° C and a minor one at 230° C prior to main melting. The appearance of a minor melting point is possibly due to the presence two different crystalline phase in the precipitated sample.[8] The sample reverts to an amorphous phase after melting and rapid cooling and shows a glass transition, $T_g$, at 143° C as indicated in the second heating scan. The DSC thermogram of coalesced PC shows a single melting point at 240° C but broader than the precipitated sample, which indicates the precipitated PC contains more uniform crystals when compared to coalesced sample. Yet, the coalesced sample has a $T_g$=149°C, which is higher than those of the as-received and precipitated PCs.

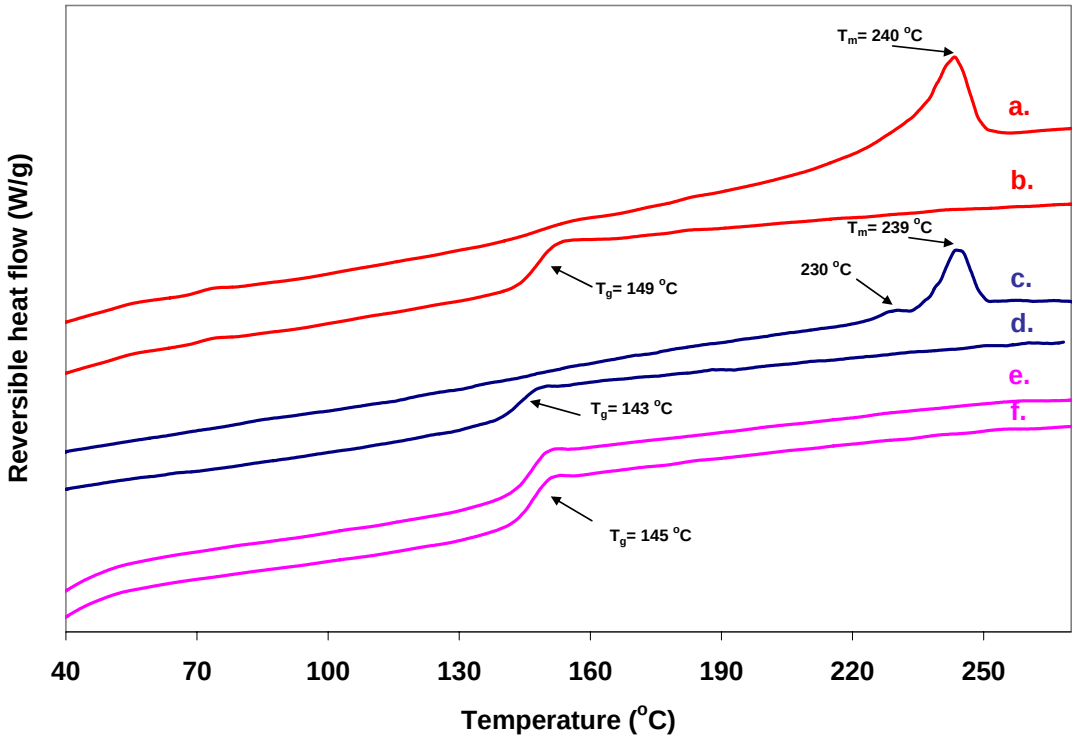


**Figure 10.** Modulated DSC thermograms of (a) first heating scan of coalesced PC (b) second heating scan of coalesced PC, (c) first heating scan of precipitated PC (d) second heating scan of precipitated PC, (e) first heating scan of as-received PC (f) second heating scan of as-received PC.

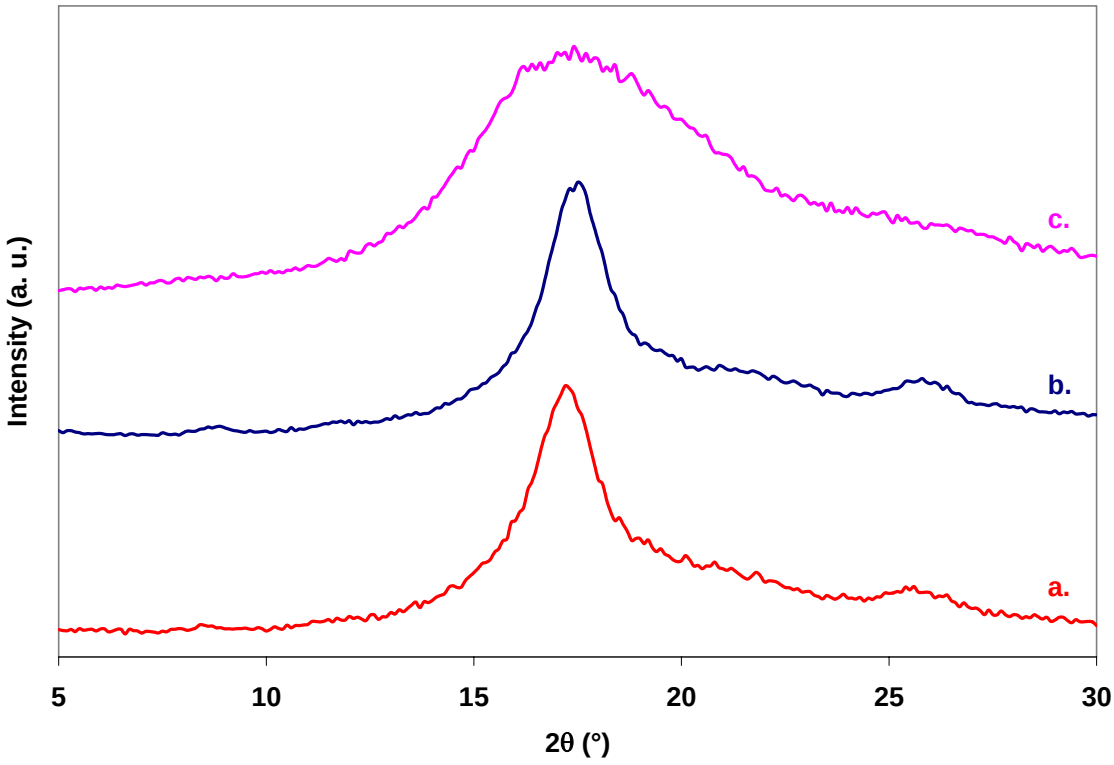


**Figure 11.** X-ray diffraction patterns of (a) coalesced PC, (b) precipitated PC and (c) as-received PC.

DSC scans recorded for coalesced and as-received PMMA and PVAc are given in Figures 12 and 13, respectively. The glass transition temperature of the as-received PMMA is observed at 83° C and is shifted to 97° C for the coalesced PMMA sample. Similar behavior is observed for the PVAc sample, where the $T_g$ is shifted from 29 to 42° C when coalesced from its inclusion compound. The increase in glass transition temperatures observed for PMMA and PVAc coalesced polymers compared to their as-received samples is significant. This behavior is commonly observed for polymers coalesced from their CD ICs [8-9] and can be explained by the

less entangled and more ordered state of the CD IC included chains upon their coalescence into bulk samples. Mi *et al.* has also observed a higher glass transition temperature for polyacrylamide (PAL) when the degree of entanglement for the polymer chains is decreased.[26] The increase in $T_g$ value of PAL was attributed to self-aggregation of unentangled chains, where the initial extended conformation transformed to a more tightly coiled conformation upon annealing. For coalesced polymers, we also suggest the presence of extended and unentangled chains, which might form tighter and more ordered structures. Additionally, we observed a remnant CD in coalesced polymer samples (section 2.5.5) and presence of few CD molecules along the polymer chain might affect and improve the thermal properties of coalesced polymers as well which results in higher $T_g$ values.

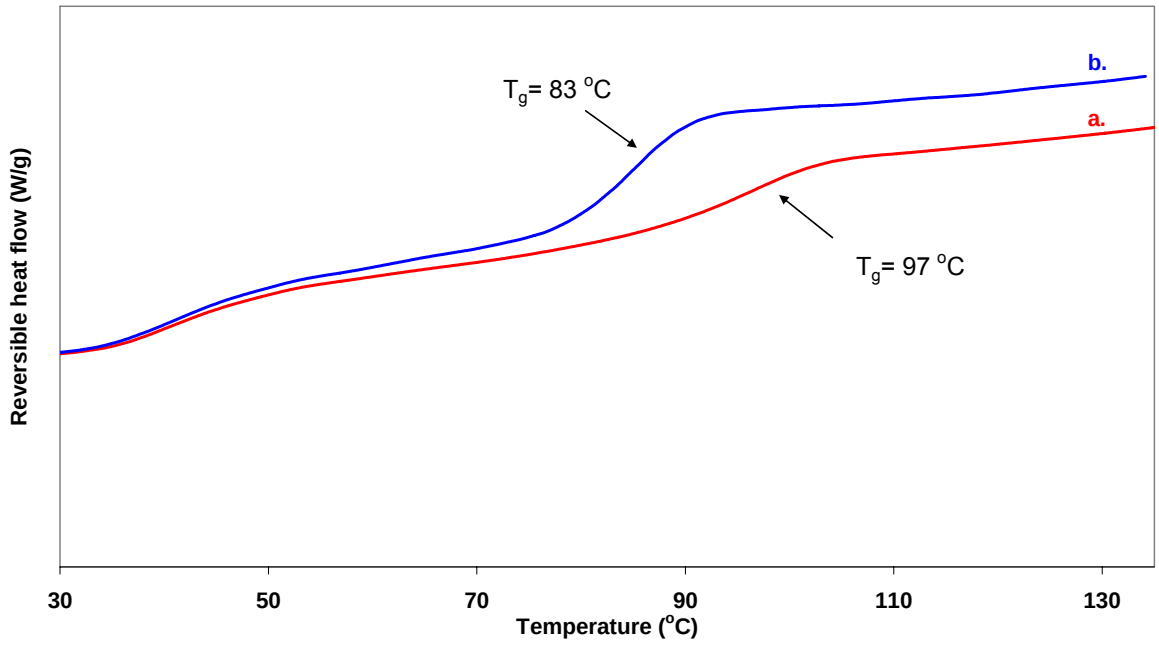


**Figure 12.** Modulated DSC thermograms of (a) second heating scan of coalesced PMMA (b) second heating scan of as-received PMMA.

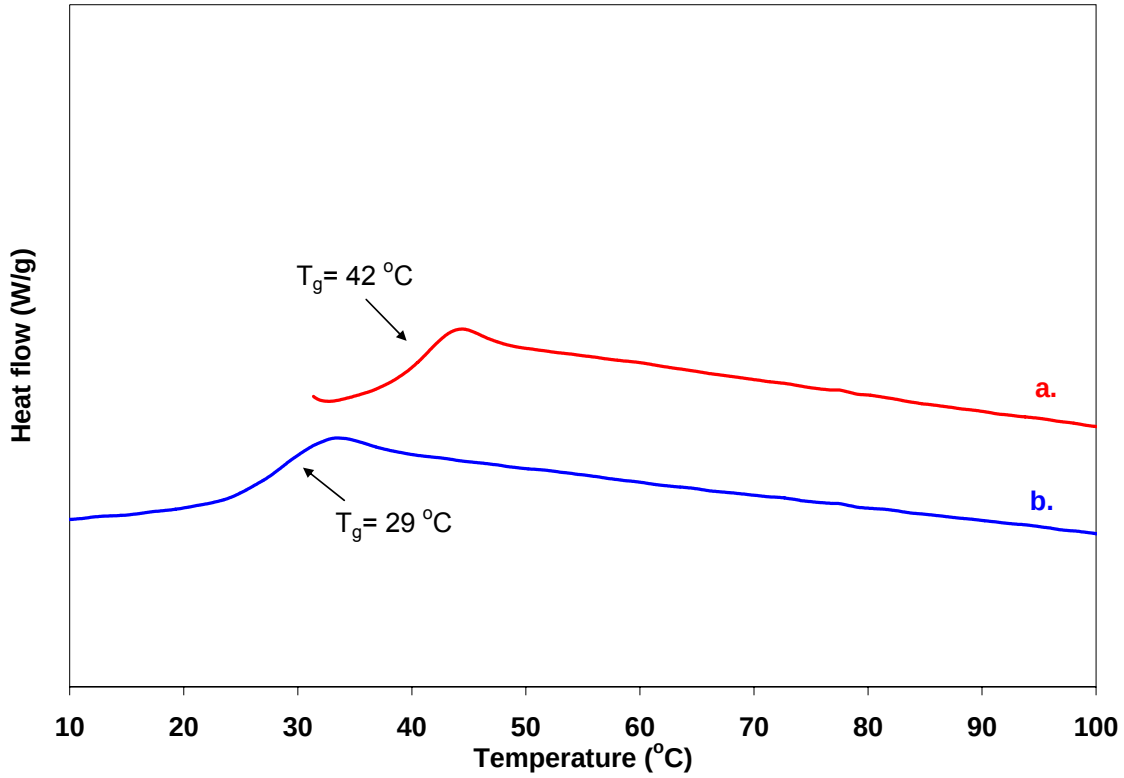


**Figure 13.** DSC thermograms of (a) second heating scan of coalesced PVAc (b) second heating scan of as-received PVAc.

### 2.5.4 Thermogravimetric Analysis (TGA)

Thermogravimetric results of pure cage γ-CD indicated two weight losses stages (Figure 14). The first weight loss below 100° C may be attributed to the removal of water, whereas the major weight loss with a maximum at 364° C corresponds to the main chemical degradation of the sample.

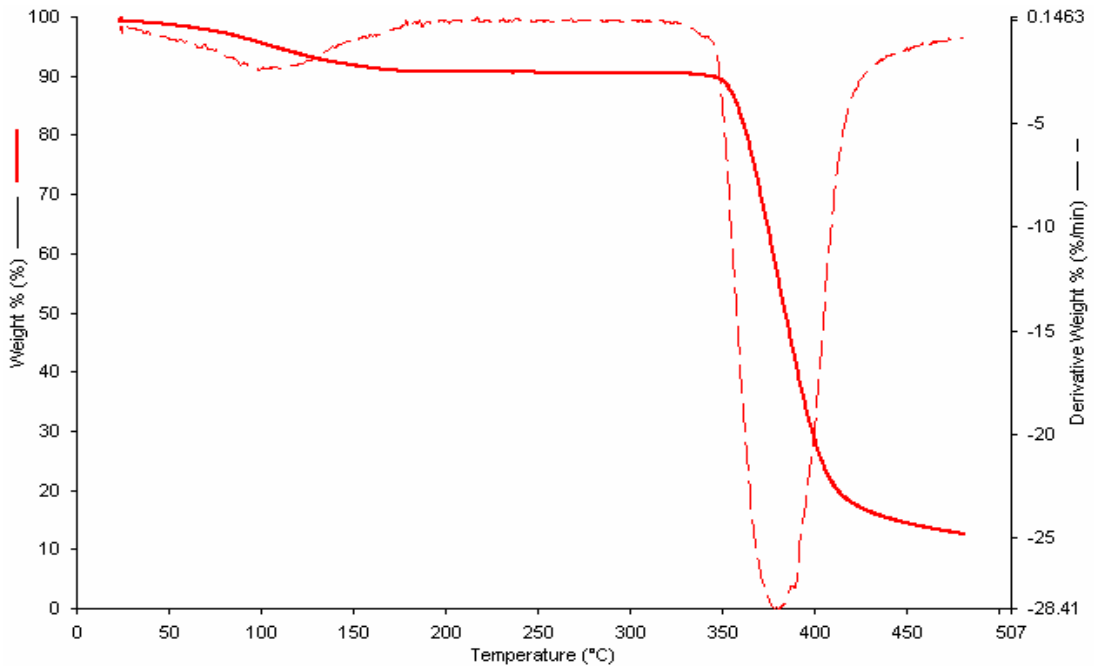


**Figure 14.** TGA thermograms of as-received γ-cyclodextrin.

Thermal degradation of PVAc, PMMA, and PC has been studied extensively.[27-32] Figure 15 displays the thermal degradation of coalesced and as-received PMMA, PVAc, and PC samples. The onset weight loss value for coalesced PMMA is lower than that of as-received PMMA, but the main degradation temperatures were shifted to higher temperature for the coalesced sample. For instance, the derivative weight loss TGA curve of as-received PMMA shows weak peaks below 300° C and a strong peak with a maximum at 410° C. In comparison, the TGA curve of coalesced PMMA shows two main degradation steps at 340° C and 423° C (higher than that of the as-received sample), the second being more intense (Figures 15 a and b).

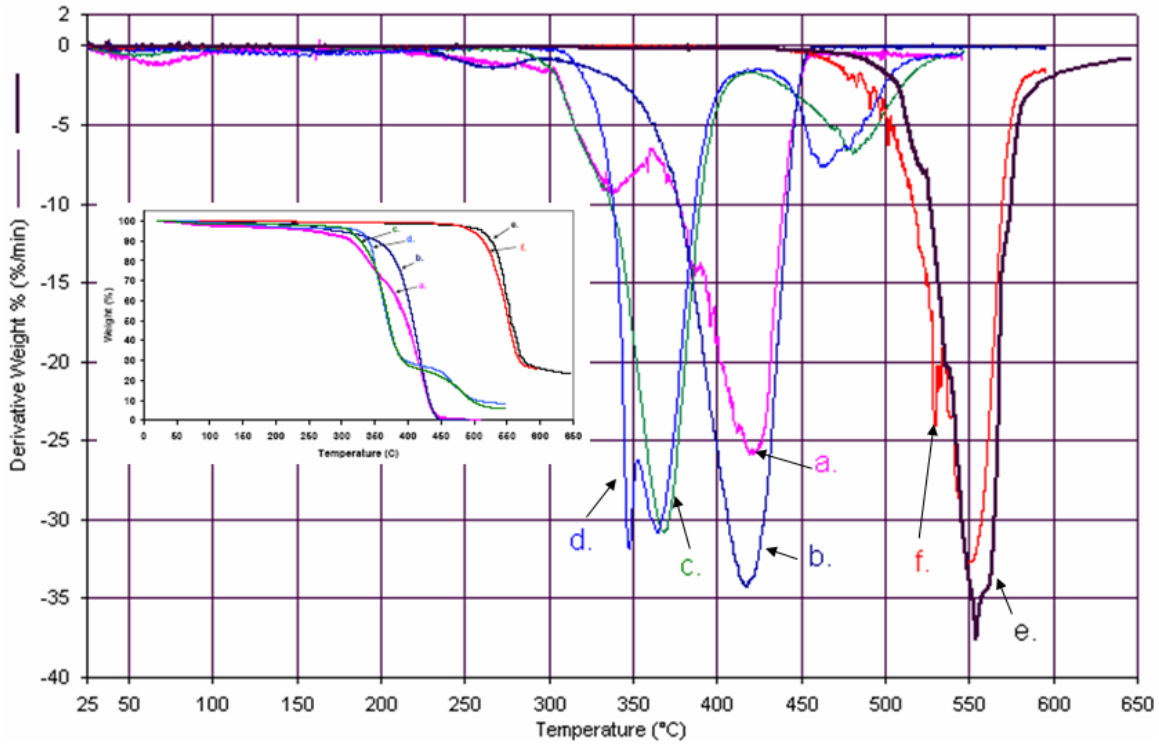


**Figure 15.** TGA thermograms of (a) coalesced PMMA, (b) as-received PMMA, (c) coalesced PVAc (d), as-received PVAc (e), coalesced PC (f), and as-received PC.

Thermal behaviors of coalesced and as-received PVAc are shown in Figures 15c and d. The decomposition temperature, $T_d$, of coalesced PVAc is observed at 369° C, whereas that of as-received PVAc is 360° C. But, the onset weight loss value for coalesced PVAc is slightly lower than that of as-received PVAc and a shoulder around 330° C is also present. The second degradation stages for the as-received and coalesced PVAc samples were recorded at 464 and 483° C, respectively, indicating an increase in thermal stability for the coalesced PVAc.

TGA analysis indicated that in the case of the coalesced PC sample, the $T_d$ of PC is shifted to 554° C, whereas as-received PC has a $T_d$ of 549° C (Figure 15e and f). In general, the TGA results reveal that the thermal stabilities of coalesced samples are increased compared to the corresponding as received polymers. The

increase in thermal stabilities of coalesced samples may due to presence of remnant CD in coalesced samples.

### 2.5.5 Direct Insertion Probe Pyrolysis Mass Spectrometry (DIP-MS)

In general, direct insertion probe pyrolysis mass spectrometry (DIP-MS) facilitates analyses of degradation mechanisms using structural information from the thermal characterization of degradation products.[33-35] However, pyrolysis mass spectra of polymers are usually very complex, as thermal degradation products further dissociate in the mass spectrometer during ionization. Furthermore, all fragments with the same mass to charge ratio make contributions to the intensities of the same peaks in the mass spectrum. Thus, in pyrolysis MS analysis, not only the detection of a peak, but also the variation of its intensity as a function of temperature, ie., its evolution profile, is important. The trends in evolution profiles can be used to determine the source of the product, or the mechanism of thermal degradation. The direct pyrolysis mass spectrometry analysis of γ-CD, as-received polymers, polymer-CD ICs, and coalesced samples have been performed to investigate the changes in their thermal degradation behavior.

#### 2.5.5.1 γ-Cyclodextrin (γ-CD)

Thermogravimetric results observed for pure γ-CD indicated two weight losses stages: the one below 100° C was attributed to removal of water and the second, with a maximum at 364° C corresponding to major weight loss, was associated with the main degradation of γ-CD (see section 2.5.4). Pyrolysis analysis indicated that the thermal degradation of γ-CD occurs over a broad temperature

range starting just above 280$^{o}$ C. The variation of total ion current (TIC) as a function of temperature shows two peaks; a sharp peak and a broad peak with a shoulder in high temperature range having maxima at 310 and 355$^{o}$ C, respectively (Fig 16.a).

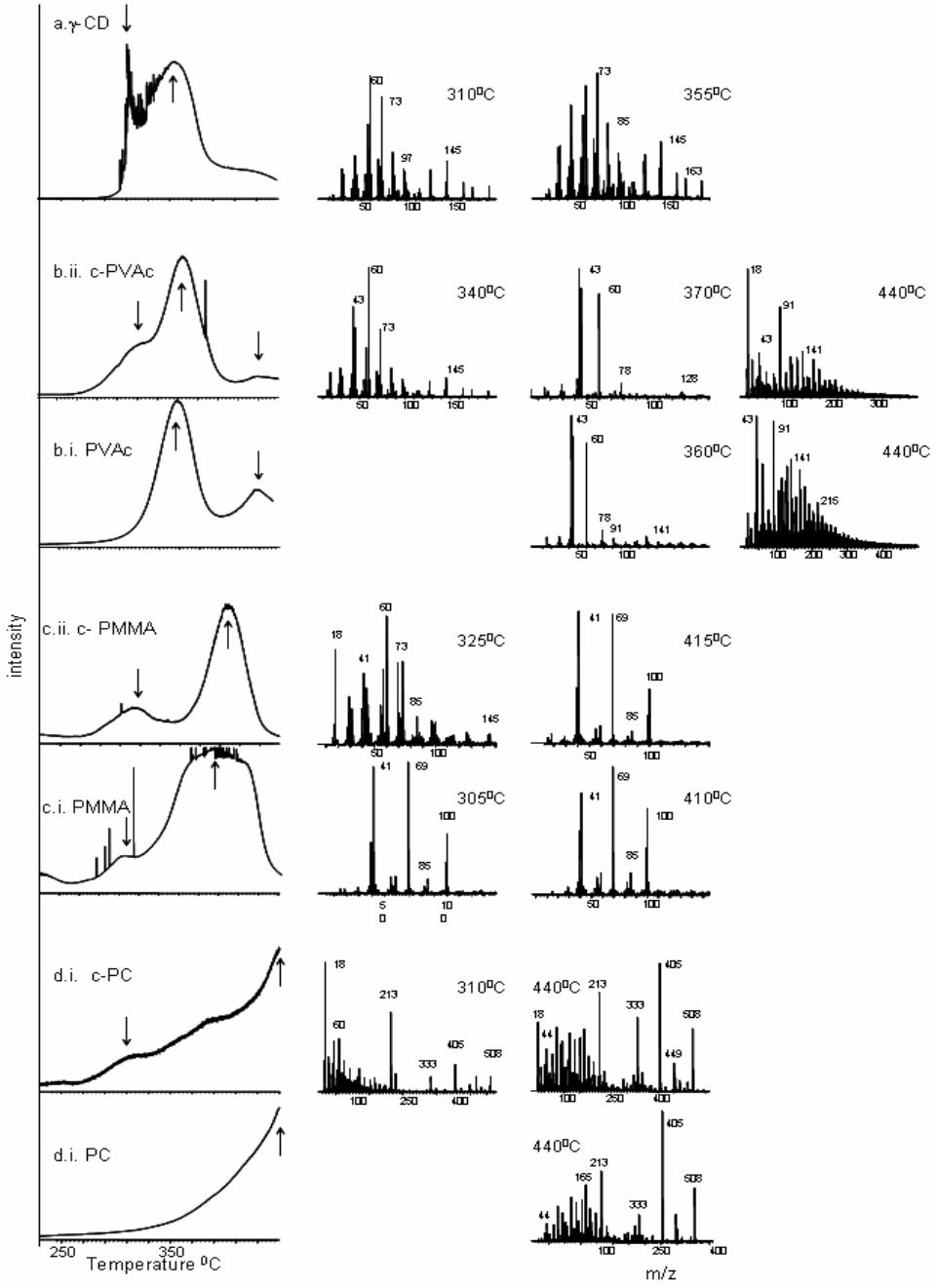


**Figure 16.** TIC curves and pyrolysis mass spectra recorded at the maximum of the peaks and shoulders in the TIC curves of a.) as-received γ-CD, b.) i. as-received PVAc, ii. coalesced PVAc, c.) i. as-received PMMA, ii. coalesced PMMA, d.) i. as-received PC ii. coalesced PC.

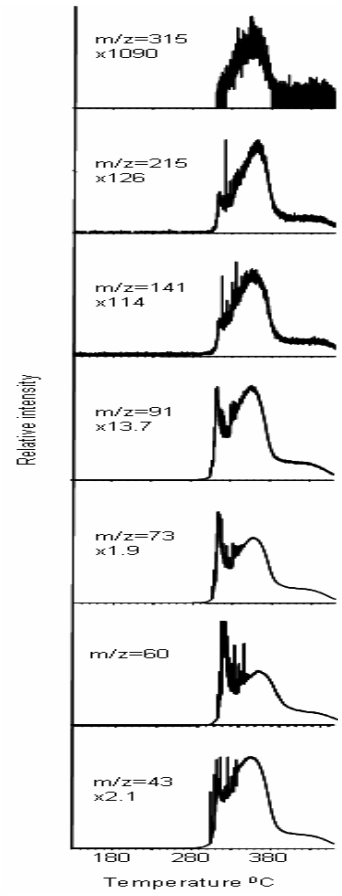


Yet, the fragmentation patterns observed in the pyrolysis mass spectra recorded throughout the pyrolysis were nearly identical and the main degradation products are due to the cleavage of weak C-O bonds yielding intense $C_2H_4O_2$ and $C_3H_5O_2$ fragments at m/z = 60 and 73 Da, respectively. Evolution profiles of some selected products are shown in Figure 17.

**Figure 17.** Evolution profiles of some characteristic products recorded during the pyrolysis of γ-CD.

### 2.5.5.2 Poly(vinyl acetate) (PVAc)

The TIC curve of as-received PVAc also showed two degradation steps, in accordance with the literature and our TGA results shown in Figure 16b(i). It is known that the thermal degradation of PVAc occurs in two stages, around 360 and 440$^o$ C, corresponding to deacetylation and disintegration of the polyolefinic backbone, respectively.[36,37] Analysis of the pyrolysis mass spectra indicated loss of side groups yielding mainly $CH_3CO$ (m/z=43Da), and $CH_3COOH$ (m/z= 60 Da) in the first stage of thermal degradation around 360$^0$ C and decomposition of the unsaturated polymer backbone formed in the second step around 440$^0$ C, also in

accordance with literature results. For the coalesced PVAc, the low temperature peak maximum was shifted slightly to 370$^{o}$ C and the relative intensity of the second peak was noticeably diminished. (Figure 16b(ii)). Furthermore, a shoulder around 330$^{o}$ C appeared in the TIC curve. The pyrolysis mass spectra recorded around the low temperature shoulder at ~330º C showed a fragmentation pattern quite similar with that of γ-CD (Figure 16.a) pointing to the presence of some γ-CD remaining even after the long coalescence process. The relative intensities and the assignments of characteristic and intense peaks in the pyrolysis mass spectra of the as-received and coalesced PVAc are collected in Table 1.

**Table 1.** The relative intensities and the assignments of characteristic and intense peaks in the pyrolysis mass spectra of as-received, and coalesced PVAc and the physical mixture of PVAc and γ-CD at temperatures corresponding to maxima in the TIC curves.

| m/z, Da | As-resceived PVAc | | Physical mixture of PVAc and γ-CD | | | Coalesced PVAc | | | Assignments |
|---|---|---|---|---|---|---|---|---|---|
| | 360$^{0}$ C | 440$^{0}$ C | 325$^{0}$ C | 360$^{0}$ C | 430$^{0}$ C | 330$^{0}$ C | 370$^{0}$ C | 440$^{0}$ C | |
| 43 | 1000 | 867 | 765 | 1000 | 793 | 580 | 1000 | 709 | $CH_3CO$, $CH_2CHO$ |
| 45 | 830 | 661 | 501 | 815 | 244 | 461 | 843 | 569 | $CCH_3O$, COOH |
| 60 | 800 | 623 | 1000 | 746 | 412 | 1000 | 785 | 1000 | $CH_3COOH$, $C_2H_4O_2$ |
| 73 | 4 | | 654 | 10 | 39 | 526 | 27 | 472 | $C_3H_5O_2$ |
| 78 | 130 | 179 | 13 | 171 | 167 | 2 | 99 | 12 | $C_6H_6$ |
| 86 | 2 | 15 | 53 | 4 | 27 | 29 | 6 | 29 | $C_4H_6O_2$, VAc |
| 91 | 40 | 1000 | 56 | 90 | 1000 | 12 | 24 | 15 | $C_7H_7$ |
| 105 | 27 | 420 | 14 | 43 | 466 | | 8 | 10 | $C_8H_{10}$ |
| 115 | 30 | 525 | 79 | 47 | 536 | 33 | 21 | 36 | $C_9H_8$ |
| 128 | 48 | 513 | 63 | 109 | 505 | 4 | 35 | 42 | $C_{10}H_8$ |
| 141 | 30 | 699 | 11 | 55 | 662 | | 9 | 12 | $C_{12}H_9$ |
| 179 | 13 | 446 | 9 | 37 | 464 | | 6 | 8 | $C_{14}H_{11}$ |
| 180 | 12 | 204 | 7 | 30 | 332 | | 6 | 7 | $C_{14}H_{12}$ |
| 215 | 4 | 341 | 10 | 11 | 359 | | 6 | 1 | $C_{14}H_{12}$ |
| 232 | 3 | 110 | 4 | 9 | 123 | | 2 | 1 | $C_{18}H_{16}$ |
| 284 | 1 | 49 | 2 | 4 | 69 | | 1 | 1 | $C_{22}H_{20}$ |
| 315 | 1 | 71 | 2 | 2 | 81 | | | | $C_{24}H_{27}$ |

A detailed study of the mass spectra recorded around $440^0$ C indicated an increase in $H_2O$ evolution together with a significant decrease in the polyolefinic product yield. In Figure 18.a and b, evolution profiles of characteristic thermal degradation products of as-received and coalesced samples are given. (Evolution of $H_2O$ and any product with m/z= 73 Da was not detected during the pyrolysis of PVAc. Thus, the related single ion pyrograms can not be given.) It is clear that the amount of polyolefinic products decreased significantly for the coalesced sample. It may be thought that crosslinking of the polyolefinic backbone by the decomposition products of γ-CD possessing two or more OH groups during the first thermal degradation stage has occurred. Crosslinking of the polyolefinic backbone should increase thermal stability and decrease the yield of unsaturated fragments. To investigate the effect of γ-CD degradation products on the thermal degradation behavior of PVAc, pyrolysis analysis was repeated for a physical mixture of γ-CD and PVAc (Figure 18.c). The relative intensities of products were comparable for pure PVAc and its physical mixture with γ-CD. The small differences in the evolution profiles were mainly due to the contribution of products generated from both PVAc and γ-CD having the same m/z peak values. It is clear that no indication for crosslinking was present for this sample, and it can be concluded that both components degraded independently. Thus, crosslinking is only effective when PVAc chains are included inside the γ-CD cavities, where the separation between the two components is very small.

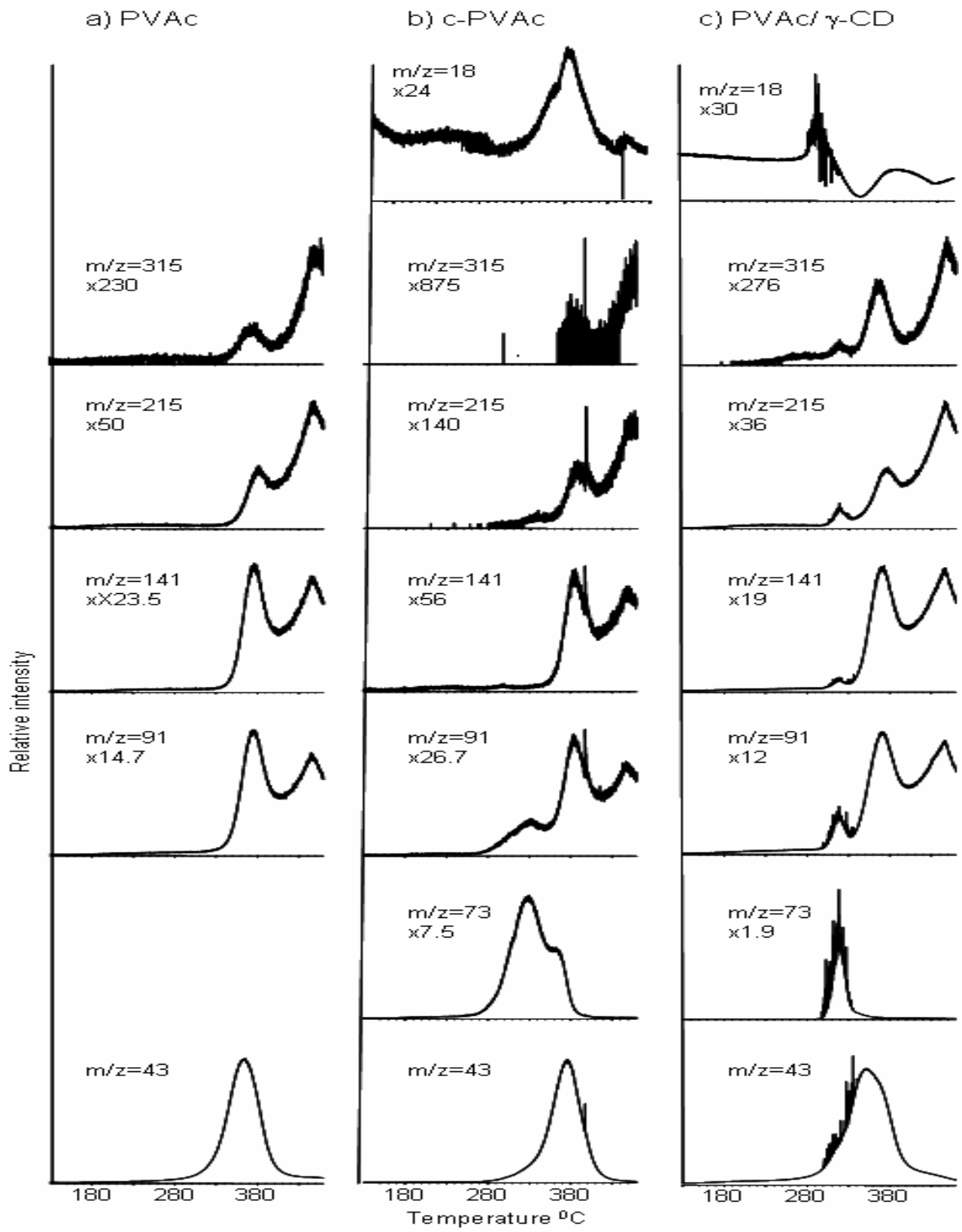


**Figure 18.** Evolution profiles of some characteristic products recorded during the pyrolysis of a) as-received PVAc, b) coalesced PVAc, and c) γ-CD/PVAc physical mixture.

### 2.5.5.3 Poly(methyl methacrylate) (PMMA)

The thermal degradation of PMMA has been studied in detail, and it has been proposed that the degradation can be initiated by different processes. Low temperature weight losses were attributed to scission of head-to-head linkages and loss of unsaturated end groups. At elevated temperatures (380 - 420$^{o}$ C) initiation of weight loss was thought to be a mixture of chain end and chain scission processes, followed by depropagation to the end of the polymer chain.[27,28]

Direct pyrolysis of as-received PMMA yielded a broad peak with several shoulders and two maxima at 330 and 400 $^{o}$ C (Figure 16c(i)). It has been proposed that in the initial stages of pyrolysis, weight losses are attributed not only to evolution of dimer and low molecular weight oligomers, but also scission of head-to-head linkages and loss of unsaturated end groups. Our pyrolysis mass spectra recorded above 300$^{o}$ C show a typical fragmentation pattern for as received PMMA confirming, depolymerization.

The TIC curve of the coalesced PMMA sample is quite similar to that of the as-received sample (Figure 16c(ii)). On the other hand, the pyrolysis mass spectra recorded around 325$^{o}$ C involves peaks diagnostic for $\gamma$-CD, indicating that total removal of $\gamma$-CD was not achieved, as in the case of coalesced PVAc. Yet, the low temperature peaks are diminished and the high temperature peaks with maxima at 325 and 420 $^{o}$ C became sharper, indicating a decrease in polydispersity and removal of low molecular weight oligomers during the inclusion processes.

The relative intensities and the assignments of characteristic and/or intense peaks in the pyrolysis mass spectra of the as-received and coalesced PMMA are collected in Table 2. In Figure 19 evolution profiles of selected degradation products of as-received and coalesced PMMA are shown. The broad evolution profiles of the thermal degradation products observed for as-received PMMA are noticeably narrower when produced during the thermal degradation of the coalesced sample. For coalesced PMMA, base product yields are also diminished significantly around $330^0$ C. It is known that cyclodextrins can selectively include molecules from their common solutions according to their molecular weights, and they can therefore be used for separation/purification/fractionation purposes.[38-39] The separation/purification of PMMA from its low molecular weight oligomers may have also been attained by forming the inclusion compound with $\gamma$-CD.

**Table 2.** The relative intensities and assignments of characteristic and intense peaks in the pyrolysis mass spectra of as-received and coalesced PMMA at temperatures corresponding to maxima in the TIC curves.

| m/z, Da | As-received PMMA | | Coalesced PMMA | | Assignments |
|---|---|---|---|---|---|
| | $315^0$ C | $415^0$ C | $325^0$ C | $420^0$ C | $430^0$ C |
| 41 | 944 | 787 | 600 | 1000 | $CH_2CCH_3$ |
| 43 | 66 | 47 | 442 | 46 | $CH_2CHO$, $CH_3CO$, |
| 45 | 28 | 31 | 198 | 27 | COOH, CHOO |
| 60 | 18 | 11 | 1000 | 9 | $CH_3COOH$ |
| 69 | 1000 | 1000 | 645 | 974 | $CH_2C(CH_3)CO$ |
| 73 | 21 | 22 | 664 | 12 | $C_3H_5O_2$ |
| 85 | 106 | 163 | 205 | 91 | $CH=CCOOCH_3$, $CH_2C(CH_3)COO$ |
| 86 | 6 | 9 | 41 | 7 | $C_4H_6O_2$ |
| 91 | 4 | 9 | 42 | 6 | $C_7H_7$ |
| 100 | 445 | 562 | 181 | 472 | MMA |

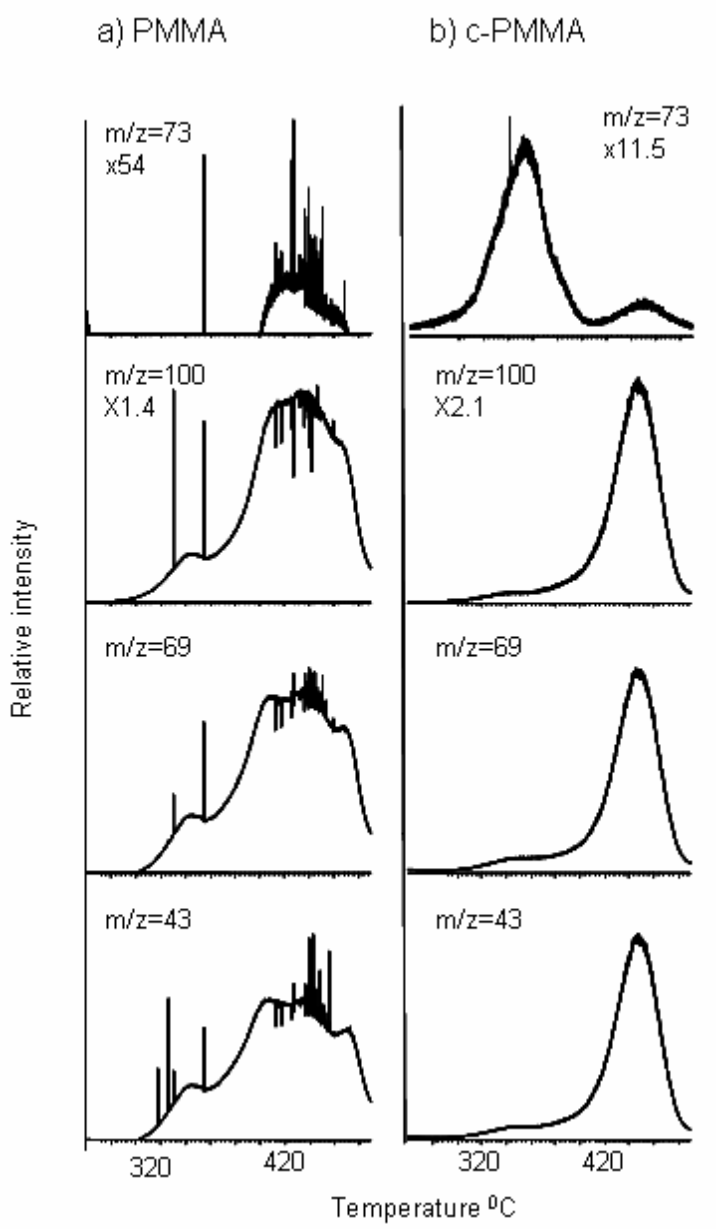


Pyrolysis of PMMA-γ-CD ICs have also been carried out, yet, PMMA based product yields are too low to make comparisons, because of the low stoichiometric contents of included polymers. Furthermore, no significant change was detected in the evolution profiles of γ-CD based on the decomposition of the IC products.

**Figure 19.** Evolution profiles of some characteristic products recorded during the pyrolysis of a) as-received PMMA, and b) coalesced PMMA.

### 2.5.5.4 Polycarbonate (PC)

It has been proposed that thermal degradation studies on poly(bisphenol A carbonate) support the evolution of cyclic oligomers and $CO_2$ in the initial stages of degradation at about 400 -500$^o$ C. Intermolecular exchange reactions lead to formation of cyclic oligomers, whereas generation of $CO_2$, is explained by

decarboxylation of the carbonate groups forming ether bridges and by hydrolysis reactions producing phenolic end groups.[31, 32] At elevated temperatures (500 -700 ° C) rearrangement of carbonate groups leads to formation of condensed groups. For our direct pyrolysis system the maximum attainable temperature, 445° C, is too low to detect the complete thermal degradation of PC. Thus, the TIC curves of as-received and coalesced PC only show the initial stages of thermal degradation as expected (Figure 16.d). The base peak in the pyrolysis mass spectra of as-received PC at m/z= 405 Da is attributed to the $C_6H_5$-$C(CH_3)_2$-$C_6H_4$-O-$C_6H_4$-$C(CH_3)_2$-$C_6H_4$ fragment generated by evolution of $CO_2$ forming ether bridges. Other intense peaks are at m/z=213 and 508 Da assigned to $C_6H_5$-O-COO-$C_6H_4$ and cyclic dimer, respectively, in accordance with the literature results.[31,32] Identical product peaks, together with peaks diagnostic for γ-CD, are identified for the coalesced sample. Yet, the evolution of degradation products shifted to lower temperatures and shoulders appear around 310 and 380° C. Drastic differences are noted when the evolution profiles of these products from as-received and coalesced PC are compared.

To gain a better understanding of the thermal degradation of coalesced PC, PC-γ-CD IC was also studied. The TIC curve of PC-γ-CD IC shows only a single, broad peak with a maximum at 400° C and is noticeably different from that of pure γ-CD and pure PC. Furthermore, unlike the PVAc and PMMA-γ-CD IC's, PC based product peaks are prominent. In Figure 20, evolution profiles of some diagnostic thermal degradation products of PC and γ-CD namely $C_6H_5$-$C(CH_3)_2$-$C_6H_4$-O-$C_6H_4$-$C(CH_3)_2$-$C_6H_4$ (m/z=405 Da), $C_6H_5$-O-COO-$C_6H_4$ (m/z=213 Da), $C_3H_5O_2$ (m/z=73Da), and $CO_2$ (m/z= 44Da) Da are shown. Evolution of low molecular weight PC based

products shifted to lower temperatures, whereas no significant change in the evolution profiles of products generated by intermolecular exchange or rearrangement reactions are indicated. It may be thought that classical degradation pathways for PC can only be followed above 400$^{o}$ C. The low temperature evolution of PC based products may be attributed to loss of polycarbonate chain ends and/or units strongly interacting with γ-CD. It is clear that both PC and γ-CD significantly affect the thermal stability of the other.

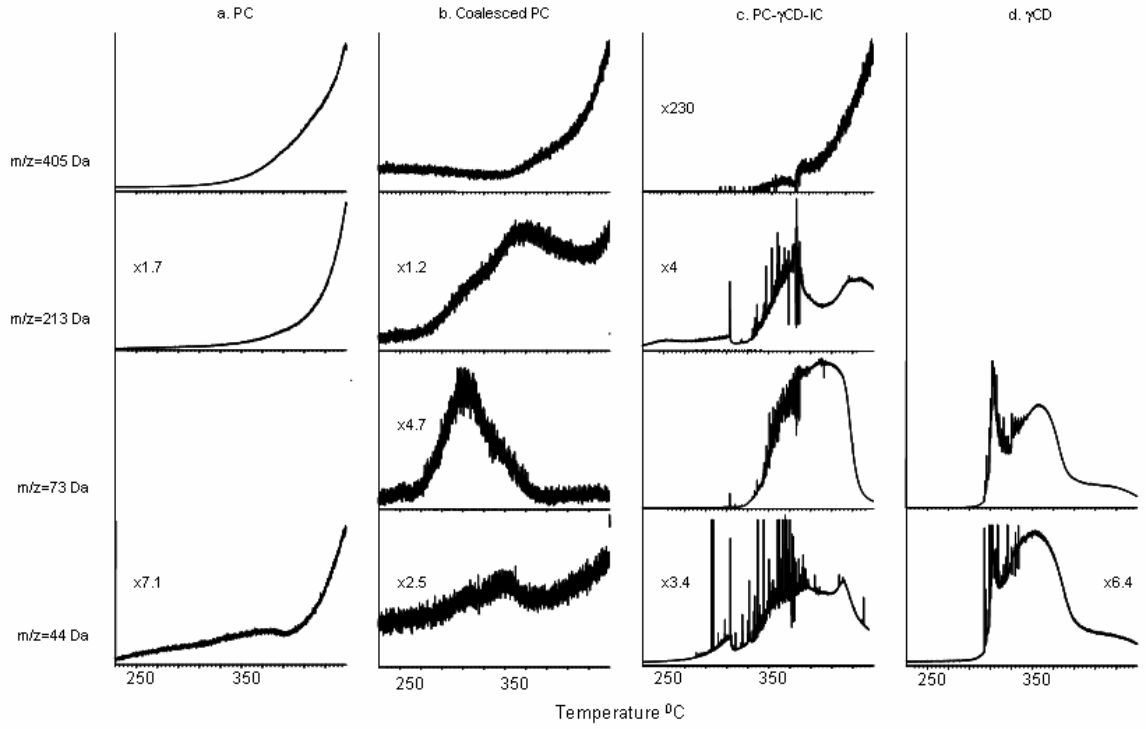


**Figure 20.** Evolution profiles of $CO_2$ (m/z= 44 Da) , $C_3H_5O_2$ (m/z=73 Da), $C_6H_5$-O-COO-$C_6H_4$ (m/z=213 Da) and $C_6H_5$-$C(CH_3)_2$-$C_6H_4$-O-$C_6H_4$-$C(CH_3)_2$-$C_6H_4$ (m/z=405 Da) recorded during pyrolysis of a.) as-received PC, b.) Coalesced PC, c.) PC-γ-CD-IC and d.) as-received γ-CD.

## 2.6 Conclusions

We have described a unique way of modifying the characteristics of commercial polymers through the formation of and coalescence from their inclusion compounds formed with cyclodextrins. The formation of ICs between γ-CD and polycarbonate (PC), poly(methylmethacrylate) (PMMA) and poly(vinylacetate) (PVAc) homopolymers was successfully achieved. The existence of extended chain conformations in the coalesced polymers was confirmed by FT-IR findings. The chain conformations of the bulk polymers were altered when they were included inside the CD channels and were partially retained their extended chain conformations when coalesced from their ICs. Significant increases in the glass transition temperatures ($T_g$) were observed for the coalesced polymers when compared to their as-received samples. Moreover, the thermal stabilities of the coalesced polymers increased slightly compared to the corresponding as-received polymers. The enhancement observed in thermal properties for polymers coalesced from their CD ICs may due to their less entangled and more ordered state or the presence of remnant CD molecules. It was also observed that the thermal stability and degradation products of the polymers are affected once the polymers chains are included inside the CD cavities.

## 2.7 References:


1. Harada A, Li J, Kamachi M. *Nature* 1994; 370: 126.
2. Huang L, Allen E, Tonelli AE. *Polymer* 1999; 40 (11): 3211-3221.
3. Lu J, Shin ID, Nojima S, Tonelli AE. *Polymer* 2000; 41(15): 5871-5883.
4. Shuai XT, Porbeni FE, Wei M, Shin ID, Tonelli AE. *Macromolecules* 2001;34(21): 7355-7361.
5. Harada A, Nishiyama T, Kawaguchi Y, Okada M, Kamachi M. *Macromolecules* 1997; 30(23): 7115-7118.
6. Do Nascimento GM, Da Silva JEP, De Torresi SIC, Santos PS, Temperini MLA. *Molecular Crystals and Liquid Crystals* 2002; 374: 53-58.
7. Li JY, Yan DY, Jiang XL, Chen Q. *Polymer* 2002 ; 43 (9): 2625-2629.
8. Bullions TA, Wei M, Porbeni FE, Gerber MJ, Peet J, Balik M, White JL, Tonelli AE. *Journal of Polymer Science: Part B-Polymer Physics* 2002; 40 (10): 992.
9. Wei M, Davis W, Urban B, Song Y, Porbeni FE, Wang X, White JL, Balik CM, Rusa CC, Fox J, Tonelli AE. *Macromolecules* 2002; 35: 8039.
10. Rusa CC, Tonelli AE. *Macromolecules* 2000; 33 (15): 5321-5324.
11. Wei M, Tonelli AE. *Macromolecules* 2001 ; 34 : 4061.
12. Bullions TA, Edeki EM, Porbeni FE, Wei M, Shuai X, Rusa CC, Tonelli AE. *Journal of Polymer Science: Part B-Polymer Physics* 2003 ; 41 (2): 139-148.
13. Rusa CC, Uyar T, Rusa M, Wang X, Hunt MA, Tonelli AE. *Journal of Polymer Science: Part B-Polymer Physics* 2004; 42 (22): 4182-4194**.**
14. Uyar T, Rusa CC, Rusa M, Wang X, Hacaloglu J, Tonelli AE. *Journal of Polymer Science: Part B-Polymer Physics* 2005; 43 (18): 2578-2593**.**

15. Rusa CC, Bullions TA, Fox J, Porbeni FE, Wang XW, Tonelli AE. *Langmuir* 2002; 18 (25): 10016-10023.
16. Lind TK, Kuge T. *Agr Biol Chem* 1970; 34(4): 568-574.
17. Mark JE. *Polymer Data Handbook*, New York: Oxford University Press, 1999.
18. Willis HA, Zichy VJ, Hendra PJ. *Polymer* 1969; 10:737.
19. Chen J, Zheng G, Xu L, Zhang J, Lu Y, Xue G, Yang Y. *Polymer* 2001; 42.
20. Oleg N, Tretinnikov ON, Ohta K. *Macromolecules* 2002; 35: 7343-7353
21. Grohens Y, Prud'homme RE, Schultz J, *Macromolecules* 1998; 31: 2545-2548.
22. Schmidt P, Dybal J, Turska E, Kulczycki A. *Polymer* 1991; 32 (10): 1862-1866.
23. Heymans N. *Polymer* 1997; 38 (14): 3435-3440.
24. Dybal J, Schmidt P, Baldrian J, Kratochvil J, *Macromolecules* 1998 ; 31: 6611.
25. Turska E, Hurek J, Zmudzinski L. *Polymer* 1979 ; 20: 321.
26. Mi Y, Xue G, Lu X. *Macromolecules* 2003; 36: 7560-7566.
27. Montaudo G, Puglisi C, Samperi F, *Journal of Polymer Science: Part A-Polymer Chemistry* 1998; 36 (11): 1873-1884.
28. Ferriol M, Gentilhomme A, Cochez M, Oget N, Mieloszynski JL. *Polymer Degradation and Stability* 2003; 79 (2): 271-281.
29. Guyot A, Bert M. Journal of Applied Polymer Science 1973; 17: 753.
30. Gupta MC, Viswanath SG. *Ind Eng Chem Res* 1998; 37: 2707.
31. Puglisi C, Sturiale L, Montaudo G. *Macromolecules* 1999; 32: 2194.

32. Ito Y, Ogasawara H, Ishida Y, et al.,. *Polymer Journal* 1996; 28: 1090.
33. Uyar T, Toppare L, Hacaloglu J. *J Analytical & Applied Pyrolysis* 2002;64(1):1.
34. Uyar T, Hacaloglu J. *J Analytical & Applied Pyrolysis* 2002; 64(2): 379.
35. Uyar T, Toppare L, Hacaloglu J. *Synthetic Metals* 2001; 123 (2): 335-342.
36. Debier D, Jonas AM, Legras R. J Polym Sci Part B: Polym Phys 1998; 36: 2197–2210.
37. Viville P, Biscarini F, Bredas JL, Lazzaroni RJ. Phys. Chem. B 2001; 105: 7499.
38. Rusa CC, Tonelli AE. *Macromolecules* 2002; 35 (5): 1813-1818.
39. Singla S, Zhao T, Beckham HW. *Macromolecules* 2003; 36 (18): 6945-6948.

# CHAPTER 3

## 3 Intimate Blending of Polymer Systems from Their Common Cyclodextrin Inclusion Compounds

### 3.1 Binary Polymer Systems: Polycarbonate/Poly(methyl methacrylate), Polycarbonate/Poly(vinyl acetate) and Poly(methyl methacrylate)/ Poly(vinyl acetate)

#### 3.1.1 Summary

A procedure for the formation of intimate blends of three binary polymer systems; polycarbonate (PC)/poly(methyl methacrylate) (PMMA), PC/poly(vinyl acetate) (PVAc) and PMMA/PVAc is described. PC/PMMA, PC/PVAc, and PMMA/PVAc pairs were included in γ-cyclodextrin (γ-CD) channels and were then simultaneously coalesced from their common γ-CD inclusion compounds (ICs) to obtain intimately mixed blends. The formation of inclusion compounds between polymer pairs and γ-CD were confirmed by wide-angle x-ray diffraction (WAXD), fourier transform infrared spectroscopy (FT-IR), and differential scanning calorimetry (DSC). It was observed [solution $^{1}H$ nuclear magnetic resonance (NMR)] that the ratios of polymers in coalesced PC/PMMA and PC/PVAc binary blends are significantly different than the starting ratios, and PC was found to be preferentially included in γ-CD channels when compared to PMMA or PVAc. Physical mixtures of polymer pairs were also prepared by co-precipitation and solution casting methods

for comparison. FT-IR, DSC, solid-state $^{1}H$ NMR, thermogravimetric analysis (TGA), and direct insertion probe pyrolysis mass spectrometry (DIP-MS) data indicated that the PC/PMMA, PC/PVAc, and PMMA/PVAc binary polymer blends were homogeneously mixed when they were coalesced from their ICs. The shifts observed in FT-IR absorption bands for the coalesced polymer blends indicated the presence of possible interactions between the coalesced polymer components. A single, common glass transition temperature ($T_g$) recorded by DSC heating scans strongly suggested the presence of a homogeneous amorphous phase in the coalesced binary polymer blends, which is retained after thermal cycling to 270º C. The physical mixture samples showed two distinct $T_g$s and $^{1}H$-$T_{1}\rho$ values for the polymer components, which indicated phase-separated blends with domain sizes above 5 nm, while the coalesced blends exhibited uniform $^{1}H$ spin-lattice relaxation values, indicating intimate blending in the coalesced samples. The TGA results of coalesced and physical binary blends of PC/PMMA and PC/PVAc reveal that in the presence of PC, the thermal stability of both PMMA and PVAc increases. Yet, the presence of PMMA and PVAc decreases the thermal stability of PC itself. DIP-MS observations suggested that the degradation mechanisms of the polymers changed in the coalesced blends, which was attributed to the presence of molecular interactions between the well-mixed polymer components in the coalesced samples.

### 3.1.2 Introduction

The blending of two or more polymer components is a very common commercial approach to obtain new polymeric materials with improved

characteristics. The conventional methods for producing polymer blends are melt blending, co-precipitation, and solvent casting.[1] When two or more polymer components are blended together, it is usually likely to obtain phase-separated materials due to a small entropy of mixing and the generally unfavorable enthalpy of mixing when there is no specific interaction (hydrogen bonds, van der Waals and/or polar interactions, etc.) between the component polymer side groups. In the case of poor mixing, the blends exhibit properties inferior to their component polymers due to the poor degree of interfacial adhesion between the phase-separated components, which create a multiplicity of defects in the system.[2] In addition to the properties of each polymer component and their compositions, the ultimate characteristics of a polymer blend depend most importantly on the miscibility of the component polymers in the blend.[1-3] The preparation of miscible polymer blends depends on many factors, such as: solvent, temperature, weight/molar ratio of the components, molecular weight etc..[3] Additionally, the presence of specific interactions (hydrogen bonds, van der Waals and/or polar interactions, etc.) between the polymer chains is usually essential to obtain miscible polymer blends.[4]

Significant studies have been carried out on PC/PMMA and PMMA/PVAc blends, while only a few studies have been reported on the PC/PVAc blend system.[4-23] The effects of solvent, solubility parameter, temperature, evaporation rate of the solvent, weight composition of the polymer components, molecular weight, tacticity etc., on generating miscible blends of these pairs were investigated. Yet, various contradictory data/results among these studies were reported.

Crispim et al. reported that the miscibility of PMMA/PVAc blends depends on the solvent and temperature when it is cast from solution. PMMA/PVAc blends were found to be miscible when cast from chloroform at 30 and 50 °C, whereas in N,N-dimethyl formamide (DMF) at the same temperatures the blends cast were immiscible and in toluene their miscibility depends on the temperature. However, none of these polymer blends retained their homogeneous phase even at relatively low temperatures (~180 °C).[5] Similar behavior was also observed by Qipeng et.al. for PMMA/PVAc polymer blends that underwent a phase separation during high temperature treatment.[6] Song et al. also studied the effect of solvents on the miscibility of the PMMA-PVAc blends. A miscible blend of PMMA-PVAc was obtained when chloroform ($CHCl_3$) was used as a solvent, but PMMA-PVAc was found to be immiscible when tetrahydrofuran (THF) was used instead of chloroform.[7] This contrasting behavior between the solvents was attributed to conformational changes. It was suggested that conformational changes would likely occur due to the hydrogen bonds between the C=O of both polymers and C-H of the solvent and the two similar polymer chains could interpenetrate. The chain movement was frozen and chains retain their conformation when the solvent was evaporated. On the contrary, PMMA was found to be almost completely immiscible with PVAc when cast from chloroform and the blends prepared from THF did show a little more partial miscibility than the ones cast from chloroform by Hsu et al.[8] It was also pointed out that using different stereoregular PMMAs (isotactic: i-PMMA, syndiotactic: s-PMMA and atactic: a-PMMA) does not have an effect on the miscibility of PMMA-PVAc blends yet i-PMMA was found to show the highest mutual solubility with PVAc when

the blends were cast from THF. In Schenk et al. it is indicated that PMMA/PVAc blend film cast from toluene is more compatible when compared to that of the blend cast-film from benzene. It was suggested that the presence of specific interactions in toluene solution makes the domain sizes smaller, which likely produce a higher compatibility level. Yet, phase segregation is observed even in the toluene cast-film when the temperature is higher than the glass transition of PVAc (Tg=~40 $^{O}$C) since PVAc macromolecules diffuse away from the interphase and form PVAc rich domains.[9] Ha et al. used the solubility parameter of the solvent to judge blend compatibility and it was claimed that immiscible blends of PMMA/PVAc would be produced from solvents if the contribution of hydrogen bonding to the solubility parameter ($\delta_h$) of the solvent is higher than 6.5 $J^{1/2}$ $cm^{-3/2}$ .[10]

The influence of solvent on the miscibility of PMMA/PVAc and the interpolymer interactions responsible for the miscibility of the blend were also examined by 2-D NMR spectroscopy (NOESY). Two different types of intermolecular interactions between (i) methoxy protons of PMMA and methyne protons of PVAc; (ii) methoxy protons of PMMA and methyl protons of PVAc were observed in miscible blends when prepared from chloroform at 40°C and toluene at 30°C. Type (ii) interactions were detected in immiscible blends when prepared in DMF and in benzene at 40°C. It was concluded that the interaction between methoxy protons of PMMA and methyne protons of PVAc contributes to the miscibility of the blend while type (ii) interactions are due to the contacts of unlike polymers in the interphase and have no effect on miscibility.[11]

Attempts to attain miscible PMMA/PVAc blends has also been carried out by introducing functional groups or a third component which promotes specific interactions like hydrogen bonds between the polymer chains.[13-15] The introduction of carboxyl acid to either of the two component polymers assisted the compatibility of PMMA/PVAc blends at the air/water interface.[13] Blending poly(methacrylic acid) (PMAA) with PVAc instead of PMMA produce homogeneous blends which is achieved by the interpolymer hydrogen bonds between the COOH groups of PMAA and the COO groups of PVAc.[14] A different approach has also been applied to achieve homogeneous PMMA/PVAc blends by the in situ polymerization of methyl methacrylate (MMA) in the presence of PVAc, which resulted in a phase-separated system.[16]

To sum up, it has been generally observed that PMMA/PVAc blends are not miscible, though casting from certain solvents at appropriate temperatures can result in partial miscibility. However, even the examples of partially miscibile PMMA/PVAc blends were observed to phase separate at temperatures above their $T_g$s.

The phase behavior of PC/PMMA blends has been investigated and certain preparation methods were found to be very effective in producing initially homogenous blends. Melt blending of PC/PMMA has been reported to yield partially miscible blends, whereas the homogeneity of blends from solvent casting techniques depends on the solvent and temperature.[18-22] Hsu et al. studied the effect of solvent for PC/PMMA blends, where the blends cast from tetrahydrofuran (THF) did not show visible phase separation, but blends cast from chloroform indicated a phase-separated structure. Conversely, opposite behavior was observed when syndiotactic

PMMA was used instead of atactic PMMA. Even though PC/s-PMMA was not found to be thermodynamically miscible, it was stated that syndiotacticity favors the miscibility between PMMA and PC.[18] This finding was supported by a previous report in which a single-phase blend system of s-PMMA/PC was demonstrated.[19]

Studies on the PC/PVAc blend system are limited in the literature. Sato et al. reported that PC forms partially miscible blends with partially saponified PVAc due to the existence of side-chain hydroxyl groups, which improves their miscibility by intermolecular hydrogen bonding, but PVAc was found to be immiscible with PC.[23]

To summarize, the homogeneity and phase behavior of the PMMA/PVAc, PC/PMMA and PC/PVAc blends showed some ambiguity due to their instability at different temperatures and in different solvent environments and show phase separation and incompatibility when they are prepared by traditional methods. Moreover, it has been revealed that the effects of solvent and temperature play a key role in the homogeneity of their polymer blends.[5-11,18-23] Processing the polymer blends *via* the formation of and coalescence from their common cyclodextrin (CD) inclusion compounds (ICs) eliminates the effects of both solvent and temperature.

Cyclodextrins (CDs) are cyclic oligosaccharides having molecular shapes like shallow truncated cones consisting of 6, 7, and 8 glucose units, and are named alpha ($\alpha$-), beta ($\beta$-) and gamma ($\gamma$-) cyclodextrins (CDs), respectively (see section 2.2, Figure 1).[24] Because of their unusual structure, CD molecules may host both polar and nonpolar guests, which include polymers as well as small molecules.[25-30]

Our research group has recently reported that CDs may act as hosts in the formation of inclusion compounds (ICs) with various guest polymers. Polymer-CD-

ICs represent crystalline compounds obtained by threading of the annular CD molecules onto the guest polymer chains. The included polymers are confined to the narrow, continuous CD channels, and so are necessarily highly extended and segregated from neighboring polymers chains by the walls of the CD stacks. We have shown that coalescence of guest polymers from their CD-IC crystals can result in a significant improvement in their bulk physical properties caused by modification of their structures, morphologies and even conformations compared to those observed in their normally produced bulk states.[28-30] Recently, we have developed a novel approach for mixing thermodynamically incompatible polymers by first obtaining a common polymer-CD-IC. Subsequently, the guest polymers are coalesced from their common CD IC crystals by removal of the CD host.[31-35] This method has successfully produced intimate blends of poly(ε-caprolactone) (PCL)/poly(L-lactic acid) (PLLA)[31], PC/PMMA[32], poly(ethylene terephthalate) (PET)/poly(ethylene 2,6-naphthalate) (PEN)[33] and the ternary blend of PC/PMMA/PVAc.[34]

Here, we summurize the intimate mixing of binary PC/PMMA, PC/PVAc and PMMA/PVAc blend pairs by coalescence from their common γ-CD-ICs, which was necessary for the formation of an intimately mixed ternary blend of PC/PMMA/PVAc.[34] The formation of ICs between γ-CD and the PC/PMMA, PC/PVAc and PMMA/PVAc pairs was successfully achieved. The coalesced binary polymer blends were obtained by removal of γ-CD, and it was found that the host γ-CD molecules preferentially include PC chains over the other two vinyl polymer guests.

### 3.1.3 Experimental

#### 3.1.3.1 Materials

The materials information for PC, PMMA and PVAc is given in section 2.3.1

#### 3.1.3.2 Formation of Binary Polymer/γ-CD Inclusion Compounds

One γ-CD molecule may host three repeat units of PMMA or PVAc or 0.66 repeat units of PC in its interior cavity.[24] On this basis we would expect a PC:PMMA or PVAc feed molar ratio of 2/3:3 = 1:4.5 would lead to 1:4.5 coalesced blends. However, as discussed subsequently, inclusion of PC by γ-CD was preferred over PMMA and PVAC, so a 1:6 molar ratio of PC:PMMA or PC:PVAc and a 1:1 molar ratio of PMMA:PVAc was used for formation of the common inclusion compounds.

A quantity of 0.208 g (0.82 mmol) of PC and 0.490 g (4.9 mmol) of PMMA were dissolved together in 100 ml of a common solvent (dioxane) at 50° C. An aqueous saturated solution of γ-CD (3.712 g (2.86 mmol) in 10 ml DI-$H_2O$ at 50 °C) was added drop-wise to the binary polymer solution, while the stirring rate was kept maximum at a temperature of 50° C. A white, turbid solution was observed once the γ-CD aqueous solution was added to the binary polymer solution (Figure 1). Subsequent to continuous stirring for three hours at 50° C, the white suspension was cooled down to room temperature while the stirring rate was adjusted to a moderate level for another three days. Polymer-CD ICs were obtained after three days of stirring at room temperature with 20-30% yields. The resulting suspension was then

vacuum filtered and the collected white powders were vacuum dried at 45° C for 24 hours. The abbreviation for this inclusion compound is PC/PMMA-γ-CD-IC.

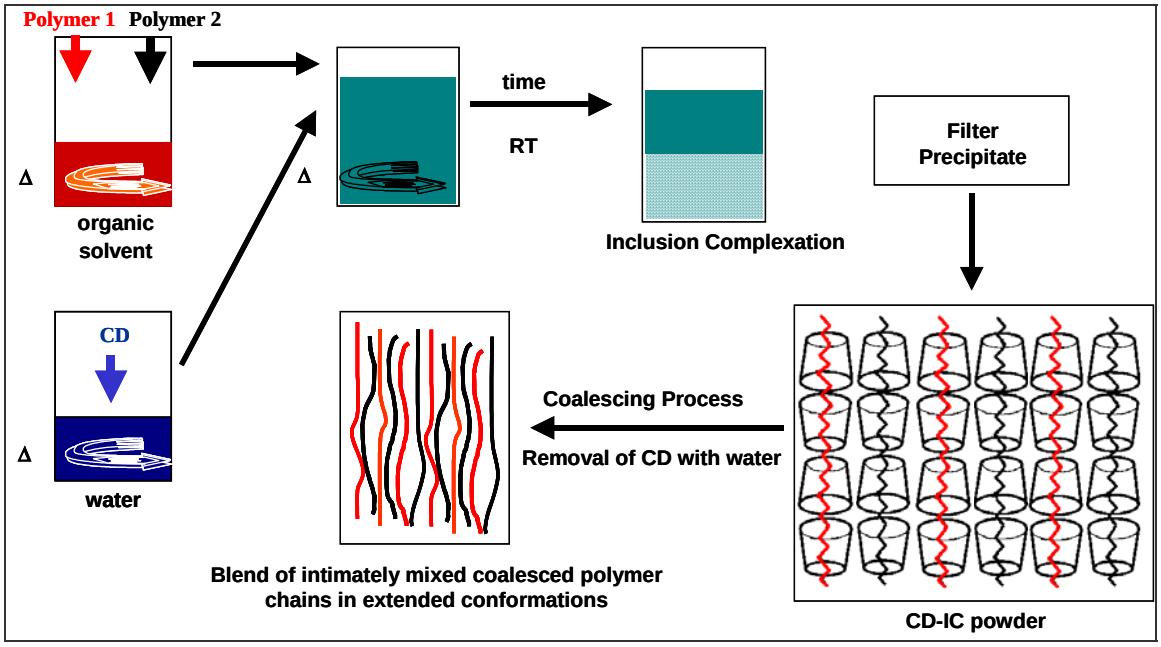


**Figure 1.** Schematic representation of polymer-CD IC formation, the coalescence process and the coalesced polymer.

The same experimental procedure was applied for the formation of the other two binary inclusion compounds (abbreviated as PC/PVAc-γ-CD-IC and PMMA/PVAc-γ-CD-IC). A quantity of 0.208 g (0.82 mmol) of PC and 0.421 g (4.9 mmol) of PVAc were dissolved together in dioxane (100 ml, at 50 °C); 0.429 g (4.29 mmol) of PMMA and 0.369 g (4.29 mmol) of PVAc dissolved together in dioxane (100 ml, at 50° C) for the formation of PC/PVAc-γ-CD-IC and PMMA/PVAc-γ-CD-IC, respectively.

### 3.1.3.3 Coalescence of Polymer Blends from their Inclusion Compounds

The host γ-CD was removed from the inclusion compounds (PC/PMMA-γ-CD-IC, PC/PVAc-γ-CD-IC and PMMA/PVAc-γ-CD-IC) by washing the white crystals with deionized water overnight at 50° C and the α-amylase enzyme (Clarase L-4000) was used when necessary. The coalesced binary polymer blends, PC/PMMA; PC/PVAc; PMMA/PVAc, were then vacuum filtered and rinsed several times with water, and finally vacuum dried at 30-40° C for 2 days. The molar composition of coalesced binary blends was identified by solution $^{1}$H-NMR spectroscopy. The molar ratios of PC:PMMA, PC:PVAc and PMMA:PVAc were found to be 2.8:1, 1.8:1 and 1:1, respectively. These coalesced binary blends were abbreviated as coalesced-PC/PMMA, -PC/PVAc and -PMMA/PVAc .

### 3.1.3.4 Preparation of Binary Blends by Precipitation and Solvent Casting

To serve as control samples, binary blends of PC/PMMA, PC/PVAc and PMMA/PVAc were prepared by dissolution in THF at the same molar concentrations as those observed in the coalesced samples. Both solvent cast and co-precipitation methods were employed to generate the physical blends. The solvent cast films were air-dried overnight and vacuum dried further at 50° C for another 24 h. Phase segregation in the cast films was macroscopically apparent. Infrared spectroscopic examination (FT-IR microscope) of these polymer blends confirmed the macroscopic phase separation of polymer domains, which was indicated by the presence of single and/or binary polymer components for different regions of the cast films. As a consequence, binary control blends of PC/PMMA, PC/PVAc and PMMA/PVAc were

also prepared by the co-precipitation method. Binary polymer components (same molar composition as in coalesced blends) were dissolved in THF and precipitated into deionized water (non-solvent). The precipitates were collected by vacuum filtering through the ceramic frit in a Büchner funnel and were vacuum dried.

### 3.1.4 Characterization

The instrumental information for Wide-Angle X-ray Diffraction (WAXD), $^{1}H$ Nuclear Magnetic Resonance (NMR), Fourier Transform Infrared Spectroscopy (FT-IR), Differential Scanning Calorimetry (DSC), Thermogravimetric Analysis (TGA), Direct Insertion Probe Pyrolysis Mass Spectrometry (DIP-MS) is given in the previous chapter (see section 2.4).

Solid-state $^{1}H$ NMR data were collected using a Bruker DSX wide-bore system with a field strength corresponding to a $^{1}H$ Larmor frequency of 300.13 MHz. Radio-frequency power levels were 71 kHz for spin-locking and decoupling, corresponding to π/2 pulse widths of 3.5 μs. Data were obtained using MAS speeds of 4.5 kHz on a commercial 7-mm probe. $^{1}H$ $T_{1\rho}$ measurements were made at room temperature using standard $^{13}C$ cross-polarization observation experiments, in which the length of the $^{1}H$ spin-lock pulse was incrementally varied prior to cross-polarization. Cross polarization contact times were 1 ms. Depending on the amount of samples, 512 to 2,000 scans were collected per relaxation time increment.

### 3.1.5 Result and Discussion

#### 3.1.5.1 Wide-Angle X-ray Diffraction (WAXD)

WAXD is a useful characterization technique for investigating the crystalline phase transition between the cage structure of as-received γ-CD·7$H_2O$ and the channel structure of γ-CD. Once the host CD molecules are threaded onto the polymer chains, it is expected that the final IC crystals adopt a channel-type crystal structure. To confirm the formation of a polymer-CD-IC, the crystals resulting from precipitation are vacuum-dried after filtration. This destroys any columnar γ-CD with only water included in the channels, since columnar γ-CD collapses into an amorphous structure upon dehydration of the crystals.[36] However, in the case of polymer-γ-CD-ICs, the polymer chains included in the γ-CD channels preserve the channel structure.

Figure 2 shows WAXD patterns for the vacuum-dried binary polymer-γ-CD-ICs. The reflections consistent with γ-CD in the channel structure persisted after vacuum drying of the polymer-γ-CD-ICs. One reflection in particular occurring at 2θ = 7.5° for polymer-γ-CD IC crystals is indicative of γ-CD in the channel structure and has been assigned to the 200 plane of a tetragonal lattice by Takeo and Kuge.[37] Yet, the diffraction pattern of our polymer/polymer-γ-CD-ICs also indicated the existence of some amorphous structure, which is due to the presence of some γ-CD with only water included that collapsed into an amorphous structure upon vacuum drying.

The presence of a peak at 2θ = 7.5° represents the first evidence that γ-CD molecules formed a channel structure IC with the possible inclusion of polymer

guests residing in the γ-CD cavities. FT-IR and DSC studies were carried out to confirm that the polymers are included in the IC channels. The presence of polymers in the IC samples was confirmed by FT-IR, where the C=O absorption bands from all three polymers were evident. None of the DSC scans of PC/PMMA-, PC/PVAc- or PMMA/PVAc-γ-CD-ICs (data not shown) exhibited glass transitions for any of the potentially uncomplexed polymers. This result reveals that polymer chains are threaded and covered by CD molecules in the polymer-CD-ICs.

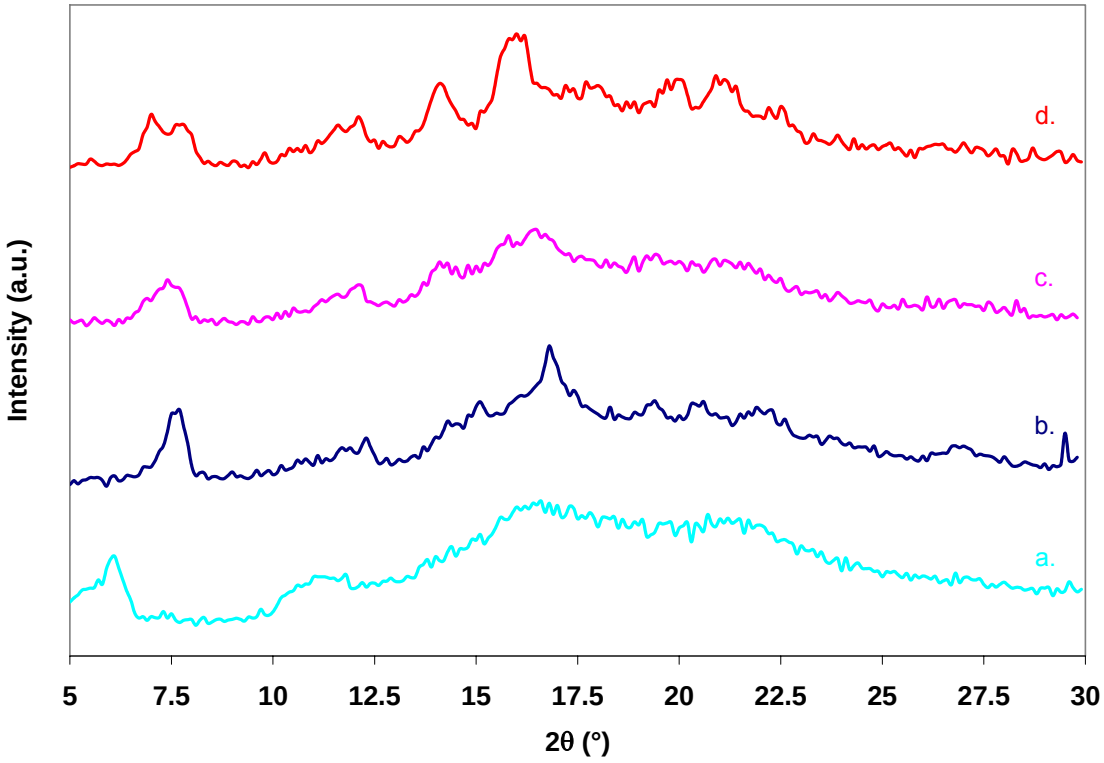


**Figure 2.** X-ray diffraction patterns of vacuum-dried crystals (a) γ-CD channel, (b) PC/PMMA-γ-CD-IC, (c) PC/PVAc-γ-CD-IC, and (d) PMMA/PVAc-γ-CD-IC.

### 3.1.5.2 $^{1}$H Nuclear Magnetic Resonance (NMR)

$^{1}$H-NMR solution spectra of the coalesced PC/PMMA, PC/PVAc and PMMA/PVAc binary blends were recorded (Figure 3). The molar ratios of PC, PMMA and PVAc in the coalesced binary blends were determined by comparison of integrals of the three distinct polymer peaks at 7.2 ppm for PC, 4.8 ppm for PVAc, and 3.6 ppm for PMMA versus TMS. The molar ratios of the coalesced PC:PMMA, PC:PVAc and PMMA:PVAc blends were found to be 2.8:1, 1.8:1 and 1:1, respectively.

Comparison to the 1:6 molar ratio of the starting solutions of PC:PMMA or PC:PVAc suggests that the host $\gamma$-CD molecules preferentially include PC chains over the other two vinyl polymer guests. The tendency of PC to form an inclusion compound with $\gamma$-CD is close to 17 times higher when compared to PMMA and 11 times higher when compared to PVAc. However, apparently there is no inclusion preference observed between PMMA and PVAc as shown by the equivalence between the initial and final molar ratios of these two polymers. Similar behavior has also been observed for the ternary system of these polymers, where PC chains are more likely to be included and reside in the $\gamma$-CD channels than PMMA and PVAc chains.[34] It has previously been reported that host $\gamma$-CD molecules posses a greater inclusion affinity for more hydrophobic, rather than hydrophilic, guest polymers.[38] Here, the preferential inclusion of PC may be explained by its hydrophobicity, which is higher than that of PMMA or PVAc. Other possible reasons for this behavior are still under investigation.

Solubility differences between the coalesced and physical blends were observed when we tried to re-dissolve the binary blends in a common solvent. We were able to dissolve the coalesced binary blends only at high temperature and after long time ultrasonication, whereas the physical blends were readily re-dissolved at room temperature. The lower solubility of the coalesced PC/PMMA, PC/PVAc or PMMA/PVAc binary blends indicated a higher degree of mixing in these systems when compared to their physical blends. When the polymer blends are intimately mixed, the entropy gained from dissolution is reduced and enthalpically favorable interchain interactions maybe established. Apparently, it requires more time and higher temperatures to break the interactions between these well-mixed chains when compared to their phase separated physical blends. Additionally, the presence of remnant CD molecules in the coalesced blends might be also the reason for their low solubility.

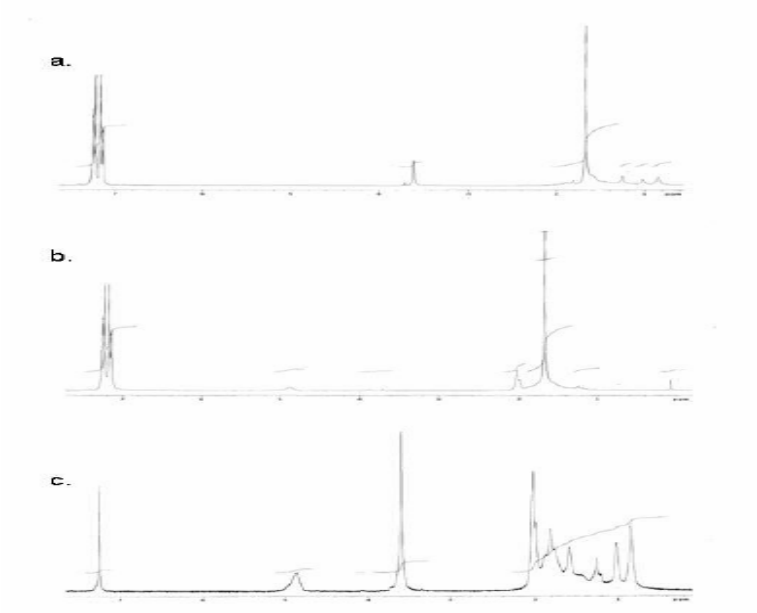


**Figure 3.** $^{1}$H-NMR spectra of coalesced (a) PC/PMMA, (b) PC/PVAc and (c) PMMA/PVAc binary blends.

### 3.1.5.3 Fourier Transform Infrared Spectroscopy (FT-IR)

The FT-IR spectra of PC/PMMA-, PC/PVAc- and PMMA/PVAc-γ-CD-ICs show the presence of two carbonyl bands (C=O) at 1775 $cm^{-1}$ , 1730 $cm^{-1}$ and 1735 $cm^{-1}$ characteristic for PC, PMMA and PVAc, respectively (Figure 4). This demonstrates that all three polymer pairs are included in the binary γ-CD-ICs.

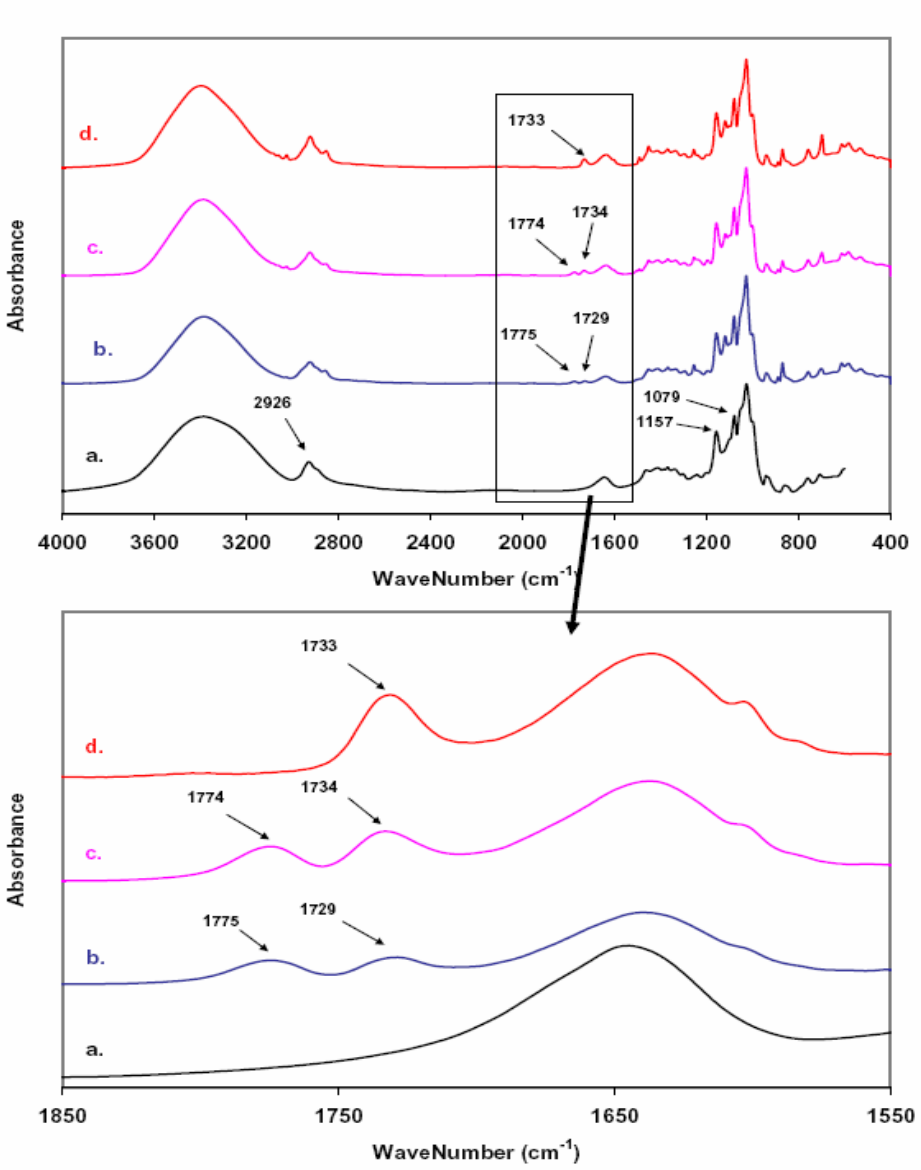


**Figure 4.** FT-IR spectra of (a) as received γ-CD, (b) PC/PMMA-γ-CD-IC, (c) PC/PVAc γ-CD-IC, and (d) PMMA/PVAc-γ-CD-IC.

In general, absorption bands are shifted in the infrared spectra of blends when there are specific interactions between or there are conformational changes in the constituent polymers. The infrared spectra of physical blends (Figure 5) and the coalesced PC/PMMA, PC/PVAc and PMMA/PVAc polymer blends (Figure 6) were examined in order to identify any possible differences between them. It was noticed that the peaks observed at 1736, 1375 ,1243 and 1022 $cm^{-1}$ in the physical blend of PMMA/PVAc were shifted to 1735, 1374,1242 and 1025 $cm^{-1}$, respectively, in the coalesced PMMA/PVAc blend. For the coalesced PC/PMMA blend, the C=O peak and carbonate aryl-O-aryl C-O peak shifted to 1775 and 1230 $cm^{-1}$ from 1776 and 1232 $cm^{-1}$, respectively, when compared to the physical mixture of this blend. In the case of the coalesced PC/PVAc blend, the carbonyl band shift was more noticeable when it was compared with its physical mixture. The C=O bands at 1735 $cm^{-1}$ for PVAc and at 1776 $cm^{-1}$ for PC in the physical blend were shifted to 1740 $cm^{-1}$ and 1774 $cm^{-1}$, respectively, for the coalesced blend. These shifts may result from interactions between polymer chains, but can also be attributed to different environments for each polymer chain in the intimately mixed coalesced binary blends.

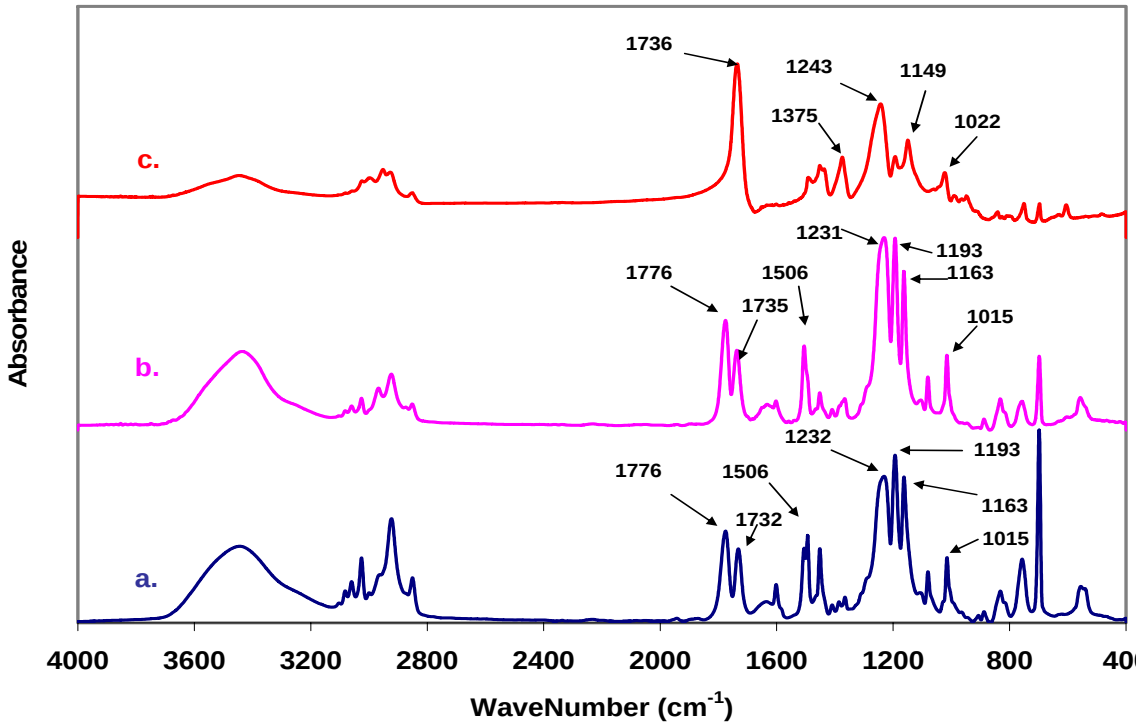


**Figure 5.** FT-IR spectra of co-precipitated polymer blends (a) PC/PMMA, (b) PC/PVAc and (c) PMMA/PVAc.

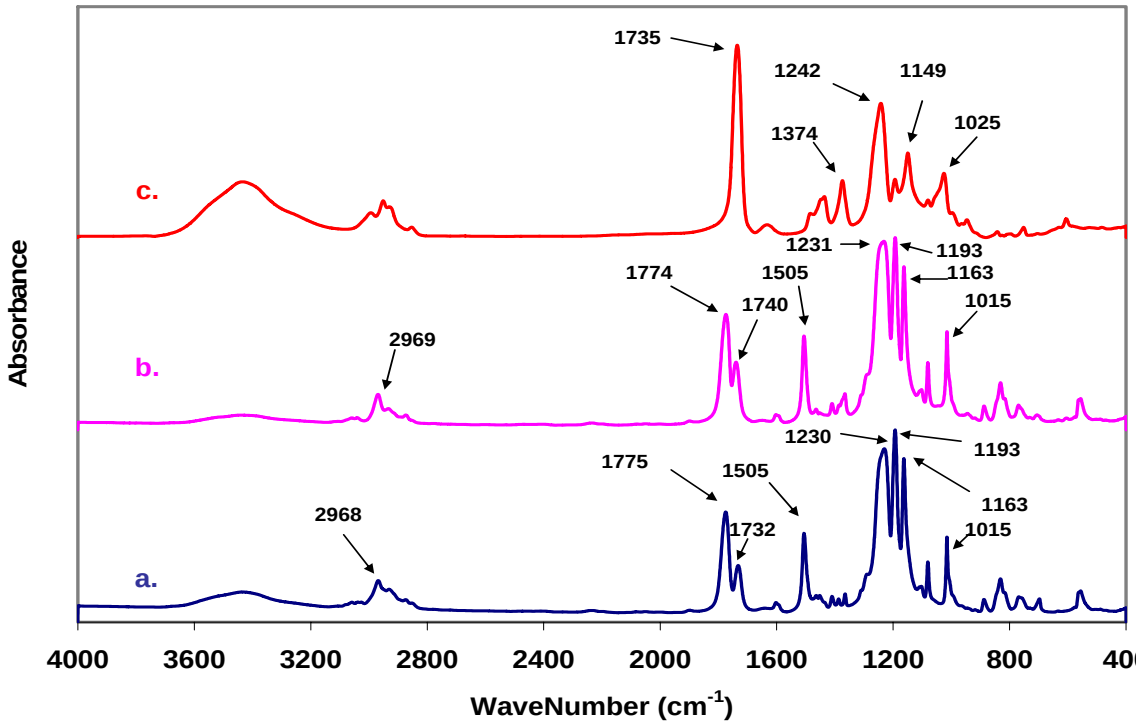


**Figure 6.** FT-IR spectra of coalesced polymer blends: (a) PC/PMMA, (b) PC/PVAc, and (c) PMMA/PVAc.

### 3.1.5.4 Differential Scanning Calorimetry (DSC)

In general, the appearance of a single glass transition temperature ($T_g$) is satisfactory verification of a homogeneous amorphous phase present in a polymer blend. However, the observation of a common glass transition temperature in a polymer blend does not necessarily mean that the homogeneous phase is in a thermodynamic equilibrium state. A polymer blend is likely to show a single $T_g$ once the homogeneous phase is trapped, but might phase separate during heating above its $T_g$ where phase segregation can occur due to the segmental mobility of the polymer chains. Therefore, it is necessary to apply several heating and cooling scans in DSC experiments performed on polymer blends. Retention of a single $T_g$ after repeated heat treatments should reveal the homogeneity of the blend system.

Figure 7 displays the DSC scans recorded for the co-precipitated physical and coalesced PC/PMMA blends. Two glass-transition temperatures ($T_g$) were observed for the co-precipitated PC/PMMA blend in the first DSC scan (Fig. 7c): a weak transition at 81° C for PMMA and a $T_g$ at 136° C for PC domains. For polymer blends, a single $T_g$ is indicative of a state of molecular dispersion, whereas the appearance of multiple distinct $T_g$s suggests the occurrence of phase separation. DSC results indicated that the physical PC/PMMA binary blend prepared by co-precipitation does not form a miscible blend. In contrast, the first scan of the coalesced PC/PMMA blend (Fig. 7a) did not show any apparent glass transition, but instead a melting of crystalline PC regions at 242° C. It is noteworthy that PC was found to be completely amorphous in the as-received sample and its co-precipitated

PC/PMMA blend, whereas PC chains form crystalline regions in the coalesced PC/PMMA blend.

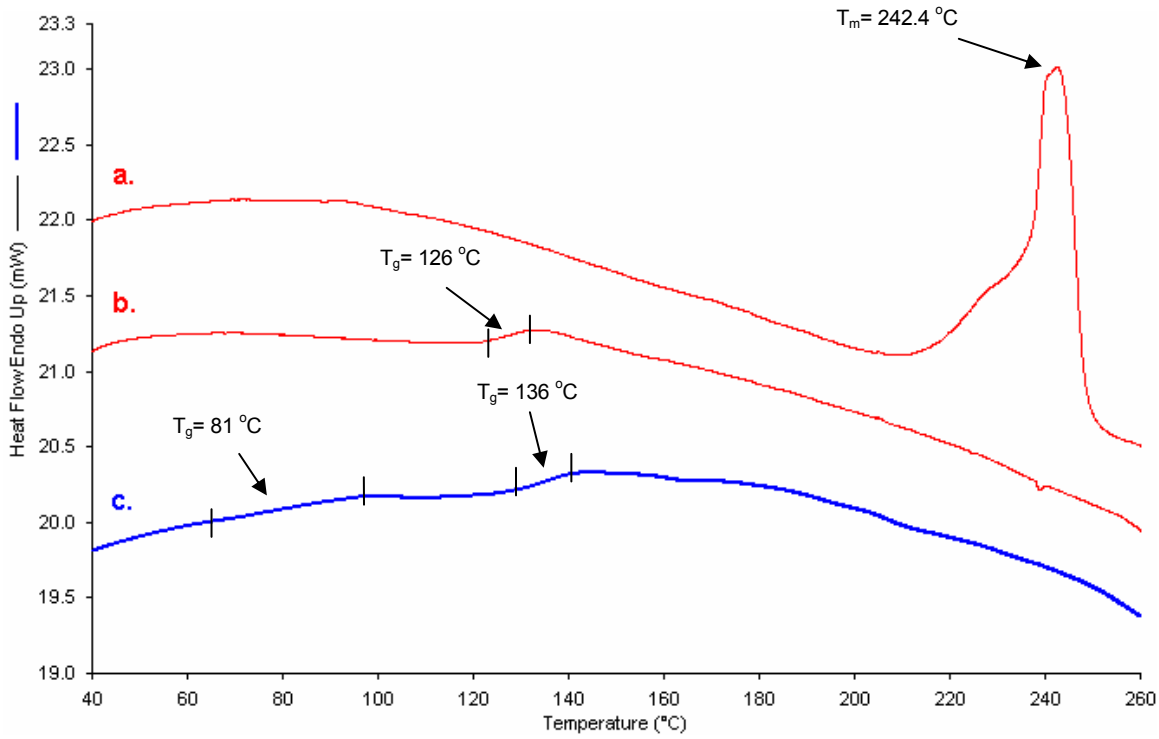


**Figure 7.** DSC thermograms of (a) first heating scan and (b) second heating scan of coalesced PC/PMMA blend (c) first heating scan of co-precipitated PC/PMMA blend.

The presence of a crystalline phase in coalesced PC/PMMA and PC/PVAc blends was also confirmed by x-ray measurement (data not shown). The x-ray diffraction from these coalesced blends showed a similar pattern with the main diffraction peak at $2\theta$= ~18º, whereas co-precipitated physical blends exhibited a broad amorphous halo in that region. This crystalline phase may be a consequence of retention of the extended conformation required by inclusion in the narrow $\gamma$-CD-IC channels for the coalesced PC, as well as their partial segregation into proximal regions of the common $\gamma$-CD-IC crystals, as discussed previously[40], as well as the preferential inclusion of PC chains mentioned above. The crystalline behavior of PC

was also observed for its coalesced homopolymer and its ternary PC/PMMA/PVAc blend.[34,41] However, PC crystals are not reformed once the blend is heated above the melting point of PC. The second DSC scan was run after quenching the sample from 270 to 0° C at a rate of 200 °C/min. In the second heating scan (Fig. 7b), the melting peak for PC crystals disappeared and a single $T_g$ at 126° C was observed, indicating the presence of a single homogeneous amorphous phase in the binary blend of PC/PMMA, where these two polymer components are intimately mixed with each other. The intimate mixing between PC and PMMA could originate from intermolecular contacts and specific interactions which generally create smaller domain sizes, thereby introducing a higher degree of compatibility.

Figure 8 displays the DSC scans recorded for the co-precipitated physical and coalesced PC/PVAc blends. The PC/PVAc blend system showed thermal behaviors similar to the PC/PMMA blend, where melting at 243° C for PC crystals was observed in the first scan of the coalesced blend (Fig. 8a). The absence of PC melting in the first DSC scan (Fig. 8c) of the co-precipitated PC/PVAc blend indicated that both polymer components were amorphous in this blend. Additionally, the DSC scan showed two distinct $T_g$s at 39° C and at 137° C due to phase separated PVAc and PC domains, respectively. The DSC of coalesced PC/PVAc blend showed a $T_g$ 40° C in the first scan (Fig 8a) indicating that PVAc domains are phase- separated in the bulk, however, the second DSC scan (Fig 8b) showed a single $T_g$ at 133 °C, which reveals the intimate mixing of these two components once the sample was subjected to heating-quenching cycle.

In both the coalesced PC/PMMA/ and PC/PVAc blends only the melting of PC crystals was observed during their first heating DSC scans, which disappeared after melting and rapid cooling during their second heating DSC scans. This suggests the presence of small PC crystals in close contact with PMMA and PVAc chains, which upon melting lead to well-mixed PC/PMMA and PC/PVAc amorphous regions that evidence single $T_g$s, though this behavior warrants further study.

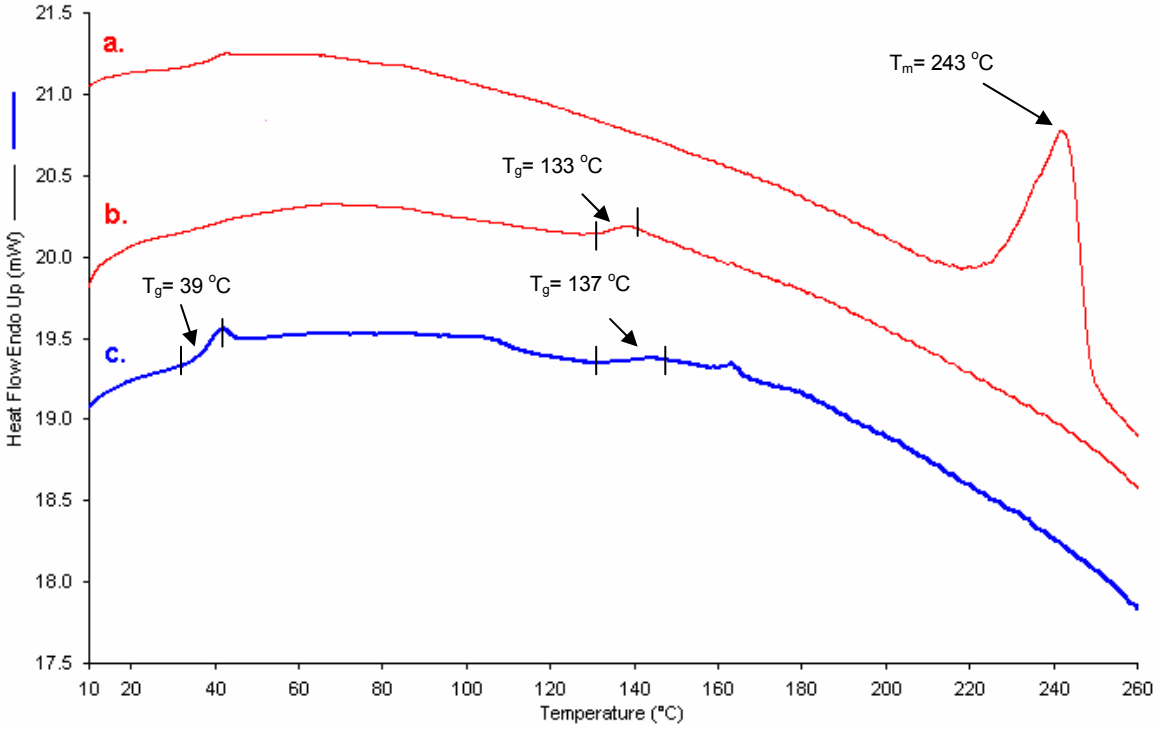


**Figure 8.** DSC thermograms of (a)1st heating scan and (b) 2nd heating scan of coalesced PC/PVAc blend (c) 1st heating scan of co-precipitated PC/PVAc blend.

Figure 9 shows the DSC scans recorded for the co-precipitated physical and coalesced PMMA/PVAc blends. The first DSC scan of the co-precipitated PMMA/PVAc blend showed a single $T_g$ at 47° C. The $T_g$ observed at 47° C is higher than the $T_g$ of pure PVAc which could be due to the miscibility of PMMA and PVAc domains. Previously, it was reported that at temperatures higher than the $T_g$ of

PVAc, PVAc macromolecules begin to diffuse from the interphase and migrate to PVAc rich domains.[9] Here, we observed the same behavior for PVAc domains in the PMMA/PVAc physical blend when it was subjected to heating-cooling cycles. The $T_g$ is shifted from 47 to 33° C in the second heating DSC scan, which indicates the phase separation of PVAc domains from PMMA domains. Figure 10c displays the second heating scan of the coalesced PMMA/PVAc blend. The thermogram shows a $T_g$ at 36° C indicating the presence of phase separated PVAc domains in the blend and a $T_g$ at 53° C, a value between the $T_g$s of the homopolymers (PMMA, $T_g$ = ~80° C and PVAc, $T_g$ = ~35° C) indicating the presence of an intimately mixed phase of amorphous PMMA/PVAc chains. The retention of the $T_g$ at 53° C even after several heating-cooling cycles reveals the presence of intimately mixed and thermally stable PMMA/PVAc domains in the coalesced blend.

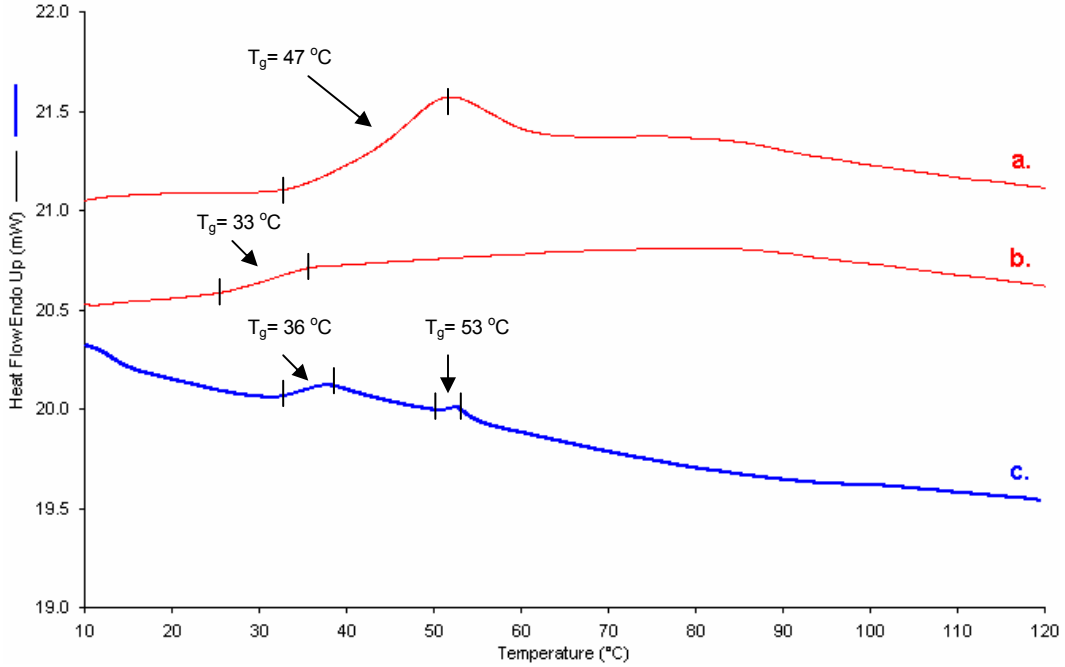


**Figure 9.** DSC thermograms of (a) first heating scan (b) and second heating scan of co-precipitated PMMA/PVAc blend and (c) second heating scan of coalesced PMMA/PVAc blend.

### 3.1.5.5 Solid-State $^1$H NMR

The $^1$H spin-lattice relaxation times of the PC/PMMA and PMMA/PVAc blend systems observed in the rotating frame ($^1$H $T_{1\rho}$) are presented in Tables I and II, respectively. The pure polymers have their own uniform $^1$H $T_{1\rho}$values, which indicates the necessary homogeneity in each pure polymer. Some $^1$H $T_{1\rho}$data are missed in the blend samples due to the overlap of the peaks with the spinning side bands of PC. For the PC/PMMA blend in Table I, the physical mixture sample shows two distinct $^1$H $T_{1\rho}$ values, one for each component, which indicates a phase-separated blend with domain sizes above 5 nm. The coalesced blend sample exhibits a uniform spin-lattice relaxation value indicating the intimate blending of PC and PMMA chains in the coalesced PC/PMMA sample. On the other hand, the similar $^1$H $T_{1\rho}$values observed for pure PVAc and PMMA shown in Table II indicate that the spin-lattice relaxation experiment may not be as an effective method to study the phase behavior of this polymer blend system. Nevertheless, the $^1$H $T_{1\rho}$ values shown in Table II suggests that the precipitation process changed the morphology of both polymers; the distinct $^1$H $T_{1\rho}$values for PMMA and PVAc in the precipitated blend show the phase segregation in this sample. In the case of the coalesced PMMA/PVAc blend, the closely similar $^1$H $T_{1\rho}$ values suggest a certain degree of intimate blending.

**Table 1.** $T_{1\rho}(^1H)$ of binary (PC/PMMA) blend (ms)

| | PC | | | | | PMMA | | |
|---|---|---|---|---|---|---|---|---|
| Peak (ppm) | 150 | 130 | 120 | 40 | 30 | 178 | 52 | 45 |
| PC | 5.1 | 5.5 | 5.5 | 5.2 | 5.6 | --- | --- | --- |
| PMMA | --- | --- | --- | --- | --- | 14.8 | 14.9 | 15.5 |
| Precipitated blend | 5.2 | 5.4 | 5.4 | 5.1 | 5.2 | --- | 16.9 | 13.0 |
| Coalesced blend | 6.8 | 7.0 | 7.6 | 6.9 | 6.7 | --- | 7.9 | 7.7 |

**Table 2.** $T_{1\rho}(^1H)$ of binary (PMMA/PVAc) blend (ms)

| | PMMA | | | PVAc | | |
|---|---|---|---|---|---|---|
| Peak (ppm) | 178 | 52 | 45 | 171 | 68 | 21 |
| PMMA | 14.8 | 14.9 | 15.5 | --- | --- | --- |
| PVAc | --- | --- | --- | 10.6 | 12.2 | 11.2 |
| Precipitated blend | 15.5 | 18.3 | 18.5 | 33.3 | 40.7 | 31.8 |
| Coalesced blend | 21.2 | 19.8 | 22.8 | 16.5 | 19.6 | 20.2 |

### 3.1.5.6 Thermogravimetric Analysis (TGA)

Figure 10 displays the TGA curves of coalesced binary blends and physical mixtures of PC/PMMA, PC/PVAc and PMMA/PVAc. Thermogravimetric results of all binary blends indicated two weight losses stages. The decomposition temperatures, $T_d$s, are at 431 and $542^0$ C for the coalesced PC/PMMA blend and are at 421 and $546^\circ$ C for the physical mixture (Figure 10a and b). The low temperature weight losses observed for individual as-received and coalesced PMMA samples[41] were not

observed for both of the binary blends. The first degradation stage of coalesced PC/PMMA is higher than the main degradation stage of coalesced PMMA (423° C) indicating an increase in thermal stability of the PMMA component. A similar behavior was also noted for the physical mixture compared to as-received PMMA (410° C). However, the second $T_d$ detected for coalesced and physical blends of PC/PMMA is lower than the $T_d$s of as-received and coalesced PC samples, at 549 and 554° C.[41]

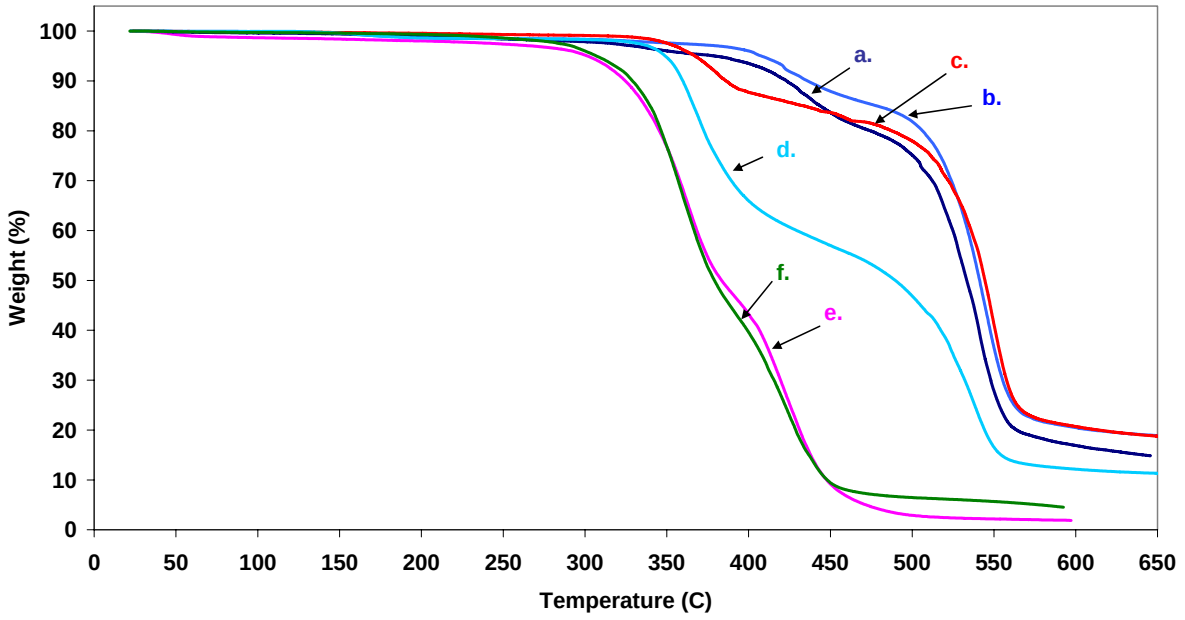


**Figure 10.** TGA thermograms of (a) coalesced and (b) co-precipitated PC/PMMA blends; (c) coalesced and (d) co-precipitated PC/PVAc blends; and (e) coalesced and (f) co-precipitated PMMA/PVAc blends.

The TGA curve of the coalesced PC/PVAc binary blend shows two $T_d$s at 377 and 551° C and that of the physical mixture of PC/PVAc shows two $T_d$s at 369 and 538° C (Figure 10 c and d). The first degradation stages of individual coalesced and as-received PVAc were observed at 369 and 360° C, respectively.[41] The second

degradation stage for the coalesced PVAc sample was shifted to 483° C from 464° C, the corresponding value of the as-received sample, indicating an increase in thermal stability for the coalesced PVAc. The second degradation stages of both of the binary mixtures are significantly higher than these values. However, the second $T_d$ for coalesced and physical blends of PC/PVAc at 551 and 538° C, respectively, are slightly lower than the $T_d$s of coalesced and as-received PC samples. The TGA results of coalesced and physical binary blends of PC/PMMA and PC/PVAc reveal that in the presence of PC, the thermal stabilities of both PMMA and PVAc increase, while the presence of PMMA and PVAc decreases the thermal stability of the PC component.

For the coalesced PMMA/PVAc blend the two $T_d$s are at 360 and 424° C, very close to the $T_d$ values of the physical mixture at 360 and 422° C and to the corresponding values for pure PVAc. The low temperature weight losses recorded for as-received and coalesced PMMA samples were not observed for PMMA/PVAc blends as in the case of PC/PMMA blends. The second degradation steps observed at 424 and 423° C are very close to that for the coalesced PMMA at 423° C, but lower than the second degradation step for PVAc at 464 and 483° C.

### 3.1.5.7 Direct Insertion Probe Pyrolysis Mass Spectrometry (DIP-MS)

DIP-MS facilitates analyses of degradation mechanisms using structural information from the thermal characterization of degradation products.[42-44] The DIP-MS technique was applied for thermal characterization of degradation products of coalesced and physical binary blends of PC/PMMA, PC/PVAc and PMMA/PVAc. As the maximum attainable temperature with our present pyrolysis system is 445° C, the

highest temperature weight losses detected in TGA curves could not be studied for PC samples.

Thermal degradation behaviors of PC, PMMA and PVAc have been detailed in the literature.[45-50] The DIP-MS results of individual polymers; PC, PMMA and PVAc were discussed in detail in the previous chapter (see section 2.5.5). To summarize, the evolution of cyclic oligomers due to intermolecular exchange reactions and evolution of $CO_2$ by decarboxylation of the carbonate groups forming ether bridges and by hydrolysis reactions producing phenolic end groups has been proposed for the thermal degradation of poly (bisphenol A carbonate) in the temperature range studied (400-500$^{\circ}$ C) here.[45,46] For PMMA the low temperature weight losses were attributed to evolution of dimer, low molecular weight oligomers, scission of head-to-head linkages, and loss of unsaturated end groups. At elevated temperatures (380 - 420$^{o}$ C), however, initiation of weight loss was thought to be a mixture of chain end and chain scission processes, followed by depropagation to the end of the polymer chain.[47,48] PVAc degrades in two stages, around 360 and 440$^{o}$ C, corresponding to deacetylation and disintegration of the polyolefinic backbone, respectively.[49,50] It is known that the probability of cleaving a particular bond during thermal degradation depends not only upon its inherent strength, but also on the stability of products formed. Thus, loss of side groups from PVAc by a mechanism similar to the Mc Lafferty rearrangement reaction[51] is favored, because a stable polyolefinic backbone and $CH_3COOH$ are generated. On the other hand, the thermal degradation of PMMA starts by cleavage of the polymer backbone, not only as a consequence of the increased stability of the tertiary carbonium radical

produced, but also due to the absence of a γ-H that can be transfered to the C=O group.

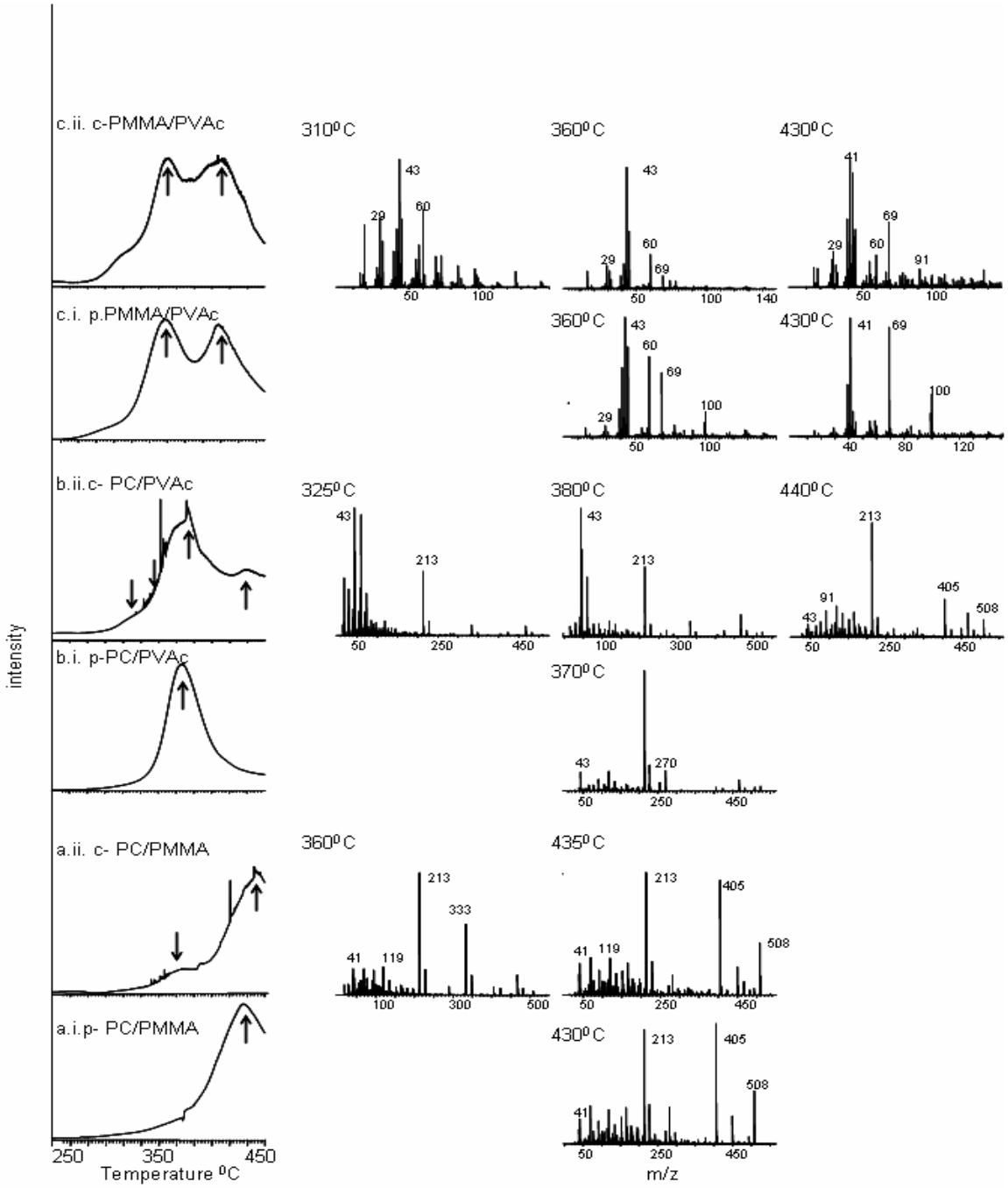


**Figure 11.** TIC curves (left) and pyrolysis mass spectra (right) recorded at the maximum of the peaks and shoulders in the TIC curves of a) PC/PMMA physical mixture, b) coalesced PC/PMMA, c) PC/PVAc physical mixture d) coalesced PC/PVAc, e) PMMA/PVAc physical mixture, and f) coalesced PMMA/ PVAc blends.

The total ion current (TIC) curves of coalesced and physical binary blends of PC/PMMA, PC/PVAc and PMMA/PVAc are shown in Figure 11. The pyrolysis mass spectra recorded at the shoulders and at the TIC maxima are also included in this figure. In general, the maxima present in the TIC curves are quite similar to the $T_d$ values in the corresponding TGA curves (see Figure 10). For all the coalesced binary blend samples, weak shoulders around 300-360° C, are detected and associated with evolution of γ-CD based products indicating that all the samples contained small amounts of remnant γ-CD.

### 3.1.5.7.1 Coalesced and Physical PC/PMMA Blends

The maxima at 435 and 430° C in the TIC curves of coalesced and physical PC/PMMA blends, respectively, are more than 20° C higher than the TIC maxima recorded for coalesced PMMA (Figures 11 a). The mass spectra recorded at the weak shoulder around 360° C in the TIC curve of the coalesced sample are dominated by peaks characteristic of PC, with the $C_6H_5$-O-COO-$C_6H_4$ fragment peak at m/z=213 Da being the base peak. Peaks diagnostic for γ-CD were also recorded in these spectra. However, PMMA based products peaks were relatively weak. In Figure 12, the evolution profiles of some characteristic fragments of pure PC, PMMA and γ-CD were observed. The maxima of the evolution profiles shifted slightly to higher temperatures for the coalesced blend. The most significant change is the low temperature evolution of the $C_6H_5$-O-COO-$C_6H_4$ fragment as in the case of coalesced PC. It is clear that thermal stability of PMMA chains increased in the presence of PC. The increase in stability is more pronounced for the coalesced sample. On the other hand, for the coalesced blend, evolution of PC based

degradation products started at significantly lower temperatures. It may be concluded that presence of PC enhances the thermal stability of PMMA.

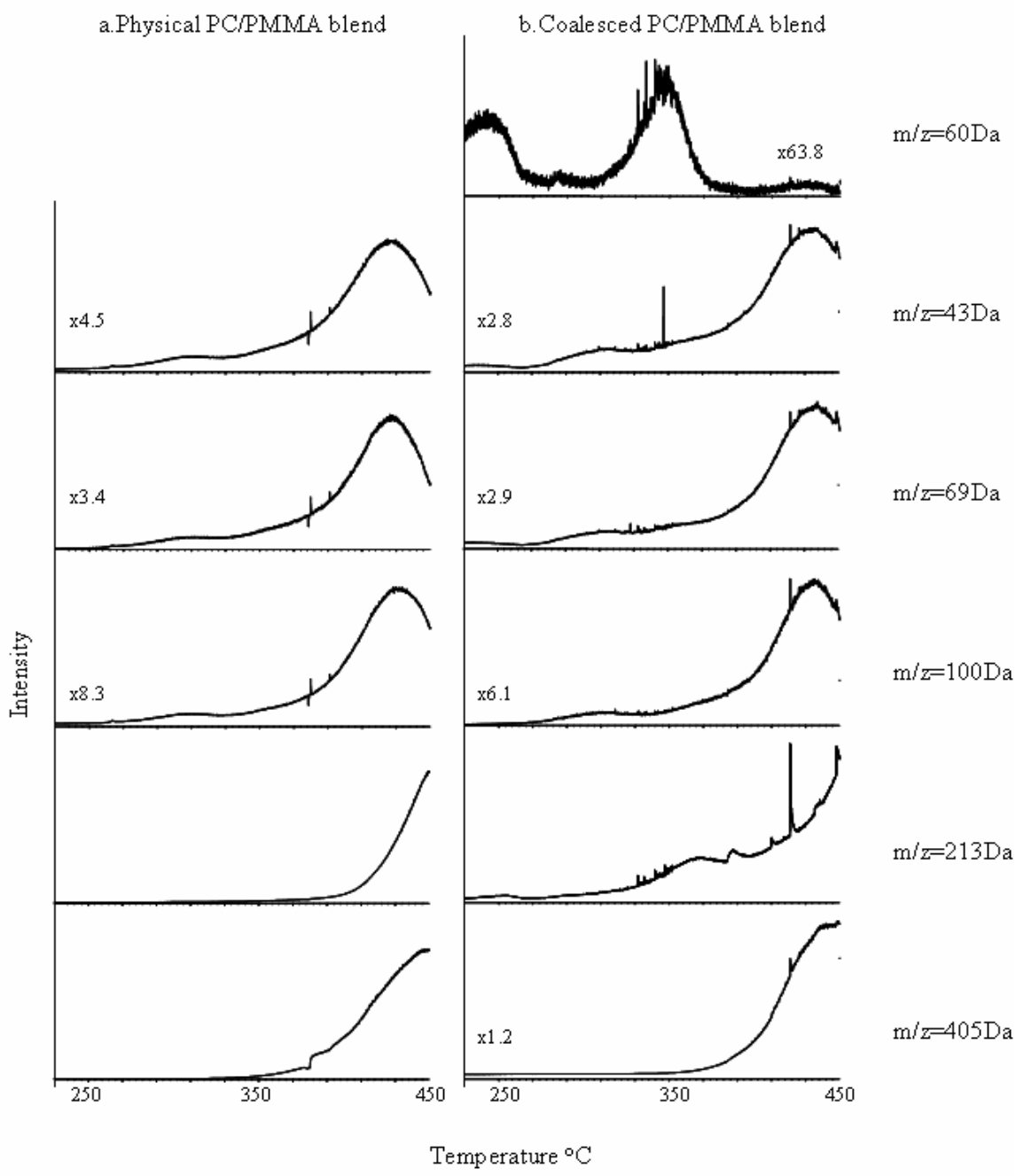


**Figure 12.** Evolution profiles of $C_6H_5$-$C(CH_3)_2$-$C_6H_4$-O-$C_6H_4$-$C(CH_3)_2$-$C_6H_4$ (m/z=405Da), $C_6H_5$-O-COO-$C_6H_4$ (m/z=213 Da), MMA (m/z=100Da), $CH_2C(CH_3)CO$ (m/z=69Da), $CH_2CCH_3$ (m/z= 41Da) , and $C_2H_4O_2$ (m/z=60Da), recorded during the pyrolysis of a) physical b) coalseced PC/PMMA blends.

### 3.1.5.7.2 Coalesced and Physical PC/PVAc Blends

The total ion current (TIC) curves of the coalesced and physical PC/PVAc blends show maxima around 370 and 380° C, respectively (Figure 11 b). For the coalesced sample a shoulder around 325° C and a second maximum on the high temperature tail at 440º C are seen. Analyses of the pyrolysis mass spectra of the coalesced binary blend indicated evolution of γ-CD around 325° C together with some PC based fragments. Unlike the PC/PMMA physical mixture, the evolution of PC based fragments were also shifted to low temperatures for the PC/PVAc physical blend (Figure 11 b). Furthermore, for the physical blend, evolution of fragments generated by decarboxylation of the carbonate groups forming ether bridges also occurred at lower temperatures in contrast to the PC/PMMA physical mixture. It may be that the acetate degradation product of PVAc occurring around 360° C activates degradation of PC even at low temperatures. In Figure 13, evolution profiles of some characteristic products are shown. Compared to pure PVAc, a significant decrease in the ratio of $CH_3COO$ to $CH_3CO$ yields was noted for the physical blend supporting the reactions of $CH_3COO$ with PC chains. However, for the coalesced blend $CH_3COO$ yield was noticeably higher. Furthermore, evolution of PC based fragments shifted slightly to higher temperatures.

### 3.1.5.7.3 Coalesced and Physical PMMA/PVAc Blends

The total ion current curves of the coalesced and physical PMMA/PVAc blends, with two maxima around 360 and $430^0$ C, are shown in Figure 14f and g. The only noticeable difference is the presence of a weak shoulder around $310^0$ C in the TIC curve of the coalesced blend, in accordance with TGA results. This weak

shoulder is again associated with evolution of γ-CD based products indicating that the sample contained small amounts of remnant γ-CD. For both blends, the mass spectra recorded around $360^0$ C are mainly dominated by peaks diagnostic for PVAc and those recorded around $430^0$ C are dominated by peaks diagnostic for PMMA. Though the TIC curves of the physical and coalesced blends are quite similar, the fragmentation pattern recorded in the related pyrolysis mass spectra are significantly different. At high temperatures the relative intensities of high molecular weight fragments were decreased for the coalesced blend. In particular, the decrease in PMMA monomer yield was quite drastic for the coalesced blend.

In Table 3 relative ion yields of intense and/or characteristic peaks in the pyrolysis mass spectra recorded at the maxima of the TIC curves of both blends are collected. It is noteworthy that the relative intensities of high molecular weight products diminished noticeably for the coalesced PMMA/PVAc blend, as was the case for coalesced PVAc. In an attempt to better understand these observations, single ion pyrograms of thermal degradation products for the physical and coalesced blends were studied and some selected results are shown in figure 15.

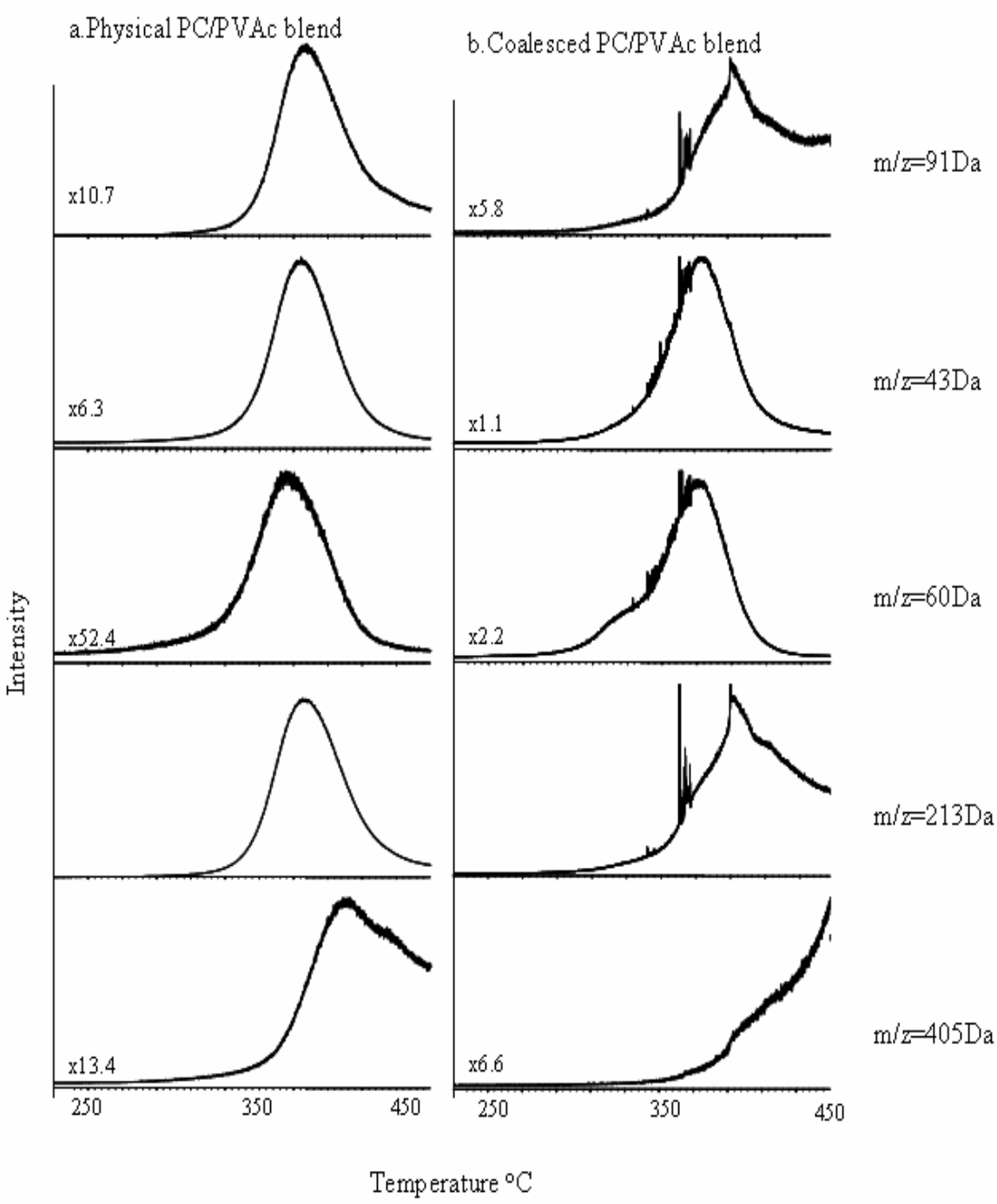


**Figure 13.** Evolution profiles of $C_6H_5$-$C(CH_3)_2$-$C_6H_4$-O-$C_6H_4$-$C(CH_3)_2$-$C_6H_4$ (m/z=405Da), $C_6H_5$-O-COO-$C_6H_4$ (m/z=213 Da), $C_2H_4O_2$ (m/z=60Da), $C_2H_3O$ (m/z=43 Da), and $C_7H_7$ (m/z= 91Da) recorded during the pyrolysis of a) physical and b)coalseced PC/PVAc blends.

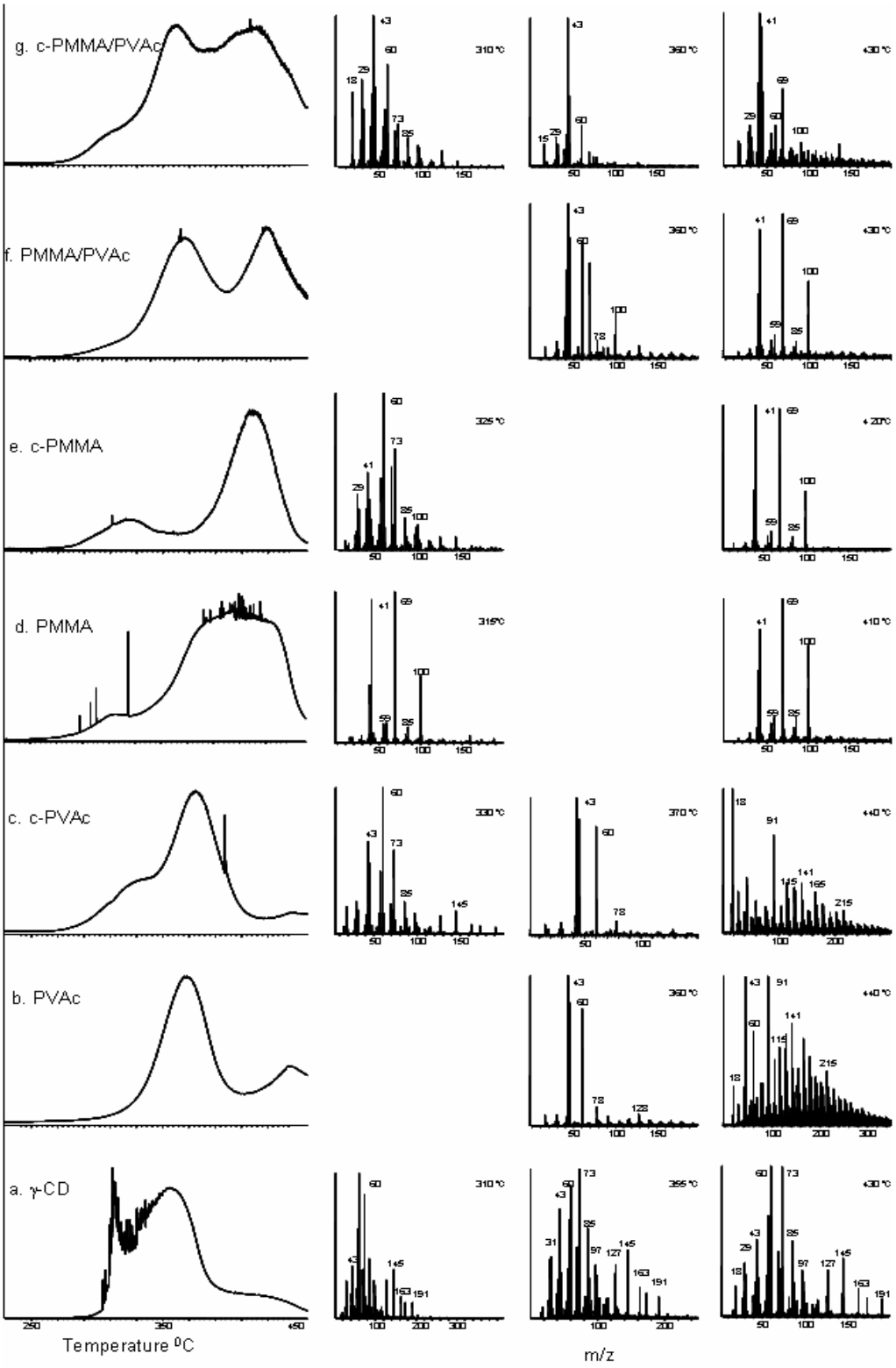


**Figure 14.** TIC curves (left) and pyrolysis mass spectra (right) recorded at the maximum of the peaks and shoulders in the TIC curves of a) γ-CD, b)as-received PVAc, c) coalesced PVAc, d)as-received-PMMA, e) coalesced PMMA, f) PMMA/PVAc physical mixture, and g) coalesced PMMA/ PVAc blend.

**Table 3.** The relative intensities and assignments of characteristic and intense peaks in the pyrolysis mass spectra of physical and coalesced PMMA/PVAc blends at temperatures corresponding to maxima in the TIC curves.

| m/z, Da | PMMA/PVAc Physical mixture | | Coalesced PMMA/PVAc | | | Assignments |
|---|---|---|---|---|---|---|
| | $360^0$ C | $430^0$ C | $310^0$ C | $360^0$ C | $430^0$ C | |
| 15 | 75 | 46 | 80 | 152 | 151 | $CH_3$ |
| 41 | 585 | 1000 | 1000 | 276 | 1000 | $CH_2CCH_3$ |
| 43 | 1000 | 207 | 979 | 1000 | 725 | $CH_2CHO$, $CH_3CO$, |
| 45 | 769 | 115 | 505 | 509 | 352 | COOH,CHOO |
| 60 | 690 | 85 | 566 | 300 | 195 | $CH_3COOH$ |
| 69 | 546 | 924 | 649 | 141 | 544 | $CH_2CCH_3$ |
| 73 | 13 | 17 | 241 | 16 | 20 | $C_3H_5O_2$ |
| 78 | 103 | 14 | 22 | 63 | 49 | $C_6H_6$ |
| 86 | 6 | 8 | 37 | 3 | 77 | $C_4H_6O_2$, VAC |
| 91 | 46 | 51 | 73 | 26 | 164 | $C_7H_7$ |
| 100 | 215 | 351 | 140 | 39 | 116 | MMA |
| 128 | 51 | 42 | 36 | 24 | 83 | $C_{10}H_8$ |
| 141 | 25 | 37 | 26 | 8 | 58 | $C_{12}H_9$ |
| 179 | 15 | 38 | 25 | 7 | 31 | $C_{14}H_{11}$ |
| 180 | 13 | 13 | 5 | 6 | 21 | $C_{14}H_{12}$ |
| 215 | 6 | 16 | 21 | 3 | 24 | $C_{14}H_{12}$ |
| 232 | 3 | 5 | 4 | 2 | 8 | $C_{18}H_{16}$ |
| 284 | 1 | 2 | | 1 | 4 | $C_{22}H_{20}$ |
| 315 | 1 | 3 | | 1 | 7 | $C_{24}H_{27}$ |

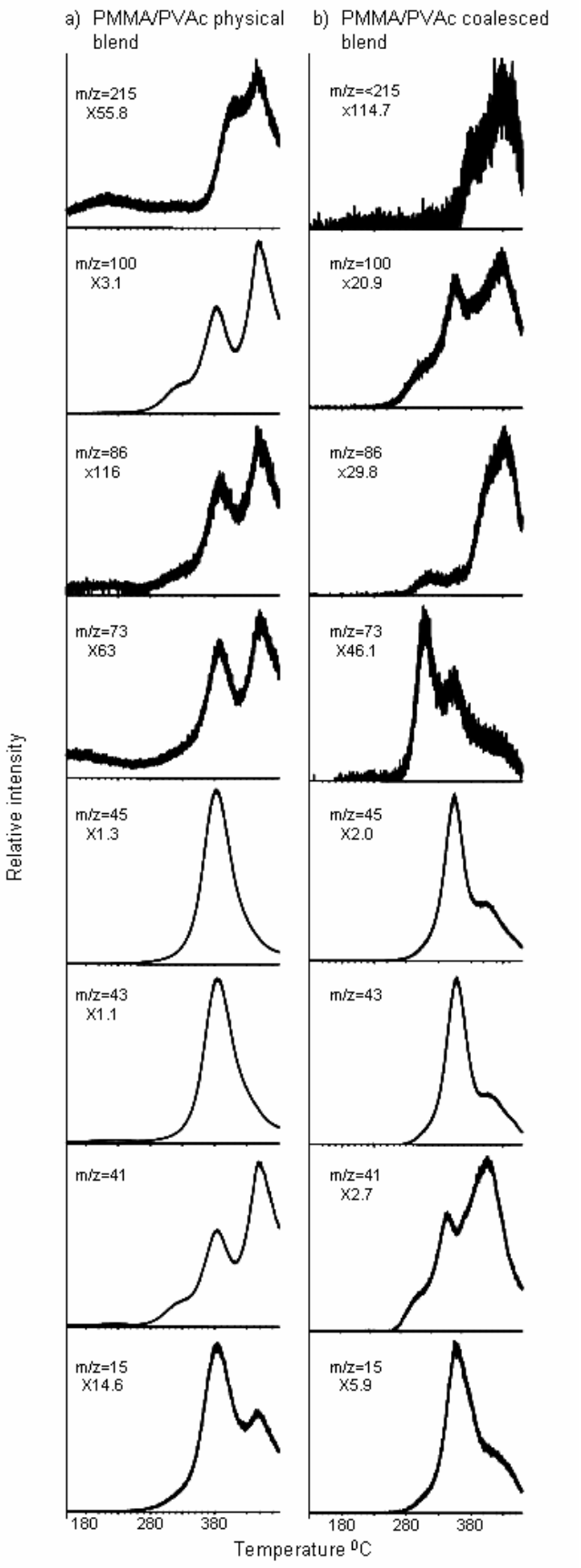


**Figure 15.** Evolution profiles of some characteristic products recorded during the pyrolysis of a) PMMA/PVAc physical mixture and b) coalesced PMMA/ PVAc blend.

In general, the evolution profiles for both blends show two peaks around 360 and 430 $^0$C, the first being mainly due to degradation of PVAc chains (Figure 14 b. and c.) and the second being mainly due to degradation of PMMA chains (Figure 14 d. and e.). Yet, significant differences in the evolution profiles are detectable. The evolution of γ-CD was recorded around 330$^0$ C for the coalesced blend, as in the case of the coalesced homopolymers (Figure 14 c. and e.). One point that should be noticed, however, is the drastic changes in the relative yields of the PVAc and PMMA based products. The evolution profiles of PVAc

based fragments recorded during the thermal degradation of the coalesced blend showed nearly similar trends up to $380^0$ C with those recorded for coalesced PVAc. Unlike the as-received and coalesced PVAc and the physical blend, shoulders around $400^0$ C appeared. Furthermore, significant decrease in the relative intensity of the MMA monomer peak, compared to those recorded for as-received and coalesced PMMA and the physical blend, was noted. On the other hand, for the coalesced blend the relative intensities of the 15 and 86 Da peaks increased noticeably, especially in the temperature region where PMMA based products evolved.

It is clear that the thermal degradation behaviors of both PVAc and PMMA have been changed in the coalesced blend. The decrease in MMA monomer yield may be associated with inhibition of PMMA depolymerization. Depolymerization of PMMA can be inhibited if the loss of side chains is favored, which implies that proton-transfer to the C=O groups of PMMA occurs. So, for the coalesced PMMA/PVAc blend, PMMA depolymerization was likely inhibited as a result of proton-transfer to the C=O groups of the MMA units.

Because both coalesced and as-received PMMA degrade mainly by depolymerization reactions, the source for the depolymerization inhibiting proton-transfer in the coalesced blend could only be PVAc. However, it is clear that the simple presence of PVAc was not sufficient for proton-transfer, as depolymerization of PMMA was also recorded for the PMMA/PVAc physical blend. Instead, it may be suggested that such a proton- transfer can only be possible if the separation between PMMA and PVAc chains is comparable to the distance between $\gamma$-H and

C=O groups within a single molecule. Actually, FT-IR findings indicated that the chain conformations of the bulk polymers were altered when they were included inside the CD channels, and extended chain conformations were retained even after coalescence from their ICs.[41] On the other hand, as coalesced PMMA also degraded mainly by a depolymerization mechanism, so it can be concluded that alterations in chain conformations cannot be the only cause of intermolecular proton-transfer reactions. Thus, it seems likely that PVAc containing $CH_3$-C=O groups, with more acidic protons, should be more effective in McLafferty type rearrangement reactions[51] and in intermolecular proton-transfer to PMMA chains, even if the distances between PVAc --- PMMA and PMMA --- PMMA are comparable, ie, PMMA and PVAc chains in the coalesced blend are very intimately mixed.

Making use of the above proposal permits the following reaction scheme to be written:

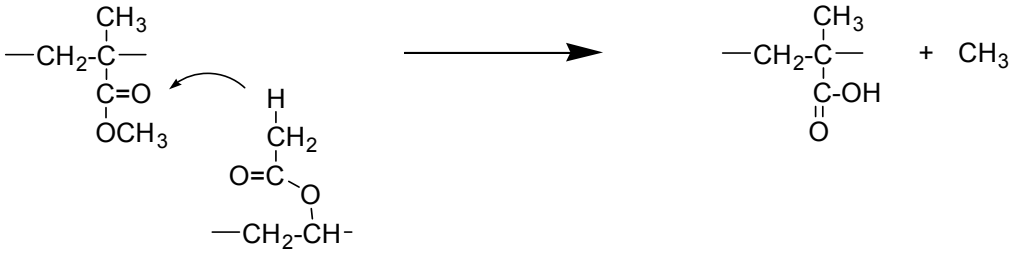

As a result of such an intermolecular proton-transfer from PVAc to PMMA, the thermal degradation of PVAc should shift to the high temperature ranges. Furthermore, thermal degradation products of poly(methyacrylic acid) (PMA) should appear in the pyrolysis mass spectra. Because of the similarities in the structures of PMMA and PMA, a depolymerization reaction yielding mainly $CH_2CCH_3COOH$,

$CH_2CCH_3$, and COOH fragment peaks at m/z= 86,43, and 45 Da, respectively, can be expected. The pyrolysis data indicating an increase in relative intensities of the 15 Da peak (due to $CH_3$), in the temperature range where PVAc degrades, and the 45 and 86 Da peaks (due to COOH and $CH_2CCH_3COOH$, respectively), in the temperature region where PMMA degradation occurs, support the proposed intermolecular proton-transfer from PVAc to PMMA in the coalesced blend. The relative intensity ratios of the above mentioned peaks in the pyrolysis mass spectra are collected in Table 4. Pyrolysis of the PVAc, PMMA and PMMA/PVAc γ-CD ICs have also been carried out. PVAc and PMMA based product yields are too low to make comparisons, because of the low stoichiometric contents of the included polymers. Furthermore, no significant change was detected in the evolution profiles of γ-CD based on the decomposition of the IC products.

**Table 4.** The relative intensity ratios of some selected peaks in the pyrolysis mass spectra of PVAc, c-PVAc, PMMA, c-PMMA, and their coalesced and physical blends, which correspond to maxima in their TIC curves.

| m/z Peak ratio | PVAc | c-PVAc | PMMA | c-PMMA | Physical blend | | Coalesced blend | |
|---|---|---|---|---|---|---|---|---|
| | $360^0$ C | $370^0$ C | $415^0$ C | $420^0$ C | $360^0$ C | $430^0$ C | $360^0$ C | $430^0$ C |
| 43/15 | 14.7 | 13.5 | | | 13.3 | | 6.6 | |
| 43/45 | 1.2 | 1.2 | | | 1.3 | | 2.0 | |
| 43/86 | 440 | 166.7 | | | 170.0 | | 33.0 | |
| 41/15 | | | 36.7 | 26.1 | | 21.7 | | 5.9 |
| 41/45 | | | 25.4 | 37.0 | | 8.6 | | 5.1 |
| 41/86 | | | 87.4 | 142.0 | | 120 | | 12.3 |
| 41/100 | | | 1.4 | 2.1 | | 2.8 | | 8.6 |

### 3.1.6 Conclusions

We have demonstrated that thermally stable and intimately mixed blends of PC/PMMA, PC/PVAc, and PMMA/PVAc can be obtained by formation of and coalescence from their common inclusion compounds with γ–CD. It was observed that the ratios of polymers in coalesced PC/PMMA and PC/PVAc binary blends are significantly different than the starting ratios, and PC was found to be preferentially included in γ-CD channels when compared to PMMA or PVAc. The intimate blends of PC/PMMA, PC/PVAc, and PMMA/PVAc with molar ratios of 2.8:1, 2.8:1 and 1:1 were prepared, respectively. Preparation of these binary blends with same molar ratios by both solvent-casting and precipitation, on the other hand, yielded phase-segregated samples. The well-mixed binary blends achieved by coalescence from their common γ–CD-ICs also exhibited thermal stabilities and thermal degradation mechanisms that were distinct from those of the pure component polymers and their binary mixtures obtained by both solvent-casting and precipitation. Thus, both the phase structures and the properties of polymer blends can be modified by processing with CDs.

## 3.2 An Intimate Polycarbonate/Poly(methyl methacrylate)/Poly(vinyl acetate) Ternary Blend *via* Coalescence from Their Common γ-Cyclodextrin Inclusion Compound

### 3.2.1 Summary

Here, we successfully report an intimate ternary blend system of polycarbonate (PC)/poly(methyl methacrylate) (PMMA)/poly(vinyl acetate) (PVAc) obtained by the simultaneous coalescence of the three guest polymers from their common γ-cyclodextrin (γ-CD) inclusion compound (IC). The thermal transitions and the homogeneity of the coalesced ternary blend were studied by differential scanning calorimetry (DSC) and thermogravimetric analysis (TGA). The observation of a single, common glass transition strongly suggests the presence of a homogeneous amorphous phase in the coalesced ternary polymer blend. This was further substantiated by solid-state $^{13}C$ NMR observation of the $T1\rho(1H)$s for each of the blend components. For comparison, ternary blends of PC/PMMA/PVAc were also prepared by traditional coprecipitation and solution casting methods. TGA data showed a thermal stability for the coalesced ternary blend that was improved over the coprecipitated blend, which was phase-segregated. The presence of possible interactions between the three polymer components was investigated by infrared spectroscopy (FTIR). The analysis indicates that the ternary blend of these polymers achieved by coalescence from their common γ-CD–IC results in a homogeneous polymer blend, possibly with improved properties, whereas coprecipitation and solution cast methods produced phase separated polymer blends. It was also found

that control of the component polymer molar ratios plays a key role in the miscibility of their coalesced ternary blends. Coalescence of two or more normally immiscible polymers from their common CD-ICs appears to be a general method for obtaining well-mixed, intimate blends.

### 3.2.2 Experimental

#### 3.2.2.1 Formation of PC/PMMA/PVAc-γ-CD Inclusion Compounds

According to the literature, we assumed that one γ-CD molecule may host three repeat units of PMMA or PVAc or 0.66 repeat units of PC.[24] Thus we would expect a 1.0:4.5:4.5:4.5 molar PC:PMMA:PVAc:γ-CD stoichiometry for the common IC if the inclusion process were completely random and unbiased toward the inclusion of any of the three constituent homopolymers, as well as for a 100 % yield of IC formation. After several attempts, we noticed that control of the molar ratios in the coalesced polymer blends is not a straightforward task, apparently because of differences in the hydrophobicities of PC, PMMA, and PVAc, resulting in the preferential inclusion of the more hydrophobic PC guest molecules by the host CD molecules from the multi-guest PC/PMMA/PVAc solution.[41,52] Consequently, here we report the formation of two PC/PMMA/PVAc-γ-CD ICs which were subsequently coalesced as described below. A quantity of either 0.1702 g (0.67 mmol) or 0.127 g (0.5 mmol) of PC, 0.4292 g (4.29 mmol) or 1.2 g (12 mmol) of PMMA and 0.3692 g (4.29 mmol) or 1.032 g (12 mmol) of PVAc were dissolved together in 160 mL or 320 mL of dioxane (a common solvent for all three component polymers) at 50 °C. An aqueous saturated solution of γ-CD (5.568 g, 4.29 mmol or 11.673 g, 9 mmol)

dissolved in 16 mL (or 32 mL) of DI-$H_2O$ at 50 °C was added drop-wise to the ternary polymer solution while the stirring rate was kept high at a temperature of 50° C. Once the γ-CD solution was added, a white, turbid solution was formed. After stirring for three hours at 50° C, the white suspension was allowed to cool down to room temperature while the stirring rate was kept low for another three days. By varying the time of the PC/PMMA/PVAc-γ-CD IC formation, the best yield of IC (~30%) was obtained after three days of stirring at room temperature. The resulting white suspension was then vacuum filtered and the collected precipitate vacuum dried at 45° C for 24 h. The abbreviations for these inclusion compounds are PC/PMMA/PVAc-γ-CD IC-1 and -2, respectively.

The X-ray diffractogram of PC/PMMA/PVAc-γ-CD IC-1 and -2 crystals show all of the diffraction peaks characteristic of γ-CD IC crystals in a channel crystal structure suggesting that the CD molecules are threaded onto the polymer chains (data not shown). The DSC thermogram (data not shown) of PC/PMMA/PVAc-γ-CD IC-1 and -2 exhibit no glass ($T_g$) transitions for any of the uncomplexed homopolymers and no melting peak for the fusion of free PC. The presence of both host and guest molecules was also evidenced by FTIR spectroscopy (see FTIR section).

Because of the preference for inclusion of PC by γ-CD, we chose to employ essentially only a slight excess of γ-CD to include all the PC, PMMA, and PVAc polymers in solution, rather than a big excess of γ-CD that might eventually allow inclusion of the entire amount of all three component polymers. In this manner we always observed IC yields well below 100%, with both component polymers and γ-

CD remaining in solution. This procedure reduces the possibility of forming PC-γ-CD IC crystals in addition to γ-CD IC crystals containing only the less readily included PMMA and PVAc component polymers, and receives confirmation from our observation (see below) that a well-mixed PC/PMMA/PVAc ternary blend consisting of a single amorphous phase was achieved.

#### 3.2.2.2 Enzymatic coalescence of a polymer blend from its CD IC

The γ-CD was removed from the ICs by washing the white crystals with deionized water in the presence of α-amylase (Clarase L-4000 enzyme) at 50° C while stirring for 18 h. The pH of this aqueous suspension was adjusted to 5 by adding HCl. The coalesced ternary polymer blends, PC/PMMA/PVAc, were then vacuum filtered and rinsed several times with water and finally vacuum dried at 30-40° C for 2 days. Solid state $^{13}C$ NMR spectra of the coalesced blends prove the absence of CD in these samples. The molar ratio of PC:PMMA:PVAc was found to be 4.4:1:1 and 1.6:1:1.4, respectively, by solution $^{1}H$-NMR spectroscopy, and these samples are named coalesced-PC/PMMA/PVAc-1 and -2 blends.

#### 3.2.2.3 Generation of PC/PMMA/PVAc Physical Blend Controls

To act as control samples, PC, PMMA and PVAc powders were dissolved together in THF at the same concentrations as those observed in the coalesced samples. Both solvent cast and co-precipitation methods were used to create the physical blends. The solvent cast films were air-dried overnight and further vacuum dried at 50° C for another 24 h. Phase separation in the cast films was noticeable even to the naked eye. Moreover, infrared microscope observations of these

polymer blends, though not presented here, showed macroscopically phase-separated polymer domains denoted by the presence of single and/or binary polymer components or sometimes ternary components for different regions of the cast films. Therefore, a ternary control blend was also obtained by a co-precipitation method by adding their clear solution in THF to deionized water (non-solvent). The precipitate was collected from the liquid by vacuum filtering through a ceramic frit in a Büchner funnel. Finally, the precipitate was vacuum dried.

### 3.2.3 Results and Discussion

#### 3.2.3.1 $^{1}$H Nuclear Magnetic Resonance

Figure 16 displays the $^{1}$H NMR spectra of the coalesced PC/PMMA/PVAc-1 ternary blend. The molar ratios of PC, PMMA, and PVAc in the precipitated control and coalesced ternary blends were determined by comparison of integrals of the three distinct polymer peaks at 7.2 ppm for PC, 4.8 ppm for PVAc, and 3.6 ppm for PMMA versus TMS. The molar ratio of the coalesced PC:PMMA:PVAc-1 blend was found to be 4.4:1:1. Comparison to the 1:6.4:6.4 molar ratio of the starting solution suggests that the host $\gamma$-CD molecules preferentially include PC chains over the other two vinyl polymer guests. The tendency of PC to form an inclusion compound with $\gamma$-CD is close to 24 times higher when compared to PMMA or PVAc. However, there apparently is no inclusion preference between PMMA and PVAc, as shown by the equivalence between the initial and final molar ratios of these two polymers. Similar behavior has also been observed for binary systems of these polymers, where PC chains are more likely to be included and reside in the $\gamma$-CD channels than

PMMA and PVAc chains.[52] It has previously been reported that host γ-CD molecules possess a greater inclusion affinity for more hydrophobic, rather than hydrophilic, guest polymers.[38] Here, the preferential inclusion of PC may be explained by its hydrophobicity, which is higher than that of PMMA or PVAc. Additional possible reasons for this behavior, including differences in the cross-sections of highly extended PC, PMMA, and PVAc chains, are still under investigation, because the molecular recognition of γ-CD molecules for more hydrophobic guest molecules might be used as a new application of γ-CD IC formation, e.g., for specific separations.

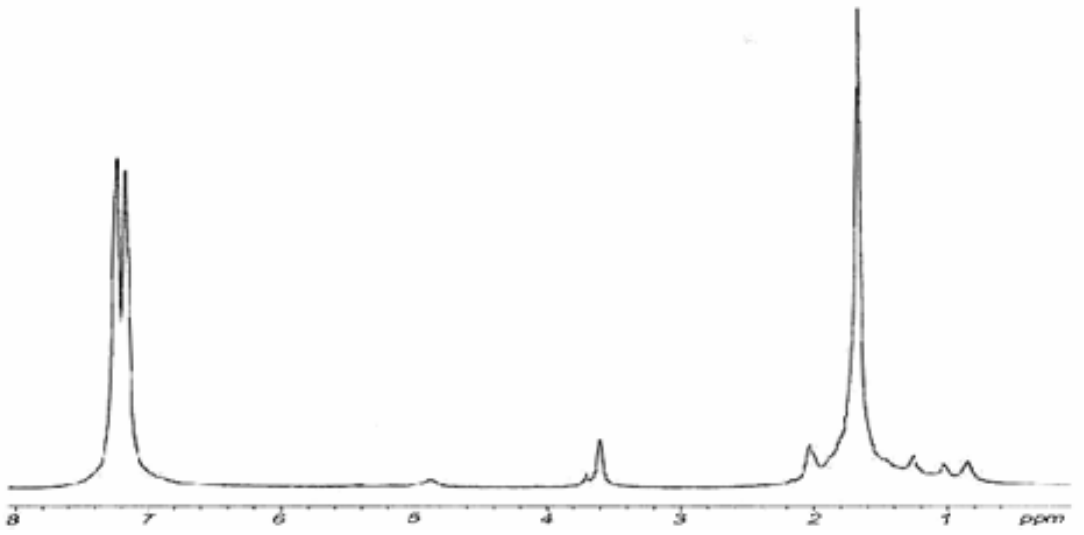


**Figure 16.** $^{1}$H-NMR spectra of coalesced PC/PMMA/PVAc-1 ternary blend.

To learn more about the hydrophobic affinity of the host γ-CD molecules, we have attempted to modify the initial molar ratio of individual polymers in order to obtain a coalesced polymer blend with a more evenly distributed molar ratio among the polymer components. From the $^{1}$H NMR spectrum of PC/PMMA/PVAc-2 blend

(not shown), the molar ratio of PC:PMMA:PVAc is calculated to be 1.6:1:1.4 compared to an initial molar ratio of 1:24:24, respectively. The PC component in the PC/PMMA/PVAc-2 blend is still prevalent over the PMMA and PVAc components, which indicates that there may be additional factors that govern the inclusion process from a multiguest system.

During redissolution of the ternary blends in a common solvent, we noticed a solubility difference between the coalesced and physical blends. The lower solubility of the coalesced PC/PMMA/PVAc ternary blends reveals information about the degree of mixing of these systems. We were only able to dissolve the coalesced PC/PMMA/PVAc blends at high temperature and after a long time under ultrasonication, whereas the physical blends were readily dissolved at room temperature. Because the mixing of the coalesced PC/PMMA/PVAc blends is achieved at the molecular level, apparently more time and higher temperatures are required to break slightly favorable interactions between component chains, when compared to the phase separated physical PC/PMMA/PVAc blends, and the interactions between component chains are likely stronger than those among pure PC, PMMA, and PVAc chains. In addition, the entropy change accompanying dissolution of the coalesced PC/PMMA/PVAc is smaller and, therefore, less favorable than that for the dissolution of the physical terpolymer blend, because of the favorable entropy accompanying the intimately mixed component chains in the coalesced blend.

### 3.2.3.2 Fourier Transform Infrared Spectroscopy (FT-IR)

The FT-IR spectra of pure γ-CD and PC/PMMA/PVAc-γ-CD-IC-1 are given in Figure 17. The absorption bands at 1079, 1157, and 2926 $cm^{-1}$ correspond to the coupled C-C/C-O stretching vibrations and the antisymmetric stretching vibration of the C-O-C glycosidic bridge and C-H vibration of γ-CD, respectively. Because the absorption bands of γ-CD cover large regions in the IR range, it is not easy to identify all the absorption peaks belonging to PC, PMMA, and PVAc guests. However, the presence of the carbonyl band (C=O) observed at 1772 $cm^{-1}$ is evidence for PC (the carbonyl band is expected at 1775 $cm^{-1}$). A closer examination of the common carbonyl band at 1733 $cm^{-1}$, due to PMMA and PVAc (expected to be at 1735 $cm^{-1}$), proves the presence of these two polymer components in this γ-CD IC sample. These shifts may indicate that there are some possible interactions between the carbonyl groups (C=O) of the polymers and -OH groups of γ-CD.

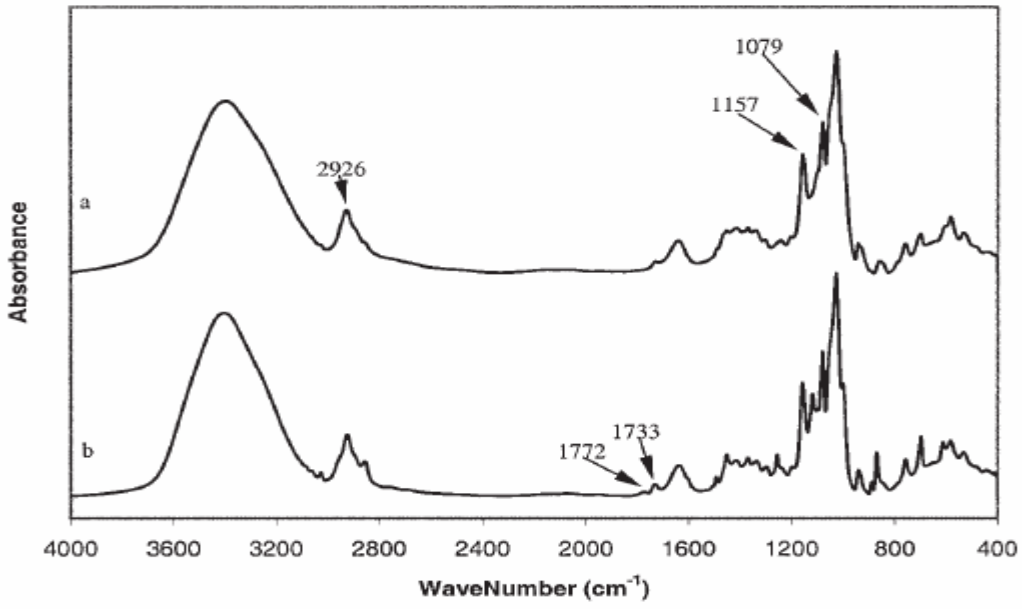


**Figure 17.** FT-IR spectra of a.)as-received γ-CD b.)PC/PMMA/PVAc-γ-CD IC.

FTIR spectra of the coalesced PC/PMMA/PVAc-1, -2, and physical ternary blends are shown in Figure 18. The infrared spectrum of the PC/PMMA/PVAc-1 blend coalesced from its γ-CD IC, for example, gives much more detail about the polymer components. The absorption bands at 1162 and 1193 $cm^{-1}$ (carbonate C-O stretch), 1234 $cm^{-1}$ (carbonate aryl-O-aryl C-O stretch), 1506 $cm^{-1}$, and 1600 $cm^{-1}$ (para-aromatic ring stretch), 1774 $cm^{-1}$ (carbonate C=O stretch), and 2968 $cm^{-1}$ ($CH_3$ asymmetric stretch) are attributed to PC in this coalesced ternary blend (Figure 18a). It is difficult to differentiate between PMMA and PVAc in the ternary blend FT-IR spectra because they do have similar chemical structures. However, the as-received PMMA shows an absorption band for the C=O stretch at 1731 $cm^{-1}$, whereas the C=O stretch of the as-received PVAc appears at 1737 $cm^{-1}$.[41] Here, a common absorption band at 1736 $cm^{-1}$, which is intermediate to both (Figure 18a), suggests the presence of PMMA and PVAc in the coalesced PC/PMMA/PVAc-1 ternary blend. The absorption bands at 1150 and 1240 $cm^{-1}$ (C-O-C stretching) attributed to PMMA and the peaks at 1374 and 1240 $cm^{-1}$ of PVAc are overlapped with PC peaks. The broad peak attributed to the combination of C-O-C stretching bands of PMMA and PVAc and the carbonate aryl-O-aryl C-O stretching band of PC appears at 1238 $cm^{-1}$ for the ternary physical blend, and are shifted to 1234 and 1240 $cm^{-1}$ for the coalesced PC/PMMA/PVAc-1 and-2 blends, respectively. Also, the carbonyl (C=O) peaks at 1776 and 1735 $cm^{-1}$ observed for PC and PMMA/PVAc, respectively, in the coprecipitated physical PC/PMMA/PVAc blend, are shifted to 1774 and 1736 $cm^{-1}$, and to 1772 and 1735 $cm^{-1}$ in the coalesced PC/PMMA/PVAc-1, -2 blends, respectively. These small shifts may result from interactions between polymer

chains, but can also be attributed to different environments for each polymer chain in the intimately mixed ternary blends.

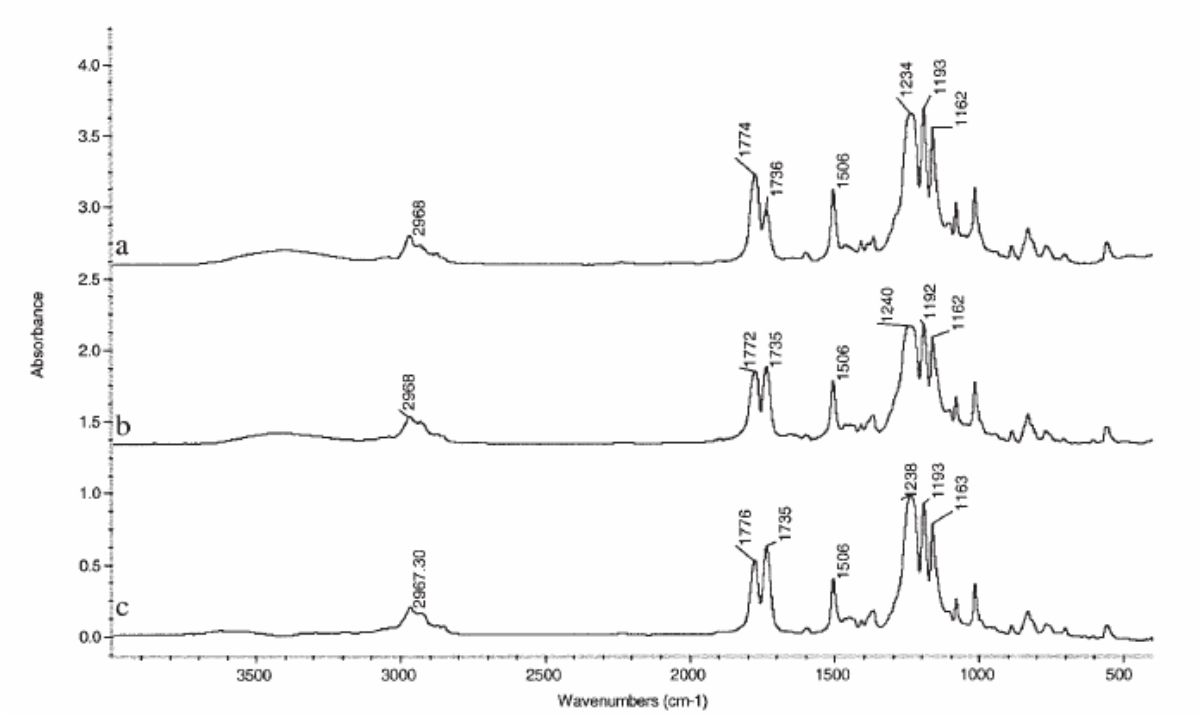


**Figure 18.** FT-IR spectra of coalesced-1 (a), -2 (b), and co-precipitated PC/PMMA/PVAc ternary blends (c).

### 3.2.3.3 Differential Scanning Calorimetry

Figure 19 displays the DSC scans recorded for the co-precipitated physical and coalesced PC/PMMA/PVAc-1 blends. Four different glass-transition temperatures ($T_g$s) were observed for the co-precipitated PC/PMMA/PVAc blend in the first DSC scan (Figure 6c): $T_g$ at 38 °C for PVAc, $T_g$ at 56 °C due to the partial miscibility of PMMA/PVAc, $T_g$ at 82 °C for PMMA, and $T_g$ at 133 °C for PC. For polymer blends, a single $T_g$ is indicative of a state of molecular dispersion, whereas the appearance of several distinct $T_g$s suggests the occurrence of phase separation.

DSC results indicate that the physical PC/PMMA/PVAc ternary blend prepared by coprecipitation does not form a miscible blend.

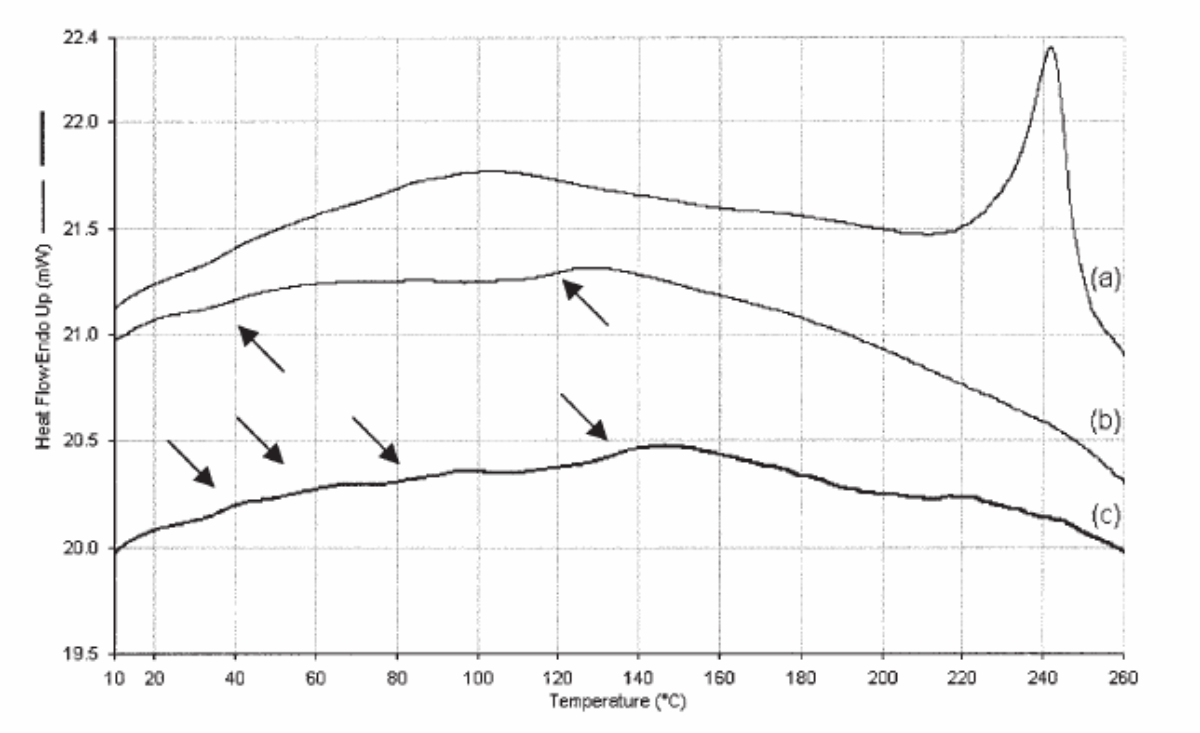


**Figure 19.** DSC thermograms of the coalesced PC/PMMA/PVAc-1 blend, first heating scan (a) and second heating scan (b); co-precipitated PC/PMMA/PVAc blend, first heating scan (c). Annealing time between first and second heating scans of the coalesced blend is 1 min.

On the contrary, the first scan of the coalesced PC/PMMA/PVAc-1 blend did not show any apparent glass transition, but instead a melting of the PC crystalline regions at 242 °C. It is noteworthy that PC was found to be completely amorphous in the as-received sample and its co-precipitated PC/ PMMA/PVAc blend, whereas PC chains form crystalline regions in the coalesced PC/PMMA/ PVAc-1 blend. This may be a consequence of retention of the extended conformation required by inclusion in the narrow $\gamma$-CD IC channels for the coalesced PC, as well as their partial

segregation into proximal regions of the common γ-CD IC crystals, as discussed above.

However, PC crystals are not reformed once the blend is heated above the melting point of PC. The second DSC scan was run after cooling the sample from 300 to 0 °C at a rate of 200 °C/min. In the second scan after quenching the sample (Figure 19b), the melting peak for PC crystals disappeared. The observation of the $T_g$ at 39 °C reveals the segregation of PVAc domains. However, the presence of a unique $T_g$ at 119 °C, a value between the $T_g$s of the homopolymers (PC, $T_g$ = 133 °C and PMMA, $T_g$ = 82 °C), strongly suggests the presence of a two-component homogeneous amorphous phase in this coalesced polymer blend. The coalesced PC/PMMA/PVAc-1 blend shows instability after annealing at a temperature higher than the $T_g$s of the polymer components. The miscibility between PC and PMMA could originate from intermolecular contacts in the interphase region because the presence of specific interactions generally creates smaller domain sizes, thereby introducing a higher degree of compatibility. In the case of PVAc, weak interactions between the PVAc domains and PC/PMMA domains would result in phase separation at high temperatures. At temperatures higher than the $T_g$ of PVAc, phase separation is likely to be observed because of the diffusion of PVAc chains from the interphases to PVAc-rich domains.[54]

Figure 20 shows the MDSC thermograms of the coalesced PC/PMMA/PVAc-2 ternary blend. The total signal of heat flow may be separated in reversing and nonreversing heat flow, as a result of the temperature modulation employed. Thermal transitions in the reversing signal arise from thermodynamic phenomena

such as the $T_g$ and melting. The nonreversing signal exhibits kinetic phenomena and includes evaporation and recrystallization. By plotting the reversing heat flow versus temperature, the effect of the solvent release as well as enthalpic recovery an endothermic peak that occurs just above the $T_g$, are eliminated, revealing a clear, single glass transition.

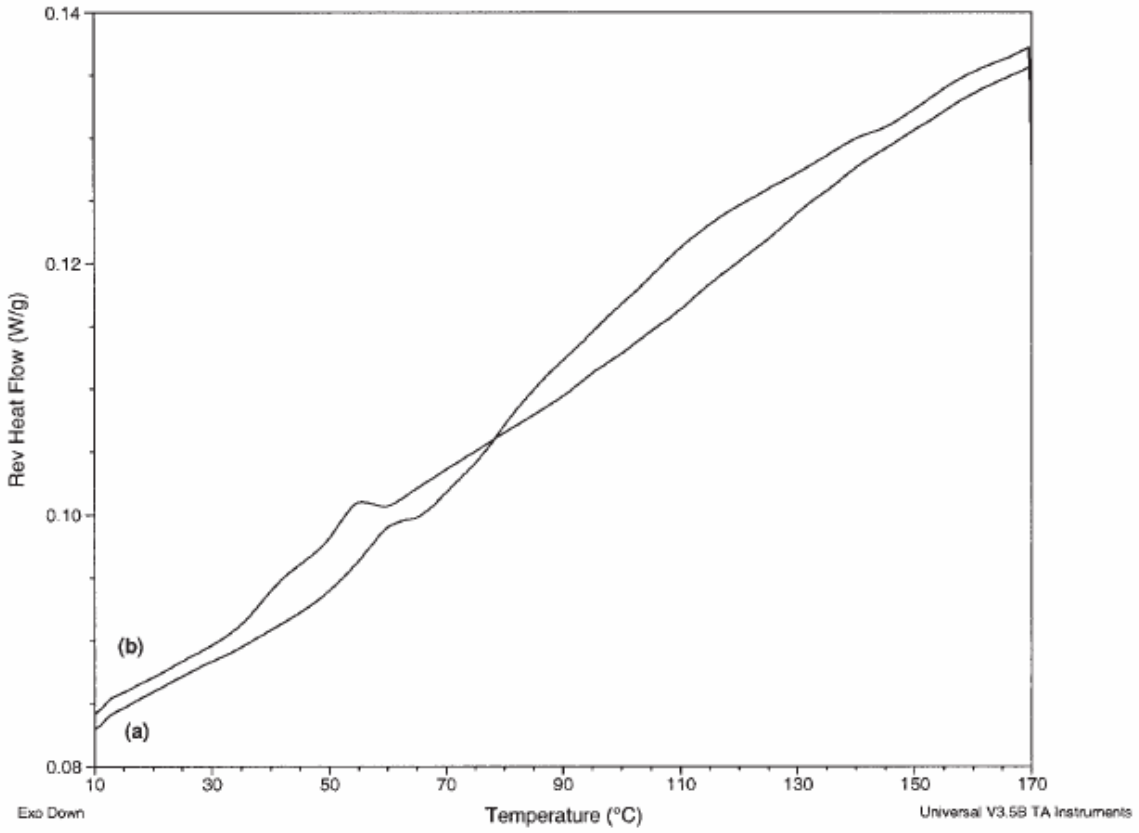


**Figure 20.** MDSC scans of the first (a), and second (b) heating runs recorded for the PC/PMMA/PVAc-2 blend. The sample was held 3 min at 170° C after the first heating.

The thermal behavior observed for the PC/PMMA/PVAc-2 ternary blend is apparently different from that of the previous coalesced blend. In both the first and second MDSC heating scans, only a single glass transition can be observed at 57 °C. This result indicates the presence of a single homogeneous amorphous phase in

the ternary blend of PC/PMMA/PVAc-2, where the three component polymer chains are intimately mixed with each other. The appearance of one glass transition in the second scan also confirms the stability and molecular degree of mixing of the PC, PMMA, and PVAc chains in the PC/PMMA/PVAc-2 ternary blend. The difference between these two coalesced PC/ PMMA/PVAc ternary blends consists primarily in the different molar ratios of their constituent polymers. The phase separation of PVAc can be explained by the presence of a larger PC-rich phase in PC/PMMA/PVAc-1. However, even this coalesced sample shows better mixing and thermal properties compared to the coprecipitated physical PC/PMMA/PVAc blend with the same molar ratio. The amount of PC in the coalesced PC/PMMA/PVAc-2 is also higher than the PMMA and PVAc contents, but the 1.6:1:1.4 ratio is apparently sufficiently homogeneous to yield an intimate blend among the PC, PMMA, and PVAc polymers when formed by coalescence from its γ-CD IC.

#### 3.2.3.4 Solid-State Nuclear Magnetic Resonance

The $^1$H spin-lattice relaxation times of the three polymers and their ternary blends observed in the rotating frame $T_{1\rho}$($^1$H) are presented in Table 5. The three pure polymers have distinct single $T_{1\rho}$ ($^1$H) values that indicates the homogeneity in each polymer. Some $T_{1\rho}$ ($^1$H) data are unobservable in the blend samples due to the overlap of resonance peaks with the spinning side bands of PC. Nevertheless, the physical mixture sample shows three distinguishable $T_{1\rho}$ ($^1$H) values for the three polymer components, which indicates a phase-separated blend with domain sizes above 5 nm. The closely similar $T_{1\rho}$ ($^1$H) values observed for PVAc and PMMA suggest the intimate blend of these two polymers in the coalesced PC/PMMA/PVAc-

2 sample. Yet, the PC is still phase-separated from the rest of the blend, as indicated by a different $T_{1\rho}$ ($^1$H) value for PC in the coalesced sample. By doing a correlation with DSC data, we may suggest that these $T_{1\rho}$ ($^1$H) values of PC are mainly provided by its oriented chains in the crystalline phase, which of course is separated from the intimately mixed amorphous phase. The structure of this coalesced blend has been investigated by X-ray diffraction (pattern not shown), which exhibits just one peak at 17.1°, corresponding to crystalline PC. This would explain the higher $T_{1\rho}$ ($^1$H) value observed for the more rigid PC chains in the crystalline phase of the coalesced blend versus its corresponding homopolymer that is completely amorphous.

**Table 5.** $T_{1\rho}$($^1$H) of Ternary PC/PMMA/PVAc Blends (ms)

| | PC | | | | | PVAc | | | PMMA | | |
|---|---|---|---|---|---|---|---|---|---|---|---|
| Peak (ppm) | 150 | 128 | 120 | 43 | 30 | 171 | 68 | 21 | 178 | 52 | 45 |
| PC | 5.1 | 5.5 | 5.5 | 5.2 | 5.6 | --- | --- | --- | --- | --- | --- |
| PMMA | --- | --- | --- | --- | --- | --- | --- | --- | 14.8 | 14.9 | 15.5 |
| PVAc | --- | --- | --- | --- | --- | 10.6 | 12.2 | 11.2 | --- | --- | --- |
| Mixture[a] | 5.7 | 6.2 | 6.3 | 6.4 | 6.0 | --- | --- | 7.6 | --- | 14.0 | --- |
| Coalesced[b] | 6.5 | 7.0 | 6.9 | 7.4 | 7.1 | --- | --- | 21.7 | --- | 20.2 | --- |

a - Physical mixture obtained by co-precipitation
b – PC/PMMA/PVAc-2 coalesced blend

In the DSC instrument, the PC/PMMA/PVAc-2 coalesced blend was also heated to 245 °C (under inert gas), which is below the melting temperature ($T_m$) of PC, held at this temperature for 5 min, then cooled at -200 °C/min, and then reheated to 260 °C at 20 °C/min. Both heating cycles evidenced small PC melting endotherms, where the endotherm observed for the second heating was reduced by about 50% from that observed in the first heating, although only a single $T_g$ was

observed in both heating scans (thermograms not shown). The heat of melting per g of PC observed in the first heating is very similar to that previously observed for in the first heating DSC scan of PC coalesced from PC-γ-CD IC. However, in the second heating scan no melting endotherm was observed, so the cooling between the first and second heating scans was sufficiently rapid (-200 °C/min) to quench the PC coalesced from its γ-CD IC into a completely amorphous material. This comparison of the DSC thermal responses of PC coalesced from its common PC/PMMA/PVAc-γ-CD IC-2 and its pure γ-CD IC is consistent with two major observations suggested above: first, the preference for inclusion of the more hydrophobic PC chains in the common PC/PMMA/PVAc-γ-CD ICs, which likely leads to some segregation of the PC chains in proximal IC channels. This is supported by the similar melting endotherm heats observed for PC coalesced from its common PC/PMMA/PVAc-γ-CD IC-2 and its pure γ-CD IC. Second, the fact that the second heating DSC scans of PC coalesced from its common PC/PMMA/PVAc-γ-CD IC-2 and its pure γ-CD IC show the presence and absence, respectively, of PC crystallinity supports the mixing of PC chains with PMMA and PVAc chains in the amorphous regions of the coalesced PC/PMMA/PVAc-2 blend, because if PC chains were completely separated from a well mixed PMMA/PVAc phase, then we would have expected the PC to be quenched into a totally amorphous phase by the rapid cooling between the first and second heating DSC scans, as observed from PC coalesced from its γ-CD IC. Following the first DSC scan, the PC/PMMA/PVAc-2 blend was dissolved and observed by $^{1}$H-NMR, and the resulting spectrum was identical to that observed prior to the high temperature (245 °C) treatment. Thus, the

coalesced PC/PMMA/PVAc-2 blend showed no evidence for crosslinking or transesterification upon brief exposure to high temperature.

### 3.2.3.5 Thermogravimetric Analysis (TGA)

The above results and the difference in blend solubilities reveal that the PC/PMMA/PVAc ternary blends are more homogeneous and stable than the physical blends. Therefore, we would also expect a different thermal stability for these two types of ternary blends. Figure 21 displays the thermal degradation of the coalesced-1 and -2 and co-precipitated PC/PMMA/PVAc ternary blends. Three distinct degradation regions were observed for the co-precipitated PC/PMMA/PVAc ternary blend. The onset temperature at 350 °C corresponds to the degradation temperature ($T_d$) of PVAc; the *T*d at 424 °C is attributed to PMMA, and the onset temperature at 498 °C corresponds to the *T*d of PC. Figure 21(a) shows a different thermal stability for the coalesced PC/PMMA/PVAc-1 blend that displays four degradation steps at 325, 411, 460, and 518 °C, assigned to the degradation of PVAc, PMMA, co-degradation of a PC/PMMA phase, and degradation of PC, respectively. The degradation temperatures of PVAc and PMMA in the coalesced ternary blend are obviously suppressed, whereas the $T_d$ of PC is elevated compared to the corresponding values observed for the physical blend. The degradation steps are not so pronounced in the TGA scan of the coalesced blend, which denotes a possible codegradation at the molecular level. By examining the slopes of the TGA scans we may conclude that the rate of degradation is higher for the co-precipitated PC/PMMA/PVAc when compared to that of the coalesced PC/PMMA/PVAc-1 blend.

Moreover, the material remaining at 650 °C after degradation of the coalesced blend is about 10 wt % higher than that of the physical blend.

By analyzing the TGA thermogram of the coalesced PC/PMMA/PVAc-2 blend (Figure 21c), which shows only one broad degradation step for all polymer components, we can again conclude that an even higher degree of mixing was achieved for this particular coalesced blend. In summary, the coalesced PC/PMMA/PVAc blends exhibited better thermal properties than the co-precipitated PC/PMMA/PVAc blend. This significant improvement in thermal stability likely comes from the presence of specific interactions between component polymer chains, which are increased due to the higher level of mixing among the polymer components in the more intimate coalesced blends.

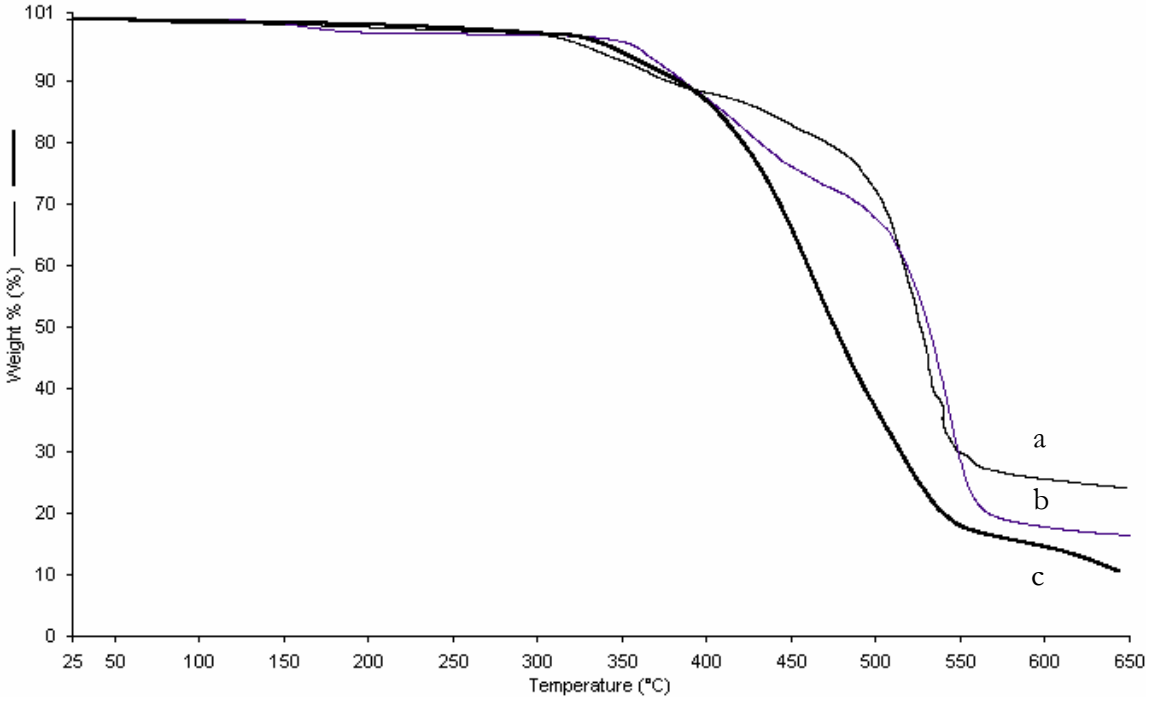


**Figure 21.** TGA thermograms of (a) coalesced (-1), (b) precipitated, and (c) coalesced (-2) PC/PMMA/PVAc blends.

### 3.2.4 Conclusion

We successfully obtained, for the first time, an intimate ternary blend of PC/PMMA/PVAc by the simultaneous formation of a common γ-CD IC with PC, PMMA, and PVAc. By removing the host CD molecules with water in the presence of a specific enzyme, a coalesced ternary polymer blend with a single amorphous homogeneous phase resulted. The observation of a common glass transition at 57 °C strongly suggests an extensive degree of mixing in the amorphous phase of this ternary polymer blend. It was shown that the CD IC coalescence method is a better way of mixing polymer components into an intimate blend than the traditional precipitation and solution- casting methods that usually lead to phase separated polymer blends.

It was also found that the molar ratio of individual polymers in the coalesced ternary blend plays a key role in producing a miscible blend. PVAc domains were found to be phase-separated in the coalesced ternary blend richer in PC, after annealing the blend at an elevated temperature (300 °C). However, the coalesced ternary blend with a more homogeneous composition of the constituent polymers showed uniform miscibility, as well as thermal stability.

We also observed that the PC chains possess a preferred ability to form inclusion compounds with γ-CD when competing with PMMA and PVAc. We believe that this preference of the host γ-CD molecules for PC chains, rather than the other two possible guests, is due to their different hydrophobicities. We are continuing to work on the procedure for controlling the molar ratio of the included polymers in the γ-CD IC channels. The final molar ratio of the coalesced ternary blend can be

somewhat controlled by modifying the initial molar ratio of polymers in the solution used to form their common γ-CD IC. Our eventual aim is to be able to adjust, as desired, the constituent polymer ratios in the coalesced ternary blends.

### 3.2.5 References


1. In *Polymer Alloys and Blends-Thermodynamics and Rheology*, Utracki, L. A., Ed., Oxford University Press: New York, 1990.
2. Krause, S. In *Polymer Blends*, Paul, D. R.; Newman, S., Eds., Academic Press: New York, 1978, p15.
3. Ellis, T. S. In *Polymer Alloys and Blends*, Shonaike, G. O.; Simon, G. P., Eds., Marcel Dekker: NewYork, 1999, p 209.
4. Coleman, M. M.; Painter, P. C. *Prog Polym Sci* 1995, 20, 1–59.
5. Crispim, E. G.; Rubira, A. F.; Muniz, E. C. *Polymer* 1999, 40, 5129–5135.
6. Qipeng, G.; Zhenhai, L. *J Therm Anal Calorimetry* 2000, 59, 101–120.
7. Song, M.; Long, F. *Eur Polym J* 1991, 27, 983–986.
8. Okamoto, M. *Journal of Applied Polymer Science* 2002, 83 (13): 2774-2779.
9. Schenk, W.; Reichert, D.; Schneider, H. *Polymer* 1990, 31, 329-335.
10. Ha, C. S.; Lee, W. K.; Cho, W. J. *Macromolecular Symp* 1994, 84, 279-288.
11. Crispim, E. G.; Schuquel, I. T. A.; Rubira, A. F.; Muniz, E. C. *Polymer* 2000, 41 (3): 933-945.
12. Lee, W. K.; Cho, W. J., Ha, C. S.; Takahara, A.; Kajiyama, T. *Polymer* 1995, 36, 1229–1234.

13. Lee, W. K.; Ryou, J. H.; Cho, W. J.; Ha, C. S.; Nakahara H. *Molecular Crystals and Liquid Crystals* 2002, 377, 337-340.

14. Asano, A.; Eguchi, M.; Shimizu, M.; Kurotsu, T. *Macromolecules* 2002, 35 (23): 8819-8824.

15. Qipeng, G. *European Polymer Journal* 1996, 32 (12): 1409-1413.

16. Zheng, S. X.; Huang, J. Y.; Li, J.; Guo, Q. P. *J of Applied Polymer Sci* 1998, 69 (4), 675-684.

17. John, K.; Reddy, G. J.; Naidu, S. V. *International J of Polymer Analysis and Characterization*, 8 (4), 295-299, 2003

18. Hsu W. P., *Journal of Applied Polymer Science*, 80, 2842-2850, 2001.

19. Kyu, T.; Ko, C. C.; Lim, D.S.; Smith, S.D.; Noda, I. *J Polym Sci Part B: Polym Phys* 1993, 31, 1641–1648.

20. Debier, D.; Jonas A. M.; Legras, R. *J Polym Sci Part B: Polym Phys* 1998, 36, 2197–2210.

21. Viville, P.; Biscarini, F.; Bredas, J. L.; Lazzaroni, R. *Journal of Phys. Chem. B* 2001, 105, 7499-7507.

22. Marin, N.; Favis, B. D. *Polymer* 2002, 43 (17): 4723-4731.

23. Sato, M.; Ooki, A.; Inamura, I.; Kubo, Y. *Macromol Rapid Communication* 2002, 23, 362-365.

24. Harada, A.; Li, J.; Kamachi, M. *Nature* 1994, 370, 126.

25. Ceccato, M.; LoNostro, P.; Baglioni, P. *Langmuir* 1997, 13 (9): 2436-2439.

26. Jiao, H.; Goh, S. H.; Valiyaveettil, S. *Macromolecules* 2002, 35 (10): 3997-4002.

27. Harada, A.; Suzuki, S.; Okada, M.; Kamachi, M. *Macromolecules* 1996, 29 (17): 5611-5614.

28. Huang, L.; Allen, E.; Tonelli, A. E. *Polymer* 1999, 40 (11): 3211-3221.

29. Lu, J.; Shin, I. D.; Nojima, S.; Tonelli, A. E. *Polymer* 2000, 41 (15): 5871-5883.

30. Shuai, X. T.; Porbeni, F. E.; Wei, M.; Shin, I. D.; Tonelli, A. E. *Macromolecules* 2001, 34 (21): 7355-7361.

31. Rusa, C. C.; Tonelli, A. E.; *Macromolecules* 2000, 33 (15): 5321-5324.

32. Wei, M.; Tonelli, A. E. *Macromolecules* 2001, 34, 4061.

33. Bullions, T. A.; Edeki, E. M.; Porbeni, F. E.; Wei, M.; Shuai, X.; Rusa, C. C.; Tonelli A. E. *J of Polymer Sci: Part B-Polymer Physics 2003*, 41 (2): 139-148.

34. Rusa, C. C.; Uyar, T.; Rusa, M.; Hunt, M. A.; Wang, X.; Tonelli, A. E. *J of Polymer Sci: Part B-Polymer Physics* 2004, 42 (22): 4182-4194.

35. Rusa, C. C.; Wei, M.; Shuai, X.; Bullions, T. A.; Wang, X.; Rusa, M.; Uyar, T.; Tonelli, A. E. *J of Polymer Sci: Part B-Polymer Phys* 2004, 42 (23): 4207-4224.

36. Rusa, C. C.; Bullions, T. A.; Fox, J.; Porbeni, F. E.; Wang, X. W.; Tonelli A. E. *Langmuir* 2002, 18 (25): 10016-10023.

37. Takeo, L. K.; Kuge, T, *Agr. Biol. Chem* 1970, 34(4): 568-574.

38. Rusa, C.C.:; Fox, J.; Tonelli, A. E. *Macromolecules* 2003, 36(8), 2742-2747.

39. In *Polymer Data Handbook*; Mark, J. E., Ed., Oxford University Press: New York, 1999, Ch. 14, 16, 19.

40. Bullions, T. A.; Wei, M.; Porbeni, F. E.; Gerber, M. J.; Peet, J.; Balik, M.; White, J. L.; Tonelli, A. E. *J of Polymer Sci: Part B-Polymer Physics* 2002, 40,(10): 992-1012.

41. Uyar, T.; Rusa, C. C.; Hunt, M. A.; Aslan, E.; Hacaloglu, J.;Tonelli, A. E. Polymer 2005, (46) 4762-4775

42. Uyar, T.; Toppare, L.; Hacaloglu, J. *Journal of Analytical & Applied Pyrolysis* 2003, 68-9: 15-24.

43. Uyar, T.; Hacaloglu J. *J Analytical & Applied Pyrolysis* 2002, 64 (2): 379-393.

44. Uyar, T.; Toppare, L.; Hacaloglu, J. *Journal of Macromolecular Science-Pure and Applied Chemistry* 2001, 38 (11): 1141-1150.

45. Puglisi, C.; Sturiale, L.; Montaudo, G. *Macromolecules* 1999, 32, 2194.

46. Ito, Y.; Ogasawara, H.; Ishida, Y.; Ohtani, H.; Tsuge, S. *Polymer Journal* 1996, 28, 1090.

47. Montaudo, G.; Puglisi, C.; Samperi, F. *J of Polymer Sci: Part A-Polymer Chemistry* 1998, 36 (11): 1873-1884.

48. Ferriol, M.; Gentilhomme, A.; Cochez, M.; Oget, N.; Mieloszynski, J. L. *Polymer Degradation and Stability* 2003, 79 (2): 271-281.

49. Guyot, A.; Bert, M. *Journal of Applied Polymer Science* 1973, 17 753.

50. Gupta, M. C.; Viswanath, S. G. *Ind Eng Chem Res* 1998, 37, 2707.

51. Smith RM, editor. *Understanding Mass Spectra: A Basic Approach*. New Jersey: 2nd Ed., John Wiley & Sons, Inc., 2004, p 208.

52. Uyar T, Rusa CC, Rusa M, Wang X, Hacaloglu J, Tonelli AE. *Journal of Polymer Science: Part B-Polymer Physics* 2005; 43 (18): 2578-2593**.**

53. Lindner, K.; Saenger, W. *Biochemical and Biophysical Research Communications* 1980, 92*,* 933-938.

54. Schenk, W.; Reichert, D.; Schneider, H. *Polymer* 1990, 31 (2), 329-335.

# CHAPTER 4

## 4 Crystalline Cyclodextrin Inclusion Complexes with Aromatic Molecules

### 4.1 The Solid Channel Structure Inclusion Complex Formed Between Guest Styrene and Host γ-Cyclodextrin

#### 4.1.1 Summary

The solid complex of guest styrene included inside the channels of host γ-cyclodextrin (styrene/γ-$CD_{channel}$-IC) was formed in order to perform polymerization of styrene in a confined environment (γ-CD channels). The experimental molar ratio of styrene to γ-CD in styrene/ γ $CD_{channel}$-IC was found to be 2:1, which is consistent with molecular modeling studies, utilizing Quantum Mechanics PM3 parameters that indicate the γ-CD/two styrene molecular complex is the most energetically favorable. Consistent with modeling of the γ-CD/two styrene molecular complex, no experimental indication of intermolecular π-π interactions between the pairs of included styrene molecules inside the γ-CD channels was observed. Once included in the host γ-CD cavities, the thermal stability of normally volatile bulk styrene to elevated temperatures (much above its boiling point) was observed until the γ-CD host molecules themselves began to degrade at ~300º C. In addition, the thermal degradation of host γ-CD from the styrene/ γ-$CD_{channel}$-IC was observed to be different from that of pure γ-CD due to co-degradation of styrene and γ-CD.

### 4.1.2 Introduction

Cyclodextrins (CDs) are cyclic oligosaccharides consisting of 6, 7, and 8 units of α-1,4-linked glucopyranose units, and are named alpha (α), beta (β), and gamma (γ)-CDs, respectively (Figure 1). The depth of the cavities for the three CDs is the same (~7.8 Å), while the cavity diameters of α-, β-, and γ-CDs are ~ 6, 8, and 10 Å, respectively.[1] Due to the unique chemical structure of the CD molecule, the cavity is hydrophobic relative to the outer surface. The hydrophobic nature of the CD cavities facilitates the ability of CDs to act as a host clathrate for both nonpolar and polar guests to form inclusion complexes (ICs).[1] Several types of driving forces, such as van der Waals interactions, hydrogen-bonding, release of high energy-water, and decrease in the strain energy in the cyclodextrin cavity, have been proposed as contributing to the formation of CD ICs.[2] Though limited by the sizes of the host CD cavities and the cross sections of included guests, CDs can include small molecules, as well as polymers, to form guest-host CD ICs.[3-6] The stability of the guest molecules significantly increase once the inclusion compound is formed, due to the binding forces between host CDs and the included guest molecules.

Solution or solid inclusion complexes of monomers i.e., styrene[7-8], methyl methacrylate[9], pyrrole[10], bithiophene[11], aniline[12-13] etc., with α-, β- and γ- CDs have been studied. In solution complexes, CDs show unique characteristic in which water-insoluble, hydrophobic monomers become water-soluble when they are complexed with host CD molecules, and this characteristic was used to synthesize polymers in aqueous media.[8-10] In the case of solid monomer-CD complexes, the monomer resides in the CD cavities and can be polymerized by solid-state polymerization[14] or

by suspending the crystals of monomer-CD inclusion compound into a solution where the inclusion compound is not soluble.[7] In order to obtain polymer, the CDs have to adopt continuous channel-type packing (Figure 1d) in which the monomer molecules reside in the channels and further react with each other once the polymerization is initiated. Polymerization cannot be achieved in cage-type monomer-CD ICs (Figure 1c), since the monomers are entrapped in the CD cavities and are segregated from each other by neighboring host CD molecules.

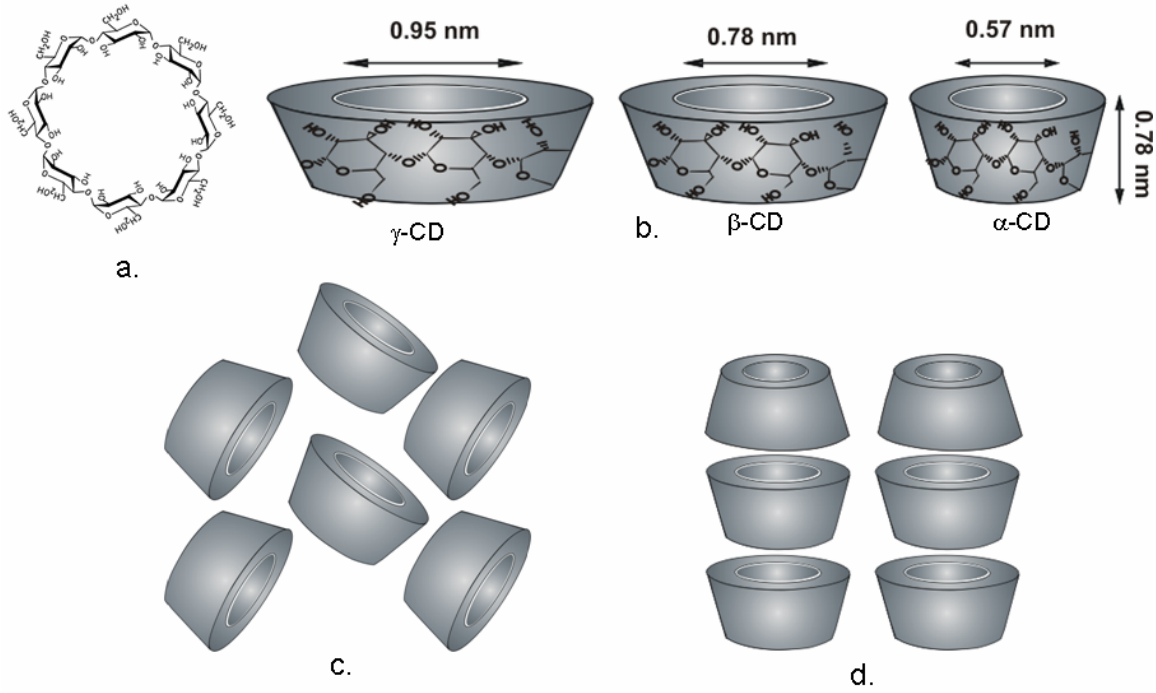


**Figure 1.** (a) γ-CD chemical structure; (b) approximate dimensions of α-, β- and γ-CDs; schematic representation of packing structures of (c) cage-type and (d) head-to-head:tail-to-head:tail-to-tail channel-type γ-CD crystals.

Polymerization of vinyl monomers, like styrene, that are located as guests in the narrow channels of their cyclodextrin-inclusion compound (CD-IC) crystals can potentially lead to polymers with microstructures that are distinct from those attained

during homogeneous polymerizations of the same monomers, since certain microstructures resulting from homogeneous polymerizations may be prevented by the conformational restrictions placed on them by the narrow CD-IC channels. Based on our conformational modeling of stereoisomeric polystyrenes (PSs) in narrow channels, we suggested that polystyrene with unusual microstructures might be obtained *via* constrained polymerization of styrene in its γ-CD-IC crystals.[15] It is crucial to have full complexation of styrene inside the γ-$CD_{channel}$ crystals prior to polymerization, since the presence of any uncomplexed styrene would jeopardize the confined polymerization. For this purpose, the solid inclusion complex of styrene inside γ-CD channels (styrene/γ-$CD_{channel}$-IC) was formed. Modeling of the styrene/γ-CD-IC was also performed with the semi-empirical Quantum Mechanics PM3 method in order to get a better understanding of the stoichiometry and interactions between guest styrenes and the host γ-CD molecules. Here, we summarize the results of the formation and characterization of the solid complex of guest styrene included in host γ-CD channels, while the polymerization of styrene inside these γ-CD channels will be the subject of the next chapter.

### 4.1.3 Experimental Section

#### 4.1.3.1 Materials

γ-cyclodextrin was purchased from Cerestar (Hammond, IN). Styrene (99.9%, Aldrich) was vacuum distilled prior to use. All the other chemicals used in this study were reagent grade and used without further purification. The water used in this study was deionized (DI-$H_2O$).

#### 4.1.3.2 Formation of Solid Styrene/Cyclodextrin Inclusion Compounds (Styrene/$CD_{channel}$-IC)

The as-received γ-CD has a cage-type crystalline structure (Figure 1c). Two different approaches can be followed to form styrene/γ–CD inclusion compounds (styrene/γ–$CD_{channel}$-ICs), where the resulting CD-IC has a channel packing structure. The first approach is a "suspension method" in which the preformed γ-$CD_{channel}$ is suspended into styrene to form the inclusion compound.[7] The second approach is a "precipitation method", which is comparatively more convenient. In this method, styrene is added directly to an unsaturated CD aqueous solution and precipitation occurs as the styrene molecules form the IC with CD molecules, where the resulting styrene/CD-IC has a channel structure. Here, we used the precipitation method to form all styrene/CD inclusion compounds.

A quantity of as-received γ-$CD_{cage}$ (6.5 grams, 0.005 mol) was dissolved in 100 ml of deionized water at room temperature (RT). Styrene (1.3 gram, 0.0125 mol) was added drop-wise to the clear aqueous solution of γ-CD, while the solution was stirred and kept at RT. The clear γ-CD solution became turbid and a white precipitate formed immediately after addition of styrene, which indicated formation of the styrene/γ-CD-IC. The resulting white suspension was stirred for an additional 24 hours at RT, and the filtered precipitate was dried in the fume hood for 24 hrs. The yield of IC was close to 100%.

X-Ray confirmed the channel packing structure for the styrene/γ-CD-IC. The presence and molar ratio of styrene to γ-CD (~ 2:1) was determined with solution $^1$H-NMR upon dissolution of the styrene-γ-CD-IC in d-DMSO. For comparison, a physical mixture of styrene and γ-CD (2:1 mol ratio of styrene to γ-CD) was prepared by mixing as- received cage structure γ-CD crystals with liquid styrene monomer.

#### 4.1.3.3 Wide-Angle X-ray Diffraction (WAXD)

Wide-angle X-ray diffraction (WAXD) measurements were performed with a Siemens type-F X-ray diffractometer using a Ni-filtered $CuK_\alpha$ radiation source ($\lambda$ = 1.54 Å). The diffraction intensities were measured every 0.1° from $2\theta$ = 5 to 30° at a rate of $2\theta$ = 3°/minute. The supplied voltage and current were 30 kV and 20 mA, respectively.

#### 4.1.3.4 Differential Scanning Calorimetry (DSC)

Experiments were performed with a Perkin-Elmer DSC-7 under nitrogen purge gas. Indium was used as a standard for calibration. The samples were subjected to heating and cooling cycles consisting of: 1.0 minute hold at -50° C, ramp to 25° C at 20° C/min, hold at 25° C for 1 minute, and quench to -50° C at a cooling rate of 200° C/min.

#### 4.1.3.5 Nuclear Magnetic Resonance (NMR)

$^1$H-NMR spectra were recorded on a Mercury 300 spectrometer in DMSO-d6, using tetramethylsilane (TMS) as the internal standard. Solid-state NMR experiments were performed on a Bruker DSX-300 instrument operating at a field strength of 7.05 T, corresponding to a 300 MHz $^1$H Larmor frequency, using 7 mm

zirconium oxide rotors. $^{13}C$ cross-polarization/magic angle spinning/with high power dipolar $^{1}H$ decoupling (CP-MAS/DD) spectra and single-pulse MAS/DD spectra were recorded with 4 kHz MAS and 3.5 μs π/2 pulse widths. Radio-frequency field strengths for $^{1}H$ decoupling (DD) were 70-73 kHz. The cross-polarization contact time was 1 ms, and the delay between two consecutive scans was 3 s, while single-pulse spectra were acquired with cycle delay times of 1 s.

#### 4.1.3.6 UV-Vis Spectrometry (UV-Vis)

Solution UV-Vis spectra of styrene were recorded in methanol on a Varian Cary 3 UV-Visible spectrophotometer. Diffuse reflectance measurements for styrene-$CD_{channel}$-IC powder were carried out on a Cary 3e UV-Visible spectrophotometer equipped with an integrating sphere. Spectra were measured following calibration with a pressed polytetrafluoroethylene powder standard. Reflectance spectra were collected and K/S data obtained using the standard Kubelka-Munk equation[16], $K/S = (1-R)^2/2R$.

#### 4.1.3.7 Thermogravimetric Analyses (TGA).

Thermogravimetric analyses of the samples were performed with a Perkin-Elmer Pyris 1 thermogravimetric analyzer (TGA). Thermal decompositions were recorded between 25 and 500° C. The heating rate was of 20° C/min and nitrogen was used as a purge gas.

#### 4.1.3.8 Direct Insertion Probe Pyrolysis Mass Spectrometry (DIP-MS)

The direct insertion probe pyrolysis mass spectrometry (DIP-MS) system consisted of a 5973 HP quadruple mass spectrometer coupled to a JHP SIS direct

insertion probe pyrolysis system. 0.01 mg samples were pyrolyzed in flared glass sample vials. The temperature was increased at a rate of 20$^{o}$ C/min and the scan rate was 2 scans/s.

#### 4.1.3.9 Computational Modeling Methods

The structures of styrene, γ-CD, and their ICs were optimized by performing an optimized geometry calculation in MOPAC using PM3 parameters.[17] The UV spectrum of styrene was predicted using ZINDO-CI/INOD1 (Zerner Intermediate Neglect of Differential Overlap-Configuration Interaction)[18] with CI = 26. In the cases of γ-CD and the styrene/γ-CD-ICs, the MOZYME algorithm[19] was used to speed up the calculations. The calculations were conducted at 298.15K and 1 atm and executed on a Pentium 4-MCPU 2.66GHz with 768 of RAM.

### 4.1.4 Results and Discussion

#### 4.1.4.1 Wide-Angle X-ray Diffraction (WAXD)

WAXD is a useful characterization technique for investigating the crystalline structure of the styrene/γ-CD-ICs. It was found that styrene/γ-CD-IC has a channel-type packing structure. The details of the WAXD study and the crystalline characteristics of the styrene/γ-CD-ICs are given in a latter section (see section 4.2.5.5).

#### 4.1.4.2 Differential Scanning Calorimetry (DSC)

DSC is a useful tool to determine whether or not the guest molecules are included inside the CD cavities: thermal transitions, such as the melting point ($T_m$) for guests, would be observed if there is any uncomplexed guest molecules present

in the CD-ICs. Figure 2 shows the DSC scans of styrene/γ-CD-IC and the physical mixture of styrene and γ-CD. It was observed that the DSC scans of the physical mixture of styrene and γ-CD exhibited a melting point for styrene at -30 $^{0}$C, whereas no melting point was observed for the styrene/γ-CD-IC, suggesting that the styrene molecules were all included inside the CD channels.

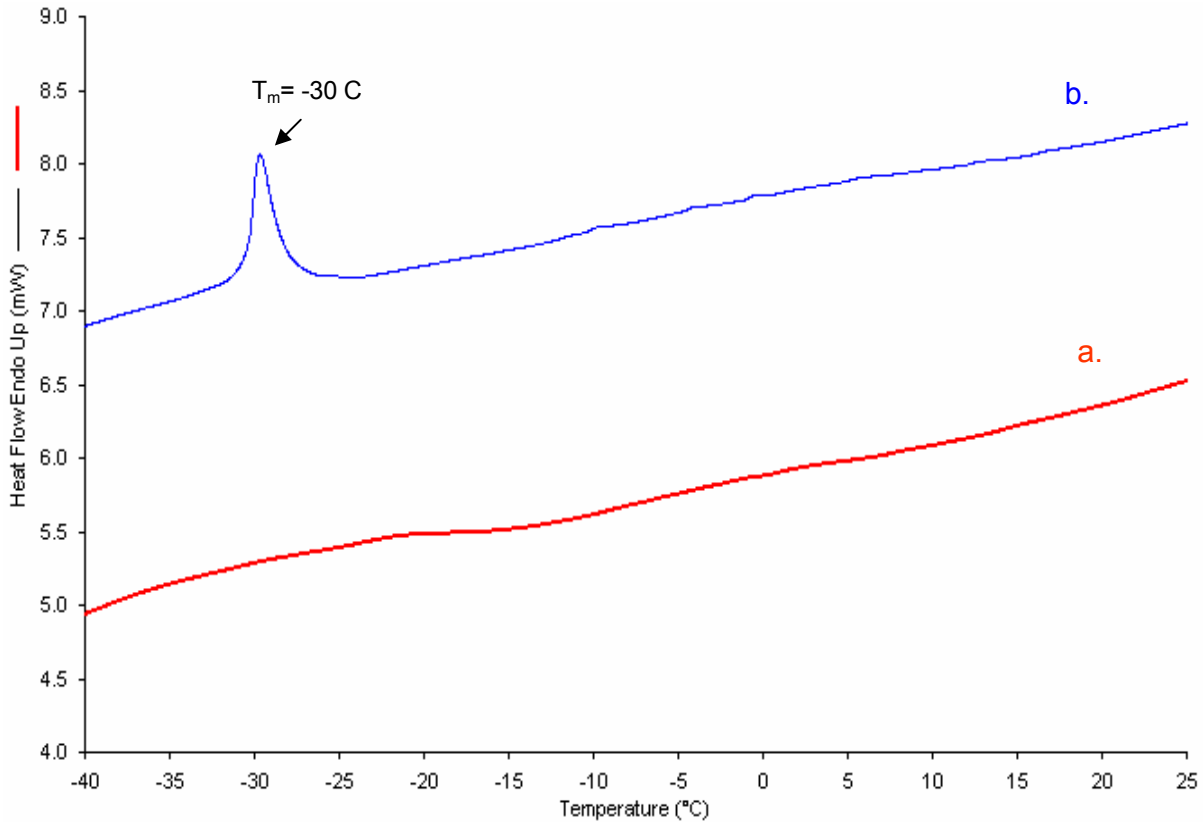


**Figure 2.** DSC scans of a.) styrene/γ-CD-IC b.) physical mixture of styrene and γ-CD.

#### 4.1.4.3 Nuclear Magnetic Resonance (NMR)

NMR is a powerful technique to determine the presence and molar ratio of guest molecules in CD-ICs. The presence of styrene in the styrene/γ-CD-IC was

confirmed by solution $^{1}$H-NMR, and the molar ratio of styrene to γ-CD was found to be ~ 2:1 for the complex. Solid-state $^{13}$C-NMR has also been carried out to get further evidence for the complexation of styrene and γ-CD. Figure 3 shows the $^{13}$C CP/MAS NMR spectra of the styrene/γ-CD-IC and the physical mixture of styrene with γ-CD. Cyclodextrin molecules assume a less symmetrical conformation in their cage structure crystals when not including a guest (other than water) in their cavities. In the CP/MAS spectrum of the physical mixture of styrene and γ-CD, the γ-CD peaks show several resolved resonances for each of the carbon types (Figure 3a). In the case of the styrene/γ-CD-IC CP/MAS spectrum, each carbon in each glucose unit can be observed as a single somewhat broadened peak (Figure 3b), which indicates that γ-CD adopts a more symmetrical conformation and each γ-CD molecule is in a similar environment due to the presence of included styrene guest molecules, whose resonances and therefore presence is also confirmed. A closer examination and comparison of the styrene resonances in the physical mixture and in the inclusion compound revealed some differences in their resonance frequencies/chemical shifts, which may due to possible interactions between γ-CD and styrene in the inclusion compound.

We have also carried out single pulse $^{13}$C-NMR experiments for styrene/γ-CD-IC (Figure 3c), to learn if the styrene molecules in the γ-CD channels are in involved in any kind of styrene-styrene π-π interactions. Judging from a comparison of $^{13}$C-NMR chemical shifts observed for pure styrene (not shown) and those observed for styrene included in the channels of its γ-CD-IC, no specific interactions between the

styrene molecules in the channels were observed, which is consistent with both the UV-Vis and modeling data discussed below.

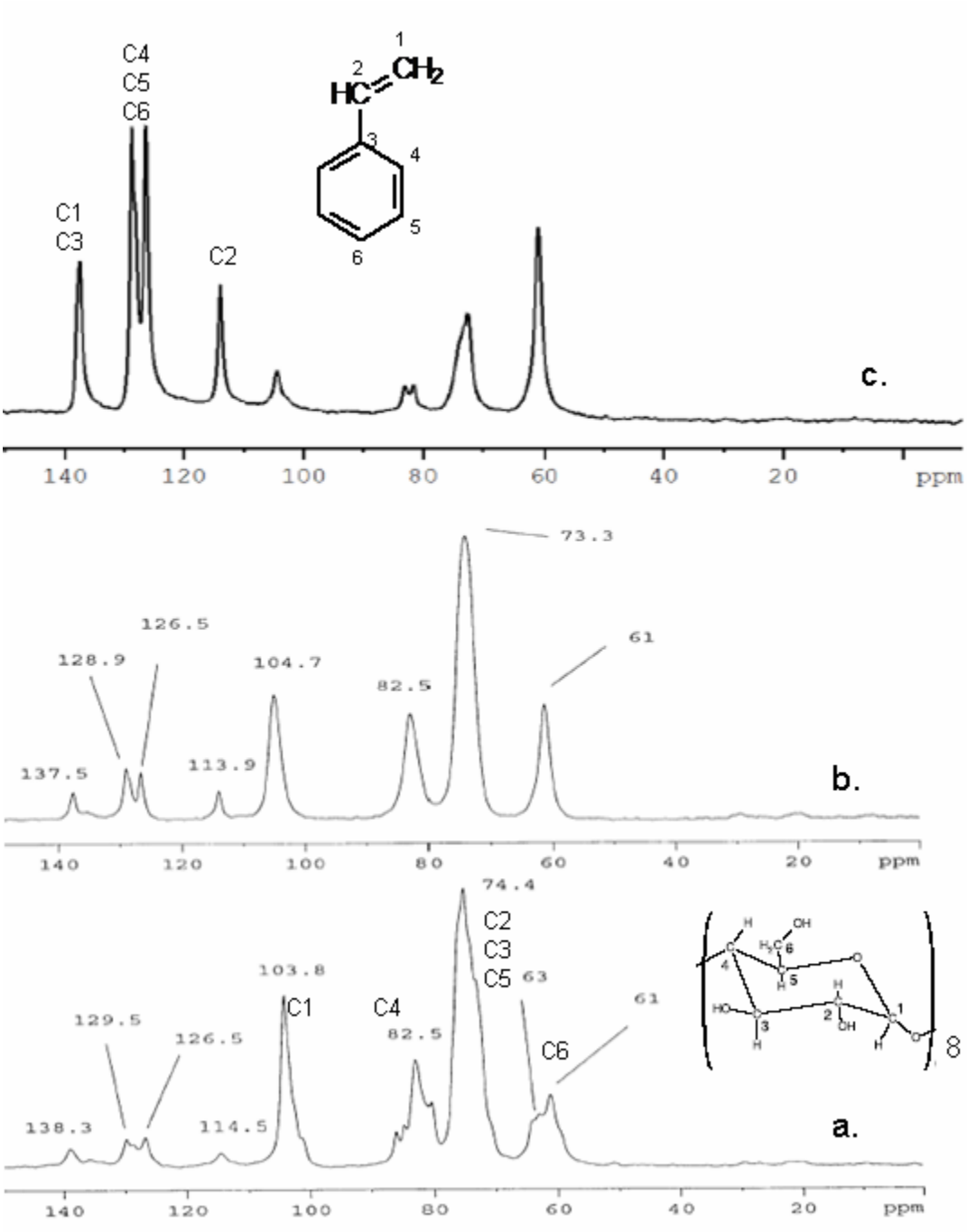


**Figure 3.** CP/MAS $^{13}$C-NMR of a.) physical mixture of styrene and γ-CD and b.) styrene/γ-$CD_{channel}$-IC, and c.) single pulse $^{13}$C-NMR of styrene/γ-$CD_{channel}$-IC.

#### 4.1.4.4 Thermogravimetric Analyses (TGA)

Thermogravimetric results observed for pure γ-CD indicated two weight loss stages (Figure 4(i)a). The one below 150° C was attributed to removal of water and the second, with a maximum at around 360° C and corresponding to the major weight loss, was associated with the main degradation of γ-CD.[20] The TGA thermogram of the physical mixture of styrene and γ-CD (Figure 4(i)c) is almost identical with the thermogram of pure γ-CD, which indicates that there is only a very small amount of styrene left in the mixture prior to the TGA experiment. Since styrene is volatile, most of the styrene is evaporated from the mixture, which proves that there is no complexation between styrene and γ-CD in the physical mixture. In the case of complexation, the stability of a volatile guest molecule would be expected to increases due to guest-host interaction, which was the case for styrene/γ-CD-IC. In the TGA thermogram of styrene/γ-CD-IC (Figure 4(i)b), there was a continuous weight loss up to the main degradation of γ-CD suggesting the presence of styrene and its stability at temperatures much higher than its boiling point (styrene $T_b$= ~$138^0$ C) . The presence and higher thermal stability of styrene at elevated temperatures is further strong evidence for the complexation of styrene with γ-CD in this sample.

Isothermal TGA study of the styrene/γ-CD-IC has also been carried out at elevated temperatures (Figure 4(ii)). The weight loss percentages were found to be 18.4, 19.8, 21.9, and 23.4 % as the temperature was kept constant at 180, 200, 220, and 265 $^0$C, respectively, for 100 minutes of thermal treatment. The higher the treatment temperature, the higher the weight loss observed for the styrene/γ-CD-IC.

This finding reveals that some of the styrene molecules are still present inside the γ-CD channels even at elevated temperatures, though less styrene remains in the γ-CD cavities after prolonged heating at elevated temperatures. Nevertheless, the presence of styrene molecules was still detected by pyrolysis mass spectrometry up until the main degradation of γ-CD (above $300^0$ C), indicating the co-degradation of the remaining styrene with γ-CD. This observation suggests that CD-ICs may provide a means to deliver volatile additives to polymers in the form of high-melting additive-CD-ICs.

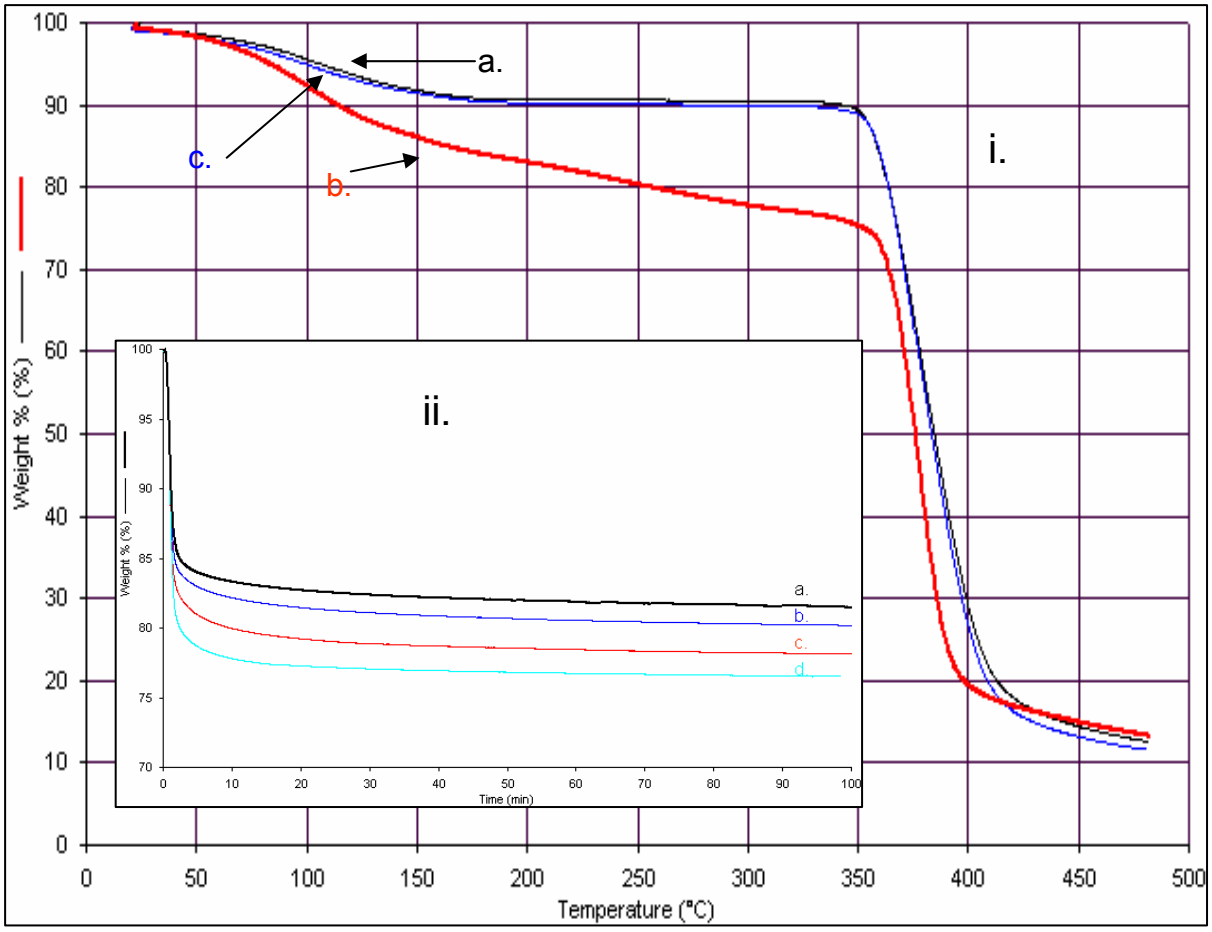


**Figure 4. (i)** TGA thermograms of a.) as-received γ-CD, b.), styrene/γ-CD-IC, and c.) physical mixture of styrene and γ-CD. **(ii)** Isothermal TGA thermograms of styrene/γ-CD-IC, a.) 180, b.) 200, c.) 220, and d.) $265^0$ C. All samples were rapidly heated ($200^0$ C/min.) to reach these constant target temperatures.

#### 4.1.4.5 Direct Insertion Probe Pyrolysis Mass Spectrometry (DIP-MS)

In general, (DIP-MS facilitates analyses of material chemical structures and their degradation mechanisms using structural information from the thermal characterization of their degradation products.[21-23] In pyrolysis MS analysis, not only the detection of a peak, but also the variation of its intensity as a function of temperature, ie., its evolution profile, is important. The trends in evolution profiles can be used to determine the source of the product, or the mechanism of thermal degradation.

The direct pyrolysis mass spectrometry analysis of styrene/γ-CD-IC and a physical mixture of styrene and γ-CD have been performed to investigate their thermal stabilities and thermal degradation behaviors (Figure 5). The presence of styrene in the sample was identified by detection of the classical mass spectrum of styrene with peaks due to $C_8H_8$, $C_6H_6$ molecular ions and $C_4H_3$,$C_3H_3$ fragments at m/z= 104,78 and 51,39 Da, respectively. Pyrolysis analysis of the styrene and γ-CD physical mixture (Figure 5b) indicated that the release of water ($H_2O$, m/z= 18 Da) and styrene from the mixture is completed at very low temperatures (below $80^0$ C). This finding is consistent with TGA data where the low temperature weight loss was recorded and attributed to removal of water and styrene for this sample. The thermal degradation of γ-CD occurs over a broad temperature range starting around $300^0$ C. The variation of total ion current (TIC) as a function of temperature shows two peaks; a sharp peak and a broad peak with a shoulder in the high temperature range having maxima at 330 and $350^0$ C, respectively. Yet, the fragmentation patterns observed in the pyrolysis mass spectra recorded throughout the pyrolysis were

nearly identical and the main degradation products are due to the cleavage of weak C-O bonds, yielding intense $C_2H_4O_2$ and $C_3H_5O_2$ fragments at m/z = 60 and 73 Da, respectively. The recorded TIC for the styrene and γ-CD physical mixture is very similar to that of pure γ-CD.[24] This indicates the absence of styrene in the physical mixture at high temperatures and points out that the degradation behavior of γ-CD in the mixture is the same as pure γ-CD.

The thermal behavior of the styrene/γ-CD IC was found to be much different compared to that of the styrene and γ-CD physical mixture (Figure 5a). The styrene/γ-CD IC pyrolysis mass spectra showed that the complete removal of water ($H_2O$, m/z= 18 Da) was again achieved at very low temperatures (below 50 $^0$C). Yet, the continuous release of styrene was observed up to the main degradation region of the γ-CD (above 300 $^0$C). This finding is consistent with TGA results which elucidate the presence of styrene in the γ-CD channels and its strong interaction with the CD cavities. Moreover, it was observed that the TIC recorded in the range of 300 - 450 $^0$C (degradation region for γ-CD) for this sample was different than the physical mixture. Although, pyrolysis mass spectra recorded above 300 $^0$C showed identical peaks, the low temperature peak with a shoulder around 300$^0$C in the single ion pyrograms of γ-CD based products became narrower while the second weak and broad peak around 390 $^0$C diminished significantly. This indicated that the degradation behavior of γ-CD was affected by the presence of styrene which may due to co-degradation of styrene and γ-CD.

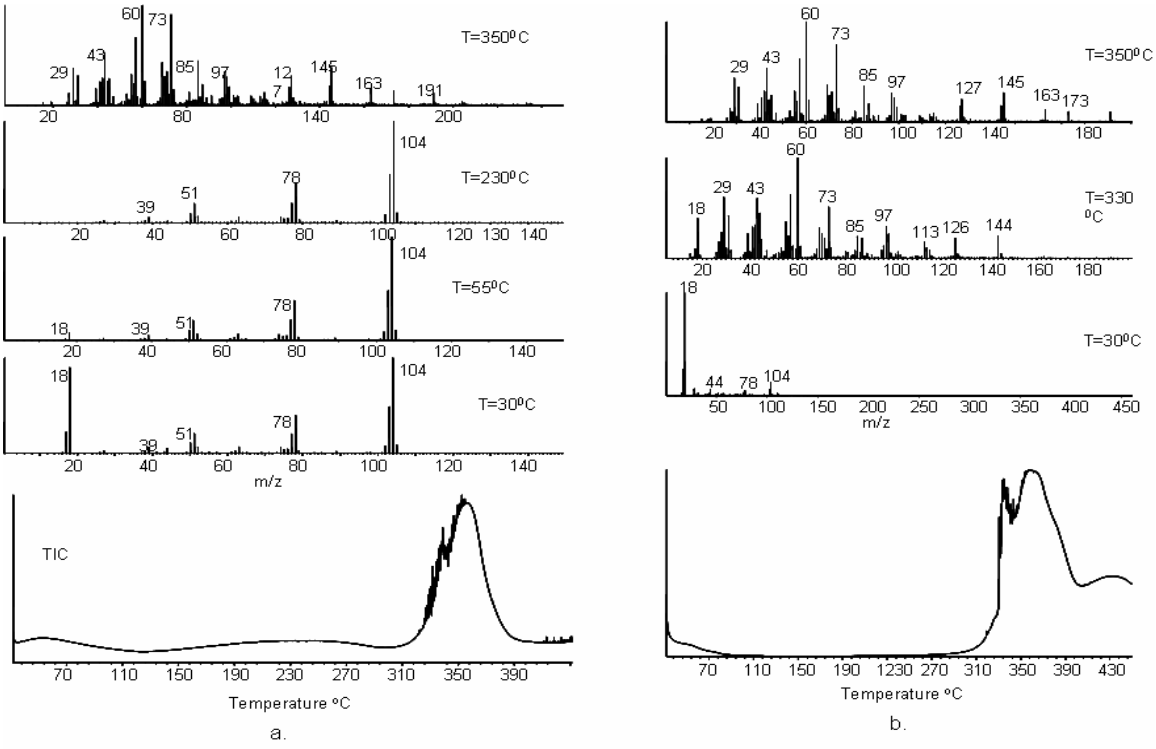


**Figure 5.** Total ion current (TIC) curves and pyrolysis mass spectra recorded at the maximum of the peaks and shoulders in the TIC curves of a.) styrene/γ-CD-IC and b.) the physical mixture of styrene and γ-CD.

In Figure 6, evolution profiles of some diagnostic thermal degradation products of styrene and γ-CD namely; $C_8H_8$ (m/z=104 Da), $C_6H_6$ (m/z=78 Da), $C_3H_5O_2$ (m/z=73 Da), and $C_2H_4O_2$ (m/z= 60 Da) are shown. Evolution of styrene based products was observed at very low temperature and diminished below $100^0$ C in the physical mixture indicating the thermal instability of styrene due to lack of complexation with γ-CD. Styrene-based products from the thermal degradation of the styrene/γ-CD-IC sample showed two maxima at low (~ $50^0$ C) and at higher temperature (~$230^0$ C). This behavior can be explained by supposing two different environments for styrene molecules in the complex. Styrene molecules having weaker interactions with γ-CDs in the host channels are released at lower

temperatures than those with stronger interactions with γ-CD. It is also noted that the quantity of styrene released at low temperature is very low suggesting that most of the guest molecules have high stability in the γ-CD channels due to strong guest-host interactions. This was also confirmed by solution $^1$H-NMR, where the styrene/γ-CD-IC that was vacuum-dried for 24 hours at $40^0$ C lost only 10 weight % of the total styrene in the complex. Moreover, significant changes were also observed for the evolution profiles of $C_3H_5O_2$ (m/z=73Da) and $C_2H_4O_2$ (m/z= 60 Da) fragments from the styrene/γ-CD-IC sample, which indicated that degradation of γ-CD was affected by styrene as mentioned earlier.

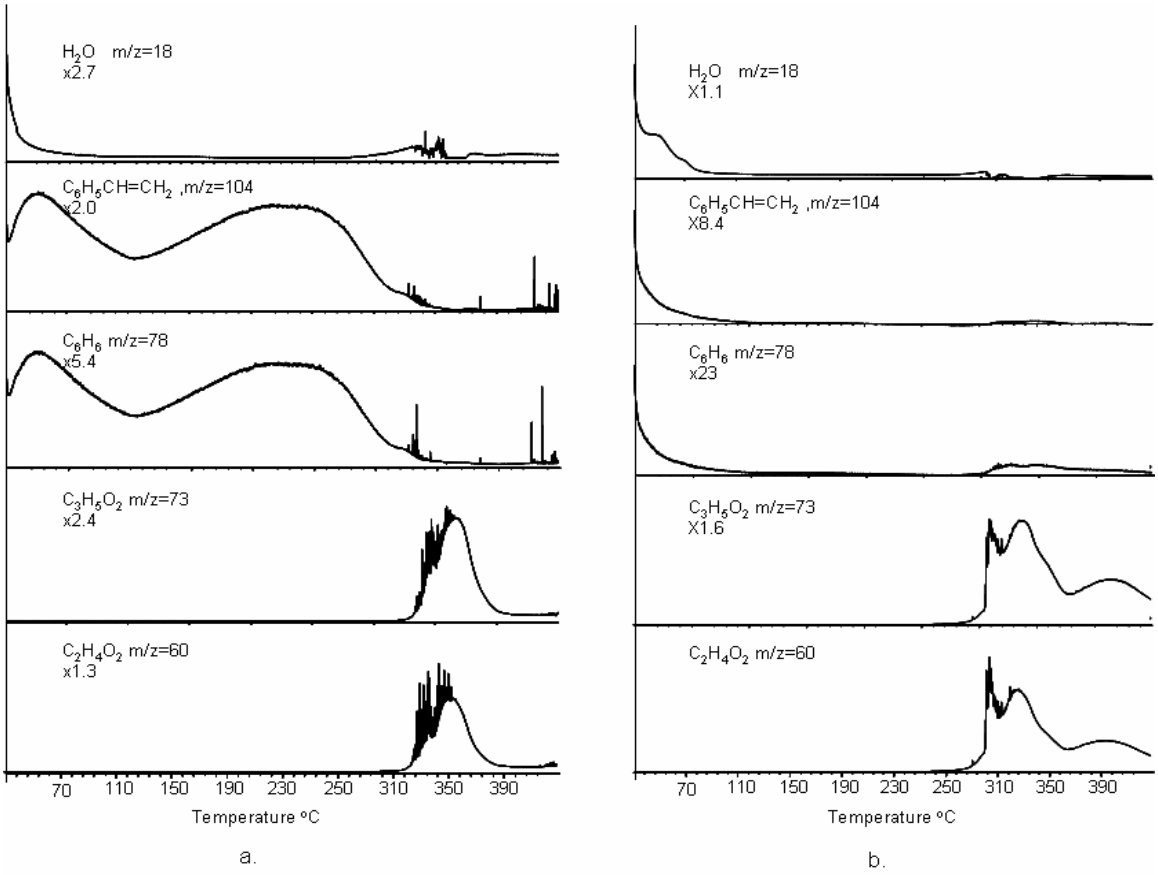


**Figure 6.** Evolution profiles of $C_2H_4O_2$ (m/z= 60 Da), $C_3H_5O_2$ (m/z=73Da), $C_6H_6$ (m/z=78 Da), $C_8H_8$ (m/z=104 Da), and $H_2O$ (m/z= 18 Da) in a.) styrene/γ-CD-IC and b.) the physical mixture of styrene and γ-CD.

#### 4.1.4.6 Quantum Mechanics Calculations

Modeling the inclusion complexation of host CDs with various organic guests can be a powerful tool, because it can potentially provide valuable and deep insights into the non-covalent, weak intermolecular interactions governing their molecular recognition, as in enzyme substrate binding.[25] Owing to the relatively large molecular size of CDs, most of the modeling studies performed on CDs employed only molecular mechanics (MM)[26], molecular dynamics (MD)[27], and Monte Carlo simulations (MC).[28] The first quantum mechanics study on CDs using a semi-empirical CNDO method was performed by Kitagawa et al. [29] in 1987. Thereafter, Yannakopoulou[30] and the Huang group[31] carried out AM1 calculations on the ICs of β-CD. Recently, the PM3 method was used to study the inclusion of different guest molecules into CDs, which proved to be a powerful tool for the conformational analysis of supramolecular systems.[32] In the present study, efforts, utilizing the semi-empirical Quantum Mechanics PM3 method, were made to estimate the number of guest styrene molecules complexed inside the host γ-CD cavity, and, if more than one is included, how they are oriented.

#### 4.1.4.7 Prediction of Styrene UV-Vis Behavior

For intermolecular π-π interaction to take place between parallel and overlapping styrenes, their intermolecular distance should be 3.3 Á or less.[33] Such interactions result in bathochromic shifts of absorption bands to longer wavelengths. The bathochromic shift decreases significantly as the intermolecular distance goes beyond 3.3 Á. With this in mind, to account for such an effect and to simulate how intermolecular π-π interactions might play a role in shifting the $\lambda_{max}$ (281nm) of

styrene, two parallel and overlapping styrene molecules were locked at an intermolecular distance of 2.55 Å. Then, the geometry was optimized using PM3 parameters. Following the geometry optimization, the UV-Vis spectrum was predicted using ZINDO/INDO1 parameters with a configuration interaction = 26.

Figure 7(i) shows the predicted absorption spectrum for two overlapping styrene molecules in the locked conformation (2.55 Å), showing the $\lambda_{max}$ at 353.9 nm, which is highlighted in red. Figure 7(ii) shows the two styrene molecules in this locked conformation with an intermolecular distance of 2.55Å, and the molecular orbitals responsible for the electronic transition at 353.9nm are superimposed on this molecular structure.

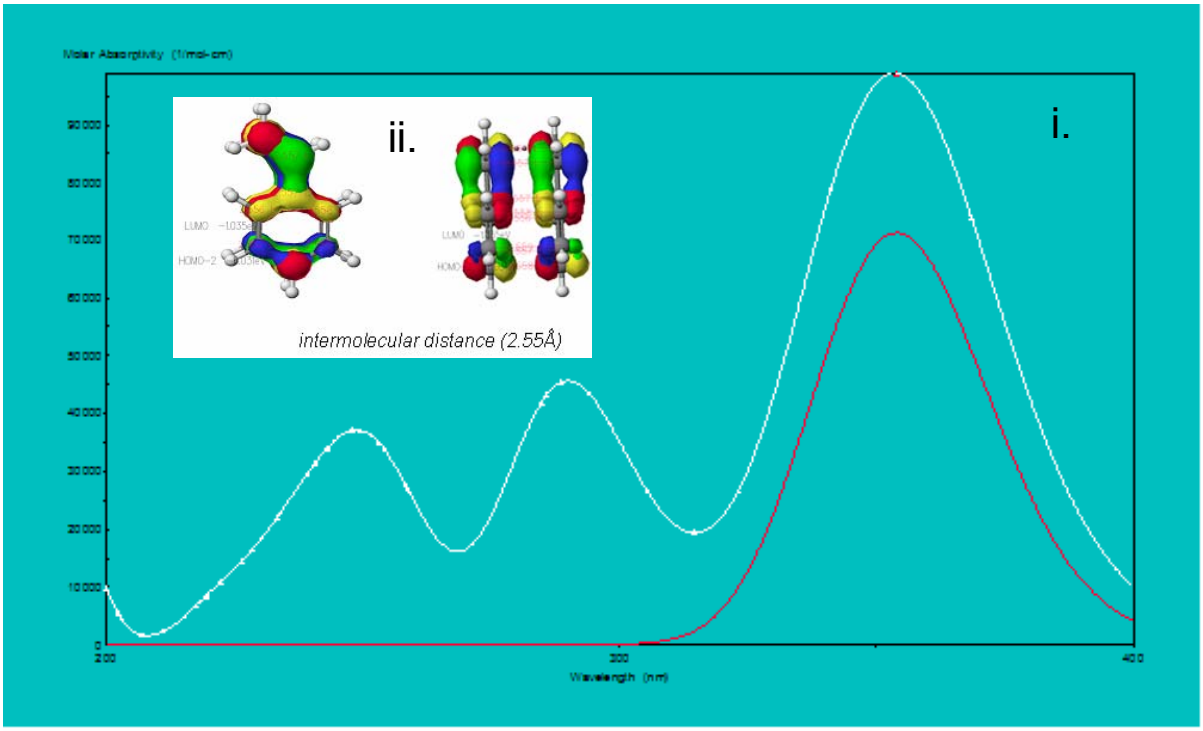


**Figure 7. (i)** Predicted absorption spectrum ($\lambda_{max}$= 353.9 nm) of two parallel and overlapping styrene molecules at an intermolecular distance (2.55 Å). **(ii)** Two views of the MO orbitals responsible for the electronic transition at 353.9nm, superimposed on two locked styrene molecules: a) two overlapped styrene molecules parallel to the plane of the paper, b) two styrene molecules perpendicular to the plane of the paper.

### 4.1.4.8 UV-Vis Absorption of Styrene in Solution and in the Styrene/γ–CD-IC

The potential for intermolecular interactions between styrene molecules inside the γ–CD channel were assessed by comparing the solution UV-Vis spectrum (Figure 8(i)) of styrene to the solid-state UV-Vis spectrum of styrene/γ-CD-IC (Figure 8(ii)). Both spectra are nearly identical, indicating that there is no intermolecular π-π interaction taking place inside the γ-CD cavity. This finding is also consistent with solid-state $^{13}$C-NMR data.

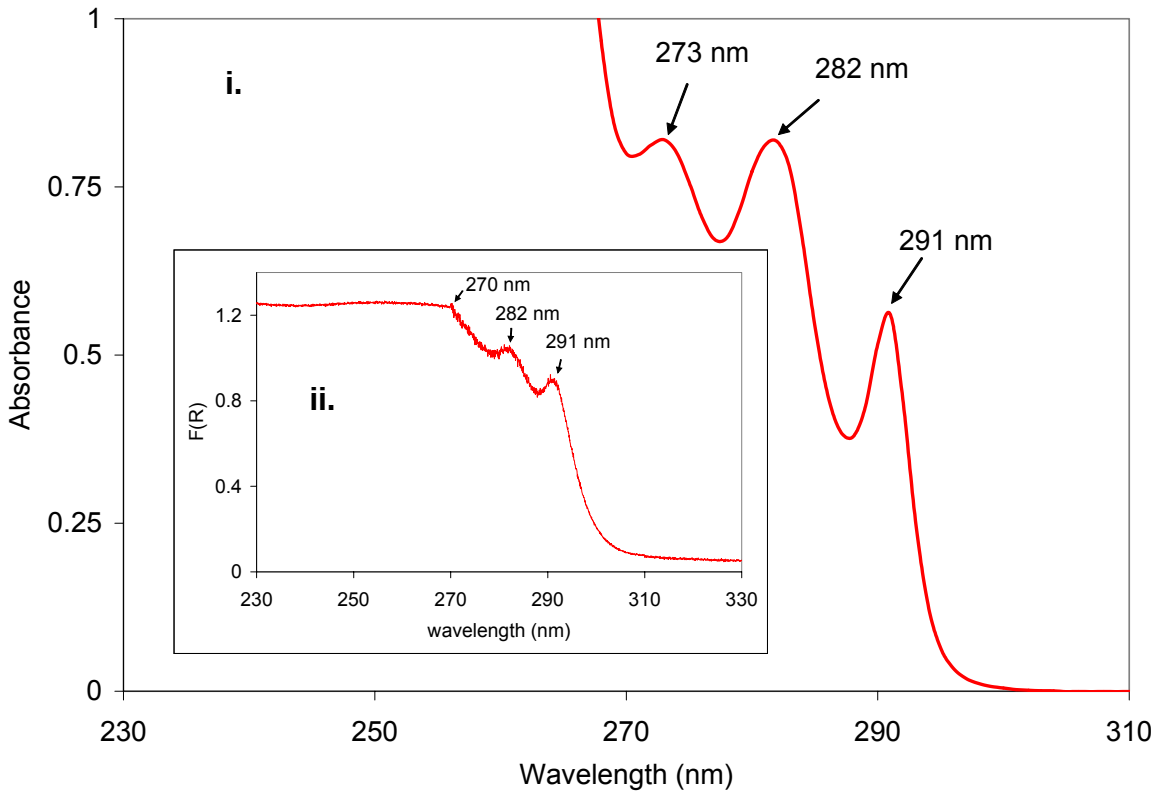


**Figure 8. (i)** UV-Vis absorbance spectrum of styrene in methanol. **(ii)** Solid-state UV-Vis spectrum of styrene/γ-CD-IC.

### 4.1.4.9 Modeling Styrene Molecules Inside the γ-CD Cavity

Quantum mechanical semi-empirical PM3 parameters were used to determine the stability of γ-CD complexes with different numbers of styrene molecules included in the host by calculating the energy difference between host and guest and their IC. Our main focus was to study the likelihood of more than one styrene molecule entering the host γ-CD, and, if so, how they are oriented and what is the intermolecular distance between them in the γ-CD cavity. To determine the stability of different complexes, the binding energy was calculated from the energy difference between the IC and the energy sum of the isolated host and guest, which are shown in Table 1.

**Table 1.** Energy of host, guest and complex, and energy of stabilization upon complexation, computed using PM3 parameters.

| **Species** (starting geometry) | | **E** (kcal/mol) | **ΔE** (optimized geometry) kcal/mol | kJ/mol | **Method** |
|---|---|---|---|---|---|
| one styrene molecule | Fig.10(i)b | 39 | ------- | | Quantum Mechanical PM3 parameters |
| 2 styrene molecules, no IMI | Fig. 10(v)a | 74 | ------- | | |
| 2 styrene molecules, at 2.55 Å | Fig. 10(ii)a | 78 | ------- | | |
| 2 styrene molecules, at 3.3 Å | Fig. 10(ii)b | 78 | -------- | | |
| γ-CD | Fig. 10(i)a | -1663 | ------ | | |
| IC/one styrene | Fig. 10(i)c | -1626 | - 2.4 | -10.0 | |
| IC/two styrene, no IMI | Fig. 10(v)b-c | -1594 | -5.7 | -23.8 | |
| IC/two styrene, at 2.55 Å | Fig. 10(iii) | -1593 | - 8.6 | -36.0 | |
| IC/two styrene, at 3.3 Å | Fig. 10(iv) | -1593 | - 8.9 | -37.2 | |

IMI = intermolecular interaction, E = total heat of formation, ΔE= stabilization energy upon complexation = $E_{complex}$- $E_{host}$- $E_{guest}$

The results obtained from semi-empirical PM3 parameters for γ-CD containing one and two styrene molecules with and without potential intermolecular π-π interactions (Figures 9 (i)-(iv)) indicated that the IC formed with γ-CD containing two styrene molecules (Figure 9(iv)b) is the most energetically favorable, as inferred from the larger negative energy changes (Table 1). This is consistent with the experimental observation, where the molar ratio of styrene: γ-CD was found to be 2:1 in the IC by solution $^{1}$H-NMR.

The binding energy of the complex with parallel and overlapped styrenes shown in Figure 9(iv) is 13.4 kJ/mol lower than that of the complex with non-overlapped styrenes shown in Figure 9(v). Although it seems that all the complexes with two overlapped and parallel styrenes (Figures 9(ii)-(iv)) are energetically favored, the intermolecular distances following geometry optimization, in the cases of 2.55 and 3.3Å initial separations, shifted to 4.146 and 4.173Å (Figures 9(iii)-(iv)), respectively, the distance at which no intermolecular π-π interactions can be expected[33] or is experimentally observed for the styrene/γ-CD complex in its UV-Vis spectrum (Figure 8(ii)). However, their binding energies were the strongest. This indicates that complexes with overlapped and parallel styrenes are more likely to exist in the γ-CD cavity at a distance ~4.1Å, where there is no intermolecular π-π interaction. This is also confirmed by the UV-Vis solution spectra of styrene (Figure 8(i)), which is nearly identical to the UV-Vis spectrum of the styrene-γ-CD complex (Figure 9(ii)), both of which show no indication of π-π interactions.

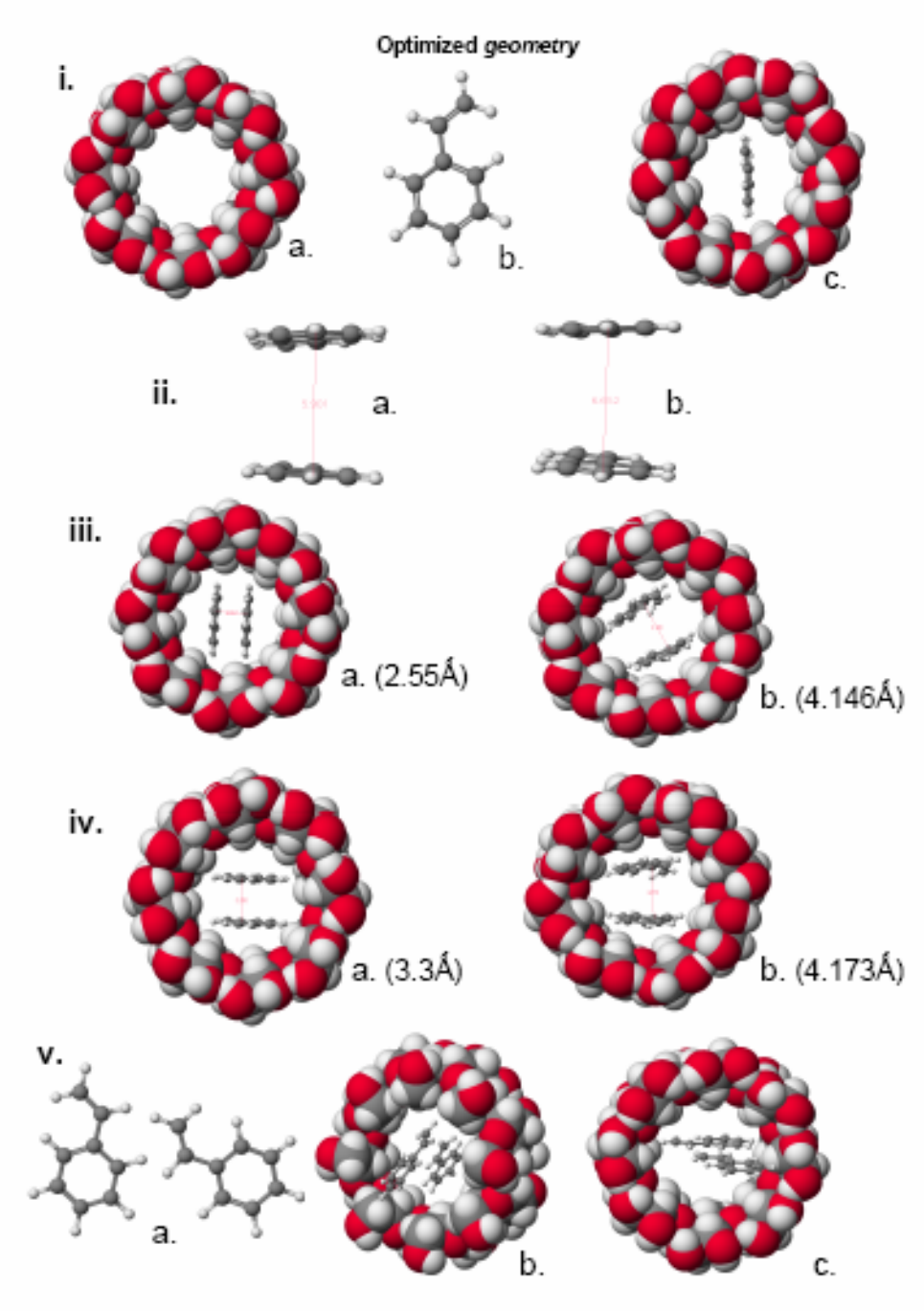


**Figure 9.** (i) Optimized geometry of host (a), guest (b), and IC (c) containing one styrene molecule using semi-empirical PM3 parameters and the MOZYME algorithm. (ii) Optimized geometry of two styrene molecules initially set at a.) 2.55 and b.) 3.3 Å. (iii) Starting a.) and optimized geometry b.) of γ-CD-IC containing two overlapped, parallel styrene molecules. (iv) Starting (a) and optimized geometry (b) of IC containing two styrene molecules. (v) Optimized geometry of non-overlapped styrenes (a) and two views (b and c) of the optimized IC containing two styrene molecules with no overlap and no π-π interactions.

#### 4.1.4.10 Microencapsulation of γ-CD Channel Structure

Table 2 summarizes the stabilization energy upon complexation of γ-CD channel structure with different number of styrene molecules in different orientation inside the channel cavity. Quantum Mechanics semi-empirical PM3 methods showed clearly that the way the styrene molecules are oriented inside the channel furnished a significant difference in the stabilization energy of the corresponding complex. The data in Table 2 show clearly that positioning three pair of styrene molecules inside a γ-CD channel (Figure 10a.), either with a starting intermolecular distance 3.3 Á (Figure 10b.) or 2.55 Á (Figure 10c.), is more energetically favorable than when the styrene molecules are aligned next to each other (Figure 10d.), inferred from the more negative enthalpy of the complex, which is also consistent with what was found with ICs of a single γ-CD molecule. Moreover, comparison of the predicted stabilization energy data of ICs produced from single γ-CD molecule and γ-CD channel structure clearly shows that the IC formation from a channel structure is more energetically favorable than that formed from a single γ-CD molecule. Following geometry optimization of ICs furnished form γ-CD channel structure, it became evident that the optimum intermolecular distance between styrene molecules was in the range 4.0-4.3 Á, which is consistent to what was found with ICs produced from single γ-CD molecule. Based on the stabilization energy of the ICs presented in Table 1, the ratio of γ-CD : styrene is 1:2, which is in agreement with what was found from $^{1}$H-NMR.

**Table 2.** Stabilization energies of ICs formed from γ-CD channel structure and different number of styrene molecules in different orientation.

| **Species (starting geometry)** | **E** Kcal/mol | **ΔE** (optimized geometry) | | **Method** |
|---|---|---|---|---|
| | | Kcal/mol | KJ/mol | |
| 6 styrene molecules, IMI=3.3 Å | 226.3547 | -------- | | Quantum Mechanics PM3 parameters with MOZYME algorithm |
| γ-CD channel structure | -5007.8852 | ----- | | |
| γ-CD channel structure/6-styrene inside the cavity, initial IMD =3.3 Å, optimized =*4.3* Å | -4812.1335 | -30.603 | -128.12 | |
| 6-styerne molecules, IMD =2.55 | 225.7248 | | | |
| γ-CD channel structure/6-styrene inside the cavity, initial IMD =2.55 Å, optimized = 4.0 Å | -4812.9575 | -30.797 | -128.94 | |
| 4-styrene molecules, next to each other | 143.0469 | -------- | | |
| γ-CD channel structure/4-styrene inside the cavity | -4877.6452 | -12.06 | -50.49 | |

IMD =intermolecular distance

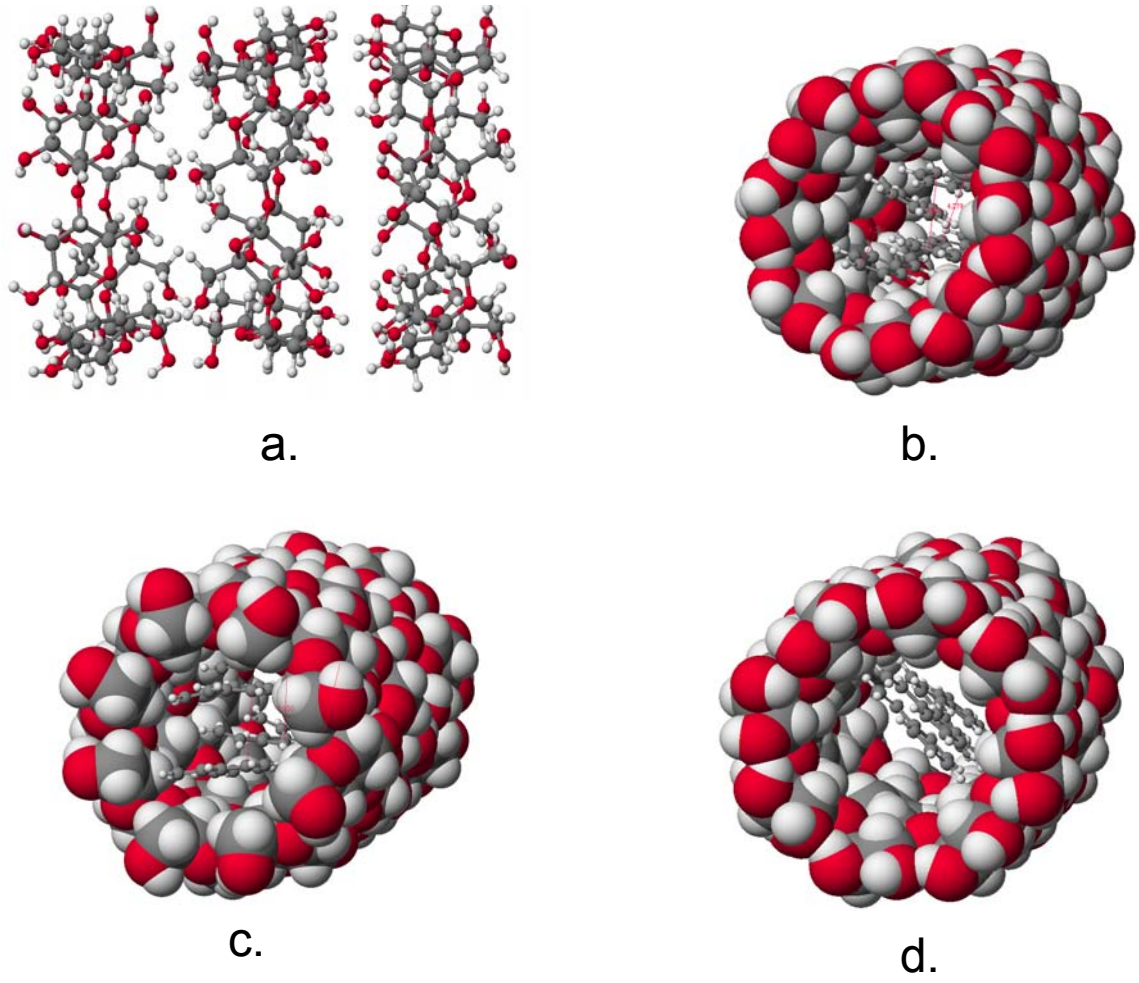


**Figure 10.** (a)Equilibrium molecular geometry of γ-CD channel structure. (b) Equilibrium molecular geometry of the IC of γ-CD channel structure and 6-styrene molecules inside. The starting intermolecular distance was 3.3 A. Following geometry optimization, it was 4.3 Å. (c) Equilibrium molecular geometry of the IC of γ-CD channel structure and 6-styrene molecules. The starting intermolecular distance was 2.55 Å. Following geometry optimization, it was 4.0 Å. (d) Equilibrium molecular geometry of the IC of γ-CD channel structure and 4-styrene molecules next to each other in a chain-like structure.

### 4.1.5 Conclusions

The formation and characterization of the channel structure solid inclusion compound formed between guest styrene and host γ-CD have been described. Two styrene guests reside in each host γ-CD. Molecular modeling has confirmed the observed 2: 1 styrene:γ-CD stoichiometry and has further suggested that the guest styrenes are arranged in a parallel and overlapped configuration at a separation distance of ~4.1Å, the distance at which no π-π interactions can be observed. This was confirmed by observation of the UV-Vis spectra of styrene in methanol and in the styrene/γ-CD-IC. TGA and DIP-MS observations demonstrate a remarkable affinity of guest styrenes to remain in the host γ-CD channels at high temperatures, even at ~300° C where the γ-CD host lattice begins to decompose. In addition, the γ-CD decomposition products observed in the degradation of the styrene/γ-CD-IC are different from those seen when pure γ-CD is thermaly degraded. This observation also affirms the strong affinity/interaction between guest styrene and host γ-CDs in the channel structure inclusion complex.

## 4.2 Crystalline Cyclodextrin Inclusion Compounds Formed with Aromatic Guests: Guest-Dependent Stoichiometries and Hydration-Sensitive Crystal Structures

### 4.2.1 Summary

A series of solid inclusion complexes (ICs) containing the aromatic guests aniline, benzene, ethylbenzene, phenol, *p*-xylene, styrene, and toluene have been formed with host γ-cyclodextrin (γ-CD). IC stoichiometry was observed to depend on the nature of the included aromatic guest. The molar ratio of styrene, aniline, and phenol guests to γ-CD host was ~ 2:1 in their individual IC crystals, whereas ethylbenzene, *p*-xylene, and toluene guests formed ~ 1:1 inclusion complexes with γ-CD. TGA analysis showed that the thermal stabilities of these volatile aromatic guest molecules increased due to guest-host interactions once they were included in their γ-CD ICs. X-ray diffraction (WAXD) observations performed on the aromatic guest/CD IC crystals showed that all of them have channel-type crystalline structures. Moreover, it was observed that the presence of guest molecules inside the γ-CD cavities stabilized the channel structure of stacked γ-CDs. However, a solid phase transition from tetragonal to hexagonal packing of γ-CD stacks was observed upon dehydration of the styrene/, toluene/, *p*-xylene/, benzene/, and ethylbenzene/γ-CD IC crystals. We have also discovered that the solid state transformation between tetragonal and hexagonal channel crystal structures is reversible upon the desorption or sorption of water. In the cases of aniline/ and phenol/γ-CD ICs, no solid

phase transition from tetragonal packing to hexagonal packing was observed upon dehydration. Instead, the tetragonal packing structure was stable even after vacuum drying at elevated temperatures for an extended period. The stability of the tetragonal packing in aniline/ and phenol/γ-CD ICs was attributed to the presence of hydrogen-bonding between the included guests and neighboring host γ-CD molecules.

### 4.2.2 Introduction

Soluble inclusion complexes of aromatic molecules, i.e., styrene[8], aniline[34], phenol[35], and their derivatives[36] with CDs have been reported in the literature. There it was found that the inclusion of substituted benzene derivatives in the CD cavities depends on a variety of factors, including their sizes, shapes, substitution positions (*ortho, meta* or *para*), ionic strengths, etc.[35-36] In this study, we have formed and studied a series of solid γ-CD inclusion complexes containing the aromatic compounds aniline, benzene, ethylbenzene, phenol, *p*-xylene, styrene, and toluene as guests. These solid inclusion compounds (ICs) were obtained by mixing the guest molecules with an aqueous γ-CD solution, and the resulting crystalline precipitate of aromatic guest/γ-CD IC crystals were recovered by filtration. Here, we summarize the characteristics of the ICs that we formed.

### 4.2.3 Experimental

#### 4.2.3.1 Materials

Cyclodextrins (α and γ) were purchased from Cerestar (Hammond, IN). Styrene (99.9%, Aldrich) and acrylonitrile (99.9%, Aldrich) were vacuum distilled

prior to use. All the other chemicals: benzene (Aldrich, 99.8%), toluene (Aldrich, 99.8%), ethylbenzene (Aldrich, 99.8%), aniline (Aldrich, 99.5%), *p*-xylene (Aldrich, 99.0%), phenol (Fluka, ~90% w/w liquid), pyrrole (Aldrich, 98 %) and methyl methacrylate (Aldrich, 99 %) were used without further purification. The water used in this study was deionized (DI-$H_2O$).

#### 4.2.3.2 Formation of Channel-type Crystalline γ-Cyclodextrin (γ-$CD_{channel}$)

γ-CD can exist in two classes of crystal structures called "cage" and "channel".[37] In the cage structure (Figure 1c), the γ-CD molecules have a "herring-bone" arrangement, where each γ-CD cavity is blocked by neighboring γ-CDs. In the channel packing crystal structure (Figure 1d), the γ-CD molecules are stacked on top of each other to form long cylindrical channels in which guest molecules can reside. For γ-CD, a cage-type complex has only been obtained with water as the guest[38], ie., pure γ-CD, whereas for other guest molecules, ie., small molecules[38,39] or macromolecules[40], the channel-type structure is formed. It was reported that the orientation of γ-CD channels is head-to-head:tail-to-head:tail-to-tail[38], resulting in a 3-molecule repeating unit in each γ-CD stack (Figure 1d).

The as-received γ-CD has a cage-type crystalline structure. We successfully obtained a channel-type packing of crystalline γ-CD (γ-$CD_{channel}$), with only water molecules included in their narrow channel cavities, by appropriate recrystallization from its aqueous solutions. The details of the preparation of γ-$CD_{channel}$ were described in our previous study[41]. To summarize, 2 grams of as-received γ-CD was dissolved in 10 ml of DI-$H_2O$ at 40$^o$ C, precipitated into 50 ml of acetone, filtered, and dried in air overnight. The channel-type crystalline structure of the sample was

confirmed by wide-angle X-ray diffractometry (WAXD), as discussed later (Figure 13b).

#### 4.2.3.3 Formation of Solid Aromatic Guest/γ-Cyclodextrin Inclusion Compounds

The solid inclusion compounds (ICs) were prepared by mixing the guest molecules with an unsaturated γ-CD aqueous solution. Precipitation occurred as the guest molecules were included in the host γ-CD molecules and then aggregated and crystallized. The as-received γ-CD has a cage-type crystalline structure and the resulting solid inclusion compounds were found to have a channel-type crystalline structure, indicating that the inclusion complexation of the guest molecules with the γ-CD molecules was successful.

6.5 grams (0.005 mol) of as-received γ-$CD_{cage}$ were dissolved in 100 ml of deionized water at room temperature (RT). 0.0125 mol of guest molecules (aniline, benzene, ethylbenzene, phenol, p-xylene, styrene, or toluene were added drop-wise to the aqueous solution of γ-CD, while the solution was stirred and kept at RT. The initially clear γ-CD solution became turbid and a white precipitate formed immediately after addition of the guest molecules, which indicated the IC formation. The resulting white suspension was stirred for an additional 24 hrs at RT, filtered, and the collected precipitate was dried in the laboratory hood for 24 hrs. The channel packing structure of the IC crystals was confirmed by X-ray study, as shown later (Figure 15a).

### 4.2.4 Characterization

#### 4.2.4.1 Wide-Angle X-ray Diffraction

Wide-angle X-ray diffraction (WAXD) measurements were performed with a Siemens type-F X-ray diffractometer using a Ni-filtered $CuK_\alpha$ radiation source ($\lambda$ = 1.54 Å). The diffraction intensities were measured every 0.1° from $2\theta$ = 5 to 30° at a rate of $2\theta$ = 3°/minute. The supplied voltage and current were 30 kV and 20 mA, respectively.

Time-dependent WAXD experiments were designed to track the phase transformation of $\gamma$-$CD_{channel}$ from tetragonal to hexagonal packing that was observed upon dehydration/hydration of the ICs. Previously vacuum-dried samples were placed in a 100% humidity chamber for different times during the experiment and placed in the diffractometer to collect diffractograms as a function of hydration time. Characteristic peaks for the hydrated tetragonal and dehydrated hexagonal 200 planes are observed at $2\theta$ = 7.5 and 6.0°, respectively.[39] To minimize the time spent outside of the humidity chamber, diffractograms for the sample were only collected from $2\theta$ = 5 – 30°, which includes the aforementioned characteristic reflections. The time spent outside of the humidity chamber was approximately 10 minutes for each x-ray scan.

#### 4.2.4.2 Fourier Transform Infrared Spectroscopy (FT-IR)

A Nicolet 510P FT IR spectrometer was utilized to obtain the infrared spectra of samples mixed with potassium bromide (KBr) and pressed into pellets. The spectra were collected over a range of 4000 to 400 $cm^{-1}$, with a resolution of 2 $cm^{-1}$ obtained after 64 scans.

#### 4.2.4.3 Differential Scanning Calorimetry (DSC)

Experiments were performed with a Perkin-Elmer DSC-7 under nitrogen purge gas. Indium was used as a standard for calibration. The samples were subjected to heating and cooling cycles, consisting of a 1.0 minute hold at the starting temperature and ramping to the target temperature at a rate of $20^0$ C/min, and quenching at a cooling rate of 200° C/min.

#### 4.2.4.4 $^1$H-Nuclear Magnetic Resonance (NMR)

$^1$H-NMR experiments were performed on a Bruker Avance 500 MHz Spectrometer. One dimensional $^1$H data sets contained 16 K data points and sufficient scans were collected to obtain good S/N. The inclusion compounds were dissolved in DMSO-$d_6$, and tetramethylsilane (TMS) was used as the internal standard. The molar ratio of guest to cyclodextrin molecules were calculated by integrating the respective characteristic $^1$H resonance peaks observed for each.

#### 4.2.4.5 Thermogravimetric Analysis

Thermogravimetric analyses (TGA) of the samples were performed with a Perkin-Elmer Pyris 1 thermogravimetric analyzer. Thermal decompositions were recorded between 25 and 500° C. The heating rate was 20° C/min and nitrogen was used as a purge gas.

#### 4.2.4.6 Water Vapor Sorption Isotherms

A custom-built gravimetric balance[42,43] was used to measure the sorption of water vapor in styrene/γ-CD IC. Samples weighing approximately 0.3 g were first dried in a vacuum oven at 40° C and then vacuum-dried in the balance chamber at

40° C to remove any water adsorbed after removal from the vacuum oven. The samples were then tested at 40° C with water activities ranging from 0.1 – 1.0. Using flow meters for regulation, dry nitrogen gas was mixed with nitrogen gas bubbled through a water-containing reservoir to achieve the desired water activity, a, [a = (partial pressure of water vapor)/(saturation pressure of water vapor)]. The humid gas was then passed through the sample chamber at a constant flow rate. Samples were allowed to sorb water until the equilibrium weight gain was achieved at each water activity. After reaching a constant weight, the water activity was increased by approximately 0.15 and equilibrium was re-established. This was repeated up to the saturation concentration of water vapor in the nitrogen gas. A desorption isotherm was also collected by decreasing the water activity in increments of –0.15, down to a water activity of approximately 0.1. The results of these experiments are plotted as sorption/ desorption isotherms at 40° C.

A sorption kinetics experiment was also conducted to determine the time-dependence of the channel γ-CD phase transformation from the dehydrated hexagonal to the hydrated tetragonal structure. Approximately 0.15 g of styrene/γ-CD IC was placed in the gravimetric balance chamber at 25° C and a = 1.0, after vacuum-drying at 40° C, and water uptake was subsequently measured as a function of time.

### 4.2.5 Results and Discussion

#### 4.2.5.1 $^{1}$H-Nuclear Magnetic Resonance ($^{1}$H-NMR)

It is widely known that cyclodextrins are used for the separation of molecules, since they are very selective for the size of the guest molecules to be included in their

cavities.[44-45] Additionally, the type of cyclodextrin used (α-, β- or γ-CD) is also very important, since the diameter of the cavity gets wider as the number of glucose units is increased from six, to seven, or to eight. For instance, α-CD was found to be more selective in the inclusion of small guests due to tight binding of the guest molecules within the cavity compared to β- or γ-CD.[1] Larger guest molecules that do not fit into the α-CD cavity can form inclusion complexes with β- or γ-CD, due to their larger cavities, but those guests forming α-CD ICs may not necessarily be included in the larger CDs. In this study, we have also found that the formation of CD inclusion compounds and their guest to host stoichiometries are highly dependent on the molecular structures and the geometrical sizes of the guest molecules.

NMR is a powerful technique to determine the presence and molar ratio of guest molecules in CD ICs. The presence of guest molecules was confirmed by the $^1$H-NMR studies by dissolution of the IC crystals in DMSO-$d_6$. Though not presented here, we observed that the molar ratio of styrene, phenol, and aniline guests to host γ-CD was ~ 2:1 in their individual ICs. The finding of a 2:1 molar ratio of styrene to γ-CD in styrene/γ-CD-IC is consistent with our recent molecular modeling studies[20], which showed that the γ-CD/two styrene molecular complex is energetically favored compared to a γ-CD/one styrene molecular complex. Similar to styrene/γ-CD IC, aniline and phenol have the same molar ratio (2:1) in their γ-CD-ICs, also suggesting that the inclusion of two aniline or phenol molecules in one γ-CD molecule is more favorable than having only one guest molecule in each γ-CD cavity.

The molar ratios of toluene, p-xylene, and ethylbenzene to γ-CD in their ICs were found to be ~ 1.1:1, ~ 1.4:1 and ~ 1.3:1, respectively. In the case of the

benzene/γ-CD IC, the molar ratio of benzene to γ-CD was ~ 0.25:1, suggesting that the benzene molecule is too small to achieve a good fit in the γ-CD cavity. As another example, we failed to form an IC of methyl methacrylate, pyrrole, and acrylonitrile with γ-CD due to a size mismatch between guest and host molecules. On the other hand, we were able to form IC crystals of these guest molecules with α-CD. We also formed IC crystals of styrene with α-CD, and the molar ratio was found to be 1:1. Hence, it can be concluded that one styrene molecule is a good fit for α-CD and two styrene molecules are a good fit for γ-CD. To conclude, the formation of inclusion compounds of cyclodextrin with these small aromatic guest molecules is highly dependent on geometrical factors.

#### 4.2.5.2 Fourier Transform Infrared Spectroscopy

The presence of guest molecules in IC samples was confirmed by Fourier Transform Infrared spectroscopy (FT-IR). The FT-IR spectra of guest/γ-CD ICs are presented in Figure 11. The absorption bands at 1080, 1158 and 2927 $cm^{-1}$ correspond to the coupled C-C/C-O stretching vibrations, the antisymmetric stretching vibration of the C-O-C glycosidic bridge, and C-H vibration of γ-CD, respectively. Since the absorption bands of γ-CD cover the entire fingerprint region, it is not easy to identify all the absorption peaks belonging to the guest molecules in the infrared spectra of their γ-CD ICs. However, a closer look at the 1600-1500 $cm^{-1}$ spectral region, where the aromatic C–C ring stretching vibrations are expected to be observed, enable us to confirm the presence of guest molecules in the γ-CD ICs. Figure 11 shows the absorption peaks observed at 1604 and 1500 $cm^{-1}$ for the

aniline and phenol ICs as well as the absorption peak near 1495 $cm^{-1}$ for ethylbenzene, p-xylene, styrene, and toluene γ-CD ICs. No distinct absorption peak was observed for the benzene/γ-CD IC sample in the 1600-1500 $cm^{-1}$ region, which indicates that the amount of benzene is very small in the inclusion compound. This is consistent with NMR results, where the molar ratio of benzene:CD was found to be 0.25:1.

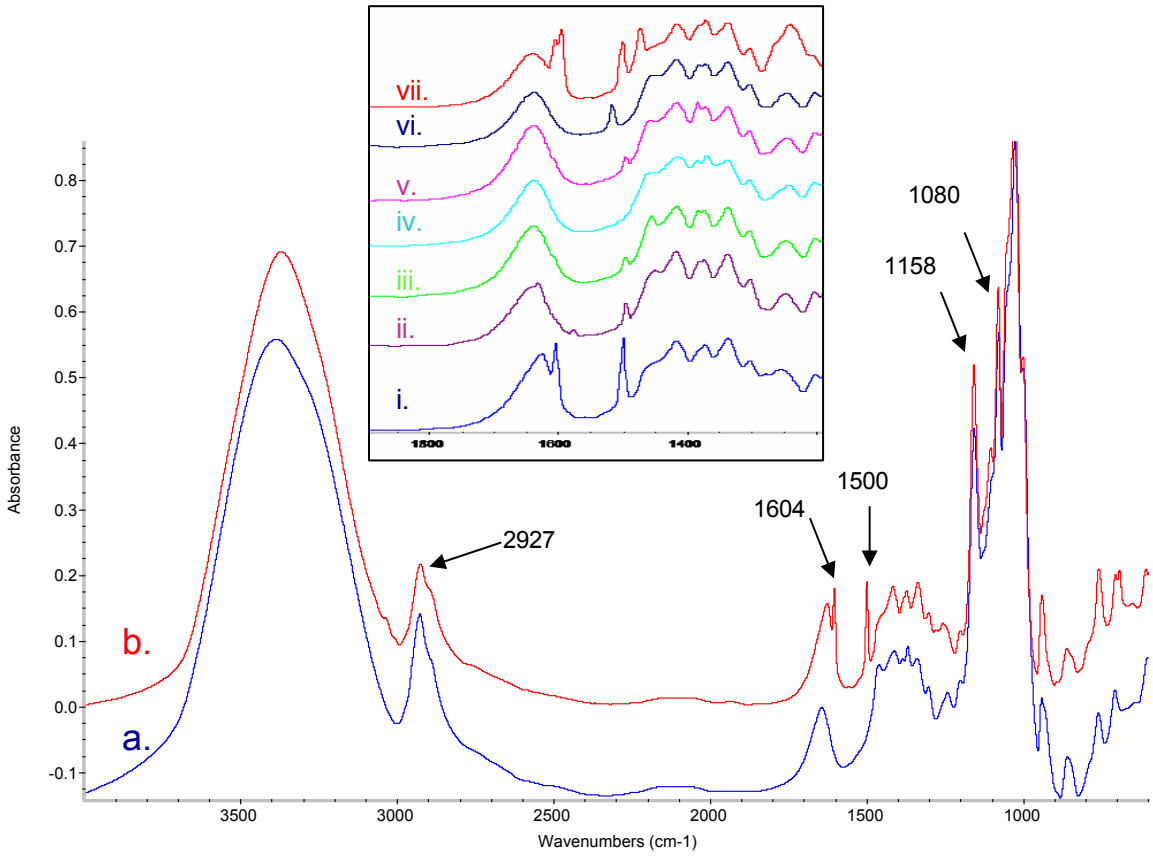


**Figure 11.** FT-IR spectra of a.) as received γ-CD and b.) aniline/γ-CD IC. The insert window shows the overlay of the expanded region (1800 - 1300 $cm^{-1}$) for i.) aniline/, ii.) styrene/, iii.) ethylbenzene/, iv.) benzene/, v.) toluene/, vi.) p-xylene/, and vii.) phenol/γ-CD ICs.

It is known that guest molecules having -$NH_2$ or -OH groups can form intermolecular hydrogen-bonds with the -OH groups of cyclodextrins. For example, circular dichroism studies have shown that aniline, phenol, and their derivatives form hydrogen-bonds with cyclodextrin in their common solutions once they are included in the CD cavities.[35] In the present case, it is possible that intermolecular H-bonding between guest and CD molecules in aniline/γ-CD IC and phenol/γ-CD IC crystals occurs. However, we were unable to isolate and identify vibrational peaks that could be attributed to hydrogen-bonding in any of the spectra, since the 3000 - 3600 $cm^{-1}$ region is dominated by the intense -OH absorptions of the host γ-CDs.

#### 4.2.5.3 Differential Scanning Calorimetry

Differential Scanning Calorimetry (DSC) is a useful tool for determining whether or not guest molecules are included inside the CD cavities. Thermal transitions, i.e., melting points ($T_m$) for guests, would be observed if there are any uncomplexed guest molecules present in the CD ICs. No guest melting peaks were observed in the DSC scans (data not shown) for any of the guest/γ-CD IC samples, suggesting that all the guest molecules were included inside the γ-CD channels.

#### 4.2.5.4 Thermogravimetric Analyses

TGA thermograms of pure γ-CD and the aromatic guest/γ-CD ICs are presented in Figure 12. Pure γ-CD evidenced two weight losses stages (Figure 12a): the one below 100° C was attributed to removal of water and the second, with a maximum above 300° C corresponding to the major weight loss, was associated with the main degradation of γ-CD.[24] In the case of complexation, the stability of

normally volatile guest molecules would increase due to guest-host interactions, which was the case for our guest/γ-CD ICs. In the TGA thermograms of guest/γ-CD ICs (Figure 12b-h), there was a continuous weight loss up to the main degradation of γ-CD, suggesting the presence of guest molecules at temperatures much higher than their boiling points. The presence and increased thermal stability of guest molecules at elevated temperatures is strong evidence of complexation with γ-CD. It is also noted that the percent weight loss for styrene/, aniline/ and phenol/γ-CD ICs was higher than the other ICs indicating the presence of a higher molar ratio of guest molecules in these ICs. This finding is consistent with the $^{1}$H NMR determined stoichiometries presented above.

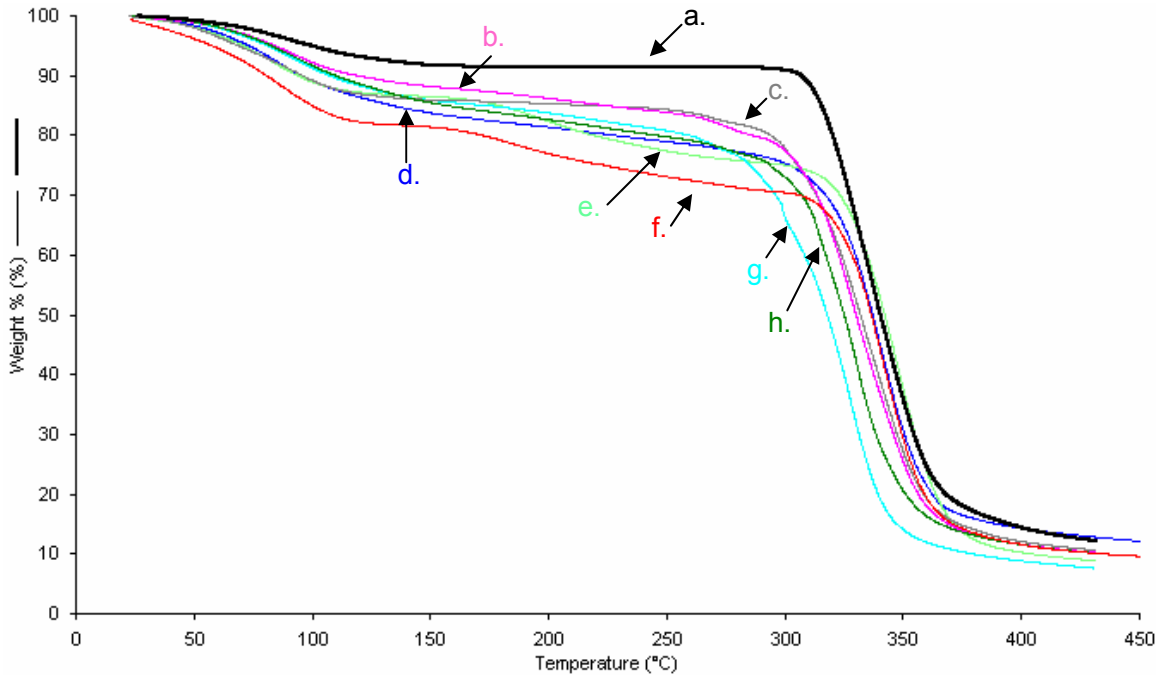


**Figure 12.** TGA thermograms of a.) as-received γ-CD and b.) toluene/, c.) benzene/, d.) styrene/, e.) aniline/, f.) phenol/, g.) ethylbenzene/, and h.) *p*-xylene/γ-CD ICs.

#### 4.2.5.5 X-ray Studies of Inclusion Compounds

WAXD is a useful characterization technique for investigating the crystalline phase transition between the cage structure of as-received γ-CD and the channel structure of guest/γ-CD ICs. Once the guest molecules are included in the γ-CD cavities it is expected that the resulting IC crystals adopt a channel-type structure. Figure 13 shows WAXD patterns for as-received γ-$CD_{cage}$ and γ-$CD_{channel}$ with only water included in the channels formed by our re-crystallization method.[15] As subsequently evident in Figure 15a, the styrene/γ-CD IC exhibits a diffraction pattern characteristic of γ-CD channel-type crystals reported in the literature.[39] The ICs of γ-CD formed with aniline, ethylbenzene, phenol, *p*-xylene, and toluene showed diffraction patterns similar to styrene/γ-CD IC, suggesting that all the ICs have channel-type packing regardless of the guest types. Therefore, the WAXD data represents strong evidence that γ-CD molecules form a channel structure with the inclusion of guest molecules residing in the γ-CD cavities.

In the case of benzene/γ-CD IC, the x-ray diffraction pattern (data not shown) exhibits peaks for both cage and channel packing indicating that the resulting IC crystals are a mixture of both cage and channel structures. The NMR data showed that there are four γ-CD molecules per benzene molecule, suggesting that ¾ of the γ-CD molecules are empty. Thus, it is not a surprise to have a mixture of cage and channel structures for this sample, since the γ-CD molecules hosting benzene would result in channel-type packing, whereas the empty γ-CD molecules would pack in cage-type crystals.

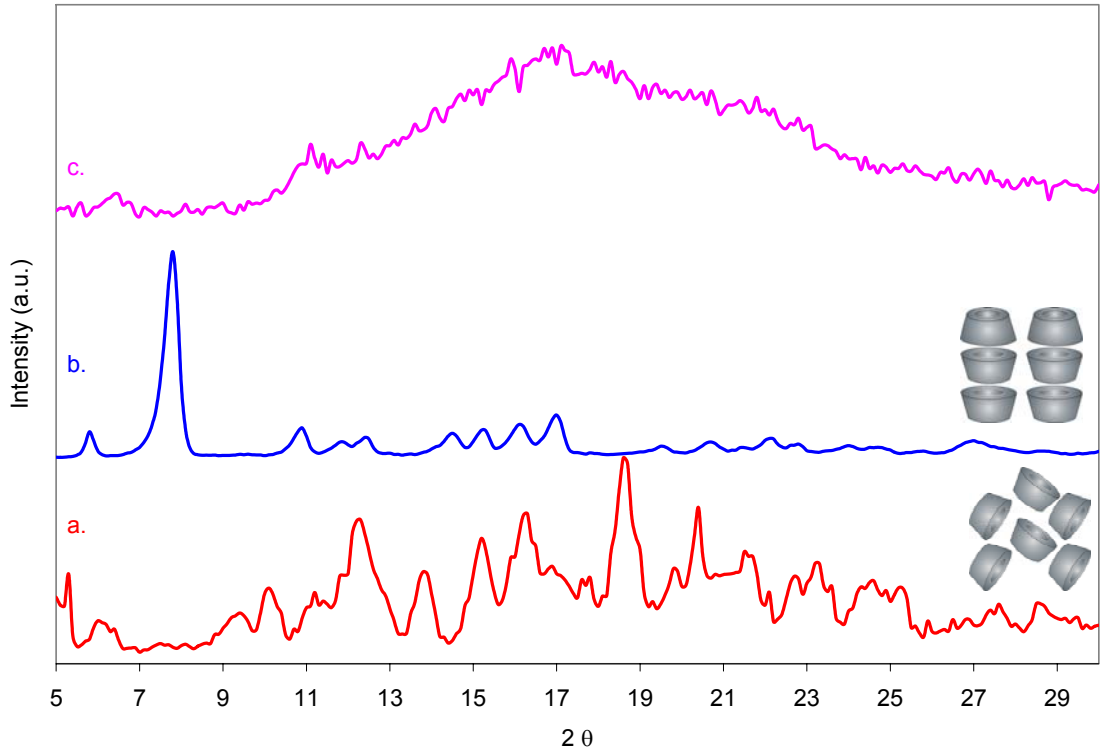


**Figure 13.** X-ray diffraction patterns of a.) γ-$CD_{cage}$, b.) γ-$CD_{channel}$, and c.) γ-$CD_{channel}$ vacuum dried for 24 hrs at $40^0$ C.

We have also formed a solid inclusion complex of styrene with α-CD (1:1 molar ratio). It is known that, unlike γ-CD, α-CD can crystallize with cage-type packing upon inclusion of small molecule guests.[38] For instance, the acrylonitrile/α-CD IC (1:1 molar ratio) that we have formed in this study has cage-type packing; conversely, styrene/α-CD IC crystals exhibit channel-type packing by WAXD. Figure 14 shows the x-ray diffraction patterns of as-received α-$CD_{cage}$ and styrene/α-$CD_{channel}$ IC. The characteristics of the diffraction patterns observed here for cage and channel structure are consistent with our earlier reports.[41,42] The as-received α-CD has three salient characteristic peaks associated with its cage-type crystal

structure occurring at 2θ = 12.0, 14.4, and 21.7° (Figure 14a). The styrene/α-CD IC has two salient peaks centered at 2θ = 12.9 (110 plane) and 19.3° (120 plane) associated with the channel-type packing structure (Figure 14b). To conclude, styrene forms solid inclusion complexes with α-CD and γ-CD, and both have a channel-type structure, containing one and two styrene guests, respectively, in each host CD cavity.

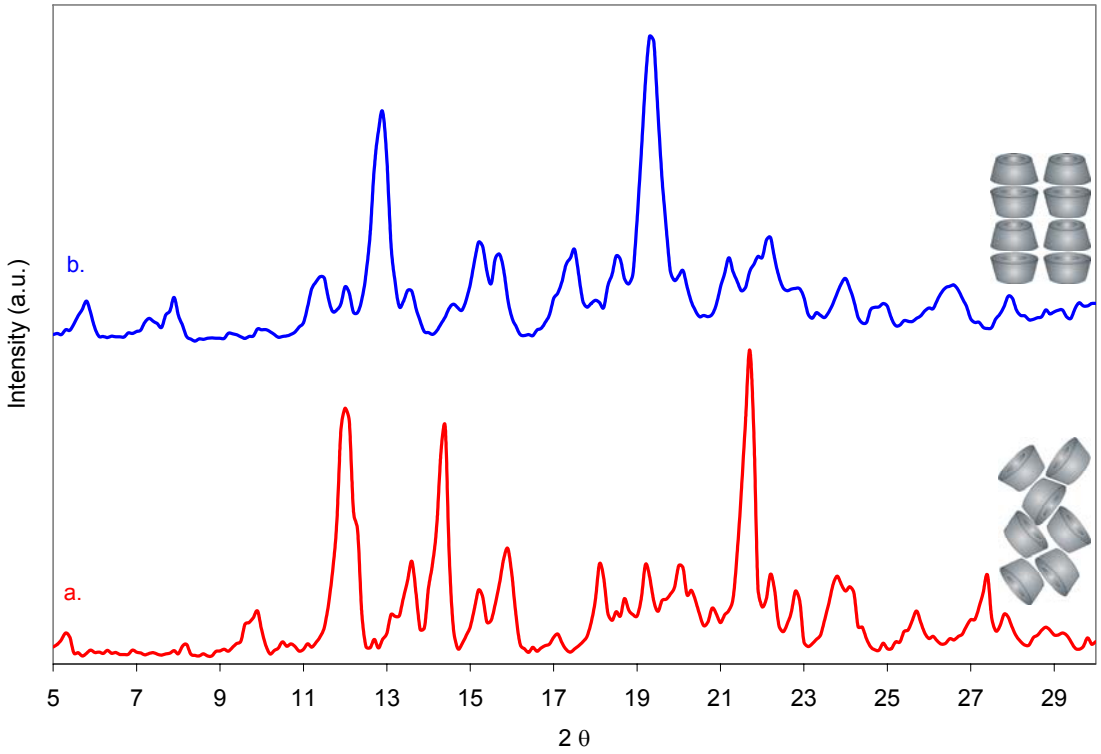


**Figure 14.** X-ray diffraction patterns of a.) α-$CD_{cage}$, b.) styrene/α-$CD_{channel}$ IC.

The crystallographic characteristics of channel γ-CD containing no guest except water of hydration (γ-$CD_{channel}$) and styrene/γ-CD IC crystals are summarized in Table 3. The calculated d-spacings from the two-dimensional tetragonal unit cell with lattice parameters[39] a = b = 23.7 Å are in good agreement with observed values

as shown in Table 3. Though it was potentially possible that guest molecules can also be entrapped in the interstitial sites between the columns of γ-CD stacks, given the size of the aromatic guest molecules under study here, an expansion of the channel γ-CD crystal would be expected if they reside within these interstitial sites. Since observed d-spacings for γ-CD channel crystals containg only water of hydration and styrene/γ-CD IC are nearly identical, we conclude that these aromatic guest molecules do not occupy intersitial sites; rather, they are only included in the γ-CD channels.

**Table 3.** Crystallographic characteristics of γ-$CD_{channel}$ and styrene/γ-$CD_{channel}$ IC.

| | γ-$CD_{channel}$ | | Styrene/γ-$CD_{channel}$ IC | | |
|---|---|---|---|---|---|
| *hkl* | 2θ(obs) (deg) | d(obs) (Å) | 2θ(obs) (deg) | d(obs) (Å) | d(calc)[a] (Å) |
| 110 | 5.8 | 15.22 | 5.6 | 15.75 | 16.76 |
| 200 | 7.8 | 11.32 | 7.7 | 11.48 | 11.85 |
| 220 | 10.9 | 8.11 | 10.8 | 8.18 | 8.38 |
| 310 | 12.4 | 7.13 | 12.3 | 7.18 | 7.49 |
| 132 | 14.5 | 6.10 | 14.4 | 6.14 | 6.21 |
| 400 | 15.2 | 5.82 | 15.2 | 5.83 | 5.93 |
| 330 | 16.1 | 5.50 | 16.1 | 5.5 | 5.59 |
| 420 | 17.0 | 5.21 | 16.9 | 5.24 | 5.3 |
| 620 | 24.0 | 3.70 | 24 | 3.7 | 3.75 |

[a]Calculated assuming a tetragonal unit cell with a = b = 23.75 Å, c = 22.92 Å [39].

We have shown that[41,43] $\gamma$-$CD_{channel}$, with no guest molecules included in the channels other than water of hydration, is destabilized by the removal of water under vacuum at 40° C, resulting in an amorphous structure, as can be seen in Figure 13c. The relatively large interstitial sites between the $\gamma$-CD channel stacks is where a portion of the adsorbed water resides in the fully hydrated structure. When this interstitial, loosely bound water is removed, the channel structure is destabilized. This would suggest that water residing in interstitial sites between $\gamma$-CD stacks stabilizes the structure through primary $\gamma$-CD--water and possibly secondary $\gamma$-CD--water--water--$\gamma$-CD hydrogen bonds. On the other hand, the $\gamma$-CD channel structure is stable upon vacuum drying and does not transform to the amorphous state when guest molecules occupy the channels. The diffraction pattern of styrene/$\gamma$-CD IC after vacuum drying at 40° C for 24 hours is shown in Figure 15b. The diffraction pattern indicates that the crystal structure of the sample is different after vacuum drying, but it is not amorphous. The diffraction pattern observed for vacuum-dried styrene/$\gamma$-CD IC is the same as the pattern for the channel structure with hexagonal packing reported by Takeo and Kuge.[39] The crystallographic characteristics of hexagonally packed styrene/$\gamma$-CD IC crystals are summarized in Table 4. The d-spacings calculated from the two-dimensional hexagonal unit cell having a = b = 32.7 Å [39] are in good agreement with the values observed in Table 3 for styrene/$\gamma$-CD IC vacuum dried for 24 hrs at $40^0$ C.

**Table 4.** Crystallographic characteristics of hexagonal styrene/γ-$CD_{channel}$ IC crystal structure.

| styrene/γ-CD IC (vacuum dried, anhydrous) | | | |
|---|---|---|---|
| *hkl* | 2θ(observed) (deg) | d(observed) (Å) | d(calculated)[a] (Å) |
| 200 | 6.0 | 14.70 | 14.16 |
| 220 | 10.9 | 8.11 | 8.18 |
| 420 | 16.4 | 5.40 | 5.35 |
| 620 | 22.1 | 4.02 | 3.93 |

[a]Calculated assuming a hexagonal unit cell with a = b = 32.7 Å [39].

The tetragonal channel packing transforms to hexagonal packing upon removal of water residing in the interstitial sites between γ-CD stacks, which results in a more closely packed structure. It is also worth mentioning that the presence of guest molecules inside the γ-CD stacks facilitates the stabilization of the channel structure, which undergoes a solid-solid phase transition from tetragonal packing to hexagonal packing upon dehydration, and not to an amorphous structure, which is the case for γ-$CD_{channel}$ with no guest molecules included other than water.

It is also of interest to note that the solid state transition of tetragonal to hexagonal packing is reversible. Figure 15c shows the diffraction pattern of vacuum dried styrene/γ-CD IC which was stored at 100 % humidity and room temperature for 51 hours. The diffraction pattern is the same as before the vacuum drying, indicating that the transformation of hexagonal packing to tetragonal packing occurs upon hydration of the previously vacuum dried styrene/γ-CD IC crystals.

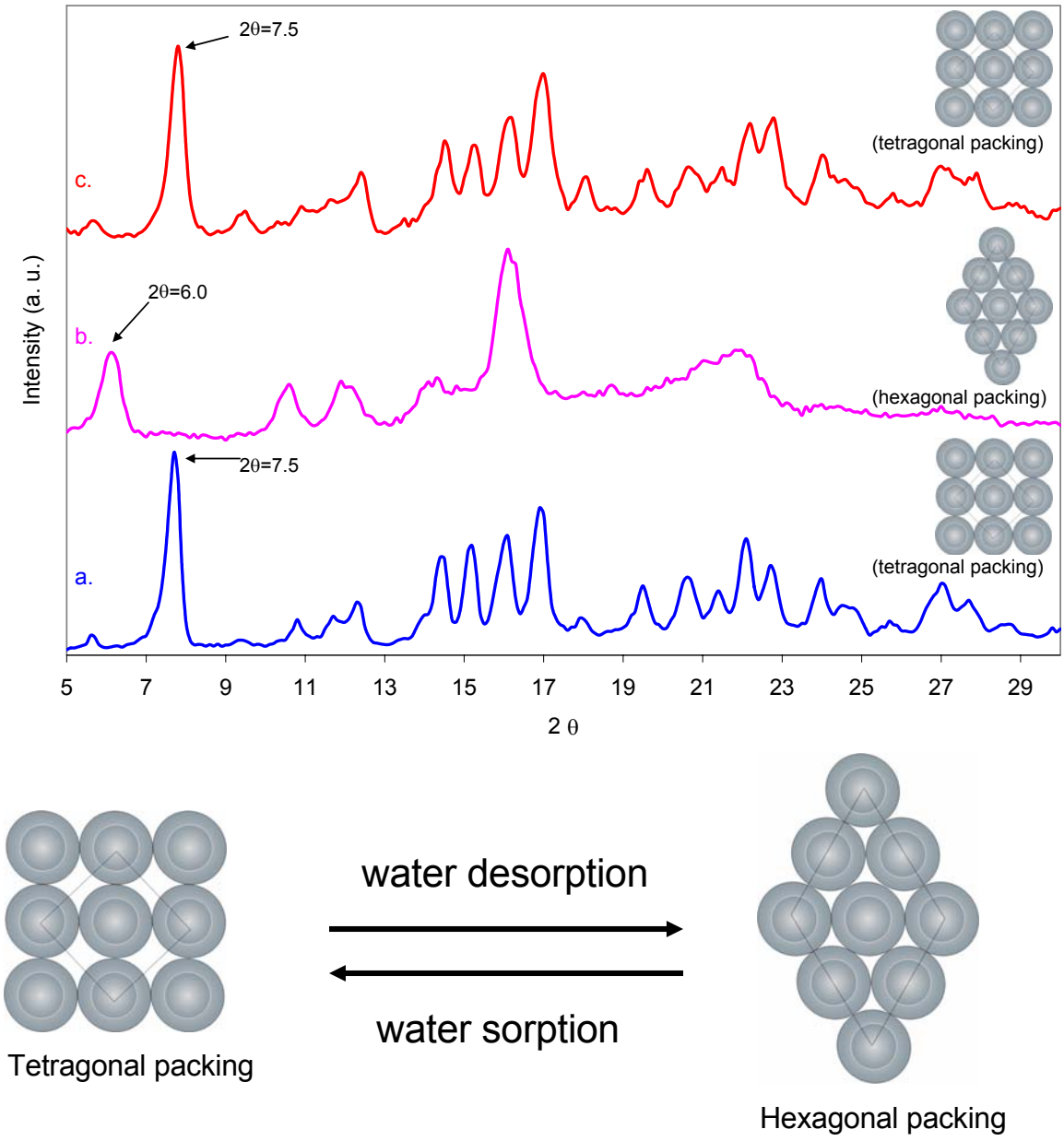


**Figure 15.** X-ray diffraction patterns of a.) styrene/γ-CD IC, b.) styrene/γ-CD IC vacuum dried for 24 hrs at 40 $^{0}$C and c.) vacuum dried styrene/γ-CD IC stored at 100% humidity for 51 hours.

Time-dependent WAXD experiments were performed to track the phase transformation of hexagonal to tetragonal structure by hydration of previously vacuum dried styrene/γ-CD IC. The WAXD patterns collected for anhydrous

styrene/γ-CD IC (vacuum dried) as a function of time subsequently stored at 100 % humidity and room temperature are presented in Figure 16. It is clear that the (200) plane at 2θ = 7.5°, which is characteristic for tetragonal packing, gradually increases as the 2θ = 6.0° peak, which is characteristic for hexagonal packing, exhibits a gradual reduction in intensity over time. The peak at 2θ = 6.0° disappeared after 12 hours suggesting that the transformation from hexagonal to tetragonal packing is essentially complete after 12 hours of hydration.

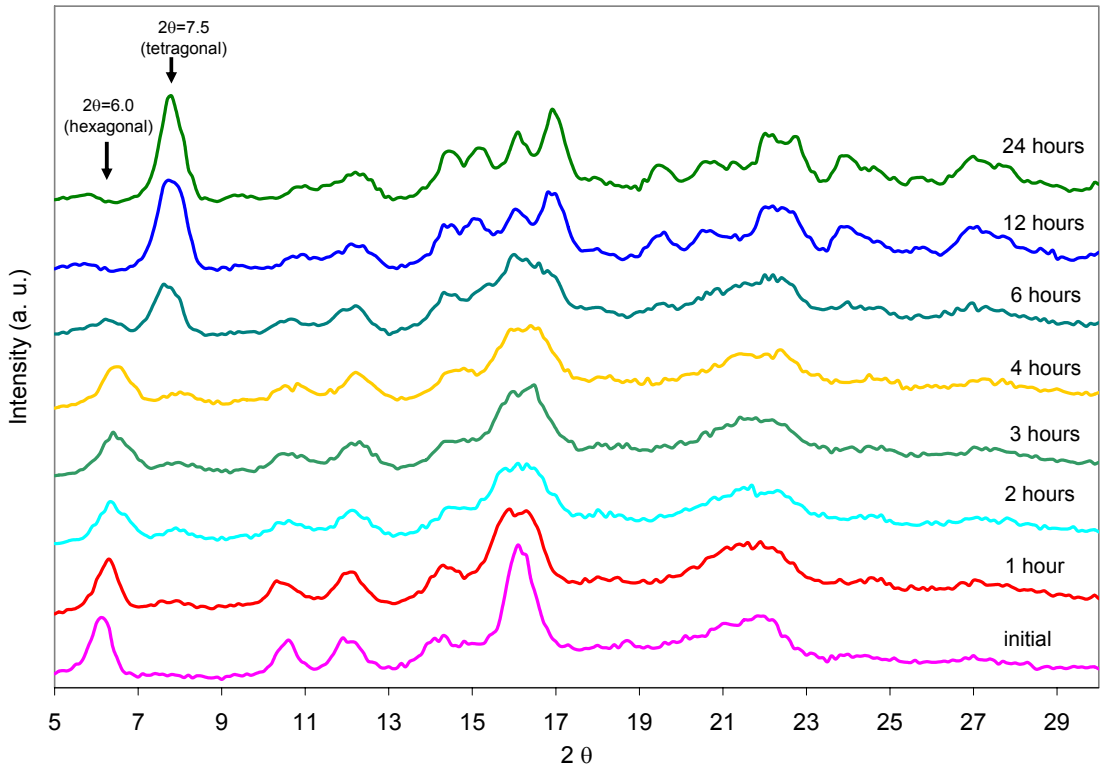


**Figure 16.** Time-dependent X-ray diffraction patterns of vacuum dried styrene/γ-CD IC subsequently stored at 100% humidity.

A sample of styrene/γ-CD IC crystals underwent multiple cycles of dehydration-hydration by repeatedly vacuum drying at 40° C and then storing at 100

% humidity and room temperature. The solid-state transformation from tetragonal to hexagonal structure and from hexagonal to tetragonal structure is clearly reversible upon water desorption and sorption, respectively. Figure 17 shows the peak intensity changes for 2θ = 7.5 and 6.0°. The increase in peak intensity at 2θ = 7.5° and the decrease at 2θ = 6.0° are used to follow the kinetics of the transition. The peak at 2θ = 6.0° disappeared after 12 hours of hydration for cycle 1 and after 6 hours of hydration for cycles 2 and 3. Similarly, the maximum peak area at 2θ = 7.5° was reached in the shortest time in cycle 3, and sooner in cycle 2 than cycle 1, indicating that the transformation from hexagonal to tetragonal packing takes place much faster after repeated desorption-sorption cycles.

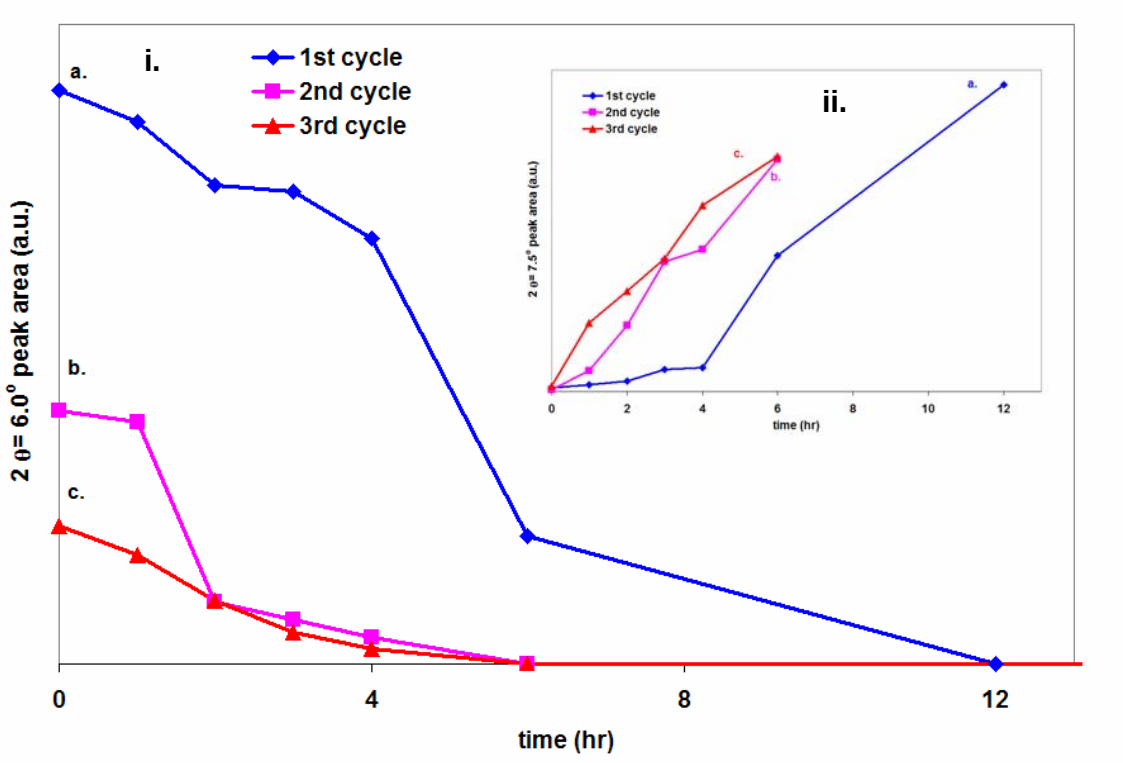


**Figure 17.** Time-dependent x-ray peak area changes for 1,2, and 3 dehydration-hydration cycles of styrene/γ-CD IC: (i) variation of the 2θ = 6.0° (hexagonal) and (ii) 7.5° peak (tetragonal) areas.

#### 4.2.5.6 Water Vapor Sorption-Desorption Studies

To further understand the water vapor-induced phase transformation from hexagonal to tetragonal structure, complementary water vapor sorption kinetics experiments were carried out under the same conditions as the aforementioned x-ray studies. Figure 18 shows the equilibrium sample weight upon desorption *via* vacuum drying at 40° C and resorption at 25° C and a = 1.0. There is a continual loss in weight after each desorption/sorption cycle. The difference in the hydrated and dehydrated weights as a function of cycle number also show a continual loss in weight, with a rate that is reduced between cycles 2 and 3. This suggests that a constant difference in anhydrous and hydrate weight would occur after a sufficient number of cycles.

The weight losses, shown in Figure 18 as a function of cycle number, are potentially a result of some loosely bound styrene in the γ-CD cavities. In the previous section, we observed that the styrene-based products from the thermal degradation of the styrene/γ-CD IC sample showed two maxima at low (~ $50^0$ C) and at high (~$230^0$ C) temperatures. This behavior was explained by supposing two different environments for styrene molecules in the complex. Styrene molecules having weaker interactions with γ-CDs in the host channels are released at lower temperatures than those with stronger interactions with the host γ-CDs. It was also noted that the quantity of styrene released at low temperature was found to be very small, suggesting that most of the guest molecules have high stability in the γ-CD channels due to strong guest-host interactions. This was also confirmed by solution $^1$H-NMR, where the styrene/γ-CD-IC that was vacuum-dried for 24 hours at $40^0$ C

lost only 10 weight % of the total styrene in the as-formed, undried, fully hydrated complex.

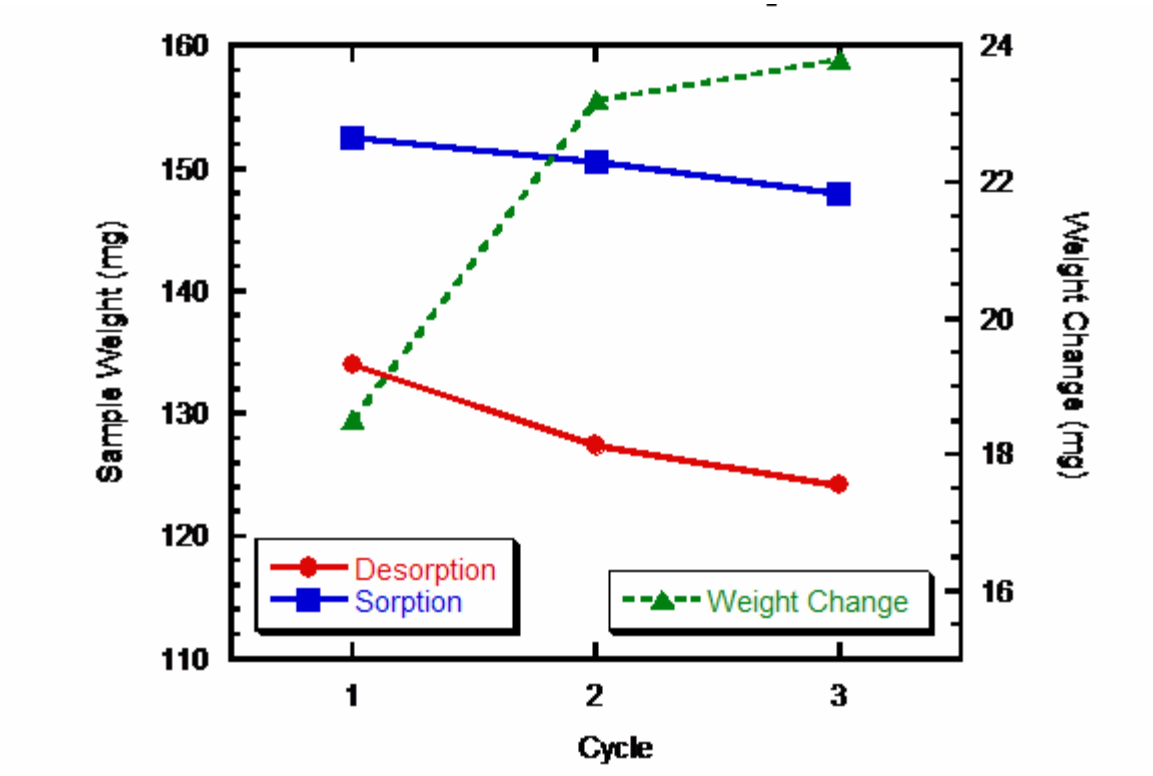


**Figure 18.** Equilibrium anhydrous weight after vacuum-drying at 40° C (●)and hydrated weight after sorption at 25° C and a = 1.0 (■) of styrene/γ-CD IC as a function of hydration cycle. The difference in anhydrous and dehydrate weights is also plotted (▲).

Interval water sorption of styrene/γ-CD IC (Figure 19) was also performed. A vacuum-dried sample was allowed to sorb water vapor at 40° C and at varying water activities. The shape of the sorption curve is similar to that of pure γ-CD in the cage structure. However, the sorption levels are slightly lower. Upon desorption, the equilibrium weight at approximately a = 0.1 is less than the initial weight. γ-CD typically exhibits similar equilibrium weight at low activities upon sorption and desorption.[43] This means that styrene was lost during either the sorption or

desorption stages of the experiment or possibly during both. This correlates with the weight loss seen in the interval sorption data of Figure 18.

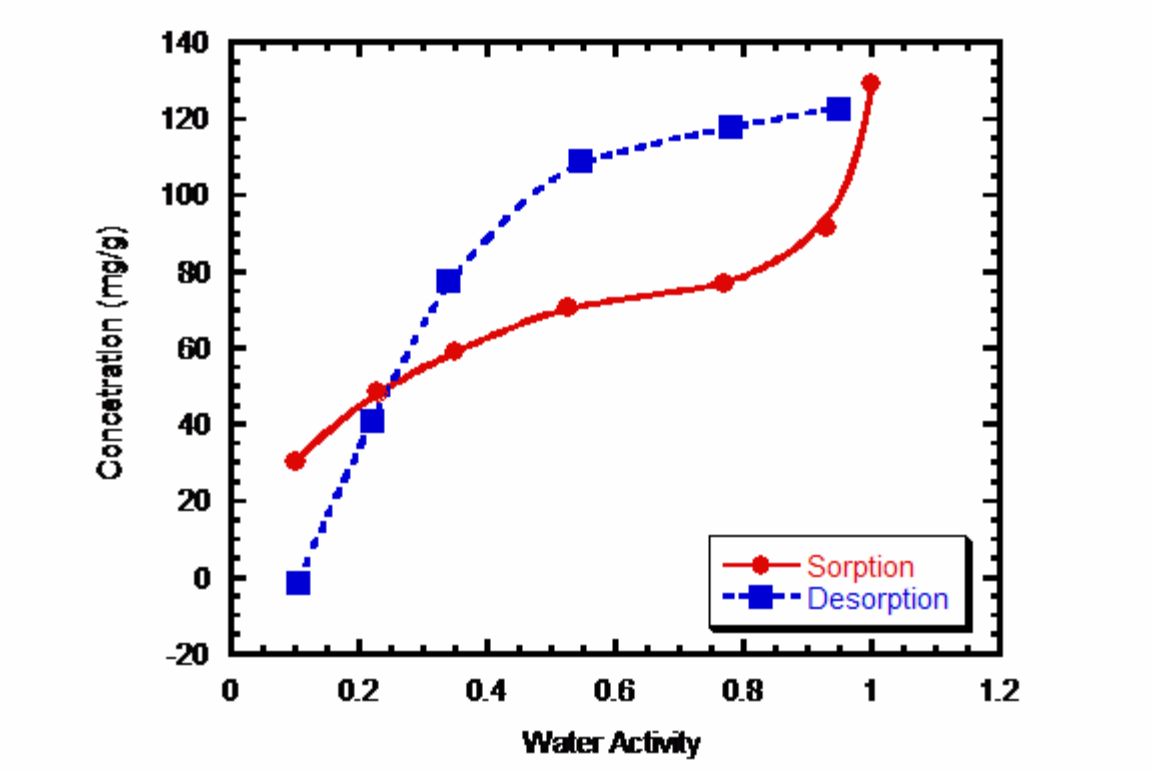


**Figure 19.** Interval sorption and desorption of styrene/γ-CD IC at 40° C.

Hexagonal packing was also observed for toluene/, *p*-xylene/, benzene, ethylbenzene/γ-CD IC crystals upon dehydration but not for aniline and phenol/γ-CD ICs. In the case of the aniline/γ-CD IC (Figure 20) and phenol/γ-CD IC (data not shown), the tetragonal packing structure was stable after vacuum drying at 40° C for 24 hours, and even after vacuum drying at 90° C for 24 hours. Phenol and aniline differ from the other aromatic guest molecules studied here because of their ability to form intermolecular hydrogen bonds with γ-CD molecules. It has been shown in solution[35,36] that the γ-CD cavity has a strong affinity for complexing with the phenyl ring due to strong hydrophobic interactions, while the hydroxyl in phenol or the

amine group in aniline hangs out of the γ-CD cavity. Therefore, hydrogen-bonding between the amine group in aniline (or the hydroxyl group in phenol) and a hydroxyl group in a neighboring γ-CD molecule is possible. Hydrogen-bonding of the included guest molecule with the neighboring γ-CD would connect γ-CD molecules along each γ-CD channel stack, thereby strengthening them and making the transformation from tetragonal to hexagonal packing unfavorable. We have also observed similar behavior for polymer/CD IC crystals.[20,40] Guest polymer chains included in the γ-CD channels make the γ-CD stacks rigid and prevent their rearrangement to hexagonal packing upon dehydration of the polymer/CD IC samples.

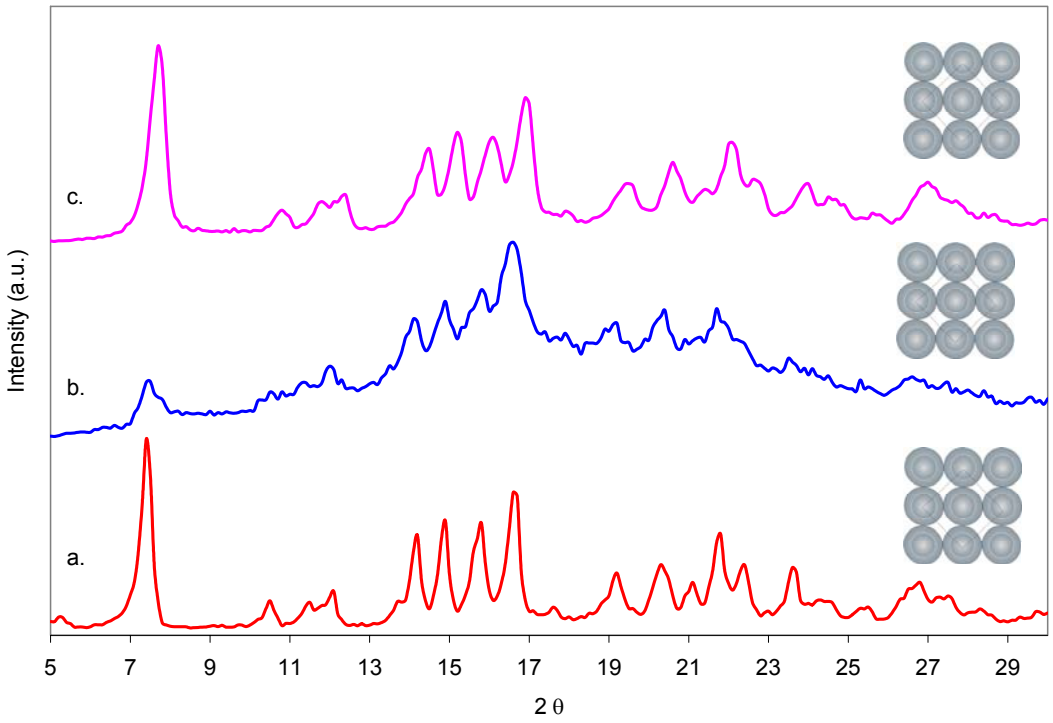


**Figure 20.** X-ray diffraction patterns of a.) aniline/γ-CD IC, b.) aniline/γ-CD IC vacuum dried for 24 hrs at $40^0$ C. and c.) vacuum dried aniline/γ-CD IC stored at 100% humidity for 24 hours.

### 4.2.6 Conclusions

The formation and characterization of channel structure solid inclusion compounds formed between the aromatic guests aniline, benzene, ethylbenzene, phenol, p-xylene, styrene, and toluene with host γ-CD have been described. $^{1}$H-NMR showed that both their inclusion complex formation and resulting complex stoichiometric ratios depend on the type of aromatic guest molecule included. It was found that the molar ratio of styrene, aniline and phenol to γ-CD was ~ 2:1 in their individual IC crystals, whereas ethylbenzene, p-xylene and toluene formed ~ 1:1 solid inclusion complexes with γ-CD. Thermal analysis showed that the thermal stability of these volatile guest molecules increased remarkably (much above their boiling points) once they were included in the γ-CD cavities, likely the result of guest-host interactions.

X-ray diffraction (WAXD) experiments confirmed that all the aromatic guest/γ-CD IC crystals have a channel-type crystalline structure. We observed that the presence of guest molecules inside the γ-CD cavity stabilized the channel packing of γ-CD stacks. However, a solid phase transition from tetragonal to hexagonal packing of the host γ-CD stacks occurred upon dehydration of the γ-CD IC crystals formed with toluene, p-xylene, benzene, and ethylbenzene guests. To our surprise, we found that the solid state transformation from tetragonal to hexagonal packing and from hexagonal to tetragonal packing was reversible, when the samples were subjected to cycles of water desorption and sorption, respectively.

For aniline/ and phenol/γ-CD ICs, the tetragonal packing structure is apparently more stable and no solid phase transition from tetragonal to hexagonal

packing was observed even after vacuum drying these samples at 90° C for 24 hours. Aniline and phenol differ from other guest molecules in their ability to form intermolecular hydrogen bonds with γ-CD molecules. The stability of their tetragonal packing might be due to the presence of hydrogen-bonding between the included guest molecules with neighboring γ-CD molecules in the same host γ-CD stack. That is, in the case of hydrogen-bonding of the included guest molecule with neighboring γ-CDs, γ-CD molecules would be connected along each channel, resulting in rigid γ-CD stacks, thereby preventing their transformation from tetragonal to hexagonal packing.

**References:**


1. Szejtli, J.; Osa, T. *Comp S Chem-V 3: Cyclodextrins* 1996, Elsevier, NY.
2. Liu, L.; Guo, Q.-X. *Journal of Inclusion Phenomena and Macrocyclic Chemistry* 2002, 42, 1-14.
3. Rekharsky, M.V.; Inoue, Y. *Chem. Rev.* 1998, 98, 1875-1917.
4. Rusa, M.; Wang, X.W.; Tonelli, A.E. *Macromolecules* 2004, 37 (18): 6898-6903.
5. Peet, J.; Rusa, C.C.; Hunt, M.A.; Tonelli, A.E.; Balik, C.M. *Macromolecules* 2005, 38 (2): 537-541.
6. Ohmura, M.; Kawahara, Y.; Okude, K.; Hasegawa, Y.; Hayashida, M.; Kurimoto, R.; Kawaguchi, A. *Polymer* 2004, 45(20): 6967-6975.
7. Uyar, T.; Rusa, M.; Tonelli, A. E. *Macromol. Rapid Commun.* 2004, *25*(15), 1382.

8. Storsberg, J.; van Aert, H.; van Roost, C.; Ritter, H. *Macromolecules* 2003, *36*(1), 50-53.
9. Storsberg, J.; Ritter, H. *Macromol. Rapid Commun.* 2000, *21*(5), 236-241.
10. Storsberg, J.; Ritter, H.; Pielartzik, H.; Groenendaal, L. *Advanced Materials* 2000, *12*(8), 567-569.
11. Takashima, Y.; Oizumi, Y.; Sakamoto, K.; Miyauchi, M.; Kamitori, S.; Harada, A. *Macromolecules* 2004, *37*, 3962-3964.
12. Velusamy, P.; Pitchumani, K.; Srinivasan, C. *Tetrahedron* 1996, *52*(10), 3487.
13. Uyar, T.; Hunt, M.A; Gracz H.S; Tonelli, A. E. *Langmuir* (in review).
14. Uyar, T.; Tonelli, A. E. (in preparation)
15. Hunt, M. A.; Jung, D. –W.; Shamsheer, M.; Uyar, T.; Tonelli, A. E. *Polymer* 2004, *45*(4), 1345-1347.
16. Wendlandt, W. W.; Hecht, H. G. *Reflectance Spectroscopy*, Interscience: New York, 1966, Chapter 3.
17. Stewart, J. J. P. *J. Comp. Chem.*1989, *10*, 221.
18. Zerner, M. C. *Review in Computational Chemistry,* (Lipkowitz, K. B.; Boyed, B. D. Volume 2, VCH, *333*, 348, (1991).
19. (a) Stewart, J. J. P. *Int. J. Quantum Chem*. 1999, *58*, 133. (b) CAChe Worksystem Pro Version 6.1.12.33, Fujitsu America Inc., Beaverton, OR 97006-5733.
20. Uyar, T.; Rusa, C. C.; Hunt, M. A.; Aslan, E.; Hacaloglu, J.; Tonelli, A. E. *Polymer* 2005 (46) 4762-4775.

21. Uyar, T.; Toppare, L.; Hacaloglu, J. *Macromol. Rapid. Commun.* 2001, *22*(3), 199-201.

22. Uyar, T.; Toppare, L.; Hacaloglu, J. *Journal of Analytical & Applied Pyrolysis* 2003, *68-69*, 15-24

23. Uyar, T.; Toppare, L.; Hacaloglu, J. *Journal of Macromolecular Science-Pure and Applied Chemistry* 2001, *38*(11), 1141-1150.

24. Uyar, T.; Aslan, E.; Tonelli, A. E.; Hacaloglu, J. *Polymer Degradation & Stability* 2006 (in press)

25. Breslow, R.; Dong, S. D. *Chem. Rev*. 1997, *98*, 1998.

26. (a) Lipkowitz, K. B. *Chem. Rev*. 1998, *98*, 1829. (b) Liu, L.; Guo, Q.-X. *J. Phys. Chem. B.* 1999, *103*, 3461. (c) Dodziuk, H.; Lukin, O.; Nowinski, K. S. *J. Mol. Struct.(Theochem)* 2000, 503.

27. Bonnet, P.; Jaime, C.; Morin-Alloy, L. *J. Org. Chem*. 2001, *66*: 689.

28. (a) Grabner, G.; Monti, S.; Mayer, B.; Koehler, G. *J. Phys. Chem*. 1996, 100. (b) Tanaka, H.; Kato, N.; Kawazura, H. *Bull. Chem. Soc. Jpn* 1997, *70*, 1255.

29. Kitagawa, M.; Hoshi, H.; Sakurai, M.; Inoue, Y.; Chujo, R. *Carbohydr. Res.* 1987, *283*.

30. Bosti, A.; Yannakopoulou, K.; Hadjoudis, E.; Waite, J. *Carbohydr. Res*. 1996, *283*, 1.

31. (a) Huang, M. J.; Watts, J. D.; Bodor, N. *Int. J. Quantum Chem*. 1997, *64*:711. (b) Huang, M. J.; Watts, J. D.; Bodor, *Int. J. Quantum Chem.* 1997, *65*, 1135.

32. Castro, R.; Berardi, M. J.; Cordova, E.; Deolza, M. O.; Kaifer, A. E.; Evanseck, J. D. *J. Am. Chem. Soc.* 1996, *118*: 10257.

33. Shiozaki, H.; Matsuoka, M. *J. Mol. Struc., Theoretical Chemistry* 1988, *427*.

34. Velusamy, P.; Pitchumani, K.; Srinivasan, C. *Tetrahedron* 1996, 52(10), 3487.

35. Kamiya, M.; Mitsuhashi, S.; Makino, M.; Yoshioka H. *J. Phys. Chem.* 1992, 96.

36. Bertrand, G.L.; Faulkner, J.R.; Han, S.M.; Armstrong, D.W. J. Phys. Chem. 1989, 93, 6863-6867.

37. Harata, K. *Crystallographic Studies, Vol. 3, Comprehensive Supramolecular Chemistry* 1996, Atwood, J.L.; Davies, J.E.; MacNicol, D.D.; Vogtle, F.; Lehn, J.M. Eds., Pergamon: Oxford.

38. Saenger, W.; Jacob, J.; Gessler, K.; Steiner, T.; Hoffmann, D.; Sanbe, H.; Koizumi, K.; Smith, S. M.; Takaha, T. *Chem. Rev.* 1998, *98,* 1787-1802.

39. Lind, T. K.; Kuge, T. *Agr. Biol. Chem.* 1970, *34*(4), 568-574.

40. Rusa, C. C.; Rusa, M.; Gomez, M.; Shin, I. D.; Fox, J. D.; Tonelli, A. E. *Macromolecules* 2004, *37*(21), 7992-7999.

41. Rusa, C. C.; Bullions, T.A.; Fox, J. D.; Porbeni, F.E.; Wang, X.W. Tonelli, A. E. *Langmuir* 2002, 18 (25): 10016-10023.

42. Hunt, M.A.; Rusa, C. C.; Tonelli, A. E.; Balik, C.M. *Carbohydrate Research* 2004, 339, 2805–2810.

43. Hunt, M.A.; Rusa, C. C.; Tonelli, A. E.; Balik, C.M. *Carbohydrate Research* 2005, 340 (9): 1631-1637.

44. Del Valle, E.M.M. *Process Biochemistry* 2004, 39 (9): 1033-1046.

45. Schneiderman, E.; Stalcup, A.M. J Chromatography B-Analytical Tech. in the Biomedical and Life Sci. 2000, 745 (1): 83-102.

# CHAPTER 5

## 5 Polymerization of Styrene in Cyclodextrin Channels: Can Confined Free Radical Polymerization Yield Stereoregular Polystyrene?

### 5.1 Summary

Modeling of polystyrenes (PS) with various stereosequences in the γ-Cyclodextrin (γ-CD) channels has been conducted and it was calculated that only isotactic PS stereoisomers can fit into the γ-CD cavity. Thus, based on the modeling of stereoisomeric polystyrenes (PSs) in narrow γ-CD channels, it was suggested that polystyrene with unusual microstructures might be produced *via* constrained polymerization of styrene monomer in its γ-CD-IC crystals. The *in situ* polymerization of styrene inside the narrow channels of its γ-CD-IC crystals was performed in aqueous media. Alternatively, the solid-state polymerization of styrene/γ-CD IC has also been carried out by radiation polymerization. It was found that most styrene monomer migrates from the γ-CD channels and polymerizes outside of the channels. Yet, a rotaxanated structure has been obtained where some γ-CD molecules entrapped along the PS chains after the polymerization. The $^{13}$C-NMR spectrum of PS synthesized in the presence of the γ-CD shows some differences when compared to the $^{13}$C-NMR spectrum of PS synthesized in toluene, which are presumably due to differences in their stereosequences.

## 5.2 Molecular Modeling of γ-CD/PS Complexation

Recently, we have conducted modeling of polystyrenes (PS) with various stereosequences in the narrow cylindrical channels corresponding to those found in γ-Cyclodextrin inclusion compounds (γ-CD ICs).[1] Isotactic PS, i-PS, is found to fit in channels with narrower diameters than syndiotactic PS, s-PS, while atactic PS, a-PS, can be included in channels with diameters intermediate to those for i-PS and s-PS. Here, we performed the molecular modeling of stereoisomeric polystyrenes in γ-CD channels. The calculations were performed in MOPAC using PM3 parameters with the MOZYME algorithm, implemented in CAChe WorkSystem 6.1.12.33. For a tetrade isotactic PS, all the distances between the carbon atoms attached to the phenyl ring and the carbons in the *p*-positions to the ethyl groups were locked. This was done to prevent the PS segment from relaxing into any other conformations other than *trans* conformation. It was calculated that isotactic PS segment (tetrade) can fit inside the γ-CD cavity. Figure 1a-b shows the equilibrium molecular geometry of i-PS tetrade and its inclusion inside the γ-CD channel. On the other hand, molecular modeling studies of syndiotactic (Figure 1c) and atactic PS showed that they don't fit spatially inside the γ-CD cavity. The molecular axes of atactic and syndiotactic PS were found to be wider than the interior diameter of γ-CD and it is not possible for syndiotactic or atactic to get inside the γ-CD cavity. Figure 1d shows a representation of the collision between the hydrogen atoms of a syndiotactic PS and the hydrogen of the γ-CD channel structure. Thus, based on the modeling of stereoisomeric polystyrenes (PSs) in narrow γ-CD channels, it was suggested that

polystyrene with unusual microstructures might be produced *via* constrained polymerization of styrene monomer in its γ-CD-IC crystals.

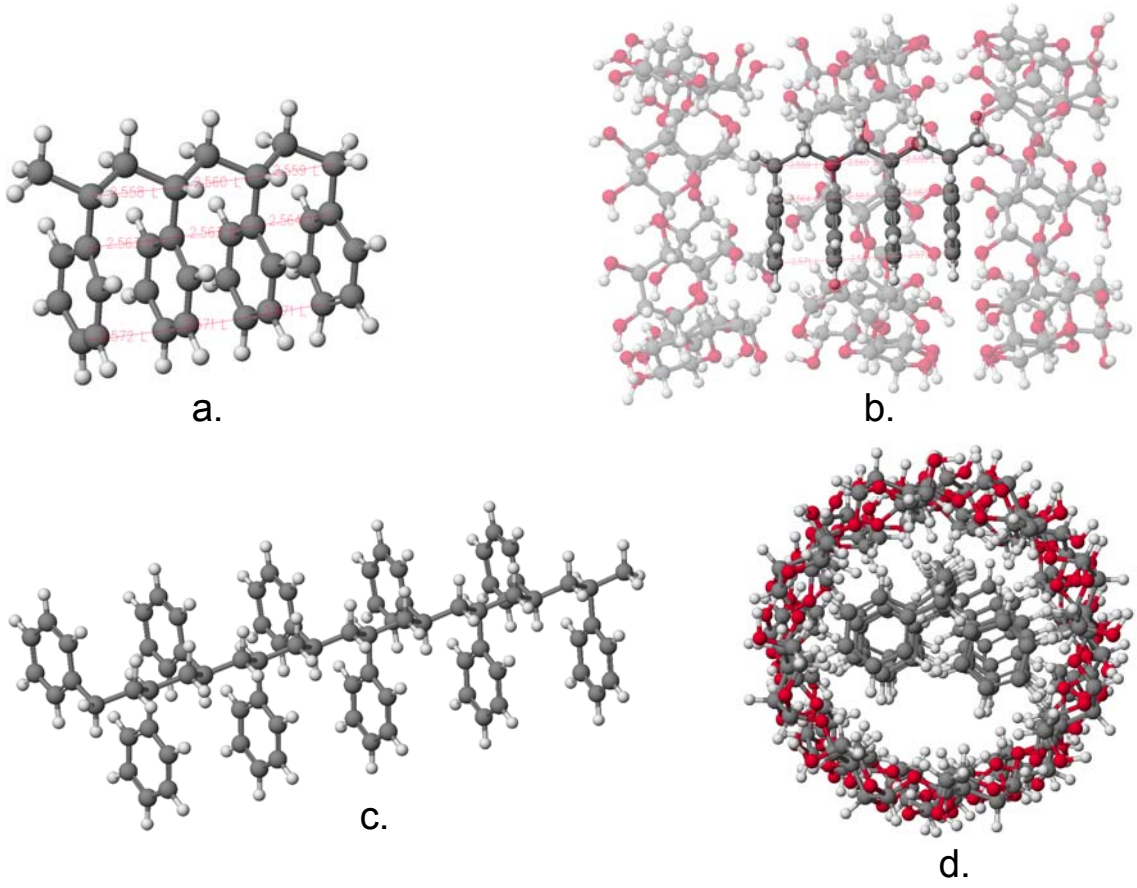


**Figure 1**. (a) Molecular geometry of a tetrade isotactic PS. (b) isotactic-PS-γ-CD inclusion compound. (c) Molecular geometry of syndiotactic PS. (d) Representation of the collision between the hydrogen atoms of syndiotactic and γ-CD.

## 5.3 Experimental

### 5.3.1 Formation of Styrene/Cyclodextrin Inclusion Compounds

The formation of styrene/γ-$CD_{channel}$-ICs can be achieved by both "suspension method" and "precipitation method" as described earlier (see section 4.1.3.2). In case

of “suspension method”, we have found that only the preformed γ-$CD_{channel}$ crystals form styrene/γ-$CD_{channel}$-ICs when suspended into bulk styrene. We have monitored the inclusion complexation of styrene with CDs by $^1$H-nuclear magnetic resonance spectroscopy ($^1$H-NMR). The kinetic study was performed by suspending as-received CDs (cage structure α- or β- or γ-CD) or the channel crystalline structure of γ-CD (γ-$CD_{channel}$) in solutions of styrene in deuterated acetone, where the insoluble CD crystals settled on the bottom of the NMR tube. γ-$CD_{channel}$ crystals and their included guests, $H_2O$ or styrene, are transparent to solution $^1$H-NMR. Subsequently, the decrease in intensity of styrene peaks and the increase in intensity of the $H_2O$ peak were recorded as a function of time as the styrene displaces $H_2O$ from the CD cavities during the inclusion and complexation process. It was observed that the styrene/acetone peak ratio decreases as a function of time when γ-$CD_{channel}$ crystals were suspended in the styrene/acetone solution. From its solution, the styrene monomer enters the channels of the γ-$CD_{channel}$ crystals, where it is not visible by $^1$H-NMR, confirming the inclusion process of styrene monomer into γ-$CD_{channel}$ to form styrene-γ-$CD_{channel}$-IC. No change in the styrene/acetone peak ratio was observed in the cases of α-$CD_{cage}$, β-$CD_{cage}$ or γ-$CD_{cage}$ (Figure 2), the latter somewhat to our surprise. Thus, styrene did not form inclusion compounds with as-received α-CD, β-CD, or γ-CD “cage type” crystals, when suspended in styrene solution, or even when suspended in pure styrene monomer. The literature has reported the inclusion complexation of styrene with various CDs (α-, β-, methylated β- or γ-CD) when styrene was added to CD solutions.[2,3] However, in the case of solid CD crystals, styrene molecules were not included in the CD cavities except for γ-$CD_{channel}$.

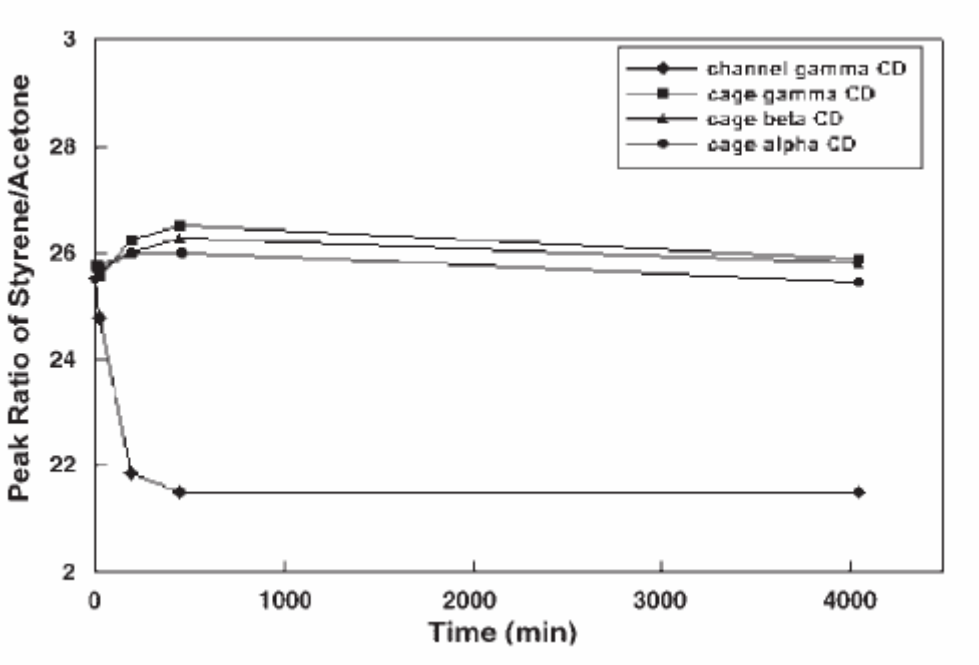


**Figure 2.** The variation of $^1$H-NMR peak intensity of styrene relative to the solvent peak in the suspensions of α-$CD_{cage}$, β-$CD_{cage}$, γ-$CD_{cage,}$ and γ-$CD_{channel.}$

We have also studied the kinetics of the "precipitation method" where the inclusion complexation of styrene with γ-CD was monitored by $^1$H-NMR. An unsaturated γ-CD solution was prepared in a NMR tube by using deuterated water ($D_2O$). Then, styrene was added to the γ-CD solution. The clear γ-CD solution became turbid and a white precipitate formed immediately after addition of styrene, which indicated the formation of the styrene/γ-CD-IC. It was observed that the γ-CD molecules disappeared from the solution as they form insoluble CD IC crystals. The decrease in intensity of γ-CD peaks and the increase in intensity of the $H_2O$ peak were recorded as a function of time as the styrene displaces $H_2O$ from the CD cavities during the inclusion process (Figure 3). It is clear from the overlay NMR spectra that γ-CD peaks have been disappeared after 1 hour of mixing time

suggesting that almost all the γ-CD molecules were complexed with styrene and form insoluble IC crystals.

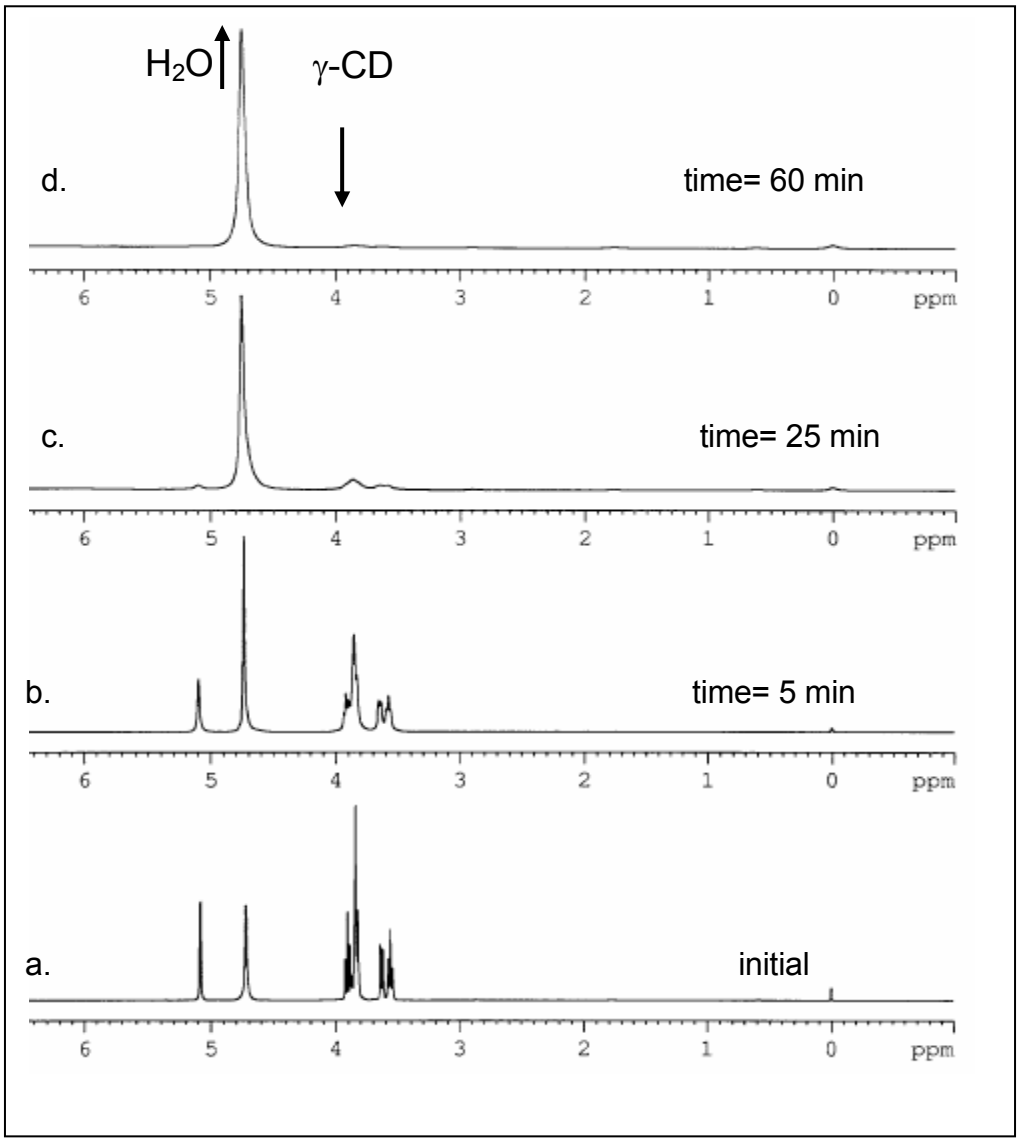


**Figure 3**. Overlay of $^{1}$H-NMR spectra of (a) γ-CD solution in $D_2O$. The addition of styrene in γ-CD aqueous solution after (b) 5 min, (c) 25 min and (d) 60 min.

### 5.3.2 Stability of Styrene/γ-$CD_{channel}$ IC in Aqueous Medium

The stability of styrene/γ-$CD_{channel}$ IC was studied under the polymerization conditions. γ-CD is soluble in water (23 g/100 ml), however, once the CD forms inclusion complex with guest molecules, the solubility of CD decreases significantly. Here, we studied the stability of the CD channels in aqueous medium at different temperatures. 1 g of styrene/γ-$CD_{channel}$ IC crystals was suspended in 10 ml of water and stirred for 24 hours at room temperature. At the end, about 80% (0.8 g) of styrene/γ-CD IC crystals were collected showing that only 20% of the CD-IC become soluble and passed through the filter during filtration. The x-ray study showed that the channel structure for styrene/γ-CD IC was preserved confirming its stability in aqueous medium. The same procedure was applied to styrene/γ-$CD_{channel}$ IC crystals at higher temperature (60$^{o}$ C). This time a 40% weight loss was observed, indicating that CD-IC became more soluble at high temperature, but again, the channel structure of styrene/γ-CD IC was preserved. This stability experiment showed that the polymerization of styrene can be performed inside γ-CD channel (confined environment) in aqueous medium at room temperature or even at higher temperatures. Therefore, we repeated the same procedure by suspending styrene/γ-$CD_{channel}$ IC crystals in aqueous medium and added a water soluble initiator for polymerization. To our surprise, we obtained about 0.1 gr of powder (90% weight loss) at the end of 24 hrs of polymerization reaction which indicates that most γ-CD molecules become free during polymerization and therefore become soluble in water. In the end, we obtained a rotaxanated polystyrene-CD structure, where some γ-CD molecules (~1 γ-CD/70 PS repeat units) were threaded and entrapped along the PS

chains after the polymerization. Though not presented here, x-ray diffraction showed that the resulting polyrotaxane has an amorphous structure.

### 5.3.3 Polymerization of Styrene/γ-$CD_{channel}$ IC

The polymerization of styrene-γ-$CD_{channel}$-IC was performed in two ways; solid-state polymerization by γ-radiation and by solution polymerization in aqueous medium. Styrene-γ-$CD_{channel}$-IC crystals were placed under a γ-radiation source ($^{60}Co$) for 240 hours and the total dose was 2.1 Mrad. The X-ray study showed that the channel structure was preserved during the polymerization. The $^{1}H$-NMR confirmed the polymerization of styrene and the conversion of monomer to polymer was about 50%.

In solution polymerization, styrene-γ-$CD_{channel}$-IC crystals were suspended in deionized water under argon atmosphere for 24 hours. Water-soluble free-radical initiator; 2,2'-azobis(2-methylpropionamidine) dihydrochloride (AMPDC) (Aldrich) (5 % molar) at 60$^{o}$ C or redox initiator $K_2S_2O_8$/$NaHSO_3$ (5 % molar) at room temperature (RT) was used. The polymerization was terminated either with 10% w/w quencher (4-methoxy phenol, Aldrich) or placing the reaction flask in an ice bath. The usual free-radical polymerization of styrene was performed in toluene solution in the presence or absence of as-received γ-$CD_{cage}$ and was initiated with 2,2'-azoisobutyronitrile (AIBN) to produce control samples for comparison. Additionally, styrene-γ-$CD_{channel}$-IC was suspended in toluene instead of water, and the polymerization was carried out under the same conditions to provide another control sample. It was found that styrene monomer migrates from the γ-CD channels and polymerizes outside of the channels when toluene (organic solvent) was used, where the resulting polystyrene did not

contain any cyclodextrin. In the case of an aqueous polymerization medium, a rotaxanated structure has been obtained, where γ-CD molecules were threaded and entrapped along the PS chains.

An overview of reaction parameters and results is given in Table 2. It was observed that the molecular weight (MW) of the PS synthesized in the γ-CD channels (aqueous medium) is much higher than the PSs synthesized in toluene, either in the presence or absence of γ-CD, along with a higher polydispersity index (PDI). The broader PDI can be due to heterogeneity of the system. It was also observed that the presence of suspended γ-$CD_{cage}$ or γ-$CD_{channel}$ in the organic medium (heterogeneous system) did not significantly affect the MW or PDI of the solution synthesized polystyrene when compared to polymer that was synthesized in the homogeneous styrene/toluene system. Yet, the presence of γ-$CD_{cage}$ produced polystyrene with a slightly higher MW and with a narrower PDI. In case of polymerization of styrene-γ-$CD_{channel}$ in toluene, higher MW polymer was produced with a broader polydispersity compare to that of the homogeneous system. But, as mentioned earlier, all these polystyrene samples have lower MWs than the polystyrene synthesized in aqueous medium.

Table 1. An overview of PS polymerization parameters and results

| **Parameters** | **$M_n$ (g/mol)** | **$M_w$ (g/mol)** | **PDI** |
|---|---|---|---|
| Styrene-γ-$CD_{channel}$-IC in water, AMPDC, 24hr, 60° C | 10,900 | 59,000 | 5.43 |
| Styrene-γ-$CD_{channel}$ -IC in toluene, AIBN, 24hr, 60° C | 2,600 | 5,000 | 1.92 |
| Styrene with γ-CD, in toluene, AIBN, 24hr, 60° C | 3,400 | 4,600 | 1.35 |
| Styrene, in toluene, AIBN, 24hr, 60° C | 2,300 | 3,600 | 1.57 |

### 5.3.4 Characterization of Polystyrene Obtained from Polymerization of Styrene-γ-Cyclodextrin Inclusion Compound

The polymerization of styrene-γ-$CD_{channel}$-IC was performed by both solid-state and by solution polymerization in aqueous medium. The resulting polystyrene-γ-cyclodextrin inclusion compound (PS-γ-CD IC) was washed with an excess of hot water at $80^0$ C for 24 hrs to remove the CD from polymer. The removal of CD from polymer-CD ICs with hot water (coalescence process) is a very common technique that we have applied to obtain coalesced polymers free of CD.[4] However, in the present case we repeatedly applied the hot water coalescence process for polystyrene-γ-CD IC, but we were unable to remove the γ-CD completely from polystyrene. Figure 4 shows the FT-IR spectra of PS obtained by solid state and solution polymerization. Both samples were repeatedly washed with hot water to remove γ-CD, but it was found that both samples did contain γ-CD molecules. The thermogravimetric analysis showed that the sample contained around 15% weight percent γ-CD (Figure 5), or roughly 1 γ-CD per 70 PS repeat units. We observed a glass transition temperature ($T_g$) of $105^0$ C for this PS. We know that polymer-CD ICs usually do not show any $T_g$ in DSC scans if the polymer chains are fully covered by the γ-CD molecules.[4] Here, the observation of a $T_g$ for PS containg a small amount of threaded γ-CDs indicated that PS chains were only partially covered by γ-CD molecules (Figure 6). We also ran a x-ray diffraction scan for this PS, which was found to be amorphous, suggesting that the γ-CD molecules were separated from each other and did not form any γ-CD crystalline structures.

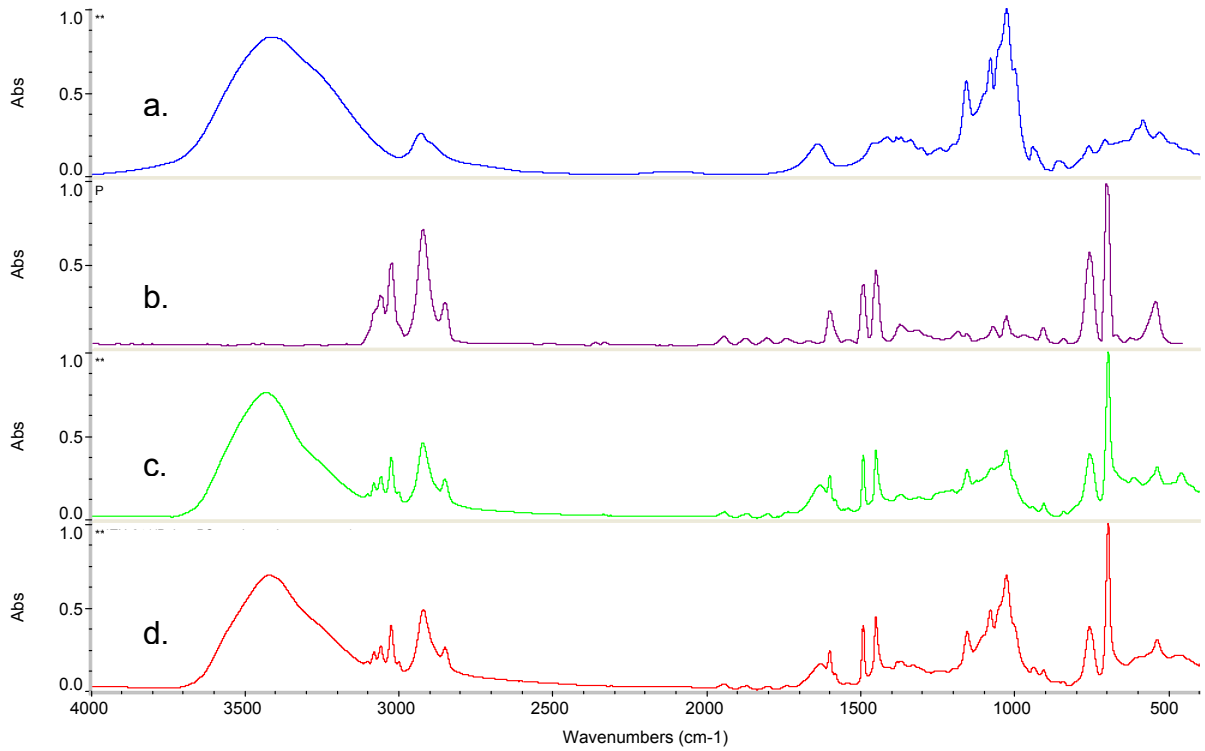


**Figure 4**. FT-IR overlay of (a) γ-CD, (b) poystyrene, (c) PS-γ-CD IC obtained by solution polymerization and (d) PS-γ-CD IC obtained by solid-state polymerization.

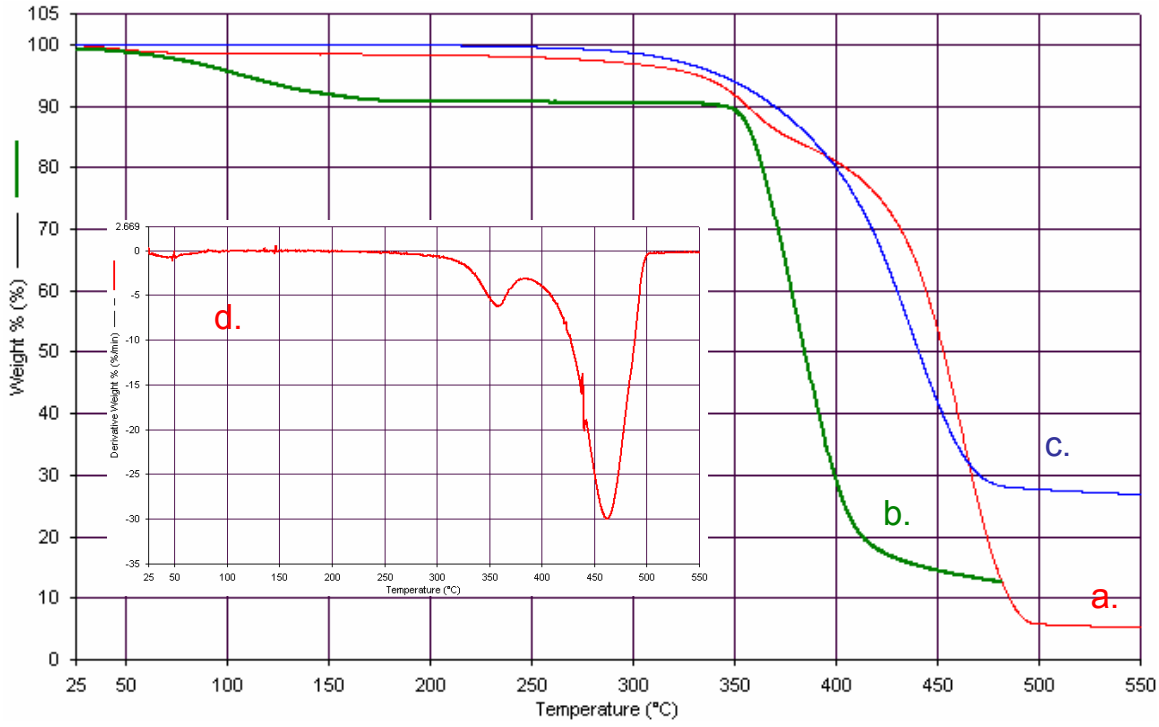


**Figure 5**. TGA overlay of (a) PS-γ-CD IC obtained by solid-state polymerization, (b) γ-CD, (c) poystyrene and (d) derivative weight % loss of PS-γ-CD IC.

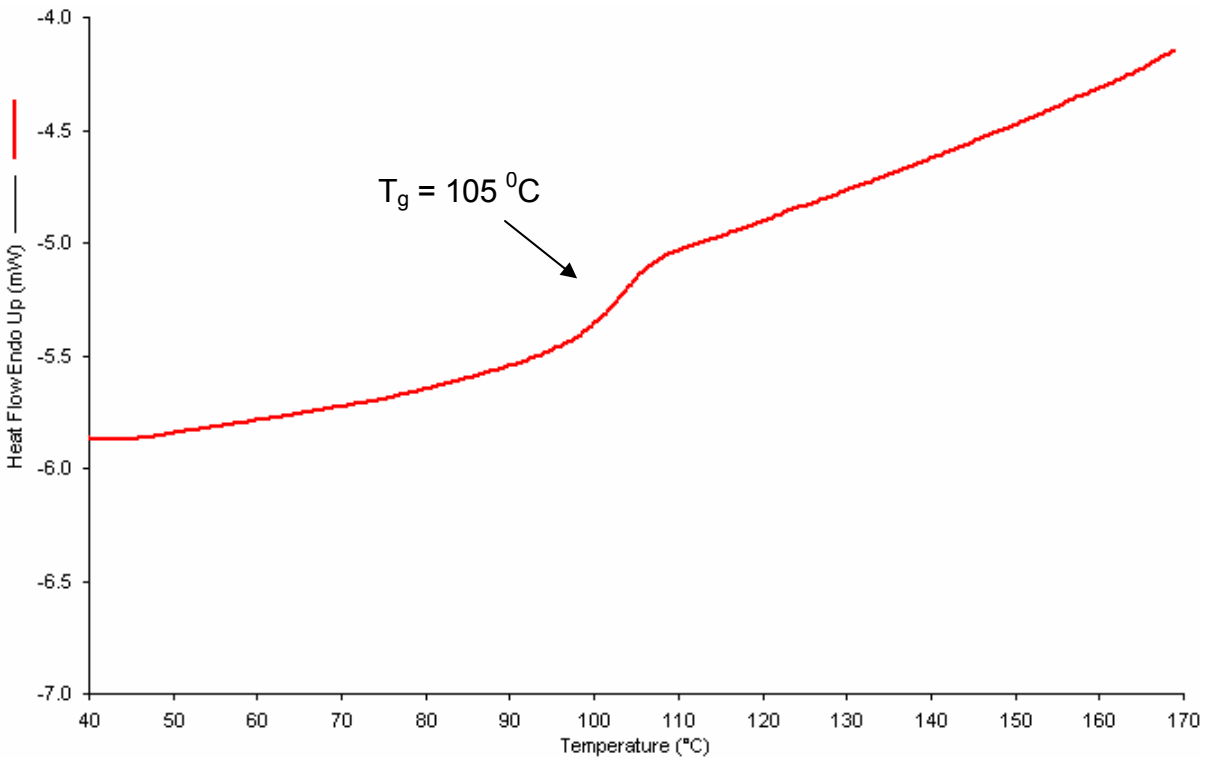


**Figure 6**. DSC scan of PS-γ-CD IC obtained by solid-state polymerization.

Based on our modeling, we expected to obtain isotactic polystyrene when styrene was polymerized inside the γ-CD channels, since only isotactic stereosequences can fit in the narrow cavity of γ-CD. We have examined the microstructures of the PS samples by $^{13}$C-NMR. The $^{13}$C-NMR spectra of PS synthesized in the channels of γ-CD were compared with that of the PS sample homogeneously polymerized in toluene (Figure 7). For the PS sample synthesized in the γ-CD channels, the most upfield aromatic C-1 peaks at ~145 ppm, which are due to syndiotactic stereosequences[5-6], are absent, whereas the rest of the peaks are similar when compared to the PS polymerized in toluene. Other noticeable differences expected for the stereosequences of PS obtained in the presence of γ-CD channels

were not observed. This may due to lack of or failure to retain the confined environment when γ-CD molecules begin to slip off during polymerization, therefore producing a largely atactic PS. Additionally, both solid-state polymerization and solution polymerization methods produced PS with similar stereosequences, indicating that the polymerization method used with styrene-γ-CD IC was not a factor.

In conclusion, these results suggested that a rotaxanated structure has been obtained with a few γ-CD molecules entrapped along the PS chains when styrene-γ-$CD_{channel}$-IC was polymerized. It is likely that γ-CD molecules are entrapped on the isotactic stereosequences, since only isotactic stereosequences can fit into the γ-CD cavity and cannot slip off the polystyrene chain due to their termination by *racemic* diads. The trapping of γ-CDs on the PS chains may also result from the disparity between the stoichiometries of stryrene- and PS-γ-CD ICs, where 2 stryrene and 3 PS repeat units are included in each γ-CD, respectively.

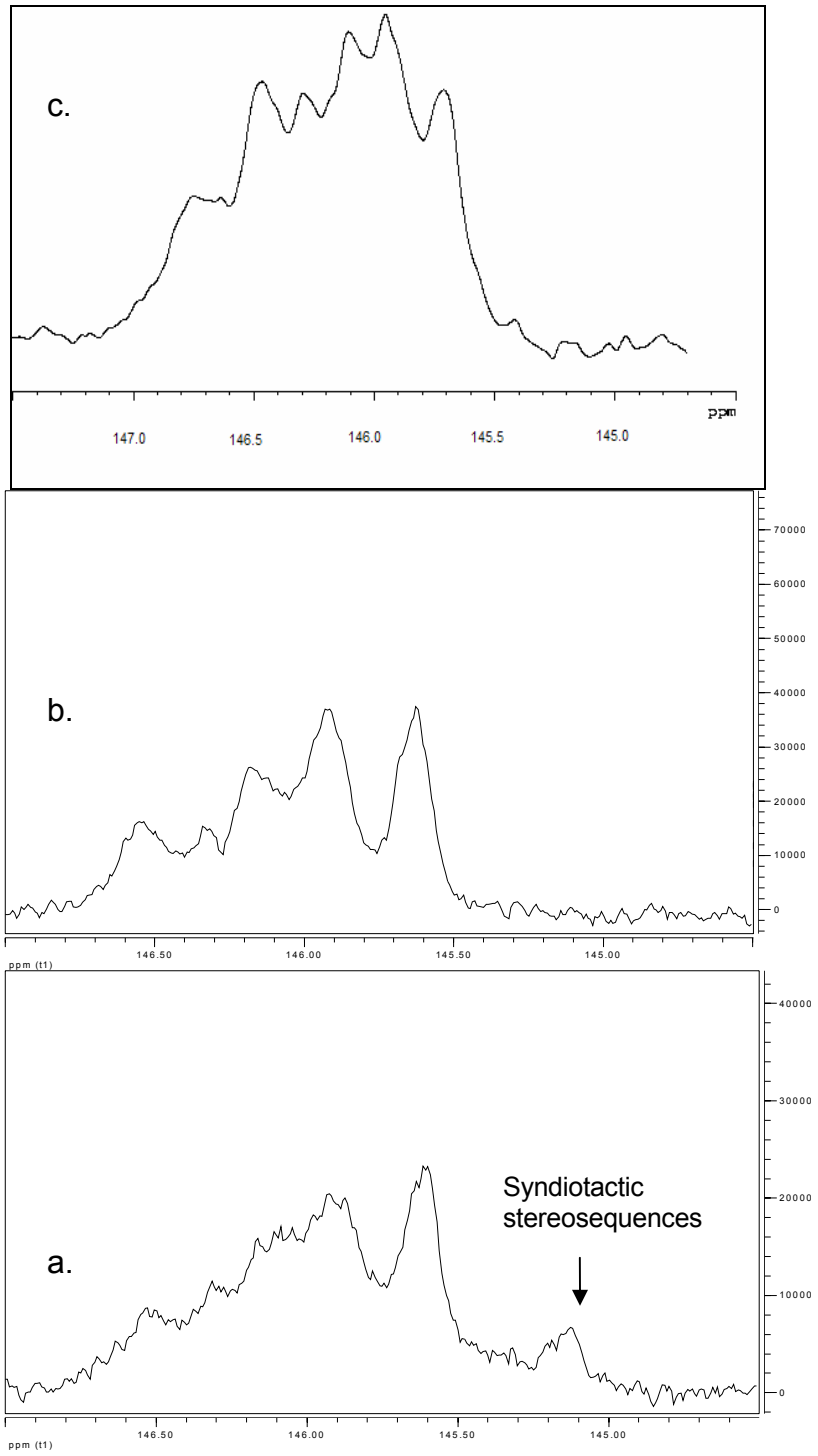


**Figure 7**. $^{13}$C-NMR of aromatic C-1 regions of PSs at 120$^{o}$ C. d-dichlorobenzene and mixture of d-dichlorobenzene/d-DMSO were used as solvent for polystyrene and PS-γ-CD IC, respectively: (a) PS synthesized in toluene, AIBN, 24hr, 60$^{o}$ C (b) PS-γ-CD IC obtained by solution polymerization and (c) PS-γ-CD IC obtained by solid-state polymerization.

## 5.4 References


1. M.A. Hunt, T. Uyar, A.E. Tonelli, et al., *Polymer,* 2004, *45* (4), 1345

2. (a) J. Storsberg, H. Ritter, *Macromol. Rapid Commun.* 2000, *21*, 236.

   (b) S.W. Choi, O. Kretschmann, H. Ritter, et al. *Macromolecular Chem. & Phys*., 2003, *204* (12), 1475.

   (c) J. Storsberg, H. van Aert, H. Ritter, et al. *Macromolecules* 2003, *36*(1), 50.

   (d) H. Ritter, M. Tabatabai, *Progress in Polymer Science,* 2002, *27* (9), 1713

3. (a) Y.J. Cao, X.H. Xiao, Q.X. Guo, et al. *J Molecular Structure*, 2003, *660* (1-3), 73.

   (b) Y.J. Cao, X.H. Xiao, Q.X. Guo, et al. *Spectrochimica Acta Part A Molecular & Biomolecular Spectroscopy*, 2004, *60* (4): 815

4. (a) Rusa CC, Uyar T, Rusa M, Wang X, Hunt MA, Tonelli AE. *Journal of Polymer Science: Part B-Polymer Physics* 2004; 42 (22): 4182-4194**.**

   (b) Uyar T, Rusa CC, Rusa M, Wang X, Hacaloglu J, Tonelli AE. *Journal of Polymer Science: Part B-Polymer Physics* 2005; 43 (18): 2578-2593**.**

   (c) Uyar, T.; Rusa, C. C.; Hunt, M. A.; Aslan, E.; Hacaloglu, J.;Tonelli, A. E. Polymer 2005, (46) 4762-4775.

5. T. Kawamura, N. Toshima, K. Matsuzaki, *Macromol. Rapid Comm.* 1994 *14*, 479

6. H. Sato, Y. Tanaka, *J Polym Sci : Polym Phys Ed.,* 1983, *21*, 1667

# 6 Conclusions and Future Directions of the Research

We achieved the formation of polymer-cyclodextrin inclusion compounds of polycarbonate (PC), poly(methyl methacrylate) (PMMA) and poly(vinyl acetate) (PVAc) guests with host γ-cyclodextrin (γ-CD). We obtained the coalesced bulk polymer samples by removal of γ-CD from their inclusion compounds (ICs). It was found that the coalesced polymers have extended chain conformations along with improved thermal properties. The improvements observed in the thermal transitions and thermal stabilities for the coalesced polymers might be due to their ordered and less entangled state. However, the presence of remnant γ-CD in the coalesced polymers may also be the reason for their improved thermal properties. As a future study, if coalesced polymers completely free of CD can be obtained, then thermal studies of these polymers can be repeated to find the answer to why do coalesced polymers have improved thermal properties? Is it due to their extended and less entangled state or is it because of remnant CD? Additionally, since the coalesced polymers chains are in extended and less entangled states, it would be valuable to study and compare the optical and mechanical properties of coalesced polymers with as-received polymers.

We developed a procedure for the formation of intimate blends of binary and ternary polymer systems; PC/PMMA, PC/PVAc, PMMA/PVAc and PC/PMMA/PVAc. PC/PMMA, PC/PVAc, PMMA/PVAc and PC/PMMA/PVAc were included in γ-CD channels and were then simultaneously coalesced from their common γ-CD-ICs to obtain intimately mixed blends. Their analyses indicated that the ternary and binary blends of these polymers achieved by coalescence from their common γ-CD-ICs

resulted in homogeneous polymer blends, possibly with improved properties, whereas co-precipitation and solution cast methods produced phase separated polymer blends. We showed that coalescence of two or more normally immiscible polymers from their common CD-ICs appears to be a method applicable for obtaining well-mixed, intimate blends. It was also observed that PC was preferentially included in γ-CD channels when compared to PMMA or PVAc. The preferential inclusion of PC may be explained by differences of its hydrophobicity and its chain cross-section compared with those of PMMA or PVAc. As a future study, hydrophobicity of PC can be changed by modifying the polymer with hydrophilic groups, and further study of the common and competitive inclusion of modified PCs with PMMA and/or PVAc in γ-CD cavities should be conducted.

Styrene/γ-$CD_{channel}$-IC was formed in order to perform polymerization of styrene in a confined environment (γ-CD channels). The *in situ* polymerization of styrene/γ-$CD_{channel}$-IC was performed both in aqueous media and by solid-state polymerization. A rotaxaned structure has been obtained where some CD molecules remain entrapped along the PS chains after the polymerization. In a future study, the rheological and physical properties of rotaxanated PS-CD can be investigated, as it is expected to have distinctive properties, since it has a unique sparsely γ-CD rotaxanated structure. Additionally, γ-CD molecules can serve as multipurpose reaction centers due to the presence of reactive –OH groups. Therefore, crosslinking of the polymer or initiating a polymerization from –OH groups to obtain co-polymers are some of the choices that can be considered in future studies of the γ-CD rotaxanated PS.

# 7 Appendix

## 7.1 List of Publications

1. ***T. Uyar**, M. Rusa , H.S. Gracz, I.D. Shin, A. Shafei and A.E. Tonelli* "Polymerization of Styrene-γ-Cyclodextrin Inclusion Compound" (in preparation)

2. *C. C. Rusa, M. Rusa, J. Peet, **T. Uyar**, J. Fox, M. A. Hunt, C. M. Balik, and A. E. Tonelli*, "The Nano-threading of Polymers" *J of Inclusion Phenomena and Macrocyclic Chem. **2005** (in review)*

3. ***T. Uyar**, M.A. Hunt , H.S. Gracz, A.E. Tonelli, "*Crystalline Cyclodextrin Inclusion Compounds Formed with Aromatic Guests: Guest-Dependent Stoichiometries and Hydration-Sensitive Crystal Structures*" Journal of Physical Chemistry **2005** (in review)*

4. ***T. Uyar**, A. Shafei, X. Wang , J. Hacaloglu, A.E. Tonelli*, "The Solid Channel Structure Inclusion Complex Formed Between Guest Styrene and Host γ-Cyclodextrin" *Journal of Inclusion Phenomena and Macrocyclic Chemistry **2005** (in press)*

5. ***T. Uyar**, E. Aslan , A.E. Tonelli, J. Hacaloglu,* "Pyrolysis Mass Spectrometry Analysis of Poly(vinyl acetate), Poly(methyl methacrylate) and Their Blend Coalesced from Their Inclusion Compounds Formed with γ-Cyclodextrin" *Polymer Degradation and Stability **2005** (in press)*

6. ***T. Uyar**, C.C. Rusa, M.A. Hunt, J. Hacaloglu, A.E. Tonelli*, "Intimate Blending of Binary Polymer Systems from Their Common Cyclodextrin Inclusion Compounds" *J of Polymer Sci: Polymer Physics* 43(18):2578-2593, ***2005***

7. ***T. Uyar**, C.C. Rusa, M. A. Hunt, J. Hacaloglu and A.E. Tonelli*, "Reorganization and Improvement of Bulk Polymers by Processing with Their Cyclodextrin Inclusion Compounds" *Polymer, 46(13), 4762–4775, **2005***

8. *C. C. Rusa, M. Wei, T. A. Bullions, X. Shuai, **T. Uyar** and A. E. Tonelli* "Nanostructuring polymers with cyclodextrins" *Polymers for Advanced Technologies, Vol 16, Issue:2-3, 269-275, **2005***

9. *C. C. Rusa, M. Wei, X. Shuai, T. A. Bullions X. Wang, M. Rusa, **T. Uyar** and A. E. Tonelli* "Molecular Mixing of Incompatible Polymers Through Formation of and Coalescence from Their Common Crystalline Cyclodextrin Inclusion Compounds" *J of Polymer Science Part B: Polymer Physics, Vol 42, 4207-4224, **2004***

10. *C.C. Rusa, **T. Uyar**, M. Rusa, M. A. Hunt, X. Wang and A.E. Tonelli* "An Intimate PC/PMMA/PVAc Ternary Blend via Coalescence from Their Common γ-Cyclodextrin Inclusion Compound" *J of Polymer Sci:Polymer Physics, 42, 4182-4194, **2004***

11. ***T. Uyar**, M. Rusa and A.E. Tonelli*, "Polymerization of styrene in cyclodextrin channels: Can confined free-radical polymerization yield stereoregular polystyrene?" *Macromolecular Rapid Comm., 25(15), 1382, **2004***

12. *MA. Hunt, DW. Jung, M. Shamsheer, **T. Uyar**, AE. Tonelli* "Polystyrenes in channels"*Polymer,45(4),1345, **2004***

13. *M. Rusa, **T. Uyar**, B.J. Busche and A.E. Tonelli*, "Nanostructuring Polymers with Cyclodextrins - Adjusting Their Conformations and Organizing Polymers on Surfaces" *Polymeric Materials: Sci. & Eng., 91,964, **2004***

14. ***T. Uyar**, M. Rusa, M. Wei, C.C. Rusa, M.A. Gomez and A.E. Tonelli*, "Reorganization of Semi-Crystalline Polymers with Cyclodextrins" *Polymeric Materials: Science and Engineering, 91, 191-192, **2004***

15. ***T. Uyar**, M. Rusa and A.E. Tonelli*, "Polymerization of Vinyl monomers in Cyclodextrin Channels: Can Confined Free Radical Polymerization Yield Stereoregular Polymers?" *Polymer Preprints, 45(2), 112, **2004***

16. *A. E. Tonelli, T. A. Bullions, M. Wei, X. Wang and **T. Uyar*** "Nanostructuring Polymer Conformations to Alter Their Properties" *Polymer Preprints, 44(2), 1-2, **2003***